Stony Brook University

The official electronic file of this thesis or dissertation is maintained by the University Libraries on behalf of The Graduate School at Stony Brook University.

Methylmercury bioaccumulation, transformation, and trophic transfer

in marine food chains

A Dissertation Presented

by

Cheng-Shiuan Lee

to

The Graduate School

in Partial Fulfillment of the

Requirements

for the Degree of

Doctor of Philosophy

in

Marine and Atmospheric Science

Stony Brook University

December 2017

Stony Brook University

The Graduate School

Cheng-Shiuan Lee

We, the dissertation committee for the above candidate for the

Doctor of Philosophy degree, hereby recommend

acceptance of this dissertation.

Nicholas S. Fisher, Dissertation Advisor
Distinguished Professor, School of Marine and Atmospheric Sciences

Glenn R. Lopez, Chairperson of Defense
Professor, School of Marine and Atmospheric Sciences

J. Kirk Cochran
Professor, School of Marine and Atmospheric Sciences

Christopher J. Gobler
Professor, School of Marine and Atmospheric Sciences

John R. Reinfelder
Professor, Department of Environmental Sciences
Rutgers University

This dissertation is accepted by the Graduate School

Charles Taber

Dean of the Graduate School

Abstract of the Dissertation

Methylmercury bioaccumulation, transformation, and trophic transfer

in marine food chains

by

Cheng-Shiuan Lee

Doctor of Philosophy

in

Marine and Atmospheric Science

Stony Brook University

2017

Monomethylmercury (MeHg) is a neurotoxic compound that causes adverse health effects in exposed wildlife and humans. It is primarily accumulated through diet and is the only mercury species to build up in aquatic food chains. However, our understanding with respect to MeHg biogeochemical cycling in marine environments and its interactions with marine organisms is still limited. In order to better understand important processes in the MeHg biogeochemical cycling and factors governing its environmental fate, uptake, accumulation, transformation, and trophic transfer of MeHg in the marine chains, I conducted a series of experiments and measurements associated with marine bacterioplankton, phytoplankton, zooplankton, and apex pelagic fish.

The largest bioconcentration step of MeHg is found between water and primary producers like phytoplankton, implying that they serve as an important entry for MeHg entering the aquatic food web. Experiments using the γ-emitting radiotracer ^{203}Hg to determine MeHg uptake rates and concentration factors in six marine phytoplankton species were performed. All algal species

greatly concentrated MeHg out of seawater, with volume concentration factors (VCFs) ranging from 0.2×10^5 to 6.4×10^6, depending on algal species. VCFs were directly related to cellular surface area-to-volume ratios, suggesting that smaller algal cells can enrich MeHg to a greater extent than larger cells. Most of the cellular MeHg was found in the cytoplasm. Temperature, light, and nutrient additions did not directly affect MeHg uptake in most species, with the exception that the dinoflagellate *Prorocentrum minimum* displayed significantly greater uptake per cell at 18°C than at 4°C, suggesting an active uptake for this species. Passive transport seemed to be the major pathway for MeHg to initially associate with most phytoplankton and the size (surface area-to-volume ratio) of algal cells seemed to be the most critical factor affecting MeHg concentrations in phytoplankton cells.

The influences of specific sulfur-containing organic compounds and naturally occurring dissolved organic matter (DOM) on the accumulation of MeHg in a marine diatom *Thalassiosira pseudonana* were investigated. At environmentally realistic and higher concentrations, the addition of glycine and methionine had no effect on algal MeHg uptake. Thiol-containing compounds such as cysteine and thioglycolic acid reduced MeHg accumulation in algal cells at elevated added concentrations (>100 times higher than naturally occurring concentrations) reduced MeHg uptake by algae, however, environmentally realistic concentrations of glutathione, another thiol-containing compound (as low as 10 nM), resulted in a decline of ~30% in VCFs, suggesting its potential importance in natural waters. Humic acid additions of 0.1 and 0.5 mg C L^{-1} also reduced MeHg VCFs by ~15% and ~25%, respectively. The bioaccumulation of MeHg for *T. pseudonana* in coastal waters with varying levels of dissolved organic carbon (DOC) was inversely correlated with bulk DOC concentrations. Generally, naturally occurring DOM, particularly certain thiol-containing compounds, can reduce MeHg uptake by phytoplankton.

MeHg is known to build up in marine food chains, resulting in higher concentrations in upper trophic level animals than their prey. To better understand MeHg bioaccumulation in marine food chains, the assimilation and retention of Hg(II) and MeHg in a marine calanoid copepod, *Acartia tonsa* were determined. Assimilation efficiencies of Hg(II) and MeHg ranged from 25% to 31% and 58% to 79%, respectively, depending on algal diets. Assimilation efficiencies were positively related to the fraction of Hg in the cytoplasm of the algal cells that comprised their diet. Efflux rates of Hg(II) (0.29 d^{-1}) and MeHg (0.21 d^{-1}) following aqueous uptake were similar, but efflux rates following dietary uptake were significantly lower for MeHg (0.11–0.22 d^{-1}) than Hg(II) (0.47–0.66 d^{-1}). The calculated trophic transfer factors in copepods were >1 for MeHg and consistently low for Hg(II) (<0.2). In general, MeHg uptake from the diet accounted for most of the body burden in copepods (>50%). For an algal diet with a MeHg dry weight bioconcentration factor $\geq 10^6$, over 90% of a copepod's MeHg body burden can derive from the diet. The model-predicted MeHg concentrations in the copepods were comparable to independent measurements for copepods in coastal and open-ocean regions, implying that the measured parameters and model in this thesis are applicable to natural waters.

The formation of Hg^0 gas from Hg(II) and MeHg by coastal bacterial assemblages was studied in controlled laboratory experiments. A rapid radioassay method was developed to evaluate Hg^0 production from seawater with added Hg concentrations in the low pM range. Hg^0 production rates were independent of dissolved Hg(II) and MeHg concentrations, and were directly a function of bacterial densities. The Hg evasion experiments showed that for 1 µm-filtered Long Island coastal waters from the Atlantic with natural bacterial assemblages of about ~1 x 10^6 cells ml^{-1}, approximately 25% of Hg(II) and 18% of MeHg were transformed to Hg^0 in 4 days at 24°C. In Long Island Sound waters, with 5 x 10^6 bacterial cells ml^{-1}, 60% of Hg(II) and 19% of MeHg

were converted to Hg^0 in 4 days. When bacterial assemblages were exposed to Hg(II), the Hg^0 production rate declined after one day, but the rate of Hg^0 evasion from bacterial assemblages exposed to MeHg remained almost constant over 4 days, suggesting two distinct production pathways for the two Hg sources. Higher Hg^0 production rates were found at 24°C than at 4°C, and bacterial mercuric reductase, *mer*-operon, was found, indicating such transformations might have been primarily driven by metabolic processes and enzymatic reactions.

Tunas are apex predators in marine food webs that can accumulate Hg to high concentrations and provide more Hg (~40%) to the U.S population than any other source. In this thesis, total Hg concentrations (mostly MeHg) were measured in 1292 Atlantic bluefin tuna (ABFT, *Thunnus thynnus*) captured in the Northwest Atlantic from 2004 to 2012. ABFT Hg concentrations and variability increased nonlinearly with length, weight, and age, ranging from 0.25 to 3.15 mg kg^{-1}, and declined significantly at a rate of 0.018 ± 0.003 mg kg^{-1} per year or 19% over an 8-year period from the 1990s to the early 2000s. Notably, this decrease parallels comparably reduced anthropogenic Hg emission rates in North America and North Atlantic atmospheric Hg^0 concentrations during this period, suggesting that recent efforts to decrease atmospheric Hg loading have rapidly propagated up marine food webs to a commercially important species. This is the first evidence to suggest that emission reduction efforts have resulted in lower Hg concentrations in large, long-lived fish.

In summary, this thesis describes the role that different marine organisms play in the bioaccumulation, trophic transfer, transformation of MeHg at the bottom and the top of marine food chains, and elucidates the importance of these processes in marine Hg cycling. The results and parameters measured in this thesis, combined with field data, could ultimately be used by

global biogeochemical models describing Hg cycling in the marine environment, allowing us to better understand the fate of Hg in the ocean.

To my family

Table of Contents

List of Tables

List of Figures

Acknowledgments

First, I would like to thank my advisor, Nick Fisher, for guiding and supporting me throughout my PhD in the past five and half years. Nick has been a brilliant mentor who always provides me with great ideas and valuable insights in oceanography. With his full support, I can do whatever experiments I want to. In addition, I was able to travel around the states and the world, attending top international conferences to present my works and meet other excellent scientists. Two ASLO meetings in Honolulu and New Orleans, the AGU meeting in San Francisco, the Mercury meeting in Providence, and the Goldschmidt conference in Paris, those are unforgettable memories and experience in my life. Nick has always encouraged me to work hard, think big, and write more! If without his selfless devotion (his time and his patience with my terrible grammar) to my writing, I could never have published 4+ papers before my graduation. I am glad that I have made the right decision to come to Stony Brook in 2012.

For their guidance in preparing this dissertation, I would like to thank my exceptional committee members, Glenn Lopez, Kirk Cochran, Chris Gobler, and John Reinfelder. Their input in various aspects has completed this dissertation. I would like to give special thanks to John and his colleagues in Rutgers University for their help in the Chapter 5, increasing the depth of my dissertation.

I am grateful to our lab manager, Shelagh Zegers for her assistance in the lab. Her extraordinary sense of humor has made my PhD life full of joy. I would also like to thank my labmates (current and former) Zosia Baumann, Cuiyu Wang, Xiayen Ye, Abby Tyrell, Daniel Madigan, Teresa Mathews, Maureen Murphy, Roxanne Karimi, Karen Warren, Derin Thomas, Zhixin Ni, Halim Ergul, Susan Silbernagel for their help and encouragement all the time.

I would like to show my gratitude to Bob Cerrato, Roy Price, Qingzhi Zhu, Gordon Taylor, David Hirschberg, and Ashley Cohen for their statistical and analytical assistance with my research. Outside of the lab, I am also grateful to my friends and officemates: Haikun Xu, Hanlu Huang, Hang Yin, Isaac Klingensmith, Irvin Huang, Joe Tamborski, Samantha Roberts, Matt Siskey, Tracey Evans, Oliver Shipley, and many other friends from Taiwanese Graduate Student Association at Stony Brook.

Last but not the least, I want to thank my family for their love and support over the years. I am indebted to my wife, Mei-Chun, for her selfless support. If without her being here, I could never have earned my PhD.

Chapter 1

Introduction

Marine biogeochemical cycling of mercury (Hg) is complicated and many processes associated with interactions with marine organisms are not yet thoroughly understood. Among various Hg species, monomethylmercury (MeHg) is known as a neurotoxic compound that can cause adverse health effects in exposed wildlife and humans. These impacts include long-term developmental delays in children and impaired cardiovascular health in adults (Grandjean et al., 2010; Mason et al., 2012; National Research Council, 2000). Moreover, MeHg is the only mercury species to accumulate in organisms and further build up at every level in marine food chains. However, our understanding of factors controlling MeHg accumulation in marine biota, especially at the bottom of marine food webs, is surprisingly limited, which is partly due to analytical difficulties (e.g., extremely low concentrations, complicated Hg speciation, and various abiotic/biotic processes involved).

MeHg can be highly assimilated in marine organisms, extending its residence time in the upper ocean. But to date, its production, uptake, release, elimination, and trophic transfer in water columns have not been well characterized. Enhanced MeHg concentration has been observed in subsurface water globally (Cossa et al., 2009; Cossa et al., 2011; Hammerschmidt and Bowman, 2012; Lehnherr et al., 2011; Mason and Fitzgerald, 1990; Sunderland et al., 2009). The mechanism leading to this phenomenon is unclear and under debate. In addition, the relationship between enhanced MeHg in seawater and MeHg uptake at the base of food webs has also not been well established. Some studies have shown higher MeHg concentrations were found in deeper-swimming fish who consume prey from below the mixed layer (Choy et al., 2009; Monteiro et al., 1996). A study on the ratios of Hg stable isotopes in fish has further fortified the idea of *in situ* MeHg production at subsurface waters (Blum et al., 2013). However, the fish dwelling in subsurface waters may have slower growth rates or longer biological half-

lifes of MeHg due to low ambient temperature, resulting in higher MeHg accumulation. Either in situ MeHg production or low temperature in the deep water could have the potential influence to enhance MeHg accumulation. Further investigation to assess which one plays the major role is needed. These studies have revealed the importance of MeHg concentrations in seawater to those in swimming fish, but how MeHg is transferred from the aqueous phase to fish still requires further investigation. In particular, the enrichment of MeHg in phytoplankton from ambient seawater is the most important factor because it is where the biggest concentration step occurs. Both field and model data have suggested that the Hg inventory in the global oceans has increased up to three times since the industrial revolution and could keep rising (Lamborg et al., 2014b; Sunderland et al., 2009). Anthropogenic input of Hg into the ocean may increase the Hg burden in marine organisms and further cause significant perturbation to marine ecosystems.

This thesis is designed to provide a better understanding of several important processes in MeHg cycling in the upper ocean. The data generated from both laboratory experiments and field work in this thesis can further be applied into a global biogeochemical Hg model, allowing us to better understand the biogeochemical processes, and better predict the fate of MeHg in the upper ocean and MeHg concentrations in our seafood.

Biogeochemical cycling of mercury in the ocean

Mercury is a naturally occurring element and provides an excellent example of complexity in its chemistry and biogeochemical cycling. It has various physical and chemical species and is difficult to analyze at typical environmental concentrations (Fitzgerald et al., 2007; Selin, 2009). Figure 1 illustrates the potential abiotic/biotic reactions, transformations, and exchanges in

marine systems. Hg is mainly found in three chemical forms in marine environments: elemental Hg (Hg^0), ionic Hg^{2+} ($Hg(II)$) in a variety of inorganic and organic complexes, and methylated forms including MeHg and dimethylmercury (DMHg). Each form can be present in dissolved, colloidal and particulate forms. MeHg can be produced from Hg(II) by both biotic and abiotic mechanisms. Substantial amounts of MeHg are produced from sediments in coastal waters (Hammerschmidt et al., 2004; Heyes et al., 2006; Sunderland et al., 2006). The MeHg concentration near coastal waters can vary considerably from one place to another. It can be up to 3.3 pM in Long Island Sound (Balcom et al., 2004; Rolfhus and Fitzgerald, 2001), but is usually at sub-picomolar levels (Fitzgerald et al., 2007; Lamborg et al., 2014a; Mason et al., 2012). The concentration in open oceans falls within the fM level (Bowman et al., 2015) and there is considerably less information on the geographical and temporal distribution and cycling of MeHg in the open oceans. As mentioned earlier, higher concentrations of MeHg and DMHg have been found in subsurface low-oxygen regions (Bowman et al., 2015; Cossa et al., 2009; Cossa et al., 2011; Hammerschmidt and Bowman, 2012; Lehnherr et al., 2011; Mason and Fitzgerald, 1990; Sunderland et al., 2009). The mechanism of MeHg production in the open ocean water column has not been discovered yet. A strong correlation has been found between methylated Hg concentrations (MeHg + DMHg) and organic carbon remineralization rates, suggesting that methylation processes are likely to occur in subsurface waters during organic carbon remineralization instead of release of preformed MeHg from decomposition (Sunderland et al., 2009). These findings reinforce the linkage between the ocean biological pump, MeHg production, and accumulation in phytoplankton in marine microbial loops. As mentioned above MeHg can accumulate in marine biota and then biomagnify in marine food chains, the average proportion of MeHg over total Hg concentrations increases from less than 10% in the water

column to about 10~50% in plankton, and over 90% in fish (Mason et al., 2012; Morel et al., 1998).

MeHg accumulation in marine phytoplankton

Most research in marine environments has focused on Hg (total Hg or MeHg) levels in commercial fish consumed by humans due to public health concerns (Fitzgerald et al., 2007; Karimi et al., 2012; Mason et al., 2012; Morel et al., 1998; Selin, 2009). In contrast, very few studies have thoroughly investigated Hg and MeHg interactions with primary producers and consumers at lower trophic levels (Mason et al., 2012). Primary producers like phytoplankton are the most critical entry where metals or pollutants enter marine food webs. Bioconcentration factors (BCFs) of MeHg between water and phytoplankton can be up to 10^6 on a dry weight basis which is the largest bioconcentration step in food webs (Lee and Fisher, 2016; Luengen et al., 2012; Morel et al., 1998; Pickhardt and Fisher, 2007). MeHg is then highly assimilated and retained in zooplankton and fish through diet, resulting in even greater BCFs compared to ambient waters (Lawson and Mason, 1998; Lee and Fisher, 2017a; Mason et al., 1996; Morel et al., 1998). Consequently, humans are exposed to high MeHg through eating contaminated fish. For this reason, understanding the MeHg cycling in aquatic ecosystems (both fresh and marine) is important for environmental risk analysis. Environmental factors and biological attributes influencing MeHg uptake by primary producers in marine environments are not well characterized yet. To date, most studies have focused on MeHg accumulation in freshwater phytoplankton (Gorski et al., 2008; Gorski et al., 2006; Miles et al., 2001; Pickhardt and Fisher, 2007; Watras et al., 1998), and its trophic transfer in freshwater environments (Pickhardt et al., 2002; Pickhardt et al., 2005). The few studies on marine environments are confined to coastal

5

diatom and cyanobacteria species (Kim et al., 2014; Lawson and Mason, 1998; Mason et al., 1996; Zhong and Wang, 2009). There is little available data of MeHg interactions with other marine phytoplankton species.

In the past two decades, extensive studies have been made on trace metal interactions with marine phytoplankton, and aqueous chemistry is critical in controlling trace metal uptake and toxicity to aquatic organisms (Campbell, 1995; Campbell et al., 2002; Sunda and Huntsman, 1998). Moreover, the extent to which some metals are bioaccumulated by diverse marine phytoplankton has also been studied extensively (Fisher, 1986; Fisher et al., 1984; Fisher and Reinfelder, 1995). However, the interactions between MeHg and marine phytoplankton (e.g., uptake, accumulation and elimination) have not been adequately and systematically studied. Given that MeHg enters marine food webs primarily via uptake by phytoplankton, it is important to evaluate the impacts of biological attributes of algae and water chemistry to uptake because they may have substantial influences on governing MeHg uptake.

Metal uptake by algal cells generally involves an initial surface adsorption and the possibility of a subsequent transport into intercellular pools (Sunda and Huntsman, 1998). The factors influencing MeHg uptake by phytoplankton can be both biological and chemical. In addition, environmental factors like temperature and nutrients can also change metabolic rates and growth rates of phytoplankton, subsequently affecting MeHg uptake. Regarding biological aspects, different algal species may have variable extents to enrich MeHg. Previous studies have shown that there is considerable variation of metal uptake among different phytoplankton species (Fisher et al., 1984; Fisher and Reinfelder, 1995). In addition, bioconcentration factors can often vary by up to one to three orders of magnitude among different species, even within the same taxonomic group (Fisher, 1986; Fisher et al., 1984; Fisher and Reinfelder, 1995). The differences

in uptake may be due to algae size, cellular surface area-to-volume ratio, cell wall composition, and extracellular organic compounds. However, as mentioned above, there are very few studies that have investigated MeHg uptake in multi-algal species, and how those biological characteristics affect MeHg bioconcentration factors remains unclear. In this thesis, a series of experiments were carried out to examine the MeHg uptake by diverse marine phytoplankton which involved several common algal species with different sizes. Previous studies have demonstrated the strong correlation between concentration factor of inorganic Hg and surface-to-volume ratio of algal cells (Fisher, 1985; Fisher et al., 1984). Thus, MeHg is hypothesized to have a similar behavior where the surface-to-volume ratio of algae is the most dominant factor governing algal MeHg uptake.

A few studies have demonstrated that metal bioaccumulation in phytoplankton can be affected by nutrient enrichment (Rijstenbil et al., 1998; Wang and Dei, 2001a; Wang and Dei, 2001b). They found an increase in nitrogen concentration remarkably enhanced metal uptake (Cd, Zn, and Se) by phytoplankton in a short-term experiment. The effects of phosphorus and silica addition on metal uptake were less significant. On the contrary, under steady-state conditions, it was found that an increase in cell growth under nutrient-enriched conditions may result in a decrease in metal concentration in the algal cells due to a growth biodilution, if the metal uptake rate stayed constant or decreased due to finite metal concentration in the dissolved phase (Sunda and Huntsman, 1998). Considering the increasing nitrogen input and eutrophication in coastal waters due to human activities, excess nutrients may have considerable influence on MeHg uptake and accumulation in phytoplankton, and may directly impact subsequent trophic transfer of MeHg along the food web. Therefore, how nutrient concentrations impact MeHg accumulation in phytoplankton needs further investigations.

Influences of dissolved organic matter on algal MeHg accumulation

Bioavailability of MeHg is chemically controlled by its speciation. Speciation of metals largely controls their behavior in the aquatic environment. For example, mercury has a strong stability constant (K) of complexation to chloride (abundant in seawater) and dissolved organic matter (DOM, not as abundant as Cl^-, but generally with higher stability constants), and MeHg has similar behavior as well (Ravichandran, 2004). As with many other metals (Campbell, 1995), the speciation of mercury can affect its uptake by phytoplankton. For example, MeHg-DOM complexation could directly reduce MeHg bioavailability to algal cells. In contrast, it is also possible that MeHg could be taken up inadvertently when it is bound to amino acids like cysteine and methionine. The higher trophic levels obtain most of their MeHg from dietary sources, so even small differences in concentration factors at the base of aquatic food web should have significant consequences on the overall biomagnification of MeHg (Pickhardt and Fisher, 2007). Thus, it is necessary to understand how DOM concentration and composition govern the interactions of MeHg with phytoplankton.

In previous studies, Mason et al. (1996) concluded that passive uptake of uncharged lipophilic MeHg-chloride complexes is the principal accumulation route in a marine diatom. Lawson and Mason (1998) examined the effect of organic and inorganic ligands to MeHg uptake in estuarine food chains, and demonstrated opposite results among three ligands. Complexation of MeHg-bisulfide decreased the phytoplankton uptake rate and the uptake rate of the MeHg-cysteine and MeHg-thiourea complexes increased with increasing complexation by these ligands (Lawson and Mason, 1998). Pickhardt and Fisher (2007) found that fresh water phytoplankton cultured in water with higher DOM accumulated more MeHg than in water with lower DOM. They

hypothesized that the phytoplankton actively took up DOM and inadvertently acquired the MeHg

associated with that organic matter. The results from Gorski et al. (2008) and Luengen et al.

(2012) were consistent in the inverse relationship between DOM concentration and MeHg

bioaccumulation in fresh water environments. Zhong and Wang (2009) suggested that DOM and

chloride control the speciation and the uptake of MeHg by a marine diatom. DOM complexation

with MeHg dominated only when the DOM concentration was relatively high, but DOM may

still partially affect the uptake of MeHg even when chloride complexes dominated. These

inconsistent results can be explained by variations in the composition and concentration of the

organic matter or differences in other chemical variables in seawater. For instance, the sulfur

content in DOM might be critical to explain this. Furthermore, the physiological differences in

phytoplankton species might also influence the bioaccumulation of MeHg.

Unfortunately, to identify the complex composition of DOM is a great analytical challenge,

resulting in sparse information on chemical structures on molecular levels. This limitation results

in a lack of suitable separation methods with sufficient sensitivity for the characterization of

DOM in seawater (Hansell and Carlson, 2002). The method of measuring bulk concentrations of

DOM is well established and easy to achieve. However, it is unable to provide the exact origin,

size, and composition of DOM. This detailed information is critical to further investigate the

DOM interactions with MeHg uptake. Several methods have been established to classify the

DOM through isolation approaches. For example, solid-phase extraction methods using XAD

and C18 resins can isolate DOM separately into hydrophobic and hydrophilic parts. Luengen et

al. (2012) reported that the hydrophobic fraction isolated from freshwater resulted in smaller

MeHg enrichment in a freshwater diatom than other fractions. This might be due to higher

aromatic contents in the hydrophobic fraction, which revealed that the composition of the DOM

was important to MeHg uptake. A recent study (Schartup et al., 2015b) used excitation emission matrix (EEM) fluorescence spectroscopy to characterize differences in the origin of DOM (from soils, rivers, or marine productivity). Their results showed marine DOM did not have effects on MeHg uptake by *Escherichia coli*, but terrestrial DOM inhibited the uptake. They hypothesized that differences in uptake were due to the larger molecular weight of terrestrial DOM which might hinder the transport through the cell membrane. Another common method, ultrafiltration, is based on the size fractionation of DOM instead of its chemical properties. Using a molecular sieve allows us to collect high-molecular-weight (HMW) DOM which is often referred to as colloids. Several studies have investigated the bioavailability of metals bound to colloids, but no Hg or MeHg were included. Wang and Guo (2000) have found that marine colloidal materials added to cultures of a diatom and dinoflagellate decreased Zn uptake but increased Cr uptake. Although it is unlikely that phytoplankton can directly take up metals bound to colloidal matter, the colloidal phase might still be an important source of metals to heterotrophic flagellates (Tranvik et al., 1993). These DOM isolation means are, nevertheless, all operationally defined methods. To compare MeHg uptake in the presence of DOM isolated from different methods will be able to provide further insight into how DOM composition and its characteristic affect bioavailability of MeHg.

Mercury is known to bind very strongly with sulfur (Fitzgerald and Lamborg, 2003; Fitzgerald et al., 2007; Ravichandran, 2004), and sulfur is an essential element required for protein synthesis by all organisms. Two major sulfur species can be produced by marine organisms: (1) volatile sulfur species like dimethyl sulfide (DMS) and carbonyl sulfide (OCS), (2) thiol compounds such as glutathione (GSH) and cysteine (Cys) (Tang et al., 2000). Among many thiol species, GSH is thought to be a major ligand for many soft, B-type metals (e.g., Cu, Pb, Cd, Zn,

Hg and MeHg) in neutral or basic conditions (Krezel and Bal, 1999). Field studies suggested that high-affinity ligands like GSH may account for most of the Hg complexation in estuarine waters (Han et al., 2006). These biogenic organic compounds may have important influences on MeHg bioavailability and its cycling through complexation. A few studies have addressed how organic ligands affect Hg and MeHg bioavailability to bacterioplankton (Hsu-Kim et al., 2013; Ndu et al., 2016; Ndu et al., 2012), However, studies assessing how complexation of MeHg by naturally occurring organic compounds affect its bioavailability for marine phytoplankton are sparse.

Trophic transfer of MeHg to zooplankton and its geochemical significance

Many phytoplankton have been found enriched in metals, but most metals are not further biomagnified in the food chain. Their concentrations in the organisms of higher trophic levels often decrease, except MeHg. The MeHg accumulation in organisms is mainly from ingesting MeHg-containing food instead of direct uptake from ambient water. Thus, the food web structure could influence the efficiency of MeHg transfer to higher level organisms (Cabana and Rasmussen, 1994; Morel et al., 1998). Zooplankton play an important role in marine food webs and they are considered a critical intermediate between primary producers (phytoplankton) and predators (fish). Metals assimilated into zooplankton tissue could be transported to fish, leading to increased concentrations through food webs. Prior studies have pointed out that zooplankton can have significant effects on vertical flux and residence times of particle-reactive metals. The dense and large fecal pellets produced by zooplankton can transport material out of surface mixed layers, influencing the cycling, residence times and fluxes of elements in the ocean metals (Fisher and Reinfelder, 1995; Fisher et al., 1987; Fowler and Knauer, 1986). Although there have been comprehensive studies of the trophic transfer and cycling of many trace metals by

zooplankton (Fisher and Reinfelder, 1995), MeHg has not been similarly studied for marine

zooplankton, where few studies have examined the transfer of MeHg from phytoplankton to

zooplankton (Lawson and Mason, 1998; Mason et al., 1996; Mathews and Fisher, 2008).

Previous work suggested that the assimilation efficiency of metals is positively correlated with

their cytoplasmic distribution because zooplankton would assimilate only the fraction that

penetrates into the cytoplasm of the algal cells (Reinfelder and Fisher, 1991). Mason et al. (1996),

Lawson and Mason (1998), and Mathews and Fisher (2008) reported a high assimilation

efficiency of MeHg in marine zooplankton feeding on marine algae, and the fractions of MeHg

accumulated in cytoplasm were strongly correlated to the assimilation efficiency in zooplankton.

Aside from assimilation efficiencies of dietary uptake, MeHg uptake from the aqueous phase

(influx rates), and MeHg deputration (efflux rates) are needed to be determined to calculate

trophic transfer factors. Once these parameters have been accurately examined, a simple model

can be established to estimate the importance of dietary and aqueous sources of MeHg, and to

predict concentrations of MeHg in marine zooplankton.

Hg and MeHg transformation by natural coastal bacterial assemblages

Hg^0 evasion from the surface ocean is known to play a significant role in marine

biogeochemical cycling of Hg (Fitzgerald et al., 1984; Kim and Fitzgerald, 1986; Mason et al.,

1994; Mason and Sheu, 2002). The sea-air exchange of Hg^0 is rapid and strongly correlated with

Hg^0 concentrations (Hg^0 saturation status), as well as other physical forces such as wind and

wave action in surface waters. Therefore, the transformation of other Hg species to Hg^0 is

important because it can alter the residence time of dissolved Hg species in the water column. In

the mixed layer, Hg^0 can be produced by biological and/or photochemical reduction of reactive

Hg(II), leading to decreased Hg(II) concentrations in the water column and therefore avoiding

further methylation of Hg(II). Moreover, MeHg can also be converted to Hg^0 through biotic

and/or abiotic demethylation processes (Barkay et al., 2003; Fitzgerald et al., 2007). Both Hg(II)

and MeHg are toxic, and the latter is bioaccumulative in aquatic organisms and can build up in

aquatic food chains. Hence, Hg^0 formation has been suggested to be beneficial to aquatic

organisms because it can not only directly remove aqueous Hg(II) and MeHg from water, but

also potentially reduce MeHg production from Hg(II) in the water column (Mason et al., 1995).

Hg^0 formation in the surface mixed layer involves a variety of complex abiotic and/or biotic

processes. Abiotic processes, for example, photochemical reduction of Hg(II) has been shown to

produce Hg^0, where solar radiation, organic matter, and inorganic free radicals are considered

key factors involved in the photochemical formation of Hg^0 from Hg(II) (Amyot et al., 1997;

Costa and Liss, 1999; Costa and Liss, 2000; Nriagu, 1994; Vost et al., 2012). In addition,

photodegradation of MeHg has also been shown to produce Hg^0 (Sellers et al., 1996; Suda et al.,

1993). Biologically mediated processes such as microbial Hg(II) reduction and MeHg

degradation have also been shown to form Hg^0 (Barkay et al., 2003; Barkay et al., 1991;

Robinson and Tuovinen, 1984). These processes can be attributable to prokaryotes possessing

the Hg-resistant *mer* operon (Morel et al., 1998; Yu et al., 1996). Microorganisms with enzymes

of Hg-resistance are considered widespread in diverse environments (Barkay et al., 1989;

Gionfriddo et al., 2016; Osborn et al., 1997; Vetriani et al., 2005). Whether the transcription of

the *mer* operon can be induced at natural Hg concentrations (pM to fM) is not fully understood.

Poulain et al. (2007) reported that *merA* genes (mercuric reductase) were present and expressed

by microbes from remote polar waters. However, some studies suggested Hg^0 formation can

occur by other uncharacterized microbial processes (Barkay et al., 2003; Kuss et al., 2015;

Oremland et al., 1991). Hg(II) reduction can also be carried out by eukaryotic phytoplankton (Ben-Bassat and Mayer, 1977; Mason et al., 1995), but the mechanism of this pathway has remained undefined. Overall, microorganisms, especially bacteria, are considered to play a fundamental role in the aquatic biogeochemistry of Hg.

This thesis demonstrates how natural assemblages of marine bacterioplankton convert MeHg to Hg^0 which is released rapidly to the overlying air. In addition, the influences of light, temperature, and bacterial abundance and metabolic activity on Hg^0 production and evasion from seawater are also investigated. Studies quantifying the kinetics of Hg^0 evasion from seawater are few, and this thesis is the first to investigate the kinetics of Hg^0 formation from MeHg by marine microorganisms. I document the successful development of a device to determine the kinetics of Hg^0 formation from either dissolved Hg(II) or MeHg and used ^{203}Hg as a gamma-emitting radiotracer of Hg^0 gas evasion.

Total Hg accumulation in bluefin tuna and a declining trend in the past decade

MeHg is known to biomagnify in aquatic food webs. It is highly enriched in organisms at the base of the food chain, and is transferred efficiently to the next trophic level. Thus, mercury levels in marine ecosystems are determined in part by food web dynamics (Cabana and Rasmussen, 1994; Morel et al., 1998). The variation in MeHg concentrations in predatory fish may be a function of varying MeHg levels at the base of the food web (Morel et al., 1998), variation in food web length (Cabana and Rasmussen, 1994), or variation in diet composition (Choy et al., 2009; Colman et al., 2015). Therefore, a small difference in MeHg enrichment at the base of aquatic food webs could have significant consequences for the overall biomagnification of MeHg in marine food chains (e.g., total Hg in tuna or shark). Here, in this

thesis, total Hg concentrations in Atlantic bluefin tuna and its variability are presented to demonstrate the variability at the opposite end of the food chain from the plankton.

Fish in higher trophic levels usually have higher MeHg concentrations than fish at lower trophic levels. It is also the major form of Hg species in fish. For example, over 90% of Hg in tunas is in the methyl form (Storelli et al., 2002). In contrast, less than 10% of Hg in open ocean is in the form of MeHg (Fitzgerald et al., 2007; Lamborg et al., 2014a). Therefore, assimilation of MeHg through diet is the dominant pathway for uptake of mercury by fish rather than direct extraction from ambient seawater. For humans, the most common route of MeHg exposure is through seafood consumption. High doses of MeHg can result in severe neurological damage, especially for children who are developing their nervous systems. Recent data have suggested an increase (approximately 3 times) in the Hg inventory of global oceans since preindustrial times (Lamborg et al., 2014b) and this could double relative from 1995 to 2050 according to modeling results (Sunderland et al., 2009). Therefore, there is a potential risk of a corresponding increase of MeHg in ocean fish (Cossa, 2013), particularly apex predator fish. Kraepiel et al. (2003) showed no increase in Hg concentrations in yellowfin tuna caught off Hawaii in 1998 compared to measurements of the same species caught in the same area in 1971. However, a recent study conducted by Drevnick et al. (2015) re-analyzed and compiled former and recent data (yellowfin tuna caught in 1971, 1998 and 2008 off Hawaii), suggesting that Hg concentrations in these fish are increasing at a rate of at least 3.8% per year from 1998 to 2008.

Several studies have reported wide variations of Hg concentrations in tuna from different geographical locations. High variations are due to several factors such as tuna species, trophic levels in food chains, life stages, size, and habitat locations. For highly migratory fish like bluefin tuna which make trans-oceanic migrations (Block et al., 2001; Block et al., 2011; Block

et al., 2005), it is complicated to associate their body Hg concentrations with their habitats. As a matter of fact, the paucity of detailed information of tuna samples is a critical problem impeding us from further data interpretation. For example, some published results do not always distinguish among tuna species when reporting mercury levels. Exact captured locations of tunas are usually unclear because fishermen are usually reluctant to divulge fishing sites. Body length (an important parameter to estimate age) and weight are often unknown, or reported in different ways. For instance, curve fork length (CFL), straight length (SL) and operculum length (OL) all have been used in different studies. Moreover, the body length of an adult bluefin tuna can be up to 300 cm, but very few studies have covered the whole size spectrum. Atlantic bluefin tuna (ABFT, *Thunnus thynnus*) and Pacific bluefin tuna (PBFT, *Thunnus orientalis*) have the largest body size and home range of any tuna species. Both of them are important fishery products with great economic value, but studies focusing on their Hg body burden associated with their age, length, weight, and habitat are few, let alone to determine the temporal trend in Hg concentrations. Since tuna is one of the most widely consumed fish in markets in several countries, including the U.S., exposure of Hg from tuna consumption has become a health issue with public concern.

General methodology

The γ-emitting radioisotope ^{203}Hg (t½ = 46.6 d) is used to trace the transfer of Hg in marine biota in this thesis. Further, ^{203}Hg(II) was methylated to $CH_3{}^{203}Hg^+$ from inorganic ^{203}HgCl$_2$ following established methods (Luengen et al., 2012; Rouleau and Block, 1997). A series of experiments involving phytoplankton, zooplankton, and bacterioplankton were conducted by using Me^{203}Hg to track the partitioning of MeHg between water and phytoplankton, assimilation

and release of MeHg in zooplankton, and transformation of MeHg by bacterioplankton. All flasks and equipment associated with MeHg experiments went through a rigorous trace metal clean treatment in order to avoid any inadvertent contamination. The use of radioisotopes for studying a variety of biological and chemical processes between the aqueous phase and aquatic biota has been widely explored and described (Fisher and Reinfelder, 1995; Wang and Fisher, 1999). In addition to that, I have developed a rapid radioassay method to collect produced gaseous ^{203}Hg, which can avoid potential contaminations.

Radioactive methods using gamma-emitters have provided several advantages for determining metal partitioning within organisms. It is a nondestructive, noninvasive and direct measurement of radioactivity which can largely avoid artifacts produced during sample treatments (e.g., digestion and dilution). Moreover, it can generate large amounts of data in a relatively short period. In terms of disadvantages for radioactive methods, first, there can be difficulties in handling radioactive materials in fieldwork or at sea. Second, when using radioactive methods, ^{203}Hg and Me^{203}Hg cannot be added at the same time in the same culture because they are not distinguishable, but a stable isotope method has the potential to add Hg and MeHg simultaneously (e.g., Me^{199}Hg and ^{201}Hg). Also, any degradation or change in speciation of Me^{203}Hg during experiments will not be differentiated. Third, in order to obtain sufficient counts of radioactivity, the MeHg concentration added in each experiment is higher than typical coastal and open ocean waters. Nevertheless, previous studies have shown that bioconcentration factors and uptake rate constants for metals in algal cells are not affected if ambient concentrations of metals are relatively high but below toxic levels. This was confirmed for MeHg by measuring its toxicity tolerance of phytoplankton and running parallel experiments with radioactive and stable isotopes.

Overview

The major goal of this thesis is to better understand important processes of MeHg in marine food chains. I have examined how MeHg enters marine food webs through algal uptake, and what/how biological characteristics and environmental variables can govern its uptake (Chapter 2). Further, influences of dissolved organic matter (especially those sulfur-containing DOM) on MeHg uptake by a diatom has been determined (Chapter 3). Subsequent trophic transfer of MeHg from marine phytoplankton to marine zooplankton, along with assimilation efficiencies and efflux rates of MeHg, have been determined. With these parameters, a reliable model to predict MeHg concentrations in zooplankton has been successfully established (Chapter 4). By developing a rapid approach to collect gaseous Hg species, the conversion of MeHg to Hg^0 by marine bacterioplankton and its formation kinetic have been evaluated (Chapter 5). Finally, I have investigated the total Hg concentrations in ABFT and its relationship to fish age, length, weight, gender, and habitat, as well as the inter-annual trends of Hg in ABFT (Chapter 6). All the generated data in this thesis can apply to a global biogeochemical Hg model, linking laboratory and field data together and allowing us to better refine biogeochemical processes of Hg (including MeHg) in marine environments.
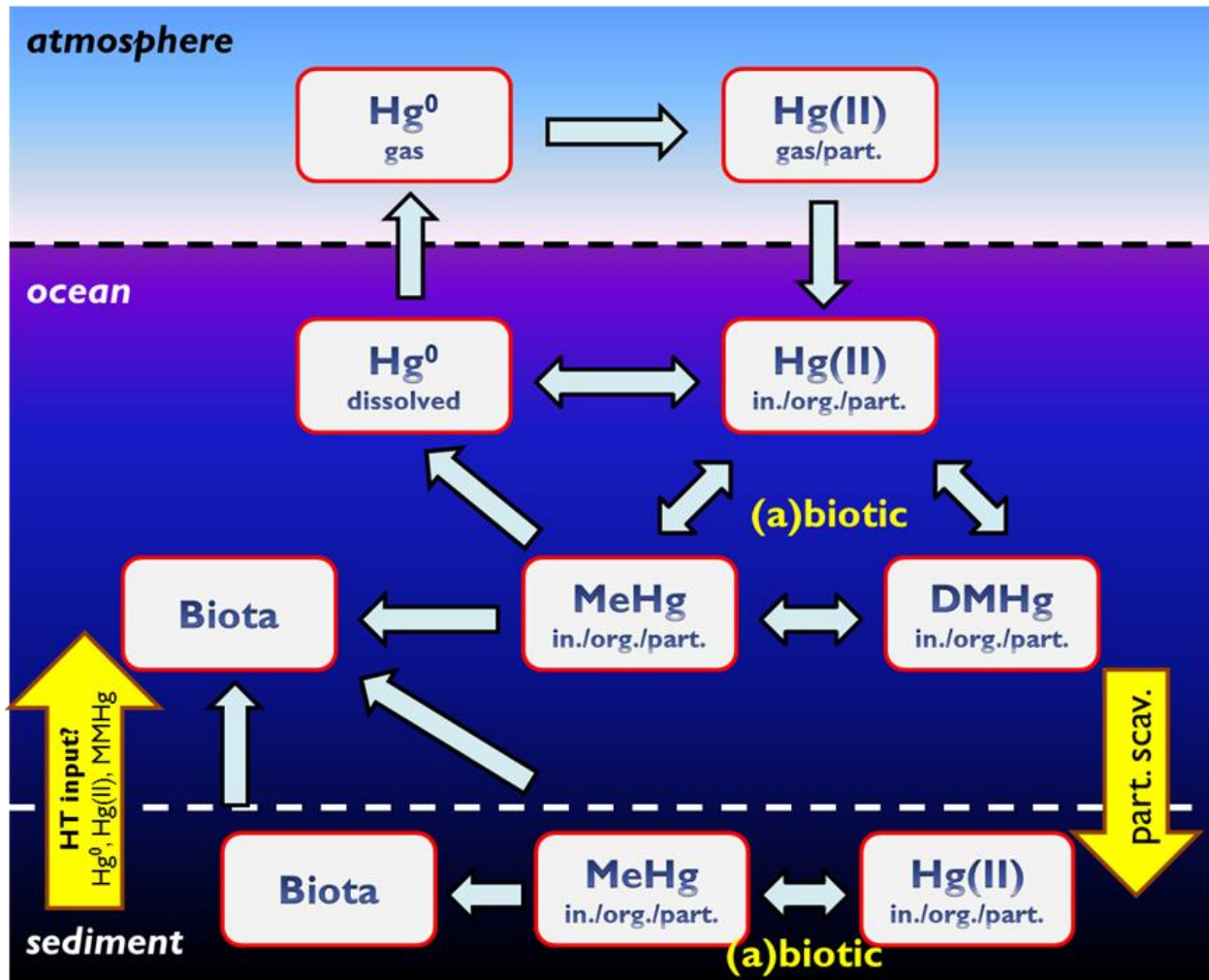
Figure 1. Biogeochemical cycling of Hg in the ocean. Modified from Fitzgerald et al. (2007) (in.: inorganic, org.: organic, part.: particulate).

Chapter 2

Methylmercury uptake by diverse marine phytoplankton

Abstract

Phytoplankton may serve as a key entry for methylmercury (MeHg) into aquatic food webs however very few studies have quantified the bioconcentration of MeHg in marine phytoplankton from seawater, particularly for non-diatoms. Experiments using ^{203}Hg to measure MeHg uptake rates and concentration factors in six marine phytoplankton species belonging to different algal classes were conducted and the influence of light, temperature, and nutrient conditions on MeHg bioaccumulation were determined. All algal species greatly concentrated MeHg out of seawater, with volume concentration factors (VCFs) ranging from 0.2×10^5 to 6.4×10^6. VCFs were directly related to cellular surface area-to-volume ratios. Most of the cellular MeHg was found in the cytoplasm. Temperature, light, and nutrient additions did not directly affect MeHg uptake in most species, with the exception that the dinoflagellate *Prorocentrum minimum* displayed significantly greater uptake per cell at 18°C than at 4°C, suggesting an active uptake for this species. Passive transport seemed to be the major pathway for most phytoplankton to acquire MeHg and was related to the surface area-to-volume ratio of algal cells. Environmental conditions that promoted cell growth resulted in more total MeHg associated with cells, but with lower concentrations per unit biomass due to biodilution. The very high bioconcentration of MeHg in marine phytoplankton is by far the largest bioconcentration step in marine food chains and variations in algal uptake may account for differences in the amount of MeHg that ultimately builds up in different marine ecosystems.

Introduction

Interest in the biogeochemical cycling of methylmercury (MeHg) in marine ecosystems stems in part from the fact that its neurotoxicity can cause adverse health effects to exposed wildlife

21

and humans (Grandjean et al., 2010; Mason et al., 2012; National Research Council, 2000).

Human exposure to MeHg is primarily from diet, especially seafood consumption (Sunderland, 2007). Although MeHg concentrations in seawater are extremely low, typically in the subpico- to femto- molar range (Bowman et al., 2015; Fitzgerald et al., 2007; Lamborg et al., 2014a), MeHg is the only mercury species to build up in aquatic food chains and display biomagnification, resulting in high MeHg levels in some common seafood items. However, our understanding of the factors controlling MeHg accumulation in marine food webs is surprisingly limited. Most research in marine environments has focused on Hg (total Hg or MeHg) levels in commercial fish consumed by humans due to public health concerns (Karimi et al., 2012; Morel et al., 1998; Selin, 2009). Very few studies have investigated Hg and MeHg interactions with primary producers at the base of marine food webs (Mason et al., 2012). Phytoplankton are the most critical entry where metals enter marine food webs (Fisher and Reinfelder, 1995). What little lab and field data exist on this issue show that MeHg is concentrated from ambient water into phytoplankton by at least a factor of 10^5 (Gosnell and Mason, 2015; Hammerschmidt et al., 2013; Pickhardt and Fisher, 2007; Watras et al., 1998), which is by far the largest bioconcentration step in aquatic food webs. Phytoplankton then serve as a highly enriched source of MeHg for herbivores which can pass this compound on to animals higher in the food chain. Subsequent enrichment with increasing trophic levels in aquatic food chains is much smaller, almost always less than a factor of 10.

To date, most studies involving algal uptake of MeHg have considered freshwater phytoplankton (Gorski et al., 2006; Luengen et al., 2012; Miles et al., 2001; Pickhardt and Fisher, 2007; Watras et al., 1998), and its trophic transfer in freshwater ecosystems (Pickhardt et al., 2002; Pickhardt et al., 2005). The few studies on marine environments are confined to a coastal

22

diatom and cyanobacterium (Kim et al., 2014; Lawson and Mason, 1998; Mason et al., 1996; Zhong and Wang, 2009). Published data on MeHg interactions with other marine phytoplankton species are sparse. Generally, bioconcentration factors of metals can vary substantially among different algal species, and for any given metal generally increase with surface area-to-volume ratios (SA/V) of cells (increasing inversely with cell size) (Fisher, 1986; Fisher and Reinfelder, 1995). Since the composition of phytoplankton assemblages often shifts seasonally, MeHg uptake by the prevailing algal assemblage might also vary, consequently affecting overall MeHg accumulation in organisms at higher trophic levels. In this study, we examined the uptake of MeHg by six marine phytoplankton species belonging to different algal classes to determine how biological attributes (e.g., size, surface area-to-volume ratio, cell wall composition, and metabolic rate) and environmental conditions (light, temperature, salinity, and nutrient levels) affect MeHg bioaccumulation in diverse marine algae. This information, combined with field data, could ultimately be used by global biogeochemical models describing Hg cycling in the marine environment.

Materials and Methods

Phytoplankton cultures

Six phytoplankton species *Thalassiosira pseudonana* (diatom), *Dunaliella tertiolecta* (chlorophyte), *Rhodomonas salina* (cryptophyte), *Prorocentrum minimum* (dinoflagellate), *Emiliania huxleyi* (coccolithophore), and *Synechococcus bacillaris* (cyanobacterium), belonging to different algal classes, were used in this study (Table 2-1). All species were held in clonal, unialgal cultures maintained axenically for generations in an incubator at 18°C under a light:dark cycle (14 h:10 h, 200 μmol quanta m^{-2} s^{-1}) provided by cool white fluorescent lamps. The f/2

medium (Guillard and Ryther, 1962) was prepared with sterile filtered (0.2 μm, Nuclepore polycarbonate membrane) surface seawater (35 psu, DOC = ~2 mg L^{-1}) collected 8 km off Southampton, New York (Lat. 40.778N, Long. 72.438W), and was used for maintaining routine cultures. However, to avoid the potential effects on MeHg speciation due to the presence of ethylenediaminetetraacetic acid (EDTA), inocula for experimental algal cultures were grown in separate flasks with amended f medium (nutrients at f/20 level and without EDTA) for 7 to 10 d prior to experiments.

Methylmercury synthesis

The gamma-emitting radioisotope, ^{203}Hg ($t_{1/2}$ = 46.6 d) was used to trace the transfer of Hg between dissolved and particulate phases in all cultures. Commercially available ^{203}Hg(II) was converted to monomethylmercury (CH$_3$^{203}Hg$^+$ or Me^{203}Hg) from inorganic ^{203}HgCl$_2$ following established methods (Luengen et al., 2012; Rouleau and Block, 1997). Briefly, inorganic ^{203}Hg solution purchased from Eckert and Ziegler Isotope Products (Valencia, California) (specific activity: 5 Ci g^{-1}) was mixed with methylcobalamin (C$_{63}$H$_{91}$CoN$_{13}$O$_{14}$P) and acetate buffer at pH 5, allowing the reaction to proceed in the dark for 18 h to 24 h and then forming Me^{203}Hg. Following extraction by dichloromethane (CH$_2$Cl$_2$) and purification procedures, Me^{203}Hg was then re-dissolved in Milli-Q$^{®}$ water and was ready to use. The conversion yield (fraction of total ^{203}Hg recovered as Me^{203}Hg) was $95 \pm 3\%$ (n = 6). A series of experiments was conducted using Me^{203}Hg to track the partitioning of MeHg between water and phytoplankton. Me^{203}Hg activities in experiments ranged from 4.46 kBq L^{-1} to 9.29 kBq L^{-1}, corresponding to concentrations of 0.29 nM to 0.42 nM. These MeHg concentrations were at the high end of those found in natural waters, however previous studies have shown that bioconcentration factors and uptake rate

constants for metals (including Hg) in algal cells are not affected by modestly elevated metal

concentrations that are below toxic levels (Fisher et al., 1984). As noted in numerous previous

gamma-emitting radiotracer studies, this approach provides a nondestructive, noninvasive and

direct measurement of metal bioaccumulation while using low metal concentrations that are in

the range of naturally occurring levels (Fisher, 2002).

General approach

The MeHg uptake experiments generally followed protocols described for metal uptake by

marine phytoplankton (Fisher et al., 1984; Stewart and Fisher, 2003b). The seawater used in all

experiments except those involving nitrate or chloride additions was 0.2 μm filtered surface

seawater (35 psu, collected 8 km off Southampton, New York), without addition of any nutrients.

Trace metal clean glass-stoppered Erlenmeyer flasks, each containing 150 mL of seawater and

microliter quantities of Me^{203}Hg solution (added 1 h prior to inoculation with phytoplankton

cells to reach equilibrium) were incubated at 18°C under the light:dark cycle. Inocula of algal

cells were concentrated by resuspending cells off 1 μm membranes or by centrifugation at 1000

g for 10 min from late log-phase cultures (without EDTA). Considering the difference in algal

biomasses, initial cell densities ranged from 6×10^3 to 6×10^4 cells mL^{-1}, depending on algal

species. Water and cell samples were periodically collected into glass tubes and onto 1 μm

polycarbonate membranes, respectively for radioassay. This approach (Fisher et al., 1983a)

measures the total radioactivity in 1 mL of suspension (water plus cells) and, in a separate

sample taken at the same time, the radioactivity in 10-mL of suspension caught on a 1 μm

polycarbonate membrane (vacuum pressure <100 mmHg) that was then washed with 2×5 mL of

unlabeled, filtered seawater. With this approach, the fraction of total radioactivity in suspension

associated with cells and the fraction in the dissolved phase could be determined. We performed

both short term (t = 1, 2, 3, 4, 8 h) and long term (t = 2, 6, 12, 24, 48, 72 h) experiments to

evaluate the uptake rate constants and bioconcentration factors of MeHg for each species. For

each culture, cell density and volume were monitored simultaneously over time using a

Multisizer[TM] Coulter Counter® and cell surface area was calculated using appropriate geometric

equations (Table 2-1).

All experiments included control flasks without algal cells which were used to correct for the

potential adsorption of Me^{203}Hg onto filter membranes. In addition, sorption of MeHg onto

culture flasks was examined by acid washing the flask walls after cell exposures. Sample

activities were determined using an LKB Wallac 1282 Compugamma NaI(Tl) gamma detector.

^{203}Hg activity was assessed at 279 keV. All samples were counted with standards and decay-

corrected. Propagated counting errors were <5%.

Effects of temperature, light, nutrient, and salinity

To examine the effect of low temperature (4°C) on MeHg uptake by phytoplankton, algal cells

cultured in medium without EDTA were acclimated at 4°C for 6 h prior to experimental

inoculation, after which the experimental procedures described above were followed. To assess

MeHg uptake by phytoplankton without light, experimental cultures were held in the dark (18°C).

In an experiment evaluating the effects of nitrate on MeHg uptake, different levels of nitrate

additions (0, 5, 10, 50 µM) to artificial seawater (prepared by adding salts to Milli-Q® water; 35

psu; DOC = ~1 mg L^{-1}) (Kester et al., 1967) were used as the experimental media; phosphate and

silicate concentrations were fixed at 1 µM and 10 µM, respectively. The nutrient concentrations

were representative of nutrient levels reported for Long Island Sound, New York (Gobler et al.,

2006). Four algal species, including the diatom, the chlorophyte, the dinoflagellate, and the coccolithophore were tested in the nutrient experiment. In a parallel experiment assessing the influence of the culture medium's ionic strength on MeHg uptake, the euryhaline diatom, *T. pseudonana*, was exposed to MeHg under four different salinities, reflected by chloride concentrations of 5.90, 27.9, 55.4, and 550 mM, prepared by mixing WCL-1 medium (Guillard, 1975) and artificial seawater. The highest chloride concentration corresponds with 35 psu seawater. The diatoms were cultured in these media for more than two generations to make sure they were fully acclimated to low salinity environments.

Cellular distribution of MeHg

The cytoplasmic distribution of MeHg in phytoplankton cells was examined in all six species after exposure to Me^{203}Hg for 3 d (two to three cell divisions) to uniformly radiolabel the cells (Fisher et al., 1983b; Reinfelder and Fisher, 1991; Stewart and Fisher, 2003b).

Results

Algal MeHg uptake

Algal growth at 18°C under a 14:10 light:dark cycle varied among species, with population doublings during the 72 h exposure period ranging from one for the dinoflagellate *P. minimum* to four for the diatom *T. pseudonana* (Fig. 2-1). All algal species accumulated MeHg (Fig. 2-1), however two patterns emerged. For those cultures (cryptophyte *R. salina*, chlorophyte *D. tertiolecta*, coccolithophore *E. huxleyi*) where <40% of the total MeHg was associated with the cells over the 72 h period, uptake generally followed increases in algal biomass, whereas when >60% of the MeHg was associated with cells (diatom *T. pseudonana*, dinoflagellate *P. minimum*,

27

cyanobacterium *S. bacillaris*), uptake slowed over time even as growth continued (Fig. 2-1), probably because there was little bioavailable MeHg remaining in the dissolved phase to support further uptake. For all species, most of the MeHg was found in the cytoplasmic fraction of the cells (Table 2-2). Among the algal species, no general patterns were observed for MeHg penetration into the cytoplasm among the various culture treatments.

MeHg mass balance

In each flask, sorption of $Me^{203}Hg$ to the glass walls accounted for <5% of the total $Me^{203}Hg$, and at least 90% of the total $Me^{203}Hg$ could be accounted for by summing dissolved, particulate, and flask wall activities of the added $Me^{203}Hg$ (Fig. 2-2). The exception was for the coccolithophore (*E. huxleyi*) cultures, where a substantial loss of $Me^{203}Hg$ (~30%) was consistently observed, implying strong volatilization from the cultures. The cryptophyte *R. salina* and the cyanobacterium *S. bacillaris* cells were prone to attach to flask walls and may not have been completely removed by acid rinsing of the walls. This may explain that ^{203}Hg recoveries for these cultures were such that mass balances were not able to achieve ~100%.

Concentration factors

Volume concentration factors (VCFs) were calculated ($[Bq\ Me^{203}Hg\ \mu m^{-3}]_{cell}/[Bq\ Me^{203}Hg\ \mu m^{-3}]_{solution}$), showing the relative degree of enrichment in the algal cells relative to the ambient water. Figure 2-3 shows VCFs of six species over time under different environmental conditions. At 18°C, VCFs ranged from 0.2×10^5 for the chlorophyte *D. tertiolecta* to 6.4×10^6 for the cyanobacterium *S. bacillaris*. Within the first 12 h, there were no differences in MeHg VCFs among environmental conditions for all species but the dinoflagellate. After 12 h of exposure,

VCFs in the dark and low temperature treatments leveled off. However, VCFs at 18°C and light/dark conditions decreased slightly and then leveled off. This decreasing trend was particularly obvious in the cultures of the diatom *T. pseudonana* and the cyanobacterium *S. bacillaris* for which growth was most pronounced. To compare MeHg sorption to abiotic and living particles, the MeHg accumulation by suspended glass beads (diameter ~5 μm), added at a density of 10^5 beads mL^{-1}, was determined. Only about 1% of the MeHg adsorbed onto the surface of the glass beads, resulting in a VCF of about 10^3 (data not shown).

Uptake rate constant

In the short-term exposure experiments, it was clear that light had no significant effect on MeHg uptake rates for any species (Fig. 2-4) but temperature did have a pronounced effect on MeHg uptake rates in the dinoflagellate *P. minimum* and to a lesser extent in the cyanobacterium *S. bacillaris*. The short-term uptake rate constant, which was normalized to the initial dissolved MeHg concentrations in the media, was calculated on per cell, per $μm^2$ cell surface, and per $μm^3$ cell volume bases for the first 4 h of exposure during which time MeHg uptake was linear (Fig. 2-5; Table 2-3). At 18°C, the uptake rate constants on cell surface area or cell volume bases were comparable for the diatom, the cyanobacterium, and the dinoflagellate, all of which were significantly higher than the other species, sometimes by more than an order of magnitude.

Effects of nutrient and salinity

Experiments to assess the effects of nitrate level on MeHg uptake showed no significant effect in four algal species. MeHg was accumulated over time but no differences were found between high and low nutrient treatments (Fig. 2-6). However, higher nutrient levels led to significant cell

growth after 48 h to 72 h (Fig. 2-7 a-d). Such increases in algal biomass would result in a "dilution" of MeHg in algal cells, and lower VCFs in high nutrient treatments were indeed observed at the end of the experiment (Fig. 2-7 e-h). For the ionic strength (salinity) experiment involving the diatom *T. pseudonana*, VCF values increased with chloride concentrations (Fig. 2-8a). Uptake of MeHg was essentially linear over the first 4 h exposure, and at this time the MeHg VCFs in the diatoms was linearly related to the log chloride concentration (Fig. 2-8b).

Discussion

This is the first report describing MeHg uptake by diverse marine phytoplankton cells, and how environmental conditions affect the uptake process. While all species greatly concentrated MeHg out of ambient seawater, significant differences among the species can be explained. VCFs among the different algal species significantly increased with cell surface area-to-volume ratios (Fig. 2-9) except for the dinoflagellate which may have a different uptake pathway. In general, the greater MeHg enrichment in phytoplankton for smaller cells with greater surface area-to-volume ratios is consistent with findings for many other metals and algal taxa (Fisher and Reinfelder, 1995).

These findings are also consistent with the conclusion that passive sorption of dissolved MeHg to cell surfaces dominates the uptake pathway. Most other metals that speciate as cations in seawater behave similarly (Fisher, 1986; Fisher and Reinfelder, 1995). The comparable uptake rate constants of MeHg by most species at 4°C, when cell growth and metabolic activity were minimal, and at 18°C when growth rates and metabolic activity were high, is also consistent with the passive uptake of MeHg. Like temperature's effects, the only effect of light on MeHg uptake by phytoplankton was an indirect one. Thus, uptake rate constants for short exposure periods

30

were unaffected by light, but after several days, illuminated cells were able to grow more than

cells held in constant darkness, leading to greater biomass and hence more total particulate

MeHg. VCFs eventually declined in illuminated cultures held at 18°C because biodilution of

cell-bound MeHg occurred when cell biomasses increased to such an extent that most of the

bioavailable MeHg in the dissolved phase was exhausted. This biodilution has been

observed for MeHg in cultures (Karimi et al., 2007) and natural assemblages (Pickhardt et al.,

2002) of freshwater algae. It would not be expected to occur in most marine waters because

plankton biomass densities are typically low enough to preclude exhausting ambient MeHg.

Further, because it is retained by aquatic organisms much more effectively than most other

metals (including inorganic mercury), MeHg is more prone to biodilution than other metals

(Karimi et al., 2010).

The pronounced loss of ^{203}Hg from the coccolithophore cultures, but not from uninoculated

medium or other algal cultures, indicates that once the Me^{203}Hg was taken up by the

coccolithophore (*E. huxleyi*), it was converted to a gaseous form of Hg, either Hg^0 or

dimethylmercury (DMHg). Henry's law constants of either of these products would suggest that

they would display evasive properties. The production of mercury gas in the coccolithophore

cultures was probably attributable to bacterial cells that were observed to be growing in cultures

of this clone. Bacteria containing the Hg resistance (*mer*) operon might explain the

demethylation and reduction of MeHg (Barkay et al., 2003) in the coccolithophore culture. We

are unaware of reports demonstrating conversion of MeHg into an evasive form of mercury,

although marine microorganisms smaller than 3 µm have been shown to reduce dissolved Hg(II)

to elemental Hg^0, an evasive form of mercury (Mason et al., 1995).

As expected, the MeHg VCFs were positively related to the surface area-to-volume ratios of

the various algal cells (inversely related to cell size) (Fig. 2-9). Expressed on a surface to volume ratio, the MeHg concentration factors were comparable to that found for the freshwater diatom *Cyclotella meneghiniana* (SA/V = 0.94 μm^{-1}) exposed under similar conditions (Luengen et al., 2012; Pickhardt and Fisher, 2007). This is broadly consistent with patterns shown for many other particle-reactive metals that sorb onto cell surfaces (Fisher and Reinfelder, 1995) and is also consistent with the idea that MeHg binds passively to them. This finding would suggest that the degree of enrichment of MeHg in algal cells in natural communities could depend on the size of the predominant cells in plankton assemblages, which in turn may vary seasonally and regionally.

The unique MeHg uptake pattern in the dinoflagellate *P. minimum* showed a significantly higher MeHg uptake rate at 18°C than at 4°C. This suggests another pathway of MeHg acquisition in this species rather than solely passive transport. As this dinoflagellate can be mixtrophic, it may be possible that MeHg bound to organic matter or other nanoparticles was acquired via an energy-requiring process such as phagocytosis. Tranvik et al. (1993) suggested that metals bound to colloidal matter might be an important source of metals to heterotrophic flagellates. Wang and Guo (2000) found that marine colloidal materials added to cultures of a diatom and dinoflagellate affected uptake of some metals. However, there was no related study for either Hg or MeHg.

Nitrogen addition to the algal cultures increased the algal biomass in cultures after 2 d, and this led to more total particulate MeHg and eventually lower VCFs. However, the MeHg uptake rate constants over the first 4 h of exposure (during which growth differences between treatments were minimal) were unaffected by nitrogen additions. In contrast, Wang and Dei (2001a, 2001b) demonstrated significant increases in short-term Cd and Zn uptake by phytoplankton enriched with nitrogen. As with light and temperature, the principal effect of nutrient additions on MeHg

uptake was an indirect one, where the greater biomass eventually resulting from higher nitrogen levels led to more total particulate MeHg in algal cells, but with each cell being less enriched in MeHg. Consequently, in eutrophic waters where algal biomasses are high, MeHg concentrations in cells may be expected to be lower, consistent with observations in lakes (Pickhardt et al., 2002) and the NW Atlantic Ocean (Hammerschmidt et al., 2013). This could be expected to result in lower MeHg concentrations in animals in eutrophic ecosystems.

The penetration of MeHg into the cytoplasm of the cells is consistent with findings for MeHg in marine and freshwater diatoms (Mason et al., 1996; Pickhardt and Fisher, 2007). This has implications for the likelihood of trophic transfer of MeHg to herbivorous zooplankton, as shown for MeHg with a marine diatom (Mason et al., 1996) and for other metals for crustacean zooplankton and molluscan larvae (Reinfelder and Fisher, 1991; Reinfelder and Fisher, 1994; Stewart and Fisher, 2003b). To our knowledge, the distribution of MeHg in other algal cell types has not been reported. Because the VCFs and uptake rate constants of MeHg were not affected by light and temperature in most algal species (Figs. 2-3, 2-4), it appears that metabolic activities did not lead to active MeHg uptake, consistent with earlier conclusions (Mason et al., 1996).

The relationship of MeHg uptake by the diatom *T. pseudonana* over a range of chloride concentrations coincides with observations of previous studies reported for the diatoms *Thalassiosira weissflogii* (Mason et al., 1996) and *Ditylum brightwellii* (Kim et al., 2014). The increased lipophilicity of chloro-complexed MeHg should increase the passive transport of MeHg with increasing Cl concentration and may therefore lead to greater MeHg enrichment in marine food chains than in freshwater food chains.

Overall, the range of VCFs of MeHg in the six algal species (log VCF = 4.3–6.8) was comparable to findings for previous lab studies involving freshwater or marine phytoplankton

(Table 2-4). Pickhardt and Fisher (2007) reported log VCF ranged from 5.1 to 6.2 and Miles et al.

(2001) reported log VCF ranged from 5.4 to 6.9 for freshwater algae. For marine algae, Kim et al.

(2014) reported log VCF values ranging from 4.9 to 6.2. Our data also agree with

bioaccumulation factors of MeHg obtained from field studies (Table 2-4), suggesting that the

experimental conditions used in this study are generally applicable to natural waters. Thus, even

though the experimental MeHg concentrations exceeded typical MeHg concentrations in marine

ecosystems, the degree of bioconcentration in phytoplankton is comparable. The field

measurements cited in Table 2-4 were originally expressed on a dry weight basis, and these were

converted to a volume basis by using a mean ratio of cell volume:dry weight of 5.0 (Fisher et al.,

1983a). The field measurements were reported for microseston in the Northeast Atlantic (log

VCF = 4.9) (Hammerschmidt et al., 2013), the subtropical North Pacific (log VCF = 5.9)

(Hammerschmidt and Bowman, 2012), and in the central Pacific (log VCF = 6.3) (Gosnell and

Mason, 2015). Relatively low VCFs were found in the North Sea (log VCF = 4.2) (Baeyens et al.,

2003), and in Long Island Sound (log VCF = 4.2) (Hammerschmidt and Fitzgerald, 2006a).

Given the variability of VCFs noted among algal cultures in this study, the concentration factors

of MeHg in natural phytoplankton assemblages in the field may be expected to vary seasonally

and spatially with the phytoplankton composition and predominant cell size. This variation in

MeHg VCFs among phytoplankton may be one order of magnitude or more (Fig. 2-9), and these

differences in MeHg bioaccumulation at the base of the food web may be reflected in variations

in higher trophic level animals, such as in fish. Moreover, the fraction of lithogenic materials

might also influence the overall concentration factor, particularly in coastal regions, since MeHg

has relatively low affinity for abiotic particles, as shown with the glass beads. VCFs in

phytoplankton were about 100-fold higher than in glass beads, suggesting that MeHg binds

principally to biochemical compounds (especially S and N-rich compounds such as proteins) (Onyido et al., 2004; Vallee and Ulmer, 1972) associated with living cells. These findings indicate that MeHg will be more enriched in living than in abiotic particles, and consequently inversely related to the abundance of lithogenic particles (Bloom et al., 1999; Hammerschmidt and Fitzgerald, 2006b; Hammerschmidt et al., 2004). Thus, the relatively low VCFs seen in coastal regions such as the North Sea and Belgian coastal waters were probably due to the higher fraction of lithogenic materials collected in suspended particulate material. In contrast, high VCFs were observed in open ocean regions such as the central Pacific where biogenic particles are dominant.

The VCFs of MeHg reported here are higher than for most other metals, even particle-reactive metals such as Zn, Cd, Ag, Pb, Po, and inorganic Hg (Fisher et al., 1984; Fisher et al., 1987; Stewart and Fisher, 2003b), and about the same as the transuranic elements Pu and Am (Fisher et al., 1983a). Importantly, MeHg penetrates into the cytoplasm of algal cells to a much greater than the other metals (particularly true for Pb, Pu, Am, and inorganic Hg), which largely remain sorbed on the surface of cells. Consequently, the MeHg is assimilated by herbivores that feed on these phytoplankton (and subsequently passed up food chains) to a much greater extent than occurs with other metals (Reinfelder and Fisher, 1991).

Table 2-1. Phytoplankton species used in this study.

Phytoplankton type	Species	Clone	Volume μm^3	Surface area μm^2	SA/V ratio[*] μm^{-1}
Diatom	*Thalassiosira pseudonana*	CCMP1335	43-62	63-89	1.44
Chlorophyte	*Dunaliella tertiolecta*	CCMP1320	141-227	127-204	0.90
Cryptophyte	*Rhodomonas salina*	CCMP1319	160-231	133-192	0.83
Dinoflagellate	*Prorocentrum minimum*	CCMP696	540-778	313-451	0.58
Coccolithophore	*Emiliania huxleyi*	CCMP375	40-75	51-97	1.28
Cyanobacterium	*Synechococcus bacillaris*	CCMP1333	1.1-1.6	4.4-6.6	4.13

[*]Surface area-to-volume ratio

Table 2-2. Percentage of total cellular MeHg in the cytoplasmic fraction under three environmental conditions.

Algal species	Conditions		
	18°C, L/D[*]	18°C, Dark	4°C, L/D
T. pseudonana	62	53	61
D. tertiolecta	75	73	53
R. salina	77	74	79
P. minimum	27	39	57
E. huxleyi	78	88	82
S. bacillaris	38	91	73

[*]L/D: 14:10 ligh-dark cycle

Table 2-3. MeHg uptake rate constants for each algal species.
Normalized to the initial dissolved MeHg concentrations in the media on per cell, per μm^2 cell surface area, and per μm^3 cell volume bases for the first 4 h of exposure.

Uptake rate constant	Conditions	Algal species					
		T. pseudonana	*D. tertiolecta*	*R. salina*	*P. minimum*	*E. huxleyi*	*S. bacillaris*
Cell basis[1]	18°C, L/D	15 ± 3	0.63 ± 0.03	1.4 ± 0.1	80 ± 6	2.2 ± 0.1	0.97 ± 0.03
	18°C, Dark	15 ± 0.1			59 ± 0.2		0.89 ± 0.03
	4°C, L/D	13 ± 1	0.56 ± 0.02	1.2 ± 0.1	6.1 ± 0.1	1.3 ± 0.1	0.64 ± 0.06
Surface area basis[2]	18°C, L/D	0.21 ± 0.04	0.0042 ± 0.0002	0.0071 ± 0.0007	0.28 ± 0.02	0.029 ± 0.001	0.15 ± 0.01
	18°C, Dark	0.21 ± 0.00			0.21 ± 0.00		0.14 ± 0.00
	4°C, L/D	0.18 ± 0.01	0.0041 ± 0.0000	0.0067 ± 0.0005	0.02 ± 0.00	0.026 ± 0.002	0.12 ± 0.01
Volume basis[3]	18°C, L/D	0.26 ± 0.05	0.0036 ± 0.0002	0.0053 ± 0.0007	0.18 ± 0.01	0.035 ± 0.002	0.62 ± 0.03
	18°C, Dark	0.27 ± 0.00			0.13 ± 0.01		0.59 ± 0.01
	4°C, L/D	0.23 ± 0.01	0.0037 ± 0.0000	0.0054 ± 0.0004	0.01 ± 0.00	0.032 ± 0.002	0.55 ± 0.01

unit:

1. amole MeHg $cell^{-1}$ h^{-1} nM^{-1} exposure

2. amole MeHg μm^{-2} h^{-1} nM^{-1} exposure

3. amole MeHg μm^{-3} h^{-1} nM^{-1} exposure

Table 2-4. MeHg VCFs from (a) culture experiments and (b) field studies.

(a) Lab study

Particle type	Diameter range[1] μm	log VCF	References
Marine algae	1.0 - 12 (6)	4.3 - 6.8	This study
	5.0 - 32 (5)	4.9 - 6.2	Kim et al. 2014
Freshwater algae	8.0 (1)	4.2 - 5.4	Luengen et al. 2012
	2.0 - 8.2 (4)	5.1 - 6.2	Pickhardt and Fisher 2007
	4.0 - 120 (4)	5.4 - 6.9	Miles et al. 2001
Glass beads	5.0	3.1	This study

(b) Field data

Sampling site	Size range μm	log VCF[2]	References
North Sea		4.2	Baeyens et al. 2003
Belgian coast		4.2	Baeyens et al. 2003
Long Island Sound	>0.2	4.5	Hammerschmidt and Fitzgerald 2006a
Northeast Atlantic	0.2 - 200	4.9	Hammerschmidt et al. 2013
North Pacific	1.0 - 51	5.9	Hammerschmidt and Bowman 2012
Central Pacific	0.2 - 200	6.3	Gosnell and Mason 2015

1. Mean diameter of algal cells. The numbers in parentheses indicate the number of algal species tested in the study.

2. Literature values were originally on a dry wt basis; they were converted to VCFs by using a mean cell volume:dry wt ratio of 5.0, based on measured values from 6 marine phytoplankton cells (Fisher et al. 1983a).
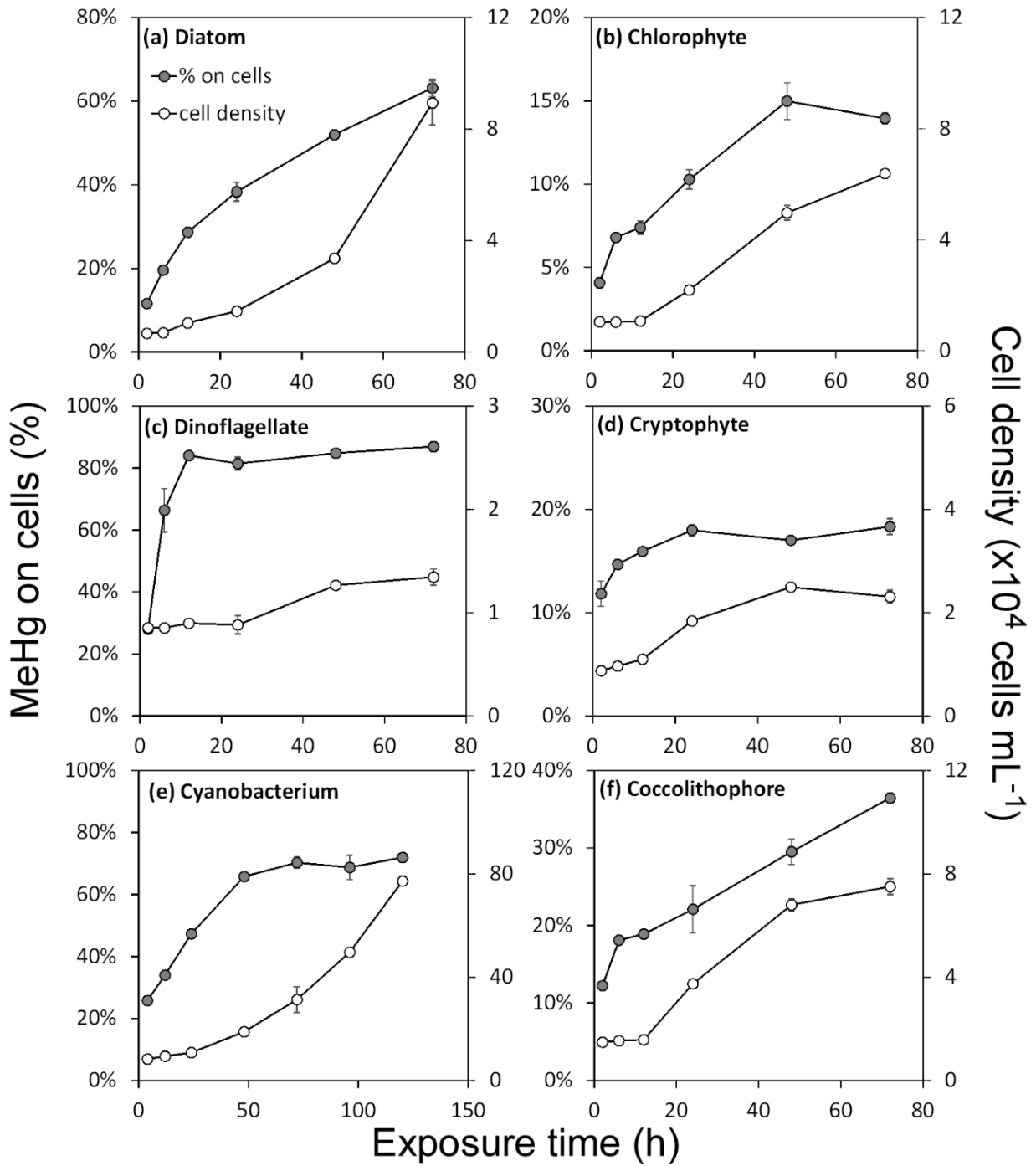
Figure 2-1. MeHg uptake and growth of algal cells among six phytoplankton species over time. The solid circles (left axis) represent the percentage (%) of total MeHg in the cultures associated with the particulate (>1 μm) phase. The open circles (right axis) represent the cell densities. Data points are the means from three replicates cultures with error bars of one standard deviation. Note the different scales on each graph.
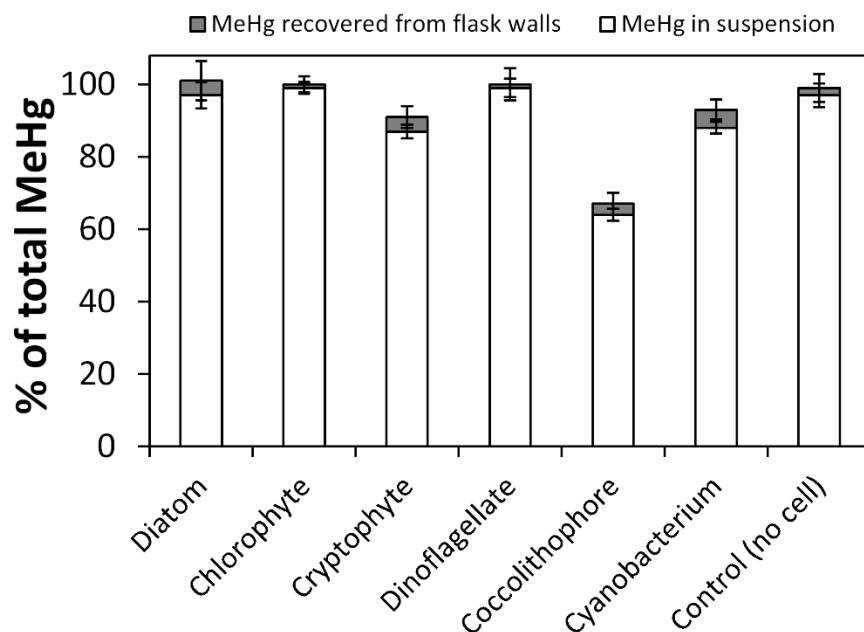
Figure 2-2. MeHg mass balance in cultures at 18°C under 14:10 light:dark cycle. The white bar represents the percentage of total MeHg remaining in suspension (dissolved plus particulate fractions after 72 h exposure). The gray bar represents the MeHg recovered from the flask wall by acid rinsing at 72 h. Recovery of less than 100% of total Me^{203}Hg from each culture is presumed attributable to evasion into the air.
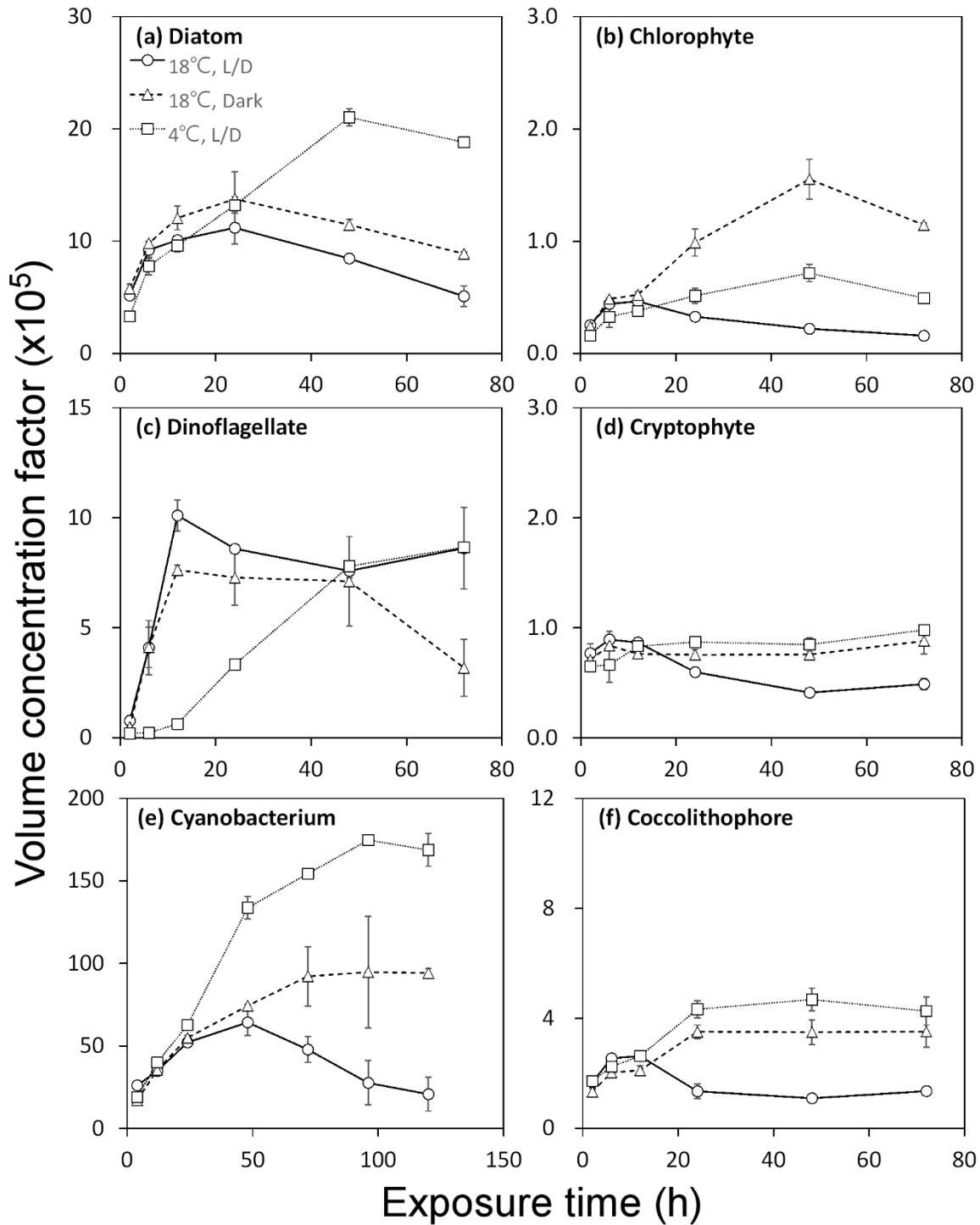
Figure 2-3. MeHg volume concentration factors over time under different environmental conditions. L/D represents 14:10 light:dark cycle. Data points are the means from two replicate cultures shown with 1 SD error bars. Note the different scales on each graph.
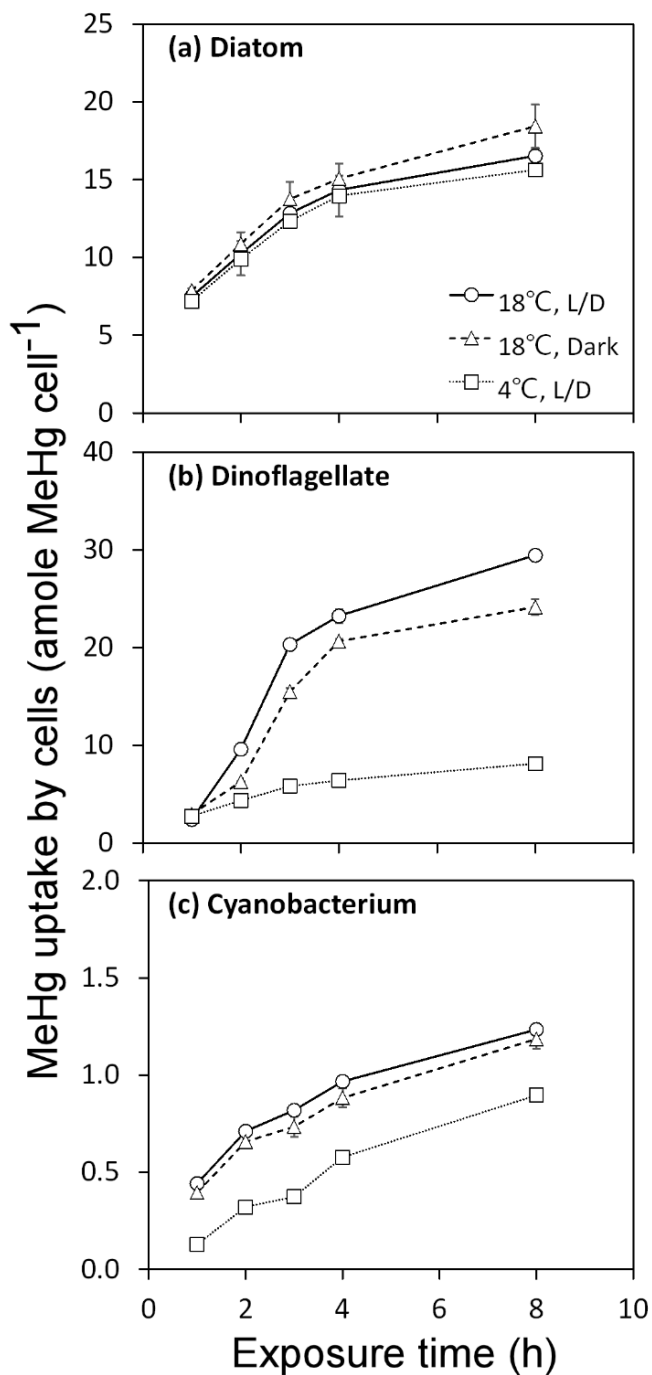
Figure 2-4. Uptake of MeHg in cells over short-term exposures for *T. pseudonana* (diatom), *P. minimum* (dinoflagellate), and *S. bacillaris* (cyanobacterium) under different environmental conditions. L/D represents 14:10 light:dark cycle. Data points are the means from two replicate cultures shown with 1 SD error bars.
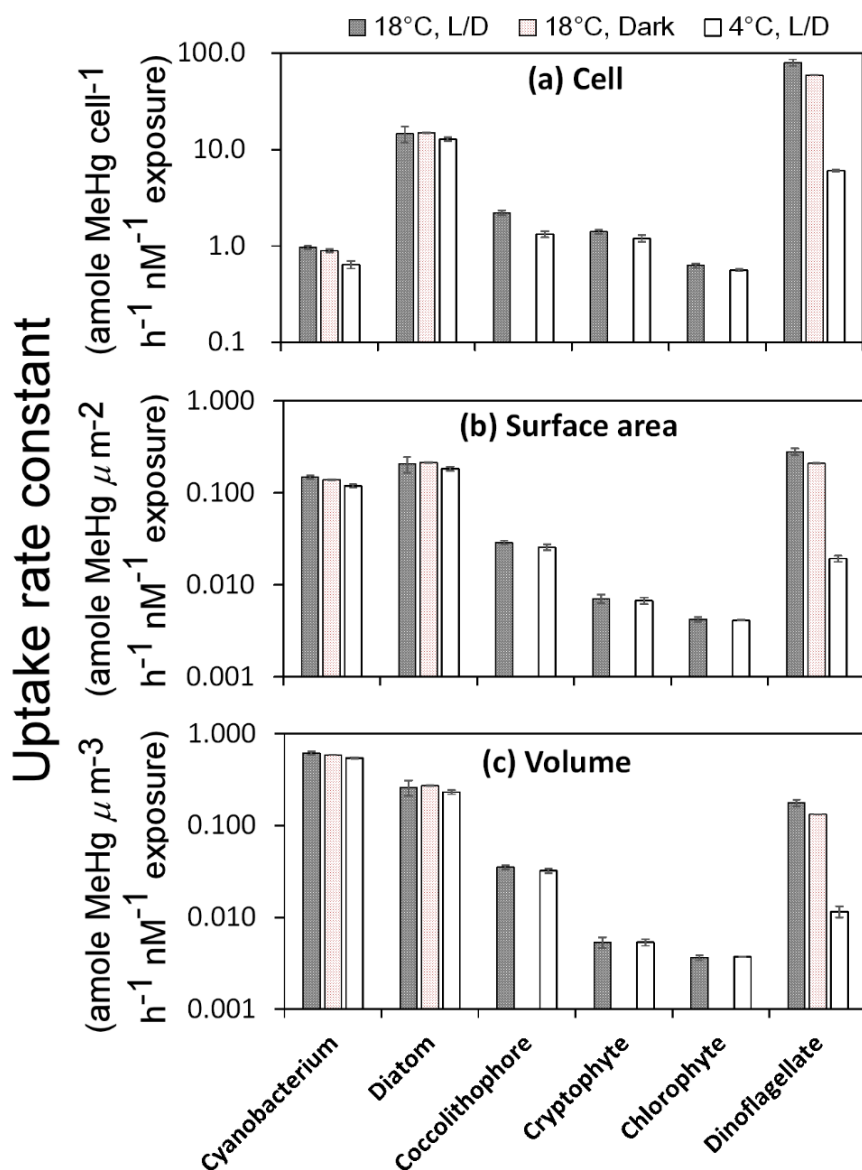
Figure 2-5. Uptake rate constants of MeHg in six different algal species over short-term exposures. Values are normalized to the initial dissolved MeHg concentrations in the media and are expressed on per cell, per μm^2 cell surface area, and per μm^3 cell volume bases for the first 4 h of exposure. Algal species on the *x*-axis are arranged in increasing size order, with the cyanobacterium being the smallest cell and the dinoflagellate the largest cell.
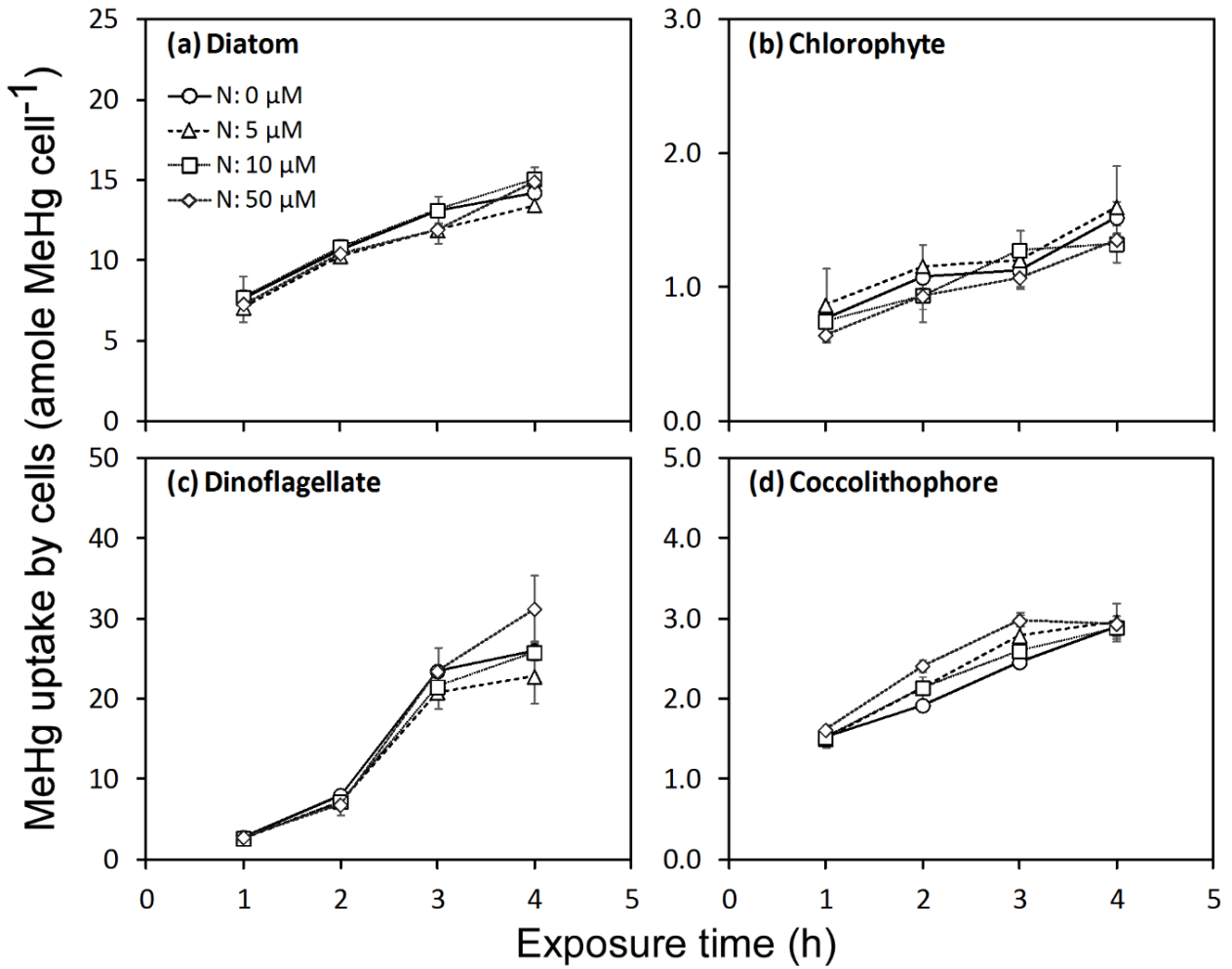
Figure 2-6. Uptake of MeHg by cells exposed under four nitrate treatments. Data points are the means from two replicate cultures shown with 1 SD error bars.
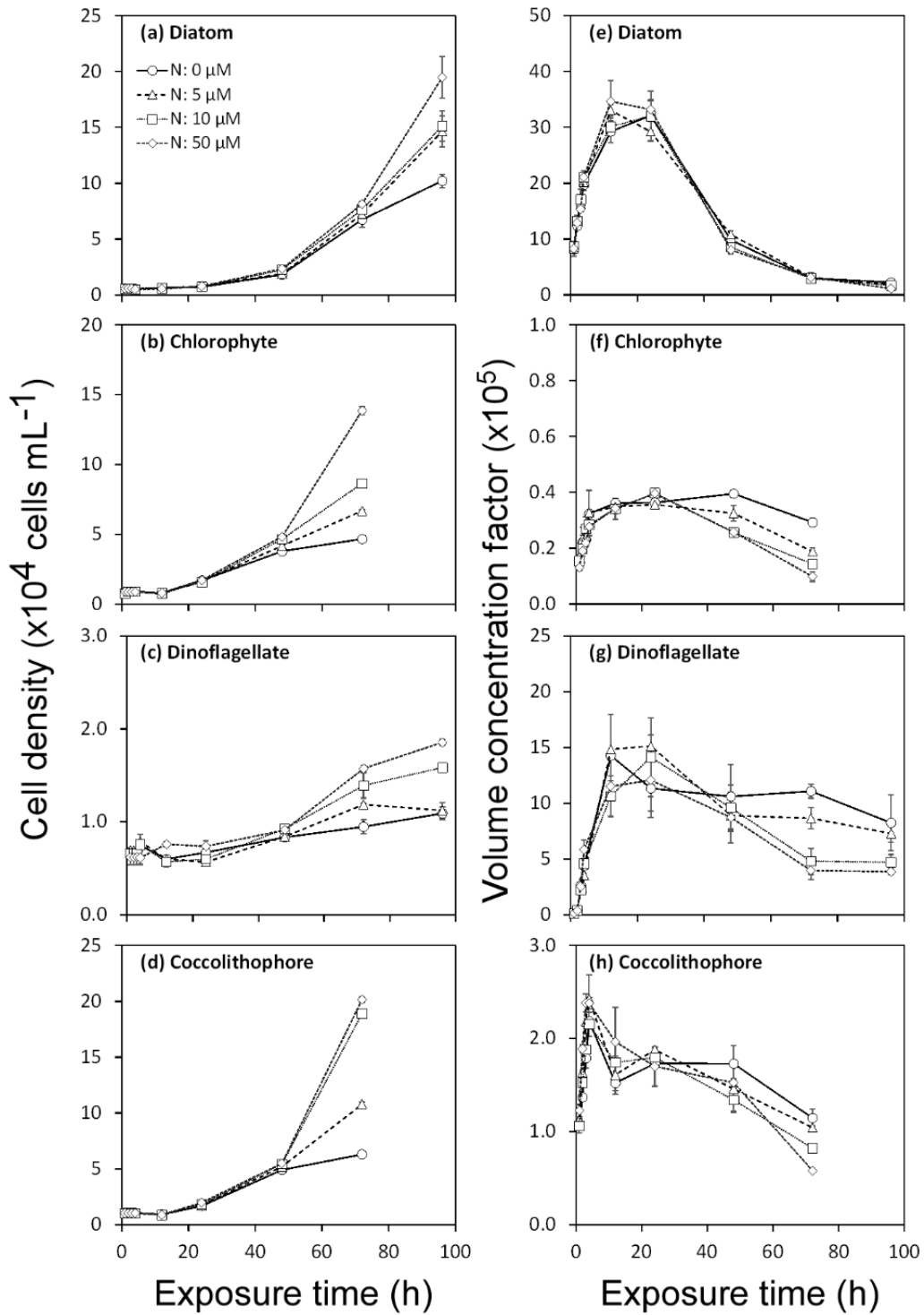
Figure 2-7. Cell growth (a–d) and MeHg volume concentration factors ($\times 10^5$, e–h) over time in cultures exposed to four different nitrate treatments. Data points are the means from two replicate cultures shown with 1 SD error bars.
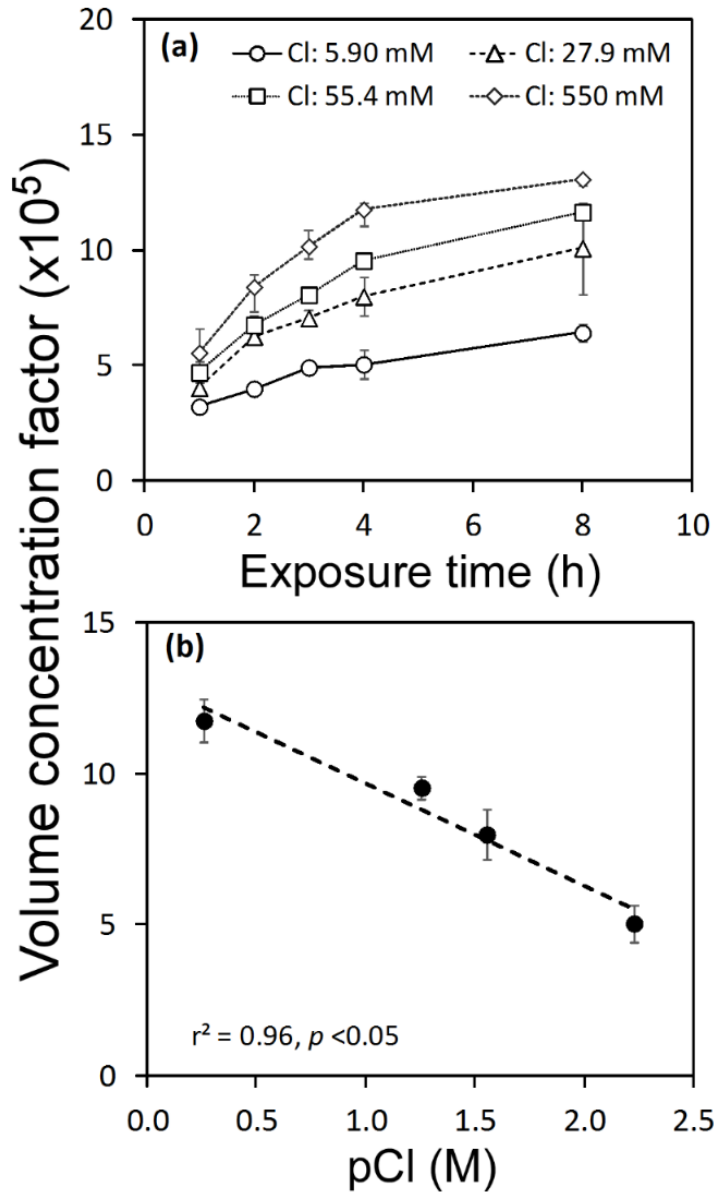
Figure 2-8. (a) Volume concentration factors ($\times 10^5$) for the diatom, *T. pseudonana*, over time at four different chloride concentrations. (b) The VCFs (t = 4 h) vs. pCl ($-$log Cl concentration). The dotted line represents the linear regression relating VCF to pCl ($r^2 = 0.96$, p <0.05). Data points are the means from three replicate cultures shown with 1 SD error bars.
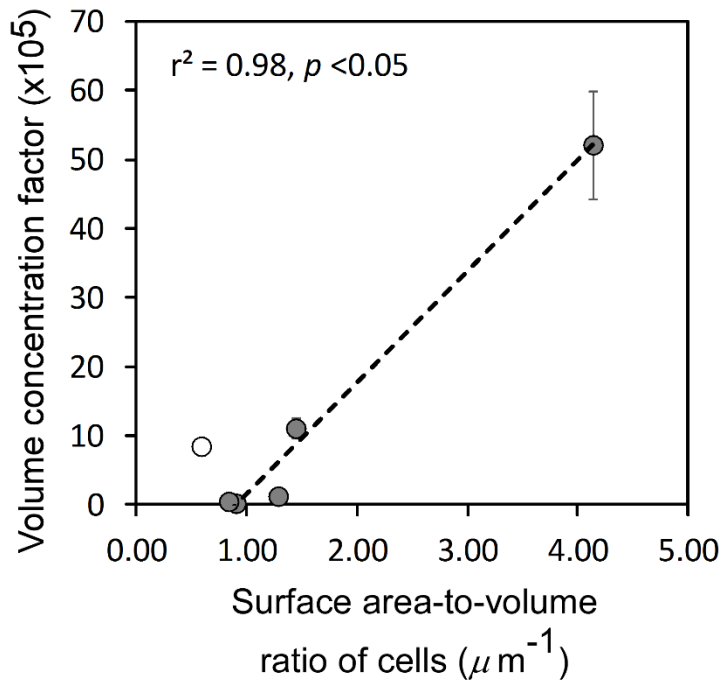
Figure 2-9. Correlation between the mean surface area-to-volume ratio of algal cells from each culture and the MeHg volume concentration factors (VCFs). Data points are the mean VCFs at 24 h (n = 3) shown with 1 SD error bars. The linear regression excludes the dinoflagellate *P. minimum* (open circle).

Chapter 3

Bioaccumulation of methylmercury in a marine diatom

and the influence of dissolved organic matter

Abstract

The largest bioconcentration step of most metals, including methylmercury (MeHg), in aquatic biota is from water to phytoplankton, but the extent to which dissolved organic matter (DOM) affects this process for MeHg largely remains unexplored in marine systems. This study investigated the influence of specific sulfur-containing organic compounds and naturally occurring DOM on the accumulation of MeHg in a marine diatom *Thalassiosira pseudonana*. Initial uptake rate constants and volume concentration factors (VCFs) of MeHg were calculated to evaluate MeHg enrichment in algal cells in the presence of a range of organic compound concentrations. At environmentally realistic and higher concentrations, the addition of glycine and methionine had no effect on algal MeHg uptake, but thiol-containing compounds such as cysteine and thioglycolic acid reduced MeHg accumulation in algal cells at high added concentrations (>100 times higher than naturally occurring concentrations). However, environmentally realistic concentrations of glutathione, another thiol-containing compound as low as 10 nM, resulted in a decline of ~30% in VCFs, suggesting its possible importance in natural waters. Humic acid additions of 0.1 and 0.5 mg-C L^{-1} also reduced MeHg VCFs by ~15% and ~25%, respectively. The bioaccumulation of MeHg for *T. pseudonana* in coastal waters with varying levels of dissolved organic carbon (DOC) was inversely correlated with bulk DOC concentrations. Generally, naturally occurring DOM, particularly certain thiol-containing compounds, can reduce MeHg uptake by phytoplankton.

Introduction

Methylmercury (MeHg) can cause adverse health effects on exposed wildlife and humans due to its neurotoxicity (Grandjean et al., 2010; Mason et al., 2012). In addition, it is one of the few

metals that biomagnifies in aquatic food chains, resulting in much higher concentrations in organisms at upper trophic levels than primary producers (Morel et al., 1998). The largest bioconcentration step (often $> 10^5$, depending on the species) is from the aqueous phase to phytoplankton primary producers, which serve as the base of most marine food webs (Lee and Fisher, 2016). Consequently, these algal cells provide highly enriched sources of MeHg for herbivores. Thus, small or moderate differences in enrichment of MeHg at the base of aquatic food chains could lead to pronounced effects on the overall MeHg concentration in marine animals.

It has been suggested that MeHg is taken up by phytoplankton mainly through passive diffusion (Lee and Fisher, 2016; Mason et al., 1996), and its uptake rate and magnitude is governed by its chemical form. Many trace metals in seawater are known to form complexes with organic ligands which could potentially mitigate their bioavailability and toxic effects to marine microorganisms (Vraspir and Butler, 2009). However, little is known regarding MeHg complexation by naturally occurring organic compounds and its influence on bioaccumulation in microorganisms in marine environments. Mercury (Hg) as well as MeHg are known to bind strongly to sulfur (Fitzgerald et al., 2007; Ravichandran, 2004), an essential element required for protein synthesis. Biogenic compounds with sulfhydryl groups (also known as thiols) such as glutathione (GSH) and cysteine (Cys) can be produced and released into seawater by marine organisms (Dupont and Ahner, 2005; Swarr et al., 2016; Tang et al., 2000; Tang et al., 2005). Among many thiols species, GSH is thought to be a major ligand for many soft, B-type metals (e.g., Cu, Pb, Cd, Zn, Hg and MeHg) in neutral or basic conditions (Krezel and Bal, 1999). Field studies suggested that high-affinity ligands like GSH may account for most of the Hg complexation in estuarine waters (Han et al., 2006). A few studies have addressed how organic

ligands affect Hg and MeHg bioavailability to bacterioplankton, motivated by their importance

in MeHg production and demethylation (Hsu-Kim et al., 2013; Ndu et al., 2016; Ndu et al., 2012;

Schaefer and Morel, 2009). For instance, the formation of a Hg-Cys complex has been shown to

promote the uptake of Hg(II) by the bacterium, *Geobacter sulfurreducens*, and further enhance

the enzymatic formation of MeHg (Schaefer and Morel, 2009). However, studies assessing how

complexation of MeHg by naturally occurring organic compounds affect its bioavailability for

marine phytoplankton are sparse.

In previous studies, Lawson and Mason (1998) examined the effect of organic and inorganic

ligands to MeHg uptake by a marine diatom, and demonstrated inconsistent results among three

ligands. Complexation of MeHg-bisulfide decreased the phytoplankton uptake rate and the

uptake rate of MeHg-Cys and MeHg-thiourea complexes increased with increasing complexation

by these ligands. Pickhardt and Fisher (2007) found that methionine (Met) had no significant

effects on MeHg bioavailability to freshwater phytoplankton. Luengen et al. (2012)

demonstrated that Cys at elevated concentrations diminished MeHg accumulation in the same

diatom. In addition to the effects of specific organic compounds, MeHg accumulation in algae

has been correlated with bulk dissolved organic carbon (DOC) concentrations. Generally, studies

reported inverse relationships between DOC concentrations and MeHg enrichment in freshwater

algae (Gorski et al., 2008; Luengen et al., 2012; Zhong and Wang, 2009), implying that binding

of MeHg-DOC reduce MeHg bioavailability for phytoplankton. Variability among studies

evaluating the effects of dissolved organic matter (DOM) on MeHg bioavailability may be

attributable to variations in DOM composition and/or the effects of ionic strength in different

water bodies. In marine environments, in addition to its high ionic strength, it is known that

chloride ions (Cl^-) are important ligands for MeHg competing against other organic ligands

(Fitzgerald et al., 2007). For this reason, the effects of marine DOM on MeHg bioavailability for algae needs further exploration.

This study performed a series of experiments to systematically assess how concentrations of specific organic compounds affect the bioavailability of MeHg to a marine diatom. Selected organic compounds included glycine (Gly), cysteine (Cys), methionine (Met), thioglycolic acid (TGA), glutathione (GSH) and humic acid (HA). Gly is the most common and abundant amino acid in the ocean. Cys and Met are amino acids with sulfur content. TGA is not commonly seen and measured in marine environments, but because it contains a sulfhydryl group and has a similar size and structure to Gly (Table 3-1), we chose to use it in our study to demonstrate the importance of sulfur on MeHg-ligand complexation. GSH is widely observed in natural waters. HA is a principal component of humic substances and a major organic constituent of many natural waters. We also examined MeHg uptake in seawater containing different concentrations of naturally occurring DOM.

Materials and Methods

Phytoplankton cultures

We used a unicellular, centric marine diatom *Thalassiosira pseudonana* (clone CCMP1335) that has been widely used to evaluate metal bioaccumulation in marine environments, including MeHg (Lee and Fisher, 2016). Unialgal clonal cultures were maintained axenically with f/2 medium (Guillard and Ryther, 1962) at 18°C under a light:dark cycle (14 h:10 h, 200 μmol quanta m^{-2} s^{-1}). Filter-sterilized (0.2 μm) surface seawater collected 8 km off Southampton, NY (Southampton seawater, SHSW, S = 35‰) was used to prepare f/2 medium for routine culture maintenance. To avoid the potential effects of ethylenediaminetetraacetic acid (EDTA) on MeHg

speciation, experimental cultures were grown in separate flasks in artificial seawater (ASW) with

amended f medium (nutrients at f/20 level) without adding EDTA for 7 d prior to all experiments.

Preparation of organic compounds and culture media

The chemical structures, stability constants with MeHg and other relevant information

regarding the organic compounds added to the diatom cultures are presented in Table 3-1. Gly,

Cys, Met, TGA and GSH are pure chemicals purchased from Sigma-Aldrich®. HA, also obtained

from Sigma-Aldrich® (H16752) is a mixture of compounds from the decomposition of organic

matter, particularly from dead plants, with a molecular weight range of 2000−500,000. Each

organic compound except HA was dissolved in Milli-Q® water individually to make a stock

solution (1 mM). To make a stock solution for HA where the molecular weight is uncertain, we

dissolved 100 mg of HA in 100 mL of ASW (S = 35‰) and added sodium hydroxide to increase

pH, enhancing its solubility. The solution's pH was then adjusted back to 8.2 and insoluble

particulate HA was removed by passing through a 0.2 μm polycarbonate membrane. Total

organic carbon (TOC) concentrations in the HA stock solution was determined using a Thermo

Finnigan Flash EA 1112 elemental analyzer.

To minimize the potential effects of natural DOM on MeHg bioavailability, we prepared

ASW with very low DOC concentrations as our experimental medium. First, all glassware and

anhydrous salts (NaCl, Na_2SO_4, KCl, $NaHCO_3$, KBr and NaF) were combusted at 450°C for 8 h

and then the salts were dissolved in Milli-Q® water subjected to UV-photooxidation of organic

matter. The produced Milli-Q® water had a background DOC concentration below the detection

limit (0.17 μM). Other noncombustible salts ($MgCl_2 \cdot 6H_2O$, $CaCl_2 \cdot 2H_2O$, $SrCl_2 \cdot 6H_2O$ and

H_3BO_3) were added as a solution. The produced ASW was then filtered by passing through a

combusted GF/F filter. The final salinity was 35‰ and the pH was adjusted to 8.2. Average

DOC concentrations in our ASW were 40±20 μM which is comparable to those in open ocean

seawater (Hansell and Carlson, 2002; Kaiser and Benner, 2009).

MeHg uptake experiments

In general, the MeHg uptake experiments followed earlier studies described for mercury

uptake by marine phytoplankton with a gamma-emitting radioisotope of Hg (^{203}Hg, $t_{1/2}$= 46.6 d)

to trace its partitioning between dissolved and algal cells (Fisher et al., 1984; Lee and Fisher,

2016). ^{203}Hg(II) was obtained from Eckert and Ziegler Isotope Products (Valencia, California)

with a specific activity of 5 Ci g^{-1} (= 185 GBq g^{-1}). Methyl-^{203}Hg (Me^{203}Hg) was synthesized in

the lab following established methods (Lee and Fisher, 2016; Rouleau and Block, 1997). In brief,

^{203}Hg was mixed with methylcobalamin ($C_{63}H_{91}CoN_{13}O_{14}P$, Sigma) at pH 5 with addition of

acetate buffer. The reaction proceeded in the dark for 18 to 24 h and Me^{203}Hg, produced

spontaneously, was then extracted by dichloromethane (CH_2Cl_2), purified, and re-dissolved in

Milli-Q$^®$ water. The conversion yield (fraction of total ^{203}Hg recovered as Me^{203}Hg) was 99±1%

(n = 2). Me^{203}Hg concentrations dissolved in seawater in our study ranged from 0.28 to 0.48 nM,

corresponding to Me^{203}Hg activities from 2.42 to 5.39 kBq L^{-1}. Radioactivity of Me^{203}Hg in

seawater or associated with algal cells was determined at 279 keV using an LKB Wallac 1282

Compugamma NaI (Tl) gamma detector. All measurements were counted with standards and

decay-corrected. Propagated counting errors were below 5%. The experimental concentrations

were below toxic levels to marine algae but were higher than those found in natural aquatic

environments. However, previous studies have shown that bioconcentration factors and uptake

rate constants for MeHg are not influenced at these concentrations (Lee and Fisher, 2016). For

those organic compounds whose sulfur content were known, the MeHg to sulfur ratios used in the uptake experiments were all less than one. The MeHg to HA and MeHg to DOC ratios used in our study were also far below the estimated MeHg binding capacities reported from previous studies (Haitzer et al., 2002; Hintelmann et al., 1997; O'Driscoll and Evans, 2000).

To assess the influence of the specific organic compound concentrations on MeHg uptake by marine algae, we used trace metal clean and organic carbon free glass-stoppered Erlenmeyer flasks, each containing 140 mL of ASW and microliter quantities of Me[203]Hg. Different levels of organic compounds from stock solutions were then added to ASW (0, 10, 100, 1000 nM for Gly and TGA; 0, 1, 10, 100, 1000 nM for Cys, Met, and GSH; 0, 0.1, 0.5, 1.0, 5.0 mg-C L^{-1} for HA). The pH in each flask was about ~8.2 and concentrations of nitrate, phosphate and silicate in each flask were fixed at 5 μM, 1 μM and 10 μM, respectively. Flasks containing Me[203]Hg and organic compounds were incubated at 18°C in the dark for 8 h to allow equilibration before inoculation of algal cells. Inocula of diatom cells were concentrated by resuspending cells off 1 μm polycarbonate membranes from experimental cultures (without adding EDTA). Initial cell densities ranged from 6 to 8×10^4 cells mL^{-1}. Water and cell samples were collected periodically (t = 2, 4, 8, 12, 24, 48, 72) for radioassays. In brief, we measured the total radioactivity in 1 mL of unfiltered water (water plus cells) and 5 mL of suspension (cells only) collected onto a 1 μm polycarbonate membranes (washed with 5 mL of unlabeled, filtered ASW; vacuum pressure <100 mmHg). Each type of treatment was run in duplicate, and control treatments (no algal cells) were performed simultaneously to correct the potential adsorption of dissolved Me[203]Hg onto membranes. Through this approach, the fractions of radioactivity in the dissolved phase and associated with the cells were determined. In addition, cell growth was monitored simultaneously over time using a Multisizer™ Coulter Counter®. Using the cellular

56

radioactivity, cell density, and cell volume, we evaluated the degree of bioconcentration of the [203]Hg in the cells at each sample time by calculating volume concentration factors (VCFs), which expresses the enrichment of MeHg in algal cells relative to the ambient seawater as:

$$VCF = (Bq\ Me^{203}Hg\ \mu m^{-3})_{cell} / (Bq\ Me^{203}Hg\ \mu m^{-3})_{water}$$

In the experiment to assess how bulk DOC concentrations affect MeHg uptake by marine algae, we prepared different seawater media with various DOC concentrations, including ASW, SHSW, and Long Island Sound seawater (LISSW). LISSW was collected from western Long Island Sound (S = 27.2‰, 40.96N, 73.58W), central LIS (S = 27.6‰, 41.14N, 72.66W), and eastern LIS (S = 30.4‰, 41.26N, 72.07W) and filtered through a 0.2 µm cartridge filter during a cruise on board the R/V *Connecticut* during September 10-12, 2014. Additionally, ASW and SHSW were mixed together in different ratios to prepare seawater with a DOC gradient between those of ASW and SHSW. The bioaccumulation of Me[203]Hg added to each water type, inoculated with *T. pseudonana,* followed the same protocols described above; for each medium, corresponding controls (without algal cells) were also examined in triplicate. DOC concentrations were measured using a Shimadzu TOC-L analyzer.

Sorption of MeHg onto flasks walls was examined by acid-rinsing (10% v/v HCl) the flask walls after each experiment. In general, adsorption of MeHg onto flask walls was very low (<2%) and the mean mass balance of MeHg in each treatment was $97 \pm 8\%$ (n = 96), suggesting no MeHg loss during the experiments.

Results

Influences of organic matter on algal MeHg uptake

After 72 h of exposure, 50~60% of MeHg was taken up by diatoms from the dissolved phase in the treatment without any addition of organic compounds (Fig. 3-1). Separate control treatments (no added organic compounds, diatoms exposed to MeHg) were tested in duplicate for each of 6 series of organic compounds, and all showed comparable results, indicating high reproducibility. MeHg uptake by algal cells was rapid in the first 12 h and reached steady-state between 12 h and 24 h. Growth of the diatoms was unaffected by any additions of organic matter other than HA additions ≥ 1 mg-C L^{-1}, which stimulated growth (Fig. 3-2). Even though algal cells kept growing in all cultures, thereby providing more cell surfaces (Fig. 3-2), the total amount of MeHg bound to cells slowed down and leveled off, probably indicative of the decline in bioavailable MeHg remaining in the dissolved phase after 24 h.

Regardless of any given concentration added in Gly, Met and TGA treatments, there were no significant influences on the MeHg uptake (Fig. 3-1). For Cys treatments, no significant effects on the uptake were found when Cys levels were below 100 nM, whereas a high level of addition (1000 nM) greatly lowered the MeHg uptake by algal cells (Fig. 3-1). For GSH treatments, a significant decrease in the uptake was observed when GSH's concentrations were higher than 10 nM. For HA treatments, low levels (0.5 to 1.0 mg-C L^{-1}) seemed to slightly decrease MeHg uptake and a high level (5.0 mg-C L^{-1}) led to a significant decline in uptake (Fig. 3-3).

MeHg volume concentration factors

Combining the MeHg uptake with cell growth, MeHg content of the diatoms was normalized on a cell volume basis (Fig. 3-3). There were no substantial differences in cell growth among

treatments (Fig. 3-2) except HA treatments. Therefore, VCFs generally showed a similar pattern with percentage of MeHg on cells (Fig. 3-1) and the difference in VCFs mainly reflect the influences from the added organic compounds. VCFs reached maximum values between 12 h and 24 h, after which they declined, reflecting subsequent cell growth and biological dilution of cellular MeHg content (Fig. 3-3). Briefly, biological dilution indicates that the total cell-bound MeHg stayed constant after the first 24 h of exposure but its concentration in cell biomass (as well as concentration factor) decreased as the cells continued to grow/divide.

Addition of Gly and Met had no significant effects on MeHg VCFs at all; high concentrations (1000 nM) of TGA and Cys lowered MeHg VCFs, but the decline was much greater in Cys treatments (>85% decline) than in TGA treatments (~15% decline). For both GSH and HA treatments, an inverse relationship was found between the MeHg VCFs and the added concentrations of GSH and HA (Fig. 3-4). The short-term uptake rate constant, which was normalized to the dissolved MeHg concentrations in the media was calculated on per cell basis for the first 4 h of exposure (Fig. 3-4, Table 3-2). In general, high uptake rate constants corresponded to high concentration factors at steady state. The uptake rate constants and mean VCFs at steady state are given in Table 3-2.

Effects of seawater with different natural occurring DOM

In the experiment comparing different types of seawater, ASW exhibited the highest VCFs for MeHg ($11.7\text{-}23.1 \times 10^5$) and LISSW had the lowest VCFs ($2.15\text{-}8.59 \times 10^5$) over time (Fig. 3-5). SHSW and mixed seawater media (ASW + SHSW) had VCFs between those in ASW and LISSW. The mean DOC concentration in ASW was 40 ± 20 μM, in SHSW was 204 ± 16 μM, in LISSW (W) was 331 ± 17 μM, in LISSW (C) was 293 ± 51 μM, and in LISSE (E) was 254 ± 28

μM. Mixed seawater media had mean DOC concentrations of 71 ± 4 μM (L), 116 ± 13 μM (M) and 154 ± 5 μM (H) (Table 3-2). The uptake rate constants for each type of seawater medium were also calculated and listed in Table 3-2. Across all experiments, a linear relationship ($r^2 = 0.77$) can be found between the uptake rate constants and mean MeHg VCFs (Fig. 3-6). The MeHg uptake rate constants and mean MeHg VCFs were inversely related to the amount of DOC in each water type (Fig. 3-7).

Discussion

There are many organic compounds in seawater that can form complexes with MeHg. Some organic complexation may reduce MeHg's ability to associate with ligands on algal surfaces or inhibit its passage across membranes of algal cells, resulting in reduced accumulation in phytoplankton. Other organic complexes of MeHg may enhance its bioavailability, leading to enriched uptake by phytoplankton. Our results clearly showed that, at sufficiently high concentrations, some dissolved organic compounds can cause a considerable decline in MeHg uptake by algae (Fig. 3-4). Such a decline can be attributed to those organic compounds complexing with MeHg and competing with algae for MeHg. Gly has a comparable size and a similar chemical structure to TGA (Table 3-1) but TGA has a sulfhydryl functional group which has a strong binding affinity to MeHg. The difference in their stability constants with MeHg may explain the reduced MeHg uptake rate constant observed in the TGA treatment at 1000 nM (Fig. 3-4). Met also has a reduced sulfur, thioether functional group in its molecule. However, its stability constant for MeHg is relatively small (Table 3-1) and it had no effects on MeHg uptake. Our results were in accordance with Pickhardt and Fisher (2007) who found no effect of 0.75 nM of Met on MeHg uptake by a freshwater diatom.

At a concentration of 1 μM, Cys, with a sulfhydryl group, lowered the MeHg uptake rate constant and its VCF significantly, consistent with results of Luengen et al. (2012) who found greatly reduced MeHg accumulation in a freshwater diatom exposed to 67 μM of Cys. Lawson and Mason (1998) showed that the MeHg uptake rate of a marine diatom decreased by >50% as Cys concentrations increased from 0.5 to 10 μM, also comparable to our results. However, the rate then increased by >100% when the concentrations increased from 10 to 50 μM in the study of Lawson and Mason (1998). The highest Cys concentration used in our study, 1 μM, is still 2-3 orders of magnitude higher than common Cys concentration in most marine environments (Dupont et al., 2006; Swarr et al., 2016).

GSH, Cys and TGA all possess a sulfhydryl group and have comparable stability constants with MeHg (Table 3-1), but 10 nM of GSH had greater effects on MeHg uptake than the same concentration of Cys and TGA (Fig. 3-3 and 3-4). This discrepancy between GSH and the other compounds was probably caused by the differences in their speciation in seawater and/or their coordination chemistry. From the given acid dissociation constants at the common ocean pH, the dominant forms of GSH, Cys and TGA are $[H_2L_{GSH}]^-$ and $[HL_{GSH}]^{2-}$, $[HL_{Cys}]^-$, and $[HL_{TGA}]^-$, respectively (Alderighi et al., 2003; Jawaid and Ingman, 1981; Rabenstein, 1973; Sharma et al., 2006). Assuming MeHg only forms a 1:1 complex, the $[HL_{GSH}]^{2-}$ has the greatest stability constant with MeHg among these complexes (Table 3-1). Hg coordination chemistry tends to form linear, two-coordinate geometric patterns (e.g., CH_3-Hg-L), but it has the potential to form complexes with a higher coordination number (>2) (Alderighi et al., 2003; Rabenstein, 1978). GSH has more potential donor atoms (S, N and two O) for MeHg than Cys (S, N and O) and TGA (S and O), which might allow for greater complexation (e.g., chelated complexes). Significant declines in algal MeHg uptake with GSH addition suggest that other similar thiols

such as phytochelatin (PC, an oligomer of glutathione), glutamine-cysteine (Gln-Cys) and γ-glutamylcysteine (γEC, a precursor of glutathione) may also have comparable effects on reducing MeHg uptake by algae. Alternatively, it is possible that GSH is not accumulated from ambient seawater by phytoplankton cells to the same extent as other thiol-containing compounds and amino acids.

Reported stability constants of natural humic substances for MeHg range from 10^{10} to 10^{15}, probably reflecting the presence of thiols in this humic material (Amirbahman et al., 2002; Hintelmann et al., 1997). Humic substances may therefore provide important ligands for MeHg, consistent with the inverse relationship found between DOC concentrations and MeHg VCFs and uptake rate constants in HA treatments in this study. The concentrations used in our study overlap with the typical ranges reported for humic substances in seawater (0.06 to 0.6 mg-C L^{-1}) (Thurman, 1985). Luengen et al. (2012) also found MeHg accumulation in a freshwater diatom was inversely related with the concentrations of humic substances isolated from natural DOM and Schartup et al. (2015b) found terrestrial DOM (containing more humic-like substances) decreased MeHg uptake by both plankton and bacteria.

The decline in MeHg bioavailability after 1 d of exposure in all treatments may be attributable to its complexation with dissolved organic matter in the aqueous phase (<0.2 μm) that greatly retards or prohibits its sorption to algal cell surfaces. As these laboratory experiments were conducted in ASW which contained very low levels of DOC (Table 3-2), the organic compounds to which the MeHg was bound – in addition to the organic compounds added to the ASW – may well have been released from the algal cells as they grew, as shown for other metals (Fisher and Fabris, 1982; Gonzalez-Davila et al., 1995; McIntyre and Guéguen, 2013). The composition of organic compounds released by cultured *T. pseudonana* into seawater during growth has been

addressed (Longnecker et al., 2015) and include polypeptides and amino acids, some of which could be expected to bind with MeHg.

Many possible mechanisms of organic-metal complex uptake by algal cells have been proposed, including the direct transport of intact organic-metal complex into cells, followed by the intracellular release of metal (Campbell et al., 2002; Morel and Price, 2003; Simkiss and Taylor, 1995; Sunda, 1989). However, since DOM usually consists of many large and complex molecules, it is unlikely that the organic-MeHg complex can penetrate intact into cells directly. Another mechanism is the metal exchange between organic ligands and membrane transporters at the surface of cell membranes, which is more likely for essential metals like Fe (Hudson and Morel, 1990) than non-essential elements like Hg. Different from many other metals, both Hg and MeHg are lipid soluble and may penetrate membranes without specific membrane transporters (Gutknecht, 1981) and neutral MeHg species such as $MeHgCl^0$ can passively diffuse through a diatom's plasmalemma (Mason et al., 1996). It is plausible that formation of a strong organic-MeHg complex, which may carry an electric charge or be very large, could therefore lessen MeHg's permeability through cell membranes. Biological reduction near cell surfaces may be another mechanism to change metal availability to algal cells (Maldonado and Price, 2001). Assuming MeHg was demethylated and then further reduced to the form of Hg^0 (elemental Hg), the produced gaseous Hg^0 would not accumulate in algal cells and would eventually be released into the overlying air. However, we did not observe any Hg loss across all treatments and the mean mass balance of MeHg in the seawater medium was $97 \pm 8\%$ (n = 96), as noted above.

In addition to the positive correlation between the uptake rate constants and mean MeHg VCFs (Fig. 3-6), the same correlation was also found between uptake rate constants and VCFs at

every time point after steady state was reached (t = 12, 24, 48, and 72 h). Two groups of outliers shown in Fig. 3-6 were LISSW and high HA treatments (5 mg-C L^{-1}). Such deviations may be attributable to the greater cell growth in these waters, leading to bio-dilution of MeHg and consequent lower VCFs.

As expected, MeHg mean VCFs and uptake rate constants both showed inverse relationships with bulk DOC concentrations (Fig. 3-7), consistent with previous studies (Gorski et al., 2008; Luengen et al., 2012). The decline in mean MeHg VCFs in freshwater diatoms with comparable increases in freshwater DOC (40 to 400 μM) was more pronounced than in seawater, ~6-fold difference (Luengen et al., 2012) vs. ~3.5-fold difference (this study). The differences may be caused by differences in the DOC composition between the waters used, and/or the chloride ions in seawater competing against DOC binding with MeHg. We did not measure the concentrations of thiols or humic substances in the SHSW and LISSW. Lamborg et al. (2004) reported that normalized mercury-binding ligand abundance (ligands to DOC ratio) in Long Island Sound (LIS) was higher than in the Mid-Atlantic Bight, which would include the collection site of the SHSW. They suggested that algal exudates and terrestrial input are the dominant sources of these ligands to the LIS, however the stability constants for MeHg were not measured.

A major role of thiols in living organisms is to defend against oxidative stress and to reduce the toxicity of metals (Ercal et al., 2001). Biogenic thiols produced within phytoplankton can be released into surrounding waters by exudation (Dupont and Ahner, 2005; Leal et al., 1999; Tang et al., 2005), cell lysis or sloppy grazing. Cys and GSH are common thiols that can be found in most aquatic systems, with GSH usually considered the dominant marine thiol. Relatively high concentrations of GSH (up to ~100 nM) can be found in anoxic and euxinic waters like the Black Sea (Mopper and Kieber, 1991), interstitial waters (Zhang et al., 2004) or lagoons (Chapman et

64

al., 2009). In estuarine, coastal and open ocean waters, their concentrations typically fall in the low nM range. Cys concentrations in the marine environments are typically lower, for instance 0.3 to 2.11 nM in the North Pacific (Dupont et al., 2006) and <0.1 to 1.5 nM in the North Atlantic (Kading, 2013; Swarr et al., 2016). These Cys concentrations are about 2 orders of magnitude lower than those (>100 nM) that reduced MeHg uptake in our study.

In contrast to Cys, our study showed that MeHg uptake was decreased by 30% in the presence of 10 nM of GSH, a concentration approaching levels observed in marine environments, especially estuarine and coastal waters. Reported concentrations of GSH ranged from <1 to 15 nM in the North-East Atlantic (Le Gall and van den Berg, 1998), 0.7 to 3.6 nM in coastal England (Al-Farawati and van den Berg, 2001), <0.1 to 2.21 nM in the North Atlantic (Kading, 2013; Swarr et al., 2016), 0.01 to 0.76 in the North Pacific (Dupont et al., 2006), 0.23 to 6.23 nM in Galveston Bay, Texas (Tang et al., 2000), 0.17 to 0.79 nM in San Diego Bay, California (Tang et al., 2004), 0.08 to 0.13 nM in Cape Gear Estuary, North Carolina (Tang et al., 2004), and 0.37 to 0.45 nM in Norfolk Estuary, Virginia (Tang et al., 2004); however electroanalytical methods used in some of these studies may lead to overestimates of GSH concentrations due to indiscriminate quantification (the authors assumed GSH was the primary component in total thiols). Notably, rather than GSH, γEC (γ-glutamylcysteine, a precursor of GSH) was found to be the most abundant thiol species (2 to 15 nM) in the North Pacific (Dupont et al., 2006). Given that γEC has a similar chemical structure to GSH, we hypothesize that it could similarly affect MeHg's availability to algae. Since thiols are mainly of biological origin, their concentrations are presumed to be associated with primary production. Dissolved GSH profiles in water column usually exhibit a maximum at sub-surface depths but do not always coincide with the chlorophyll maximum. Al-Farawati and van den Berg (2001) found that GSH-equivalent thiols were

65

positively correlated with chlorophyll in coastal waters. However, this relationship was not observed in the North Pacific (Dupont et al., 2006), Northwest Atlantic (Kading, 2013; Swarr et al., 2016), and Galveston Bay, Texas (Tang et al., 2000). Dupont et al. (2006) suggested that biological exudation was the primary source of dissolved GSH and other thiols in the mixed layer, but this exudation process was mainly controlled by environmental conditions (e.g., light or metals) rather than primary productivity (Ahner et al., 2002; Dupont and Ahner, 2005; Dupont et al., 2004; Tang et al., 2004). Assuming a large amount of biogenic thiols was released into surrounding waters due to exudation, cell lysis or grazing after an algal bloom, MeHg uptake by phytoplankton may be reduced subsequently, resulting in overall reduction in MeHg biomagnification in this ecosystem.

The sharp increases in MeHg VCFs after 72 h in the high treatments of Cys and GSH (Fig. 3-3) were possibly due to the degradation of those organomercuric complexes, releasing the bioavailable MeHg. These results suggest that while assessing a thiol's impact on MeHg accumulation in the field, its turnover rate in the water column needs to be taken into consideration. Free dissolved thiols are known to be unstable; for example, the reported half-lives of thiols through photochemical degradation were <1 d (Laglera and van den Berg, 2006; Moingt et al., 2010) and thiols can be readily oxidized (RSH→RSSR, which has no thiol group) in the presence of strong oxidants (Winterbourn and Metodiewa, 1999). However, the formation of strong metal complexes like Hg-thiol retard degradation, lengthening their residence times to several days in the water column (Hsu-Kim, 2007; Moingt et al., 2010). Kading (2013) assumed that thiols are components of the labile DOC in the ocean and suggested their turnover times may be on the order of hours to days based on the estimate from Carlson and Ducklow (1995). Dupont et al. (2006) used simple calculations based on the observed particulate and dissolved

66
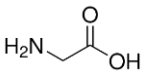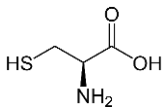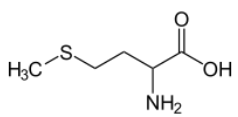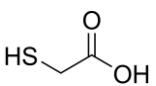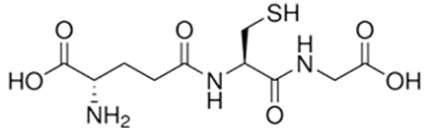
thiols concentrations and concluded that their turnover times were on the order of weeks or even longer assuming the system is at steady state.

Although thiols, HA (or humic substances), as well as bulk DOC, are capable of reducing MeHg uptake by phytoplankton, they can also lead to positive or negative feedbacks (directly or indirectly) on production, degradation and accumulation of MeHg in aquatic environments. For example, Schaefer and Morel (2009) reported that Cys was able to stimulate the production of methylmercury by the Fe-reducing bacterium *G. sulfurreducens*. However, binding of Cys with MeHg can increase its bioavailability for some Hg-resistant bacteria, leading to enhanced MeHg degradation (Ndu et al., 2012). The role of humic substances and DOC in the methylation of Hg and the degradation of MeHg remains more uncertain because of the variability in their concentrations and composition. DOM has been hypothesized to enhance methylation by stimulating the activity of heterotrophic bacteria or through direct abiotic methylation by humic or fluvic substances (Ullrich et al., 2001), but Hg methylation may also be inhibited due to Hg complexation with humic substances and DOC, reducing Hg bioavailability to bacteria (Ndu et al., 2012; Ullrich et al., 2001). A study in Arctic lakes further suggested that total Hg bioaccumulation was determined by binding thresholds on DOC, resulting in a bell-shaped relationship between total Hg accumulation and DOC concentrations (French et al., 2014). In brief, prediction of overall bioaccumulation and biomagnification of MeHg in an aquatic ecosystem cannot merely rely on measurements of bulk DOC or some ligands.

Thus, our study examined the effects of specific dissolved organic compounds (especially for thiols) and dissolved organic carbon (DOC) concentrations on the bioaccumulation of MeHg in a marine diatom. Overall the results indicated that under natural conditions glutathione and humic substances can play an important role on reducing MeHg uptake by phytoplankton, whereas

glycine, methionine, cysteine, and thioglycolic acid at representative seawater concentrations do not affect MeHg bioaccumulation. Future studies involving other algal species, including natural plankton assemblages, may provide the extent to which these findings can be applied to natural ecosystems.

Table 3-1. Organic compounds used in this study and their chemical structures and stability constants with MeHg.

Ligand name	Chemical structure	log K	Reaction	Reference
Chloride		5.13^a	$M^+ + L^- \rightarrow ML$	[1]
Glycine (Gly)		7.52^a 2.00^b	$M^+ + L^- \rightarrow ML$ $M^+ + HL \rightarrow M(HL)^+$	[1-3]
Cysteine (Cys)		16.46^c 15.11^c	$M^+ + L^{2-} \rightarrow ML^-$ $M^+ + HL^- \rightarrow M(HL)$	[1], [3-6]
Methionine (Met)		7.17^a	$M^+ + L^- \rightarrow ML$	[1], [4], [6]
Thioglycolic acid (TGA)		16.93^c 10.53^c	$M^+ + L^{2-} \rightarrow ML^-$ $M^+ + HL^- \rightarrow M(HL)$	[1], [3], [5]
Glutathione (GSH)		15.99^c 15.55^c 10.24^c	$M^+ + L^{3-} \rightarrow ML^{2-}$ $M^+ + HL^{2-} \rightarrow M(HL)^-$ $M^+ + H_2L^- \rightarrow M(H_2L)$	[1], [5]
Humic Acid (HA)		10-15		[7-9]

a: ionic strength = 1, temperature = 25°C
b: ionic strength = 0.15, temperature = 25°C
c: ionic strength = 0.1, temperature = 25°C
Reference: [1] NIST (2004), [2] Jawaid and Ingman (1981), [3] Alderighi et al. (2003), [4] Berthon (1995), [5] Arnold and Canty (1983), [6] Rabenstein (1978), [7] Fitzgerald and Lamborg (2003), [8] Amirbahman et al. (2002), [9] Hintelmann et al. (1997)

Table 3-2 (a). MeHg uptake rate constants (per cell basis for the first 4 h of exposure) and mean volume concentration factors (VCFs, the average of the 12, 24, 48, and 72 h time points) in all experiments.

(a)

Type of organic compound	Added amount	Uptake rate constant	mean VCF
	nM (mg C/L for humic acid)	*atto-mole MeHg / cell / h / nM exposure*	$\times\ 10^5$
Glycine (Gly)	0	16.3 ± 0.4	17.1
	10	14.3 ± 0.3	15.8
	100	15.0 ± 0.3	16.8
	1000	15.4 ± 0.8	14.8
Cysteine (Cys)	0	17.8 ± 0.7	16.6
	1	16.7 ± 1.9	15.6
	10	15.5 ± 3.3	14.8
	100	14.8 ± 0.2	14.8
	1000	0.3 ± 0.1	2.5
Methionine (Met)	0	17.1 ± 0.5	16.9
	1	16.9 ± 0.2	16.8
	10	15.5 ± 0.5	16.5
	100	17.1 ± 1.5	16.2
	1000	14.8 ± 0.7	15.1
Thioglycolic acid (TGA)	0	18.3 ± 2.2	17.1
	10	17.6 ± 1.8	17.3
	100	17.2 ± 1.3	15.5
	1000	13.5 ± 0.3	14.5
Glutathione (GSH)	0	17.7 ± 2.2	18.2
	1	17.8 ± 1.1	18.4
	10	12.8 ± 1.5	13.5
	100	7.1 ± 1.3	6.8
	1000	0.5 ± 0.0	1.7
Humic acid (HA)	0	18.1 ± 1.1	16.8
	0.1	15.2 ± 1.0	13.7
	0.5	14.2 ± 1.1	12.3
	1	11.9 ± 1.5	11.8
	5	11.6 ± 1.3	3.1

Table 3-2(b). MeHg uptake rate constants (per cell basis for the first 4 h of exposure) and mean volume concentration factors (VCFs, the average of the 12, 24, 48, and 72 h time points) in all experiments.

(b)

Type of seawater	bulk DOC μM	Uptake rate constant *atto-mole MeHg / cell / h / nM exposure*	mean VCF $\times\ 10^5$
ASW	40 ± 20	18.7 ± 2.6	17.0
ASW + SHSW (L)	71 ± 4	17.0 ± 0.9	14.1
ASW + SHSW (M)	116 ± 13	16.1 ± 1.4	13.8
ASW + SHSW (H)	154 ± 5	15.4 ± 0.1	12.8
SHSW	204 ± 16	15.6 ± 0.7	12.2
LISSW (W)	331 ± 17	9.2 ± 0.3	4.9
LISSW (C)	293 ± 51	12.3 ± 0.4	6.0
LISSW (E)	254 ± 28	11.4 ± 0.2	5.8
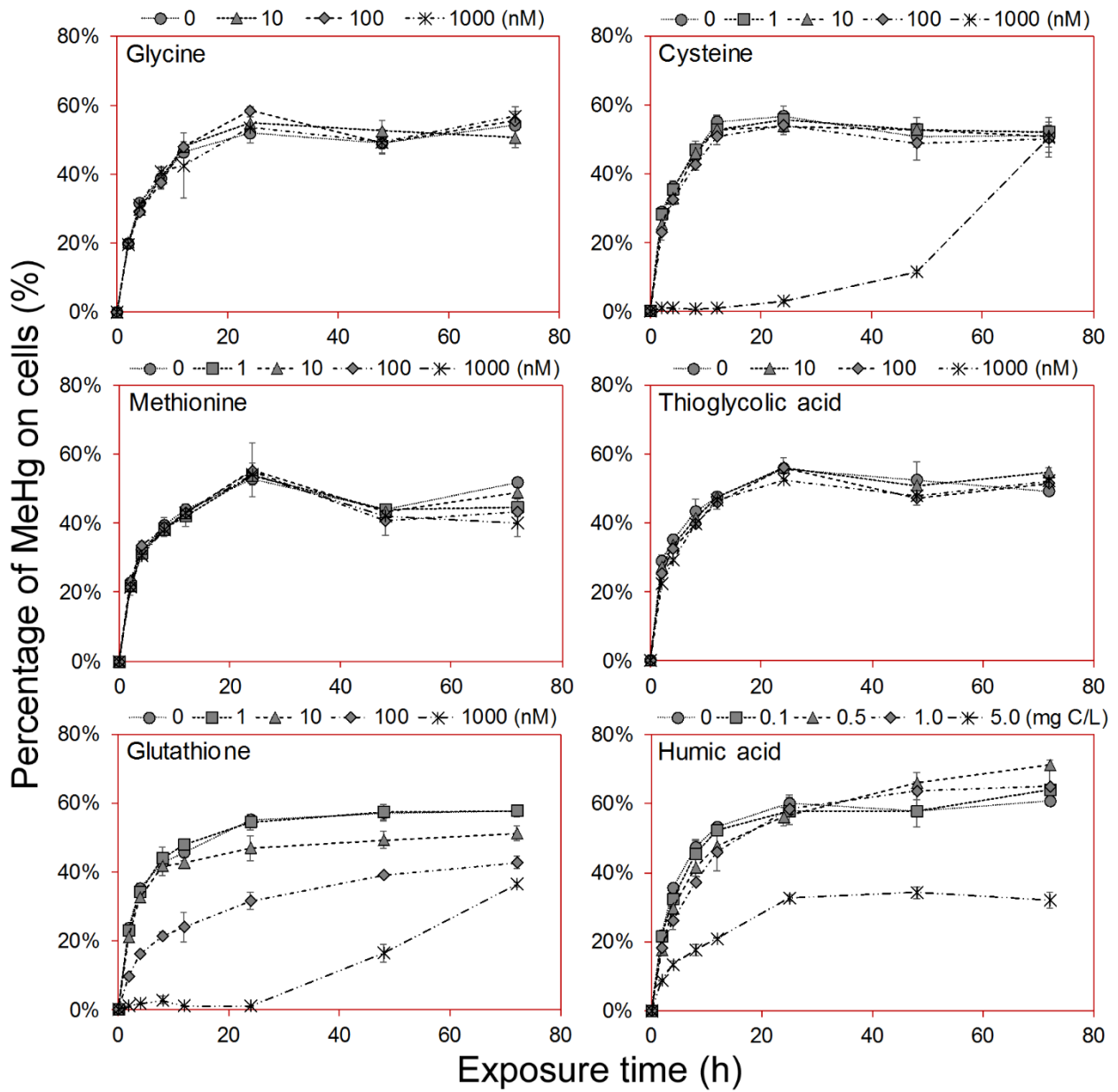
Figure 3-1. Effects of varying concentrations of different dissolved organic compounds on the bioaccumulation of MeHg by cells of *T. pseudonana*. Data points, the means from two replicates cultures ± 1 SD at each sample time, indicate the fraction of total MeHg associated with cells over time.
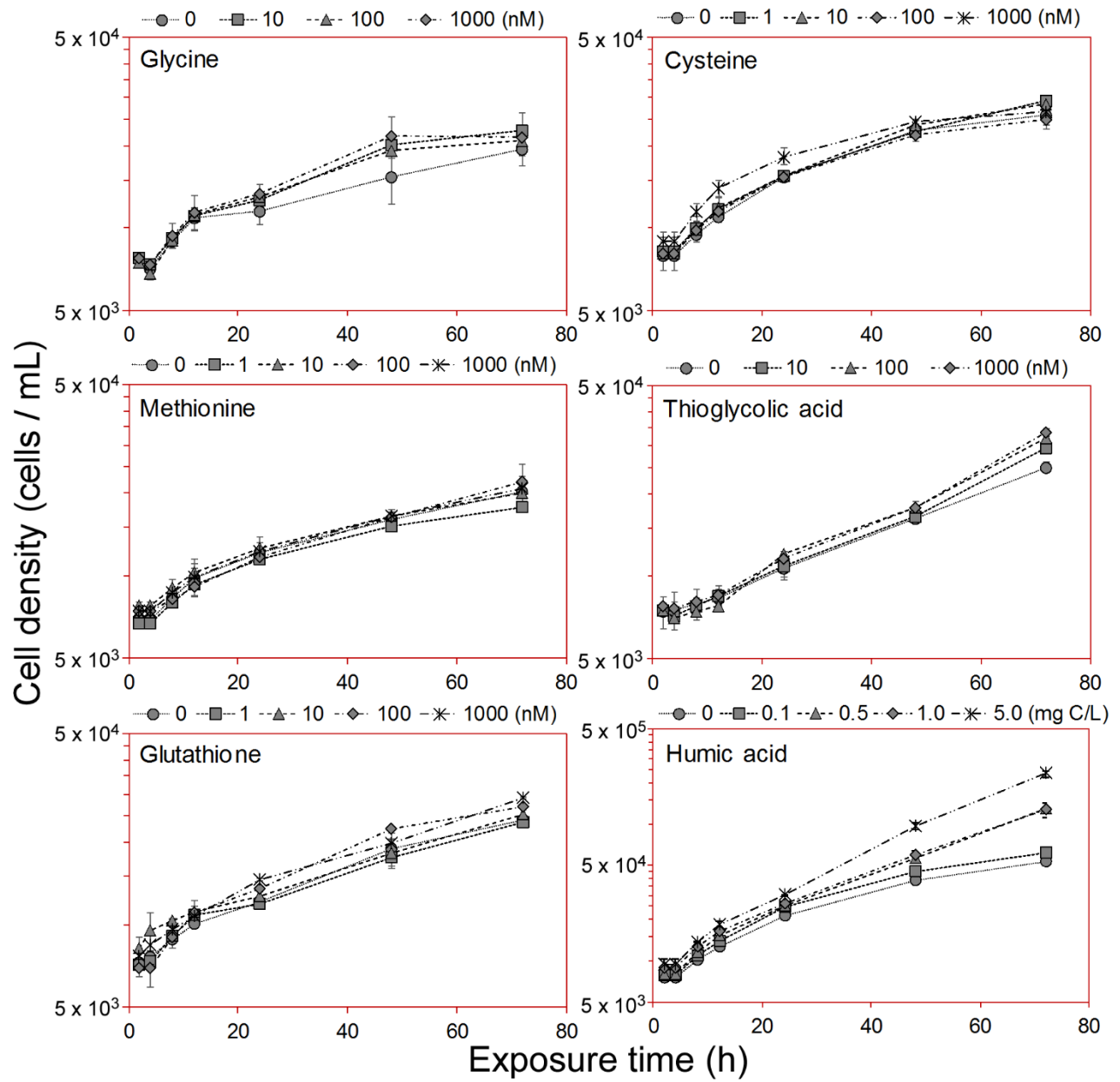
Figure 3-2. Growth of *T. pseudonana* cells exposed to six different organic compounds at varying concentrations. Data points are the means from two replicates cultures ± 1 SD at each sample time
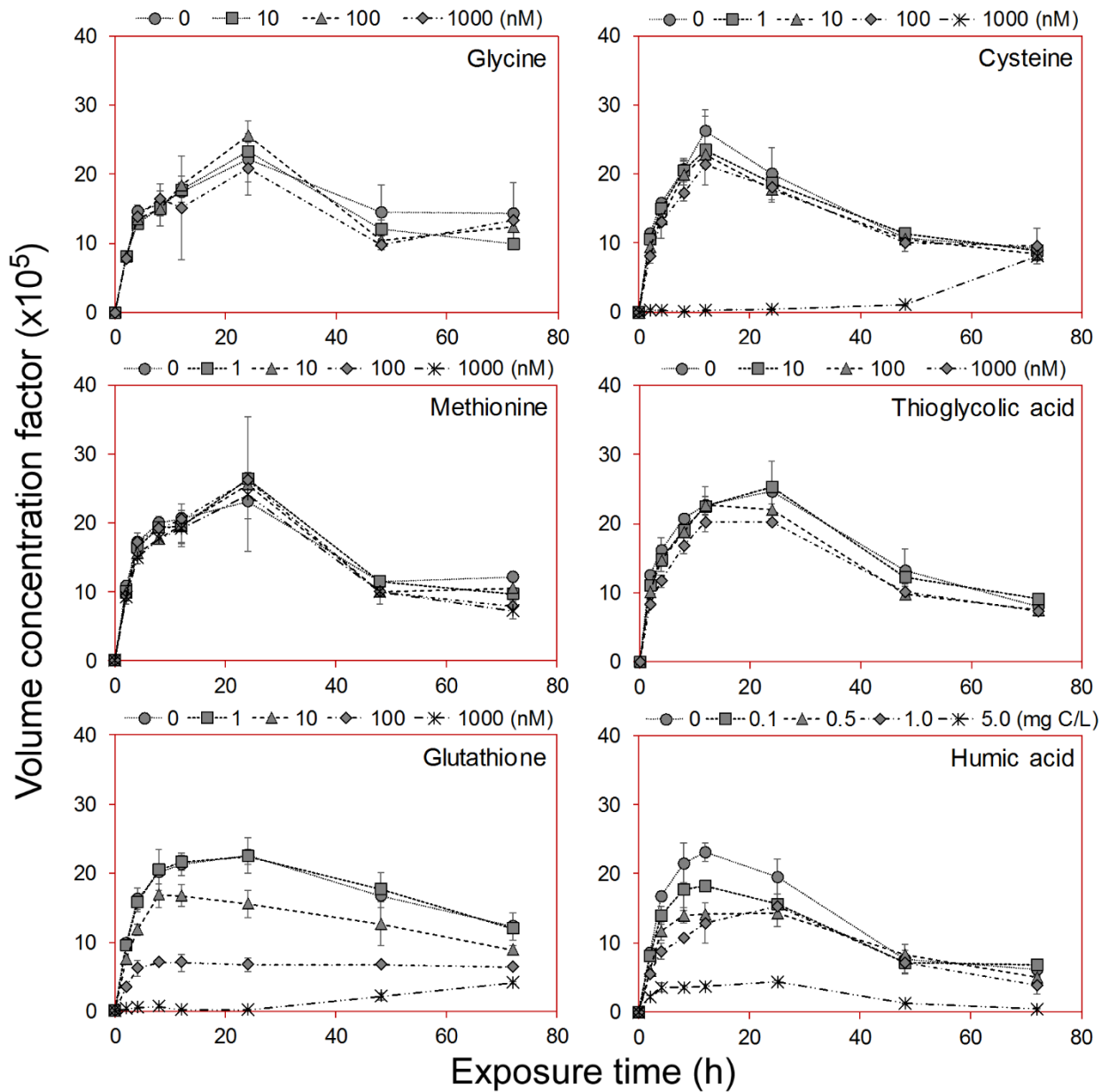
Figure 3-3. Effects of varying concentrations of six different dissolved organic compounds on MeHg volume concentration factors (VCFs) in *T. pseudonana*. Data points are the means from two replicate cultures ± 1 SD at each sample time.
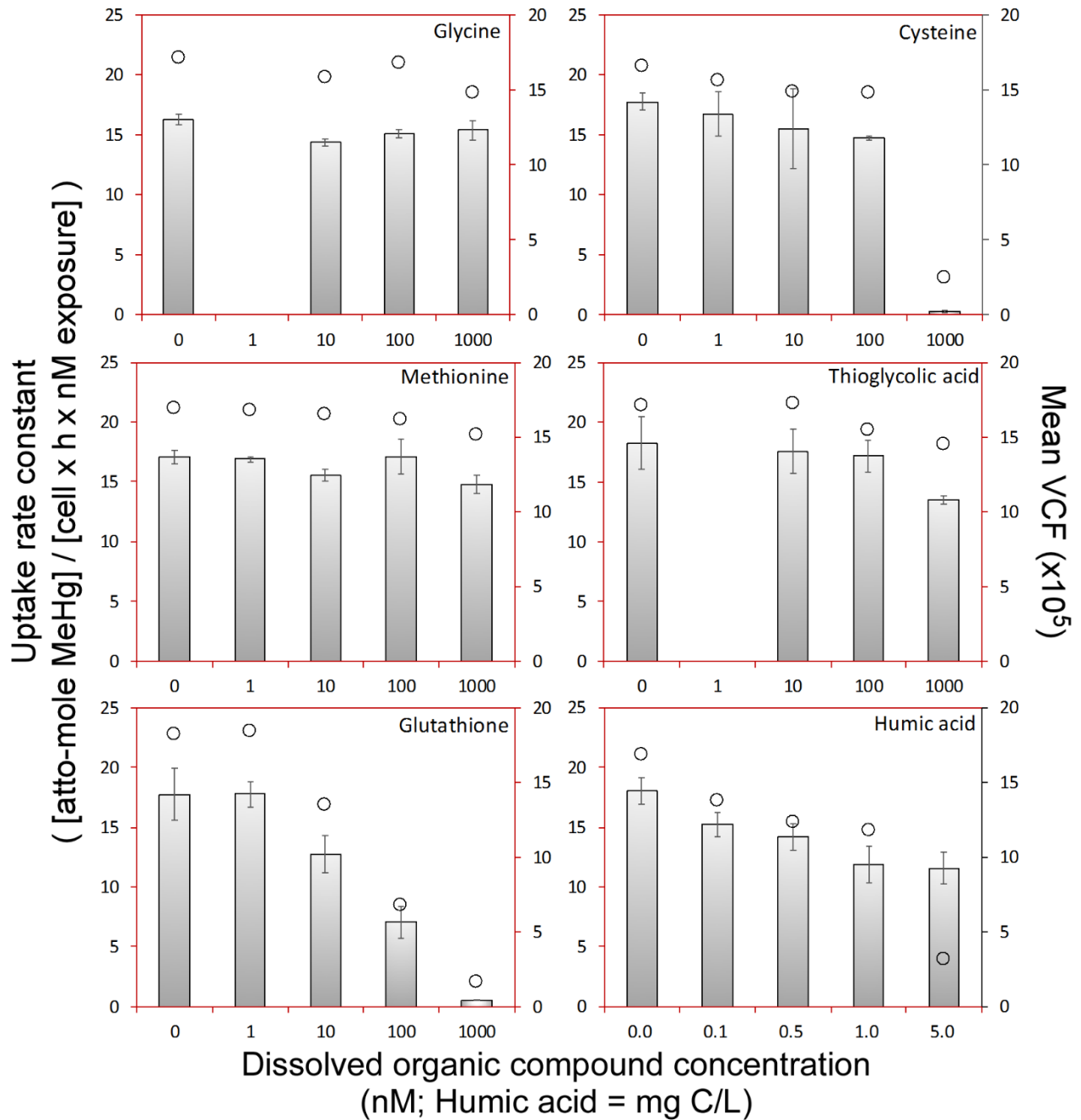
Figure 3-4. Calculated MeHg uptake rate constants (bar) and mean volume concentration factors (open circle) among varying concentrations of six organic compounds in ASW. All treatments shown are for 2 replicate cultures. The uptake rate constants were normalized to the ambient dissolved MeHg concentrations in the media and were expressed on a per cell basis for the first 4 h of exposure. The mean VCFs are the average of the 12-, 24-, 48-, and 72-h time points. Error bars are ± 1 SD
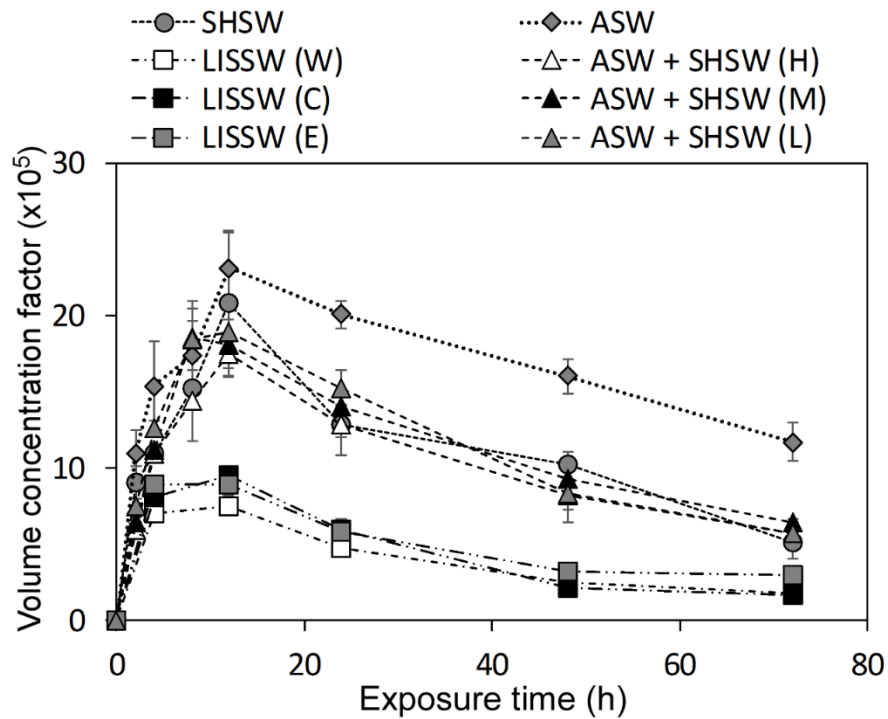
Figure 3-5. Effects of different seawater media on MeHg volume concentration factors (VCFs) for *T. pseudonana*. Data points are the means from three replicates cultures ± 1 SD at each sample time. LISSW (W): Western LIS; LISSW (C): Central LIS; LISSW (E): Eastern LIS; ASW+SHSW (L): Low DOC; ASW+SHSW (M): Medium DOC; ASW+SHSW (H): High DOC; ASW: Artificial seawater; SHSW: Southampton seawater.
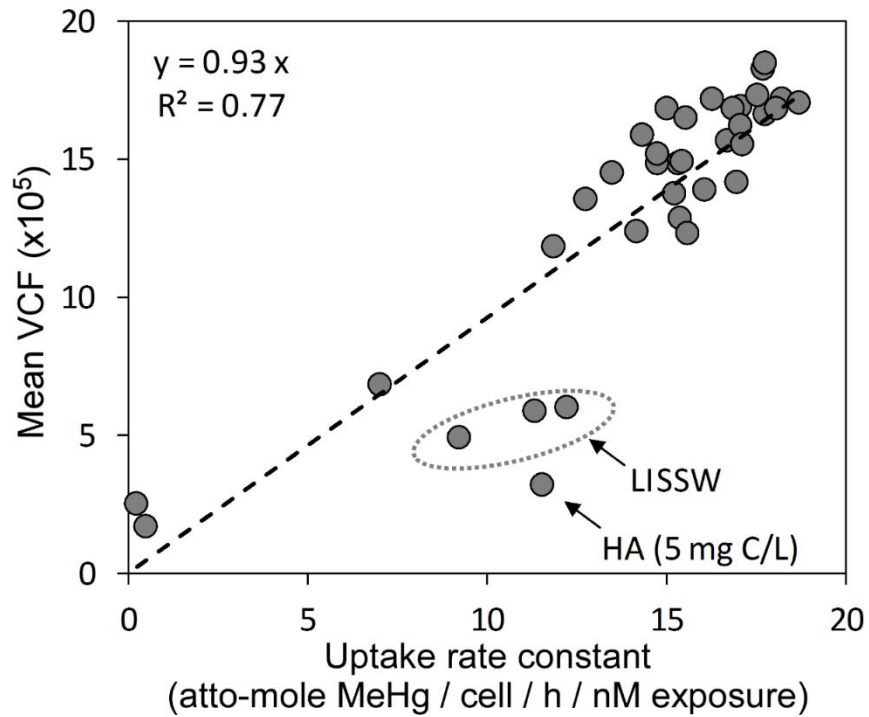
Figure 3-6. Correlation between MeHg uptake rate constants and mean volume concentration factors (VCFs) across all experiments. The mean VCFs are the average of the 12, 24, 48, and 72 h time points. The dashed line and the equation shown reflect all data.
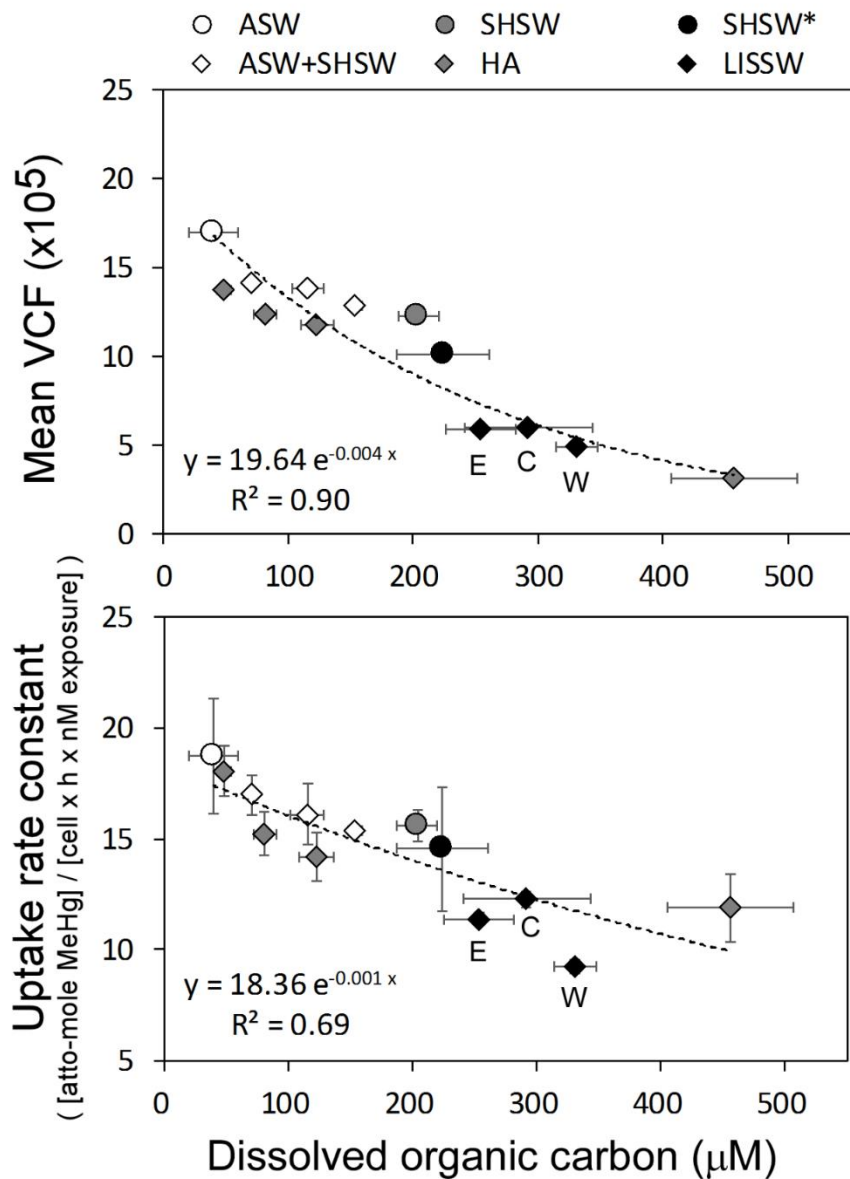
Figure 3-7. MeHg uptake rate constants and volume concentration factors (VCFs) as a function of dissolved organic carbon (DOC) in different seawater media. SHSW* represents the data from Lee and Fisher (2016). E, C, and W indicate eastern, central, and western Long Island Sound samples.

Chapter 4

Bioaccumulation of methylmercury in a marine copepod

Abstract

Methylmercury (MeHg) is known to biomagnify in marine food chains, resulting in higher concentrations in upper trophic level animals than their prey. To better understand how marine copepods, an important intermediate between phytoplankton and forage fish at the bottom of the food chain, assimilate and release MeHg, we performed a series of laboratory experiments using the gamma-emitting radiotracer ^{203}Hg(II) and Me^{203}Hg with the calanoid copepod *Acartia tonsa*. Assimilation efficiencies (AEs) of Hg(II) and MeHg ranged from 25 to 31% and 58 to 79%, respectively, depending on algal diets. The AEs were positively related to the fraction of mercury in the cytoplasm of the algal cells that comprised their diet. Efflux rates of Hg(II) (0.29 d^{-1}) and MeHg (0.21 d^{-1}) following aqueous uptake were similar, but efflux rates following dietary uptake were significantly lower for MeHg (0.11-0.22 d^{-1}) than Hg(II) (0.47-0.66 d^{-1}). The calculated trophic transfer factors (TTFs) in copepods were >1 for MeHg and consistently low (≤0.2) for Hg(II). We used the parameters measured in this study to (1) quantitatively model the relative importance of MeHg sources (water or diet) for copepods, and to (2) predict the overall MeHg concentrations in copepods in different marine environments. In general, MeHg uptake from diet accounted for most of the body burden in copepods (>50%). For an algal diet whose MeHg dry weight bioconcentration factor (BCF) is ≥10^6, over 90% of a copepod's MeHg body burden can be attributable to diet. Our model-predicted MeHg concentrations in the copepods were comparable to independent measurements for copepods in coastal and open-ocean regions, implying our measured parameters and model are applicable to natural waters.

Introduction

Phytoplankton concentrate many trace metals out of seawater (Fisher, 1986) and serve as highly enriched sources of these metals for herbivorous animals, including zooplankton and bivalve mollusks (Fisher and Reinfelder, 1995; Wang and Fisher, 1998; Wang et al., 1996). Zooplankton are of particular interest as their sinking waste products and cast exoskeletons can vertically transport metals (Fowler and Knauer, 1986) and in so doing affect their oceanic residence times (Fisher and Fowler, 1987; Fisher and Reinfelder, 1995). Overall, zooplankton play an important role in the bioaccumulation of metals in marine food webs because they link phytoplankton, whose bioconcentration of metals is the single largest enrichment step in food chains, with fish and other metazoans; thus, trace metals that are assimilated into zooplankton could ultimately be transferred to higher trophic level organisms (Fisher and Reinfelder, 1995).

Although phytoplankton has been found greatly enriched in many essential and nonessential metals, most of the nonessential metals are not appreciably assimilated from phytoplankton food by zooplankton, let alone further biomagnifying in marine food chains (Fisher and Reinfelder, 1995). Indeed, the concentrations of most metals in organisms at higher trophic levels typically decrease with increasing trophic level; the exception is methylmercury (MeHg) which is the only trace metal species known to substantially biomagnify in food chains. This biomagnification is due to its high assimilation efficiency in organisms at every trophic level and very slow release rates from animal tissues (Mathews and Fisher, 2008; Reinfelder et al., 1998). As a consequence, MeHg is efficiently transferred from one trophic level to the next and is ultimately enriched in fish. It is known that MeHg accumulation in heterotrophic organisms is mainly from ingesting MeHg-containing food instead of direct uptake from water. Thus, food web structure could influence the MeHg transfer to higher trophic level organisms (Cabana and Rasmussen, 1994;

81

Morel et al., 1998). Because seafood consumption is the primary route for human intake of MeHg (Sunderland, 2007) and such exposure may lead to adverse health consequences to exposed humans (Grandjean et al., 2010), there is interest in the food chain build-up of MeHg in marine ecosystems among public health agencies and the general public. While there have been comprehensive studies of the trophic transfer and cycling of many trace metals by zooplankton (Fisher and Reinfelder, 1995), MeHg has not been similarly studied for marine zooplankton, where few studies have examined the transfer of MeHg from phytoplankton to zooplankton.

Previous work has shown that a high assimilation efficiency (>90%) and low release rate (<5 %/d) of MeHg in a fresh water daphnid, *Daphnia pulex* feeding on a chlorophyte (Karimi et al., 2007), led to a significant transfer of MeHg from phytoplankton to zooplankton. For marine organisms, Mason et al. (1996) reported a high assimilation efficiency (>60%) of MeHg in marine copepods feeding on a diatom. This value was four times greater than Hg(II) and the fractions of MeHg and Hg(II) accumulated in algal cell cytoplasm were strongly correlated to the assimilation efficiencies in copepods. This correlation of cytoplasmic distribution in algal cells and AE in herbivorous copepods is consistent with findings for other elements (Reinfelder and Fisher, 1991). Lawson and Mason (1998) also found high assimilation efficiencies (>50%) of MeHg in marine copepods and amphipods feeding on diatoms. Mathews and Fisher (2008), examining trophic transfer of MeHg in a simple estuarine food chain, reported a high assimilation efficiency of MeHg (>76%) for both zooplankton feeding on phytoplankton and small planktivorous fish feeding on zooplankton.

In this study, we conducted a series of laboratory experiments to evaluate assimilation efficiencies of both Hg(II) and MeHg in marine copepods that fed on three marine phytoplankton species belonging to different algal classes, and compared this with Hg(II) and MeHg uptake

82

from the aqueous phase. We estimated Hg(II) and MeHg efflux rates from copepods and trophic

transfer factors from phytoplankton to copepods. With those parameters, we used a simple model

to estimate the relative importance of dietary and aqueous sources of MeHg in zooplankton and

compared modeled MeHg concentrations in marine zooplankton with field data.

Materials and Methods

Preparation of plankton

   Three marine phytoplankton species were used to feed zooplankton, the diatom *Thalassiosira*

pseudonana (clone 3H), chlorophyte *Dunaliella tertiolecta* (CCMP1320) and cryptophyte

Rhodomonas salina (CCMP1319). These species, representing three different algal classes, have

significantly different MeHg bioconcentration factors (Lee and Fisher, 2016) as well as different

cell wall characteristics and photosynthetic storage products, which may influence the trophic

transfer of MeHg to copepod grazers. All species were held in clonal, unialgal cultures

maintained axenically for generations at constant temperature (18°C) and 14 h:10 h light:dark

cycle (200 μmol quanta m^{-2} s^{-1}) with cool white fluorescent lamps. Routine cultures were

maintained in sterile filtered (0.2 μm) surface seawater (35 psu) and enriched with f/2 nutrients

(Guillard and Ryther, 1962).

   The coastal calanoid copepod *Acartia tonsa,* was collected in early summer from Stony Brook

Harbor, New York with a plankton net (160 μm mesh) and transferred into 0.2 μm filtered

seawater. Immediately after collection, adult *A. tonsa* individuals were visually identified using a

dissecting microscope and separated from other plankton. The separated copepods were

maintained in a tank with filtered seawater under shimmer light and fed the algae *R. salina* and

Isochrysis galbana every 12 h to allow them to acclimate to laboratory conditions for 2 d. Prior

to experiments, the copepods were transferred to another tank with 0.2 μm filtered seawater without food for 12 h in order to evacuate their guts of ingested material. To put the amount of bioaccumulated Hg in copepods into context, we measured total background Hg concentrations in *A.tonsa* collected from Stony Brook Harbor. Total Hg, determined by analyzing freeze-dried copepods using a DMA-80 direct mercury analyzer (Milestone, Inc.), was found to be 30.2 ± 4.6 ng g^{-1} dry weight (n = 6, water content = 86 ± 1 %). The reported fraction of total Hg in the form MeHg in marine zooplankton generally ranges from 12 to 45% (Mason et al., 2012).

Hg Assimilation and depuration by copepods from food

The protocol of using radioisotopes to evaluate the accumulation and assimilation of elements in copepods has been well established (Reinfelder and Fisher, 1991; Wang and Fisher, 1998). In this study, we used the gamma-emitting radioisotope, ^{203}Hg, as a tracer to track the transfer of Hg (Hg(II) and MeHg) from phytoplankton to zooplankton. Short pulse-feeding experiments were performed to help avoid extensive excretion and recycling of Hg which would lead to ambiguous results.

Inorganic ^{203}Hg(II) solution was obtained from Eckert and Ziegler Isotope Products (Valencia, CA) (specific activity: 5 Ci g^{-1}). It was further converted to methylmercury (Me^{203}Hg) following methods described elsewhere (Lee and Fisher, 2016; Rouleau and Block, 1997). In brief, the ^{203}Hg(II) solution was adjusted to pH 5 with acetate buffer and mixed with methylcobalamin ($C_{63}H_{91}CoN_{13}O_{14}P$). Allowing the reaction to proceed in the dark for 18 to 24 h, Me^{203}Hg was formed and then extracted by dichloromethane (CH_2Cl_2) and re-dissolved in Milli-Q$^®$ water. The conversion yield (fraction of total ^{203}Hg(II) recovered as Me^{203}Hg) was $95 \pm 3\%$ (n = 6).

Algal cells for feeding experiments were cultured in f/2 medium without adding EDTA. Late-log phase cells were concentrated from water by either filtering onto polycarbonate membranes or centrifuging and resuspending into 0.2 µm sterile-filtered seawater. The algal cells were then radiolabeled with ^{203}Hg(II) or Me^{203}Hg (55-78 kBq L^{-1}, corresponding to concentrations 0.6-2.0 µg L^{-1} of Hg). The concentrations of Hg(II) and MeHg used in these experiments were higher by about 10^3 and 10^4 times, respectively, than those in natural waters. Because ^{203}Hg(II) was prepared in 1 M hydrochloric acid, corresponding amounts of 1 M Suprapur NaOH were added immediately afterwards to maintain the seawater pH (~8.2). In order to have uniformly radiolabeled cells, the cultures were grown for at least 2 days (several cell divisions) to reach equilibrium. The analysis of the cellular distribution of the ^{203}Hg (for both Hg(II) and MeHg) followed the protocol described in Reinfelder and Fisher (1991).

Radiolabeled algal cells were concentrated and resuspended as described above and then added into transparent Teflon feeding bottles containing 100 mL filtered seawater with a cell density of 6 to 8×10^4 cells mL^{-1}, depending on algal species. Three replicates were used for each algal food treatment. In each bottle, 60 copepods fed on radiolabeled cells in the dark for 45 minutes. After feeding, the copepods were collected with a 160 µm nylon mesh, rinsed twice with 10 mL of unlabeled, filtered seawater and immediately transferred to 25 mL clean filtered seawater for radioanalysis (t = 0, assigned as the starting point of the depuration period). Fecal pellets egested by copepods during the feeding experiment were also collected with a 20 µm nylon filter, rinsed with filtered unlabeled seawater, and radioassayed. The copepods were transferred back to the original Teflon bottles with clean filtered seawater to depurate their ingested radiolabeled food. They were maintained under the same conditions as the feeding experiments but with non-radiolabeled food of the same species. The radioactivity of copepods

and their fecal pellets was determined periodically (t = 4, 12, 24, 36, 48, 60, 72 h) over the 3-d depuration period. The food was added and the seawater was replaced at each time point. The gentle handling throughout resulted in negligible mortality of copepods.

Hg(II) and MeHg may desorb from radiolabeled algal cell surfaces into the dissolved phase during the feeding experiment. Consequently, it was possible that the copepods may have acquired Hg from both water and food sources. Thus, a control treatment was used to assess the copepod uptake of ^{203}Hg (for both Hg(II) and MeHg) that had desorbed from the algae during the same time period used for radioactive feeding (45 min). To accomplish this, 100 mL of filtered seawater was exposed to radiolabeled algal cells and was then passed through 0.2 μm membrane to remove all particles. Uptake of desorbed radioactive Hg by copepods from this seawater constituted the control treatment for the feeding experiments.

MeHg uptake from the dissolved phase

Two experiments were conducted to measure MeHg uptake by copepods from the dissolved phase, one in which uptake was evaluated over time, the other in which MeHg was added at varying concentrations. For the former, Me^{203}Hg was added to 0.2 μm filtered seawater at 0.35 nM and equilibrated for 2 h. Copepods were then exposed to this radioactive seawater (60 individuals in a beaker containing 100 mL filtered seawater, total of 8 beakers). Periodically, at 2, 4, 8, 12 h, all 60 copepods were collected from each of the two replicates onto 20 μm nylon membranes and rinsed with filtered clean seawater in preparation for radioanalysis. To evaluate the uptake over a range of MeHg concentrations, Me^{203}Hg was added to 0.2 μm filtered seawater at five different concentrations (20, 50, 100, 250, 500 ng L^{-1}) and equilibrated for 2 h. Each treatment had two replicates. 60 copepods were exposed to each MeHg for 4 h, after which they

were collected onto 20 μm nylon membranes and rinsed with filtered clean seawater for radioanalysis.

^{203}Hg measurements

Radioactivity of ^{203}Hg ingested by copepods was determined noninvasively using a large-well NaI(Tl) gamma detector. Radioactivities of labeled phytoplankton and seawater were measured using an LKB Wallac 1282 Compugamma NaI(Tl) gamma detector equipped with a well detector. ^{203}Hg activity was assessed at 279 keV. Intercalibration between the two gamma counters was performed, and all samples were counted with standards and decay-corrected. Propagated counting errors were <5%.

Results

The copepods ingested radiolabeled cells during all feeding experiments. Figure 4-1 shows the percentage of ^{203}Hg (^{203}Hg(II) or Me^{203}Hg) retained in them over different periods of depuration. All values shown are net values after subtracting radioactivity from control treatments; controls typically accounted for 5 to 15% of the total radioactivity acquired during feeding. The percentage of Hg was calculated as the radioactivity in the copepods divided by the radioactivity measured in the copepods at time zero of depuration (immediately after feeding). ^{203}Hg in copepods decreased over time in all experiments during depuration. Depuration patterns typically displayed an initial, rapid loss of Hg from the copepods, followed by a more gradual decline after 24 h of depuration. The initial rapid loss reflects loss of unassimilated boluses of ingested algal food through defecation, whereas the slowly exchanging pool reflects loss of assimilated Hg driven by metabolic activity (Wang and Fisher, 1998; Wang and Fisher, 1999). Assimilation

87

efficiencies (AEs) were calculated from the second stage of depuration (1-3 d), using the

equation described by Wang and Fisher (1998):

$$\%A = A_0 e^{-kt} \qquad (1)$$

where $\%A$ is the percentage of radioactivity retained in copepods at time t and k is the depuration

rate constant during 1 to 3 d of depuration. A_0 is the y-axis intercept of radioactivity retained in

copepods and is defined as the AE of the ingested mercury. Calculated mercury AEs and efflux

rate constants (k_e) are shown in Table 1. Copepods ingesting MeHg-labeled food had higher AEs

(58-79%) than those ingesting Hg(II)-labeled food (25-31%). AEs for both Hg(II) and MeHg

among different algal species did not differ significantly. Efflux rate constants following uptake

from the aqueous phase (k_{ew}) were similar among the two Hg species, 0.29 d^{-1} for Hg(II) and

0.21 /d for MeHg. Efflux rate constants (k_{ef}) following ingestion of Hg-labeled algal food were

significantly lower for MeHg (0.11-0.22 d^{-1}) than for Hg(II) (0.47-0.66 d^{-1}). In both Hg(II) and

MeHg feeding experiments, Hg loss in the form of fecal pellets during the depuration period

accounted for 10-40% for Hg(II) and 1-13% for MeHg of total Hg released by copepods,

suggesting that excretion of Hg into the dissolved phase was the primary route of Hg loss.

There was a strong relationship between AEs and cytoplasmic distribution of Hg in algal cells

($r^2 = 0.95$); the slope of this regression line was about 1 and the y-intercept was about 0 (Figure

4-2a). The clear separation of MeHg from Hg(II) in AEs in *A. tons*a reflects their different

penetration into algal cytoplasm of the different algal species (Figure 4-2a).

MeHg uptake from the dissolved phase by copepods increased linearly during the 12 h of

exposure (Figure 4-3a), suggesting that MeHg uptake did not reach equilibrium within the first

12 h of exposure. The dry weight concentration factor ([Me^{203}Hg Bq g^{-1}]$_{copepod}$ / [Me^{203}Hg Bq

mL^{-1}]$_{dissolved\ phase}$) reached 3×10^4 at 12 h. Figure 4-3b shows the relationship between MeHg

influx rates and dissolved MeHg concentrations after 4 h of exposure. The higher aqueous MeHg

concentration led to a greater influx rate, suggesting the influx rate was directly dependent on the

ambient MeHg concentration. The metal influx rate constant of 35 (L g^{-1} d^{-1}, dry weight basis)

was obtained from the regression slope of Figure 4-3b.

Discussion

Hg assimilation and depuration from ingested food

Calculated AEs of Hg(II) and MeHg in copepods were comparable to previous studies. Fisher

et al. (1991) found that 21% of Hg(II) was assimilated by a marine copepod, *Anomalocera*

pattersoni, fed a prymnesiophyte diet, *I. galbana*. Mason et al. (1996) reported that 15% of Hg(II)

and 62% of MeHg were assimilated by marine copepods (*A. tonsa*, *Temora longicornis*,

Centropages sp.) fed a diatom diet, *Thalassiosira weissflogii*. A similar experiment conducted by

Lawson and Mason (1998) using marine copepods (*Eurytemora affinis*) and amphipods

(*Hyallela azteca*) fed *T. weissflogii* obtained an AE for MeHg in zooplankton of >50%. Williams

et al. (2010) reported AEs of Hg(II) and MeHg in the marine amphipod *Leptocheirus plumulosus*

fed *I. galbana* to be 6% and 81%, respectively. Overall, these results suggest that the AEs of

MeHg are much higher than the AEs of Hg(II), and that diet composition does not have a

pronounced influence on the assimilation of Hg(II) and MeHg in marine copepods.

As shown in Figure 4-2a, the pattern of AEs and cellular distributions of mercury in algal diets

agrees with other elements reported by Reinfelder and Fisher (1991). As noted above, Hg(II) and

MeHg showed two distinct groups. MeHg penetrated into the cytoplasm of algal cells more than

Hg(II) did, and AEs in zooplankton feeding on these algae followed correspondingly. Moreover,

we further compared our Hg data with other elements taken from previous copepod studies (Figure 4-2b). Generally, there was a strong linear relationship between AE and cytoplasmic distribution of the elements ($r^2 = 0.97$), with the slope close to 1 and the y-intercept close to 0. MeHg, which is biologically nonessential, has an AE that exceeds some essential metals (e.g., Zn, Cu and Fe) and is comparable to S and P (Figure 4-2b). Stewart and Fisher (2003a) reported that AEs of polonium in marine copepods varied significantly with different algal diets and ranged from 19 to 55%, which was also correlated to the percentage of Po in cytoplasm of algal cells. However, we did not observe significant differences in AEs and cytoplasmic distributions among the three algal diets for either Hg(II) or MeHg. The positive relationship of elemental distribution in algal cytoplasm with AEs in herbivorous animals probably reflects the degree to which the metal is released from ingested algal cells into the gut fluid of the copepod in a form that can cross the gut lining (Reinfelder and Fisher, 1991; Stewart and Fisher, 2003a). Thus, metals bound to compounds in algal cytoplasm that are sought by the animal (such as proteins or amino acids) may more effectively cross the gut lining (become assimilated) than metals bound to cellular components (such as cell walls) that remain undissolved in the gut.

The efflux rate constants of Hg(II) (0.29 d^{-1}) and MeHg (0.21 d^{-1}) from the copepods following uptake from the aqueous phase (k_{ew}) were 1.5 to 3-fold higher than other elements such as Ag (0.17 d^{-1}), Cd (0.11 d^{-1}), Co (0.12 d^{-1}) and Zn (0.11 d^{-1}) (Wang and Fisher, 1998) and an order of magnitude greater than Po (0.01-0.03 d^{-1}) (Stewart and Fisher, 2003a). For efflux rate constants following dietary uptake (k_{ef}), Hg(II) (0.47-0.66 d^{-1}) was much higher than MeHg (0.11-0.22 d^{-1}), as well as other elements like Ag (0.29 d^{-1}), Cd (0.30 d^{-1}), Co (0.28 d^{-1}), Se (0.16 d^{-1}), Zn (0.08 d^{-1}), and Po (0.01-0.07 d^{-1}) (Stewart and Fisher, 2003a; Wang and Fisher, 1998). Our results indicate that loss rates from copepods following uptake from food were generally

greater than those obtained from water, consistent with findings of Wang and Fisher (1998). Whether this difference is attributable to different copepod tissue distributions of accumulated metal from diet vs. water remains to be determined.

Methylmercury uptake from the dissolved phase

The calculated concentration factor and influx rate of MeHg were closer to Ag (10.42 L g^{-1} d^{-1}) than other elements (Wang and Fisher, 1998). The study of the physiology of trace element uptake in crustaceans by Rainbow (1997) noted that metals could enter these animals through either passive carrier-mediated transport or active transport through either ionic or protein channels. Like Ag and Cu, it is known that Hg (including MeHg) has a very strong affinity for sulfur and this may account for MeHg's very high concentration factors and influx rates from the dissolved phase.

Trophic transfer factors of Hg

Various models have been developed to assess and quantify bioaccumulation and biomagnification of elements and compounds in aquatic ecosystems. The combination of high assimilation efficiencies and low efflux rate constants of MeHg in copepods would result in potential biomagnification in food chains. Here we use a simple equation to evaluate the trophic transfer factor (TTF) for Hg(II) and MeHg (Reinfelder et al., 1998):

$$TTF = (\text{AE} \times \text{IR})/(k_{ef} + g) \qquad (2)$$

where AE is assimilation efficiency (%), IR is weight-specific ingestion rate (g g^{-1} d^{-1}, dry weight), k_{ef} is efflux rate constant from dietary uptake (d^{-1}) and g is growth rate constant (d^{-1}). For TTF values >1, biomagnification is expected. We used AE and k_{ef} values obtained from this

study and literature values for growth rate (0.03 d^{-1}) for *A. tonsa* (Mauchline, 1998). A range of

ingestion rates (0.33-0.43 g g^{-1} d^{-1}) of marine copepods from previous studies (Berggreen et al.,

1988; Lonsdale et al., 1996; Mauchline, 1998) were taken to calculate TTF. Calculated TTFs are

listed in Table 4-2. As expected, TTFs of Hg(II) were consistently low (≤0.2) and TTFs of MeHg

were all >1, suggesting that marine copepods concentrate MeHg and act as an important

intermediate between phytoplankton and forage fish to transfer MeHg in marine food chains.

Modeling of Hg uptake pathways in copepods

Metal accumulation in aquatic organisms can be depicted as a balance between metal uptake

and loss from aqueous and dietary routes. We used a simple first-order equation to describe the

relative contribution from each route and predict the overall final concentrations in zooplankton.

At steady-state, when metal uptake is balanced by metal elimination and growth, the metal

concentration in a given organism can be described by the following equations (Reinfelder et al.,

1998; Thomann, 1981):

$$C_{ss} = C_{ss,w} + C_{ss,f} \qquad (3)$$

$$C_{ss} = [(k_u \times C_w)/(k_{ew} + g)] + [(AE \times IR \times C_f)/(k_{ef} + g)] \qquad (4)$$

where C_{ss} is the metal concentration (μg g^{-1} dry weight) in an organism at steady-state, $C_{ss,w}$ is

the metal concentration (μg g^{-1}) obtained from the dissolved phase, $C_{ss,f}$ is the metal

concentration (μg g^{-1}) acquired from diet, k_u is the metal uptake rate constant (L g^{-1} d^{-1}) from the

dissolved phase, C_w and C_f are the metal concentration in the water (μg L^{-1}) and the prey (μg g^{-1}),

respectively, k_{ew} and k_{ef} are the efflux rate constants (d^{-1}) following aqueous and dietary uptake,

respectively, AE is the metal assimilation efficiency (%), IR is the weight-specific ingestion rate

(g g^{-1} d^{-1}, dry weight), and *g* is the growth rate constant (d^{-1}). We applied equation 4 to

understand MeHg accumulation in the copepods, and used average values of k_u (35 L g^{-1} d^{-1}), k_{ew} (0.21 d^{-1}), k_{ef} (0.16 d^{-1}) and AE (72%) obtained from our experiments. Maximum IR (0.43 g g^{-1} d^{-1}, dry weight) and average g (0.03 d^{-1}) were taken from the previous studies mentioned above (Berggreen et al., 1988; Lonsdale et al., 1996; Mauchline, 1998). C_{ss} may vary due to variability in biologically mediated parameters such as AE and IR (which may vary due to food quality and/or concentration, and other physiological and/or environmental conditions) as well as variability in geochemical parameters (such as C_w and C_f which may vary regionally and temporally) in different aquatic environments. First, we used the reported bioconcentration factor (BCF, C_f-to-C_w ratio on a dry weight basis) of MeHg between water and phytoplankton to model the relative importance of aqueous and dietary uptake to marine copepods. The volume concentration factors of MeHg in diverse marine algae ranged from $10^{4.2}$ to $10^{6.8}$ (Lee and Fisher, 2016), which was equivalent to BCFs of $10^{4.9}$ to $10^{7.5}$ (assuming mean cell volume-to-dry weight ratio of 5.0 (Fisher et al., 1983a)). Figure 4-4 shows the model predicted percentage of MeHg uptake from aqueous vs. dietary sources as a function of MeHg BCFs in algal food. Overall, diet is the major source (>50%) for MeHg accumulation in copepods. As the MeHg BCF increases, the MeHg uptake contributed from the dissolved phase decreases sharply. In the open ocean where MeHg BCFs in phytoplankton are typically greater than 10^6 (Gosnell and Mason, 2015; Hammerschmidt and Bowman, 2012), our model suggests that the dietary route would be the predominant pathway (>90%) for copepods to acquire MeHg.

In addition, we incorporated field data into our model and compared the outcome with independently measured data. To date, the applicable field data we found were from five different marine environments (Table 4-3), including the NW Atlantic (Hammerschmidt et al., 2013), the Central Pacific (Gosnell and Mason, 2015; Munson et al., 2015), Long Island Sound

(Hammerschmidt and Fitzgerald, 2006a), Groswater Bay, Canada (Schartup et al., 2015a) and the Gulf of Lions, France (Cossa et al., 2012). In Table 4-3, we present the field data and normalized them onto a dry weight basis. If the water content of biota samples was not clearly noted in the original paper, we assumed a water content of 95% for phytoplankton and 90% for zooplankton. We used a 200 μm cut-off to differentiate between phytoplankton (microseston) and zooplankton. The size range used in each study was also noted in Table 4-3. Although parameters used in our model referred specifically to the copepod *A. tonsa*, previous work found no pronounced differences for other metals among different calanoid copepod species (Reinfelder and Fisher, 1991). Our model-predicted values of MeHg are comparable with those directly measured in bulk zooplankton (Table 4-3). Zooplankton collected in the Long Island Sound study were primarily composed of calanoid copepods (*Acartia* spp.) (Hammerschmidt and Fitzgerald, 2006a), and the predicted values closely match the measured values. In the Groswater Bay study, there was only one sample for microseston which may have biased the predicted value. The size range used for collecting microseston in the Gulf of Lions study was 80 to 200 μm, which did not comprehensively cover the size spectrum of marine nanophytoplankton and therefore may increase the uncertainty of the predicted value. Note that the k_u value for our modeling was based on experiments using elevated C_w values of Hg(II) and MeHg. That the model prediction of C_{ss} in zooplankton matched independent field values (Table 4-3) suggests that this k_u value is applicable to Hg concentrations in natural waters.

Overall, our model results suggested that it is possible to predict the concentration of MeHg in copepods given the concentration of MeHg in water and phytoplankton. Of course, it is easier to test model predictions in the field when there is a clear delineation of phytoplankton and zooplankton from other suspended particles in the same size ranges. Complications can arise

when suspended abiotic particles (e.g., sediment particles) co-occur with the plankton. Recently, Lee and Fisher (2016) reported that MeHg concentration factors in diverse marine phytoplankton cells are related to algal cell size. Therefore, the MeHg concentration in both phytoplankton and zooplankton can be calculated with only a few measured parameters. The parameters measured in this study along with the established model should be useful in refining the global biogeochemical models describing Hg cycling in the marine environment.

Table 4-1. The calculated assimilation efficiencies (AEs, %) and efflux rate constants (k_e, d^{-1}) of Hg(II) and MeHg in the copepod *A. tonsa* from different uptake routes.

Uptake route	Hg(II)		MeHg	
	AE (%)	k_e (1/d)	AE (%)	k_e (1/d)
Diatom	31	0.64	79	0.22
Chlorophyte	31	0.66	78	0.16
Cryptophyte	25	0.47	58	0.11
Water		0.29		0.21

Table 4-2. The estimated trophic transfer factors (TTFs) of Hg(II) and MeHg in the copepod *A. tonsa* following uptake from different food types.

Food type	IR (g g^{-1} d^{-1})	g (d^{-1})	TTF	
			Hg(II)	MeHg
Diatom			0.15-0.20	1.04-1.35
Chlorophyte	0.33-0.43	0.03	0.15-0.19	1.37-1.78
Cryptophyte			0.16-0.21	1.40-1.83

AEs and k_e's are given in Table 4-1. IR = ingestion rate; g = growth rate.

Table 4-3. Comparison between measured MeHg concentrations in zooplankton collected from different regions and predicted MeHg concentrations from the model using lab-derived and field-collected parameters.

Study area	Water (ng L^{-1})	Microseston (ng g^{-1} d.w.)	Zooplankton (ng g^{-1} d.w.) measured	predicted	Reference
NW Atlantic	0.0066 ± 0.0020	2.8 ± 1.2 (0.2-200 μm)	5.6 ± 5.6 (>200 μm)	5.5 ± 2.0	Hammerschmidt et al., 2013
Central Pacific	0.019 ± 0.023	11.7 ± 10.4 (0.2-200 μm)	2 - 34 (>200 μm)	21.5 ± 16.9	Munson et al., 2015 Gosnell and Mason 2015
Long Island Sound	0.03	4.7 ± 2.8 (0.2-200 μm)	11 ± 2 (>200 μm)	12 ± 4	Hammerschmidt and Fitzgerald 2006
Groswater Bay	0.023 ± 0.012	0.16 (5-200 μm)	7.0 (200-500 μm)	3.6 ± 1.7	Schartup et al., 2015
Gulf of Lion	0.0045 ± 0.0026	1.4 ± 1.0 (80-200 μm)	5.2 ± 3.9 (200-500 μm)	2.9 ± 1.6	Cossa et al., 2012

Thus, C_w for these calculations equals the MeHg concentration reported for water at each site, C_f equals the MeHg concentration in microseston at each site, and other parameters for MeHg from equation 4 are means from values given in Table 1. Thus, k_{ef} = 0.16 (d^{-1}), AE = 72 (%), IR = 0.43 (g g^{-1} d^{-1}), g = 0.03 (d^{-1}), k_u = 35 (L g^{-1} d^{-1}), k_{ew} = 0.21 (d^{-1}). Model-predicted values for copepods are compared with independently measured MeHg concentrations in zooplankton at each site. Propagation of uncertainty (1 SD) was calculated if applicable.
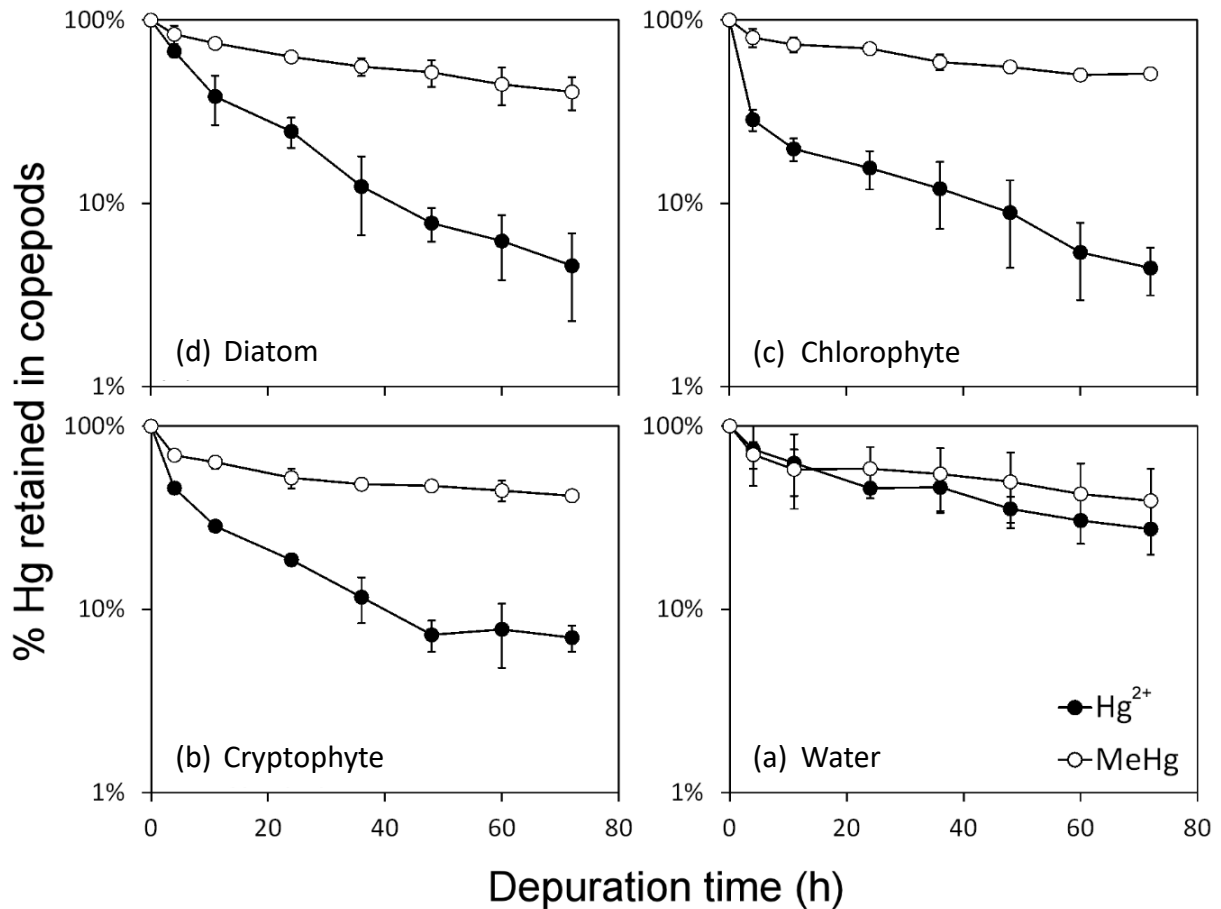
Figure 4-1. Depuration curves of Hg(II) and MeHg in the copepod *A. tonsa* from all the experiments. Hg sources in (a) to (c) are different algal foods and (d) is the dissolved phase. Time zero represents the radioactivity measured immediately after feeding, which is assigned as 100%. In (a)-(c), radioactivity from controls (dissolved phase) were subtracted from radioactive measurements following feeding. Each point represents the average from three replicates and error bars denote 1 SD.
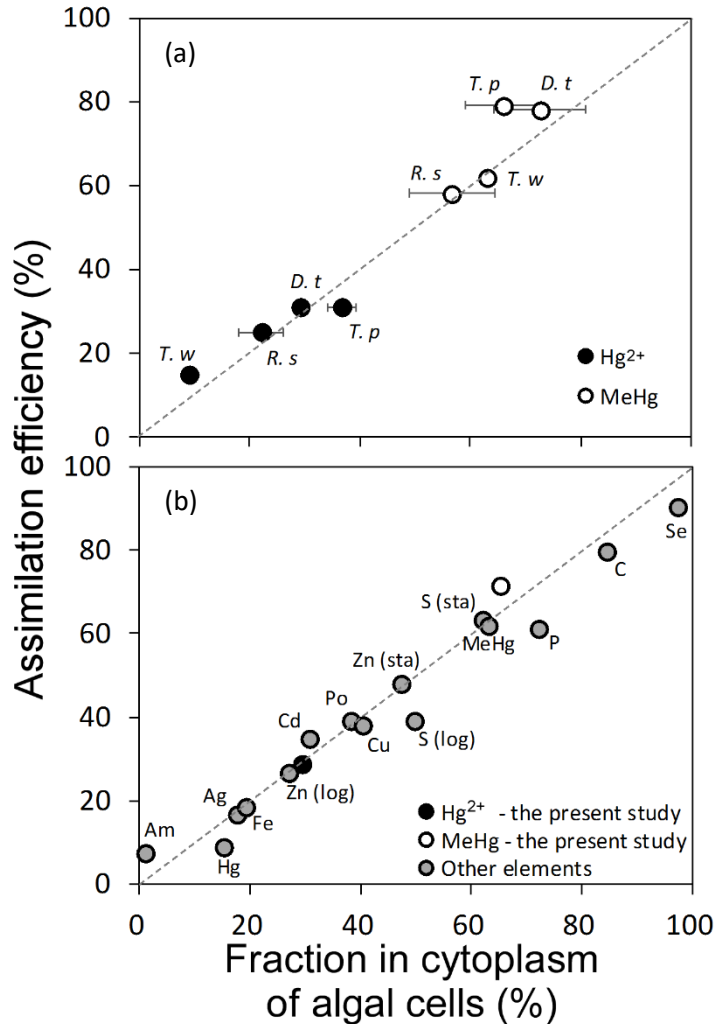
Figure 4-2. (a) Relationship between assimilation efficiencies of Hg in the copepod *A. tonsa* and cytoplasmic distributions of Hg in algal cells. (b) Assimilation efficiency of ingested elements in copepods as a function of the cytoplasmic distributions of those elements in the ingested algal cells. The solid and open circles represent Hg(II) and MeHg, respectively. The dashed line is the 1:1 ratio line. *T. p*: *Thalassiosira pseudonana*, *D. t*: *Dunaliella tertiolecta*, *R. s*: *Rhodomonas salina*, *T. w*: *Thalassiosira weissflogii; T. w* data in (a) is from Mason et al. (1996). The linear regression equation in (a): $y = 1.04x + 1.01$, $r^2 = 0.95$. Data in (b) are average values from Reinfelder and Fisher (1991), Hutchins et al. (1995), Mason et al. (1996), Chang and Reinfelder (2000), Stewart and Fisher (2003a) and this study. "Sta" and "log" denote stationary phase and exponential growth phase of the phytoplankton cells, respectively, consumed by the copepods. The linear regression equation in (b): $y = 0.91x + 2.38$, $r^2 = 0.97$.
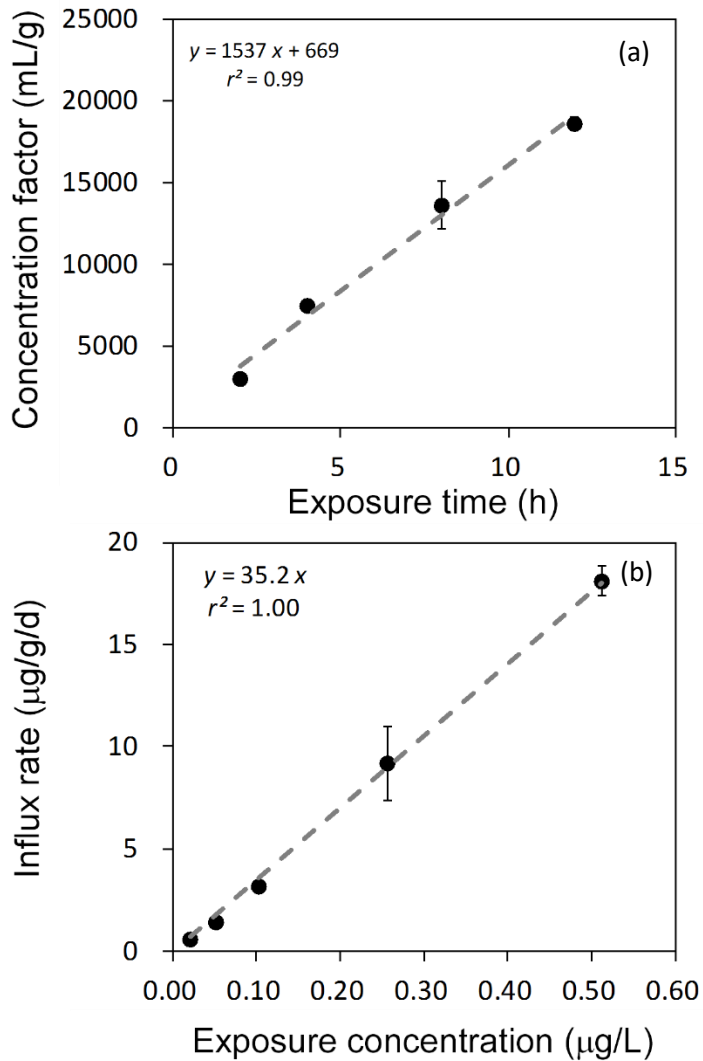
Figure 4-3. (a) The calculated concentration factors of MeHg in copepods exposed to dissolved MeHg as a function of exposure time. (b) The influx rate of MeHg in *A. tonsa* from the aqueous phase as a function of ambient dissolved concentrations. Concentration factors represent the $[MeHg]_{copepods}$ to $[MeHg]_{water}$ ratio for each treatment. Each point represents the average from two replicates and error bars denote 1 SD.
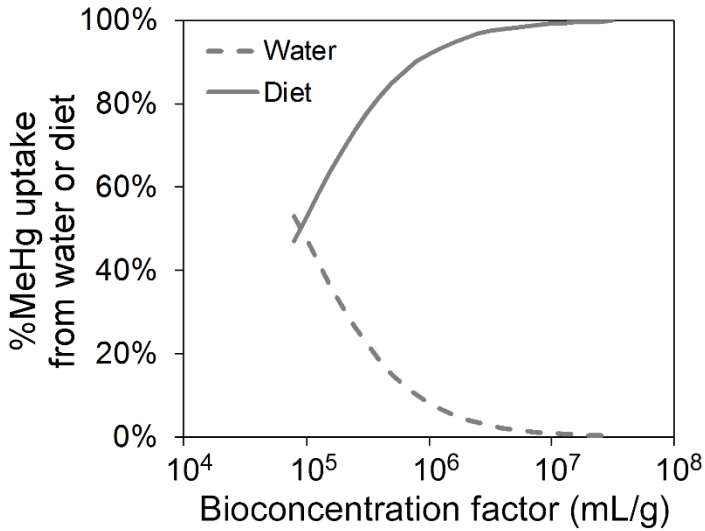
Figure 4-4. The model prediction of percentage of total MeHg uptake in the copepod *A. tonsa* from dissolved or dietary sources as a function of MeHg bioconcentration factor (BCF) in algae, which is proportional to C_f (Eqn. 4). The assumed BCF ranged from $10^{4.9}$ to $10^{7.5}$ (see text, Fisher et al. (1983a); Lee and Fisher (2016)). The solid and dashed lines represent the contribution from diet and water, respectively. The parameters used in this calculation were the mean values from Table 4-1 and 4-2.

Chapter 5

Microbial generation of volatile mercury from dissolved methylmercury in seawater

Abstract

Elemental mercury (Hg^0) formation followed by subsequent evasion from surface seawater plays a principal role in the marine mercury cycle, and is mainly controlled by abiotic (photochemical) and biotic (microbial) processes. However, the relative importance of microbial-mediated conversion of Hg^0 from either Hg(II) or monomethylmercury (MeHg) in seawater remains unclear. The gamma-emitting ^{203}Hg was used as a tracer and a rapid radioassay method was developed to evaluate the kinetics of Hg^0 production by natural coastal bacterial assemblages under controlled lab conditions. Natural bacterial assemblages in seawater were found to produce Hg^0 from seawater containing Hg(II) and MeHg and this Hg^0 was rapidly lost to the overlying air, even after storage at 4°C for 6 years. Hg^0 production rates were independent of dissolved Hg(II) and MeHg concentrations, and were directly a function of bacterioplankton cell densities. That low temperatures inhibited Hg^0 formation and bacterial mercuric reductase was detected in our samples suggest that bacterial metabolic activities and enzymatic reactions are involved in Hg^0 gas formation. These findings demonstrate the importance of Hg^0 evasion mediated by natural marine bacteria, and the subsequent decline in Hg(II) and MeHg concentrations may have significant implications for the amount of Hg entering marine food webs.

Introduction

Elemental Hg (Hg^0) can be found at all depths in the ocean and is usually supersaturated in surface waters (Fitzgerald et al., 2007), resulting in its subsequent evasion from the sea surface to the overlying air. Several studies have demonstrated the significance of Hg^0 evasion from the surface ocean (Fitzgerald et al., 1984; Kim and Fitzgerald, 1986; Mason et al., 1994; Mason and Sheu, 2002; Rolfhus and Fitzgerald, 2001). The sea-air exchange of Hg^0 is rapid and is

associated directly with Hg^0 concentrations in surface waters. Therefore, the transformation of other Hg species to Hg^0 is an important process in marine Hg cycling. In the mixed layer, Hg^0 can be produced by biological and/or photochemical reduction of reactive Hg(II), leading to decreased Hg(II) concentrations in the water column and therefore avoiding further methylation of Hg(II). Moreover, monomethylmercury (MeHg) can also be converted to Hg^0 through biotic and/or abiotic demethylation processes (Barkay et al., 2003; Fitzgerald et al., 2007). Both Hg(II) and MeHg are toxic, and the latter is bioaccumulative in aquatic organisms and can build up in aquatic food chains (Morel et al., 1998). Hence, Hg^0 formation has been suggested to be beneficial to aquatic organisms because it can not only directly remove aqueous Hg(II) and MeHg, but also potentially reduce MeHg production from Hg(II) in the water column (Mason et al., 1995).

Hg^0 formation in the surface mixed layer can involve a variety of complex abiotic and/or biotic processes. Abiotic processes such as photochemical reduction of Hg(II) ~~has~~ have been shown to produce Hg^0, where solar radiation (visible and ultraviolet), dissolved organic matter, and inorganic free radicals are considered key factors involved in the photochemical formation of Hg^0 from Hg(II) (Amyot et al., 1997; Costa and Liss, 1999; Costa and Liss, 2000; Nriagu, 1994; Vost et al., 2012). In addition, photodegradation of MeHg can also produce Hg^0 (Sellers et al., 1996; Suda et al., 1993). Biologically mediated processes like microbial Hg(II) reduction and MeHg demethylation have also been shown to form Hg^0 (Barkay et al., 2003; Barkay et al., 1991; Robinson and Tuovinen, 1984). These processes can be attributable to prokaryotes possessing the Hg-resistant *mer* operon at a relatively high Hg exposure condition (Morel et al., 1998; Yu et al., 1996). For example, the bacterial mercuric reductase enzyme, *merA* governs the conversion of dissolved Hg(II) to volatile Hg^0. Microorganisms with enzymes of Hg-resistance are

widespread from diverse environments (Barkay et al., 1989; Gionfriddo et al., 2016; Osborn et al., 1997; Vetriani et al., 2005). Whether the transcription of the *mer* operon can be induced at natural Hg concentrations (pico- or femtomolar range) is not fully understood. Poulain et al. (2007) reported that *merA* genes were present and expressed by microbes from remote polar waters. However, some studies suggested Hg^0 formation can occur by other uncharacterized microbial processes (Barkay et al., 2003; Kuss et al., 2015; Oremland et al., 1991). Hg(II) reduction can also be carried out by eukaryotic phytoplankton (Ben-Bassat and Mayer, 1977; Mason et al., 1995), but the mechanism of this pathway has remained undefined. Overall, microorganisms, especially bacteria, are considered to play a fundamental role in the aquatic biogeochemistry of Hg.

In this chapter, we demonstrate how marine bacterioplankton convert MeHg to Hg^0 which, at prevailing ocean temperatures, is released rapidly to the atmosphere. We focused on Hg^0 formation mediated by natural assemblages of marine microorganisms exposed to picomolar Hg concentrations. Studies quantifying the kinetics of Hg^0 evasion from seawater are few, and our study is the first to investigate the kinetics of Hg^0 formation from MeHg by marine microorganisms. We developed a device to determine the kinetics of Hg^0 formation from either dissolved Hg(II) or MeHg and used ^{203}Hg as a gamma-emitting radiotracer of Hg^0 gas evasion. We further investigated how light, temperature, and bacterial abundance and metabolic activity influence Hg^0 production and evasion from seawater.

Materials and Methods

^{203}Hg preparation and Me^{203}Hg synthesis

The gamma-emitting radioisotope, ^{203}Hg (half-life = 46.6 d) was used in this study to trace the transformation of Hg species between dissolved and gaseous phases. A solution of ^{203}Hg(II) in 1 M HCl was obtained from Eckert and Ziegler Isotope Products (Valencia, California) with a specific activity of 185 GBq g^{-1} and was further converted to methyl-^{203}Hg (Me^{203}Hg) in the lab following established methods (Lee and Fisher, 2016; Rouleau and Block, 1997). In brief, ^{203}Hg(II) solution was mixed with methylcobalamin ($C_{63}H_{91}CoN_{13}O_{14}P$) and acetate buffer at pH 5. Allowing the reaction to proceed in the dark for 18 to 24 h, Me^{203}Hg was formed spontaneously. Following extraction by dichloromethane (CH_2Cl_2) and purification processes, Me^{203}Hg was re-dissolved in Milli-Q® water and was ready to use. The conversion yield (fraction of ^{203}Hg recovered as Me^{203}Hg) was $98 \pm 2\%$ (n = 3). Activities of ^{203}Hg and Me^{203}Hg used in this study ranged from 0.019 kBq L^{-1} to 2.23 kBq L^{-1}, corresponding to concentrations of 1 to 100 pM of total (stable plus radioactive) Hg. This approach with radiotracer ^{203}Hg can provide precise, rapid and direct measurement of Hg evasion from seawater to the atmosphere, avoiding lengthy analytical procedures and potential contamination.

Natural bacterioplankton assemblages

The natural bacterial assemblages used in this study were collected from Southampton, NY (8 km offshore, Lat. 40.77°N, Long. 72.43°W, 35 psu) and Stony Brook, NY (Lat. 40.92°N, Long. 73.15°W, 30 psu). Southampton seawater (SHSW) was collected with coarse filtration (~100 μm) in June 2011, stored at 4°C in the dark, and brought to room temperature (22°C) 2 d before experiments after 6 years of storage at 4°C. Further considerations on the possible artifacts associated with this storage are presented in the Discussion section. Stony Brook seawater (SBSW) was collected during high tide one day prior to experiments. Background concentrations

of Hg(II) were ~5 pM, and MeHg were close to the detection limit (~5 fM) in these two waters,

as determined using Tekran 2600 and 2700 mercury analyzers, respectively. Seawater used for

experiments was filtered through sterile 1 μm polycarbonate membranes to remove all large

particles including phytoplankton and zooplankton, leaving only bacterioplankton and similarly

sized (or smaller) particles in the seawater. In general, SHSW and SBSW contain bacterial

densities of about $0.2–0.4 \times 10^6$ cells mL^{-1} and $4–5 \times 10^6$ cells mL^{-1}, respectively. We used

$SHSW_{1 \, μm}$ and $SBSW_{1 \, μm}$ to indicate 1 μm-filtered seawater with bacteria, and $SHSW_{ctrl}$ and

$SBSW_{ctrl}$ to represent seawater without bacteria (experimental controls).

Experimental setup and general approach

Figure 5-1 shows a schematic of the experimental apparatus used in this study. All the

experiments were performed in 250 mL Pyrex® Erlenmeyer flasks with Teflon-lined screw caps

(containing two holes drilled through the caps for an air inlet and outlet). 200 mL of seawater

with bacteria was injected with microliter quantities of ^{203}Hg or $Me^{203}Hg$ solutions (dissolved in

1 M HCl and Milli-Q® water, respectively), yielding ranges of concentrations of 1 to 100 pM.

Flasks were incubated at a constant temperature under a 14 h:10 h light/dark cycle provided by

cool white fluorescent lamps. Seawater was continuously bubbled gently with particle-free and

Hg-free air and the produced gaseous ^{203}Hg species was then collected in a Hg trap through the

air outlet. The Hg trap was made of a quartz tube, glass wool and gold-coated beads purchased

from Brooks Rand Instruments (Seattle, Washington) (Fig. 5-1). Radioactivity of ^{203}Hg in the Hg

traps from each culture was determined with an LKB Wallac 1282 Compugamma NaI(Tl)

gamma detector at 279 keV. All samples were counted with standards and decay-corrected.

Propagated counting errors were <5%. From measured activities on traps, the percentage of Hg species transformed to Hg^0 gas can be calculated as:

$$\%Hg^0 \text{ evolved} = \frac{[Bq\ ^{203}Hg]_{trap}}{[Bq\ ^{203}Hg]_{added}}$$

The rate of Hg^0 formation attributed to bacterial activity can be calculated as:

$$\frac{[Hg^0 evolved]_{bacteria} - [Hg^0 evolved]_{control}}{[Hg(II)\ or\ MeHg]_{dissolved} \times Time}$$

Assuming Hg(II) reduction and MeHg demethylation as irreversible pseudo-first order kinetics, the following equations apply:

$$\frac{d[Hg(II)\ or\ MeHg]_{dissolved}}{dt} = -k_r[Hg(II)\ or\ MeHg]_{dissolved} = \frac{d[Hg^0]_{evolved}}{dt}$$

Where k_r is the pseudo-first order rate constant for gross reactions under the experimental conditions. Reversible reactions such as Hg^0 oxidation and Hg(II) methylation were neglected because they were unlikely to occur during our experimental incubations.

Of the various Hg species, the Henry's law coefficients of Hg^0 and dimethylmercury (DMHg) indicate they are highly volatile and could volatilize from the dissolved phase at ambient temperatures. To distinguish Hg^0 from DMHg in the gas traps, we used another Hg trap, Bond Elut ENV (Agilent Tech., Santa Clara, California), which effectively collects volatile organomercury compounds (Baya et al., 2013). In preliminary experiments, produced gaseous Hg was first passed through a Bond Elut trap followed by a gold trap without exceeding the reported breakthrough volume of the Bond Elut trap. We found very little Hg retained in the

Bond Elut trap and >95% of the Hg was collected in the gold trap. The Bond Elut trap can also collect a small fraction of Hg^0 (Baya et al., 2013). Thus, we concluded that Hg^0 was the dominant gaseous species produced in our study.

Short-term incubation experiments

We first performed a short term (1d) incubation experiment to test the influence of Hg concentrations and bacterial densities on Hg gas production. For Hg concentration experiments, triplicate samples of 200 mL SHSW with the same initial bacteria density were injected with $^{203}Hg(II)$ or $Me^{203}Hg$ at three different concentrations (1, 10, and 100 pM) and were then incubated for 24 h at 24°C under a light/dark cycle. For bacterial density experiments, duplicate samples of 200 mL SHSW with varying initial bacterial densities were prepared; all cultures were from different carboys, each with its own bacterial community and cell density. There was an addition of 10 pM of $^{203}Hg(II)$ or $Me^{203}Hg$ in each treatment, and all cultures were incubated for 24 h. After 24 h, Hg traps and 1 mL of unfiltered seawater were collected for radioanalysis, and the bacterial densities were measured.

Long-term incubation experiments

A series of long-term (4 d) incubation experiments were carried out in order to evaluate the rates at which Hg gas evolved from each flask to overlying air. First, we determined the Hg gas evasion from three different types of controls, 0.2 μm filtered SHSW (removing all bacteria detectable with DAPI staining), autoclaved SHSW (120°C for 30 min), and SHSW with antibiotics (1% GE HyClone™ Penicillin-Streptomycin). Second, we examined how temperature (24°C vs. 4°C) and light (light vs. dark) influenced the Hg gas evolved from SHSW. Third, we

examined the Hg gas production in freshly collected SBSW, as well as the difference between unfiltered SBSW and 1 μm-filtered SBSW.

Experimental procedures for long-term incubations were similar to those described in short-term incubation experiments. Briefly, 200 mL seawater was injected with ^{203}Hg(II) or Me^{203}Hg at concentrations from 40 to 80 pM, and incubated at either 4°C or 24°C with or without light. The Hg trap was collected and replaced with a new one at each sample time (4, 8, 12, 24, 36, 48, 72, and 96 h). In addition, 1 mL of unfiltered seawater was collected for bacterial density determination at each sample time. Control treatments (seawater without bacteria) containing equivalent amounts of ^{203}Hg were performed simultaneously. To calculate the Hg mass balance ($[Hg]_{added} = [Hg]_{suspension} + [Hg]_{trap} + [Hg]_{flask\ wall}$) in each flask, sorption of Hg(II) or MeHg onto culture flasks was examined by acid washing (1 M HCl) the flask walls at the end of the experiment. Across all experiments, the mass balance of Hg(II) and MeHg treatments were 94 ± 10% and 97 ± 2%, respectively.

Bacterial density and bacterial production

A modified DAPI (4',6-diamidino-2-phenylindole) staining method (Sherr et al., 2001) was used to count bacterial densities. Bacterial cell samples were fixed with 2% glutaraldehyde solution and were stored at 4°C. Prior to cell counts, cell samples were mixed with DAPI (1 μg mL^{-1}) and stained cells were then filtered onto a 0.2 μm black polycarbonate membrane at a vacuum pressure <300 mm Hg. Cell counts were obtained with the use of epifluorescence on an inverted microscope under ultraviolet light excitation.

Bacterial production measurements were performed as a parallel experiment to the Hg evasion experiments, using leucine incorporation (Kirchman, 1993). Radiolabeled L-[4,5-^{3}H]-leucine

was purchased from PerkinElmer. In brief, 20 mL of unfiltered seawater was collected in an incubation vial at each time point (6, 12, 24, 48, 72, and 96 h), injected with ^{3}H-leucine to yield a concentration of 20 nM (corresponding to 24.8 kBq per vial) and incubated for 6 h. Incubation was terminated by adding trichloroacetic acid (TCA) at a concentration of 5%. After heating for 20 min at 80°C, bacterial cells were collected onto a 0.22 μm cellulose acetate filter at a vacuum pressure <300 mm Hg. The filter with cells was dissolved by adding ethyl acetate in a scintillation vial, mixed with Ultima Gold™ XR liquid scintillation cocktail, and radioactivity determined using a PerkinElmer Tri-Carb® 2810 TR liquid scintillation analyzer.

Conventional PCR analysis for mercuric reductase merA

Total DNA was extracted from seawater, using a PowerWater® Sterivex™ DNA isolation kit (MO BIO, Carlsbad, CA). About 10 L of SHSW and 2 L of SBSW were filtered to collect enough DNA concentrations for analysis and *merA* was measured following the procedure of Poulain et al. (2015). PCR was performed using a Biometra® T3000 Thermocycler. PCR conditions consisted of a 10-min incubation at 95 °C, followed by 35 cycles of 95°C for 30 s, 63°C for 15 s, 72°C for 30 s, and a final extension step at 72°C for 5 min. Final concentrations of the PCR mixture were $1\times$PCR buffer, 2.5 mM MgCl$_2$, 0.2 μM forward/reverse primers (merA2 F: CCTGCGTCAACGTCGGCTG, merA2 R: GCGATCAGGCAGCGGTCGAA), 0.2 mM dNTPs, and 1 U Taq Polymerase. Samples were analyzed with a positive control (*Pseudomonas aeruginosa* containing the Hg resistance plasmid pVS1) (Lloyd et al., 2016), and a negative control (reagents only). Amplicons were separated by electrophoresis and visualized under ultraviolet light.

Results

Short term incubations

Figure 5-2 shows the total percentage of Hg^0 gas evolved after 24 h as a function of (a) dissolved Hg(II) and MeHg concentrations and (b) average bacterial density. The %Hg^0 evolved from each culture stayed almost constant across three different Hg concentrations (1 to 100 pM) at ~20% for Hg(II) treatments and ~5% for MeHg treatments (Fig. 5-2a). In these cultures, the initial bacterial densities were $0.34–0.40 \times 10^6$ cells mL^{-1}, and the bacterial densities at 24 h were $0.81–1.2 \times 10^6$ cells mL^{-1}. In separate experiments which used cultures with varying bacterial cell densities and only 10 pM of Hg(II) or MeHg, the %Hg^0 that evolved as a gas ranged from 6.2% to 31% in Hg(II) treatments and from 2.1% to 13% in MeHg treatments depending on the bacterial abundance (Fig. 2b); Hg^0 released was positively correlated with bacterial density. We performed each experiment twice and got very similar results. At the same bacterial density, Hg^0 production was always higher from Hg(II) treatments than from MeHg treatments.

Long term incubations (SHSW- Background evasion)

Figure 5-3 shows the Hg^0 evasion kinetics from three different control treatments. Generally, in Hg(II) treatments (Fig. 5-3a), 0.2 μm sterile-filtered SHSW and autoclaved SHSW had very similar patterns, rapid Hg^0 formation in the first 12 h then followed by very slow formation, with an overall 5–9% of Hg^0 evolved. Controls with antibiotics showed almost no Hg^0 production in the first 24 h, but increased Hg^0 evasion was observed after 36 h (Fig. 5-3a). In MeHg treatments (Fig. 5-3b), all three types of controls showed very low Hg^0 formation over 72 h (overall < 1%), suggesting MeHg was very stable in seawater without bacteria. For the all other experiments, we used 0.2 μm sterile-filtered seawater for controls.

Long term incubations (SHSW- Temperature and light)

Figure 5-4 shows the Hg^0 evasion from (a) Hg(II) and (b) MeHg treatments in SHSW over 96 h at two different temperatures, and (c) their corresponding bacterial cell densities. Rapid evasion of Hg^0 from Hg(II)-treated SHSW with bacteria within 24 h was observed (Fig. 5-4a). Total $\%Hg^0$ evolved was $32.6 \pm 1.6\%$ at 24°C after 96 h, but at 4°C it was only $8.0 \pm 2.3\%$. The total %Hg evasion in controls was $7.6 \pm 3.5\%$ at 24°C and $5.6 \pm 1.4\%$ at 4°C. Total Hg^0 evasion from MeHg-treated SHSW with bacteria after 4 d was $18.9 \pm 1.7\%$ at 24°C and was $10.2 \pm 0.4\%$ at 4°C, and both showed the same linear increasing patterns over time (Fig. 5-4b). Controls at two temperatures both showed very low Hg^0 production after 96 h ($< 0.4\%$) and no bacterial growth. Bacterial growth was more pronounced at 24°C (more than one doubling after 96 h) than at 4°C, where scant growth occurred (Fig. 5-4c). The results of bacterial production at 24°C are shown in Fig. 5-4d. The bacterial production, as inferred from leucine uptake, increased over time, ranging from 0.09 to 0.35 µg-C L^{-1} h^{-1}. Normalized to bacterial density, the estimated production rate ranged from 0.21 to 0.44 fg C $cell^{-1}$ h^{-1}; normalized to bacterial carbon (20 fg C $cell^{-1}$) (Lee and Fuhrman, 1987) the bacterial production increased at a rate of 1.1 to 2.2% h^{-1}. As the lower estimated value, which is the rate reflective of the initial production rate, closely matches the observed growth rate of the bacteria (increase in cell number day^{-1}) (Fig. 5-2c), it appears from the leucine incorporation rates that all the cells observed by DAPI were metabolically active.

For both Hg(II) and MeHg treatments, there was no significant difference in Hg^0 evasion between light and dark conditions (Fig. 5-5). In addition, Hg^0 evasion in controls and bacterial growth were not affected by light (data not shown).

Long term incubations (SBSW)

The results of Hg^0 evasion from freshly collected SBSW are shown in Figure 5-6 (note that presented data contain unfiltered and 1 µm-filtered SBSW). For Hg(II)-treated SBSW, $70.5 \pm 5.4\%$, $53.4 \pm 3.1\%$, and $11.2 \pm 1.3\%$ of Hg^0 evolved from $SBSW_{unfiltered}$, $SBSW_{1\ \mu m}$, and $SBSW_{ctrl}$ after 96 h, respectively (Fig. 5-6a). For MeHg-treated SBSW, $18.8 \pm 0.6\%$, $7.9 \pm 0.2\%$, and $0.4 \pm 0.1\%$ of Hg^0 evolved from $SBSW_{unfiltered}$, $SBSW_{1\ \mu m}$, and $SBSW_{ctrl}$ after 96 h, respectively (Fig. 5-6b). Bacterial densities in SBSW ranged from 4.3 to 7.1×10^6 cells mL^{-1} (Fig. 5-6c).

Hg^0 production rate

After correcting for abiotic Hg^0 production (evasion in controls), average Hg^0 formation rates by bacteria in different treatments over 4 d of incubation are presented in Table 1. The Hg^0 production rates by bacteria at different time intervals were also calculated (Figs. 5-7a, 5-7b, data from $SBSW_{unfiltered}$ not shown). For Hg(II)-treated seawater, the production rate was high at the first day (0-24 h) and then declined afterward (Fig. 5-7a). Notably, a significant decline after 1 day can be found in SHSW (both 24°C and 4°C treatments). In contrast, a significant decline can be found after 3 days in SBSW. For MeHg-treated seawater, the production rate gradually increased over time (Fig. 5-7b). Calculated Hg^0 production rate in figure 7a-b could have been biased by differences in the bacterial biomass among treatments. Therefore, we further normalized the Hg^0 production rate to bacterial density (Figs. 5-7c, 5-7d).

Discussion

Effects of Hg concentrations and bacterial densities

Regardless of the concentrations of dissolved Hg(II) or MeHg, the percentage of the total that resulted in Hg^0 formation in $SHSW_{1\mu m}$ stayed constant over a 1-day incubation (Fig. 5-2a). These results suggest that the fraction of total Hg that was bound to bacterial cells remained constant and reached equilibrium rapidly across three concentrations. Limited by the specific activity of ^{203}Hg, the lowest Hg concentration used in this study was 1 pM, which was still higher than typical concentrations (fM to pM range) in nearly all marine ecosystems (especially for MeHg). Because there was no significant difference in mercury behavior across three concentrations (over 2 orders of magnitude), extrapolation of the experimental results to lower Hg concentrations may be valid.

Hg^0 evasion from Hg(II)- and MeHg-treated seawater both positively correlated with bacterial density, consistent with observation of Rolfhus and Fitzgerald (2004) in coastal seawater. The striking consistency of our results from different experiments suggests that the bacterial assemblages did not differ from SHSW in different storage containers after 6 years of storage at 4°C. The *y*-intercept of regression lines observed in Fig. 5-2b represents the percentage of abiotic Hg^0 formation from each treatment, ~9% for Hg(II) and ~1% for MeHg. These values are comparable to the results of background evasion described above in Results (background evasion).

Abiotic Hg^0 production from control treatments

The Hg^0 formation in SHSW controls that were 0.2 μm sterile-filtered or autoclaved was consistent with findings that reactive Hg(II) might be reduced abiotically in a very short time in

116

the presence of reductants in seawater or on flask walls (Mason et al., 1995). For controls of 0.2 μm-filtered SHSW with antibiotics, no rapid Hg(II) reduction was observed in the first 24 h, which might be attributable to complexation of Hg(II) by the antibiotics, thereby inhibiting abiotic Hg(II) reduction. However, the effectiveness of antibiotics lasted only one day and the subsequent degradation of antibiotics seemed to enhance Hg^0 formation (up to 18% in 48 h). No significant Hg^0 evasion was found among all MeHg-treated controls of SHSW or SBSW, suggesting that MeHg was very stable in seawater without the presence of bacteria and/or particles larger than 0.2 μm.

Effects of Temperature and light

Nearly the same amount of Hg^0 was collected in controls between 24°C and 4°C, suggesting that continuous bubbling of air can sufficiently remove all produced Hg^0 from the dissolved phase and therefore the influence of changes in Hg^0 solubility due to varying temperatures can be ignored. It was clear that more Hg^0 was produced at 24°C than 4°C in either Hg(II)- or MeHg-treated $SHSW_{1\mu m}$ (Fig. 5-4 a,b). For Hg(II) treatments, total $\%Hg^0$ production from $SHSW_{1\mu m}$ was about four times higher at 24°C than at 4°C and the Q_{10} (calculated over the period 0-96 hours) for the evasion rate process was 2.03 for Hg(II), consistent with a biologically mediated process ($Q_{10} = 2\sim3$). It is unlikely that abiotic reduction of Hg(II) occurring on bacterial cell surfaces also contributed to the evasion because Hg^0 formation from $SHSW_{ctrl}$ at 4°C was close to $SHSW_{1\mu m}$ at 4°C where bacteria cells were present (Fig. 5-4a), suggesting that surface reduction only accounted for a small part of Hg^0 evasion. In contrast, for MeHg-exposed cells, the Q_{10} of the evasion calculated over the first 96 hours was only 1.11. The Q_{10} values calculated over the first 24 hours for Hg(II) and MeHg were 2.09 and 1.38, respectively. There was a much

sharper decline in Hg evasion rates for Hg(II) than for MeHg after the first 24 hours of exposure, expressed either on a whole culture basis or normalized to a bacterial cell basis (Table 5-1).

The likeliest mechanism of Hg^0 formation from MeHg involves cleavage of the carbon-mercury bond by the organomercurial lyase, producing Hg(II), followed by the reduction of Hg(II) to Hg^0 by mercuric reductase (Ullrich et al., 2001). Because the latter process seems to be influenced by temperature greatly (Fig. 5-4a), we suggest that the demethylation process might not be very sensitive to temperature. Alternatively, the demethylation process might be driven by an uncharacterized abiotic reaction which is not affected appreciably by temperature. The higher bacterial production at 24°C than at 4°C (Fig. 5-4d), as inferred from leucine uptake, coincided with increased bacterial cell densities over time (Fig. 5-4c). The measured values of bacterial production were comparable to reports for natural assemblages of bacteria in field studies (Anderson and Taylor, 2001; Shiah and Ducklow, 1994).

Photochemical reactions through radiation of ultraviolet and visible light are known to reduce Hg(II) (Amyot et al., 1994; Costa and Liss, 2000; O'Driscoll et al., 2007) and degrade MeHg (DiMento and Mason, 2017; Hammerschmidt and Fitzgerald, 2006c; Lehnherr and St. Louis, 2009; Sellers et al., 1996; Suda et al., 1993), resulting in Hg^0 formation. However, we did not observe significant differences in Hg^0 evolution between light and dark treatments (Fig. 5-5). The reason was probably due to our experimental settings where cool-white fluorescent light without ultraviolet radiation was used in our study. Moreover, its light intensity was less than one-twentieth of incident irradiation at full sunlight. Regardless of any light effects that may occur in nature, it was clear from the laboratory experiments that biologically mediated processes significantly enhanced the evasion of Hg from these cultures.

Unfiltered SBSW vs. 1μm-filtered SBSW

We compared the difference in Hg^0 production between unfiltered SBSW and 1 μm-filtered

SBSW. Hg^0 production from Hg(II)-treated seawater was higher in $SBSW_{unfiltered}$ than in

$SBSW_{1μm}$ (Fig. 5-6a). Microbes smaller than 1 μm accounted for 71% of Hg(II) reduction in

SBSW, suggesting that these organisms are the primary Hg^0 producers, consistent with the

conclusion of Mason et al. (1995). Hg^0 was also produced in MeHg-treated $SBSW_{unfiltered}$ to a

greater extent than in $SBSW_{1μm}$ (Fig. 5-6b), but microbes smaller than 1 μm only accounted for

41% of MeHg degradation. This discrepancy may be attributable to the broad distribution of

mercuric reductase (*merA*) which is the core enzyme of bacterial mercury resistance. In contrast,

organomercurial lyase (*merB*) is not as prevailing as *merA* among bacteria (Barkay et al., 2003).

Comparison of Hg^0 formation between SHSW and SBSW

The greater production of Hg^0 in Hg(II)-treated $SBSW_{1μm}$ than in Hg(II)-treated-$SHSW_{1μm}$

(Figs. 5-4a, 5-6a) was probably attributable to the greater bacterial biomass in SBSW. However,

less Hg^0 production was found in MeHg-treated $SBSW_{1μm}$ than in MeHg-treated $SHSW_{1μm}$ (Figs.

5-4b, 5-6b) which cannot be explained by differences in bacterial biomass or other factors like

salinity, dissolved organic matter and nutrient concentrations. Further, the Hg^0 evasion from

SBSW was significantly lower than from SHSW when normalized to bacterial biomass (Figs. 5-

7c, 5-7d). Assuming Hg^0 formation was mainly driven by bacterial enzymatic processes, the

discrepancy between SHSW and SBSW may have been a consequence of different bacterial

communities in these two waters. Although the Hg-resistance gene, *mer* operon, is considered

broadly distributed among bacteria probably due to horizontal gene transfer in evolution (Osborn

et al., 1997), fractions of Hg-resistant bacteria of total bacterial numbers vary from one place to

another (Barkay et al., 2011). Further investigations using metagenomic analysis could elucidate the bacterial community composition in SHSW and SBSW.

Bacterial mercuric reductase merA

There are two known MeHg degradation processes mediated by microbes, reductive demethylation by *merAB* yielding CH_4, and oxidative demethylation related to C1 metabolism in anaerobic prokaryotes yielding CO_2 and CH_4 (Barkay et al., 2011; Barkay et al., 2003). The former process probably occurred in our experiments (assuming the demethylation was mediated by microbes), because the latter process is favored at low redox potentials.

Following the procedure described by Poulain et al. (2015), *merA* genes in our positive control were successfully amplified at 300 bp (Fig. 5-8). Moreover, bacterial *merA* genes were detected in both SHSW and SBSW (Fig. 5-8). The results suggest that the Hg^0 formation in our study might have been driven by bacterial mercuric reductase. It has been suggested that *merA*-mediated reduction is induced at high ambient Hg(II) concentrations of >50 pM (Morel et al., 1998); such a "threshold" concentration of Hg(II) is much higher than in most marine environments. Several field studies indeed showed detectable transcription of *merA* genes in highly contaminated environments (Nazaret et al., 1994; Schaefer et al., 2004). However, Poulain et al. (2007) reported detectable *merA* transcription in microbes in the Canadian Arctic where the ambient total Hg concentrations were about 10 pM, implying that bacteria may have continuous activity of Hg reductase even at natural, low Hg concentrations. In fact, *mer* induction should not only depend on absolute Hg concentrations but also other factors that affect actual Hg bioavailability to bacteria (Barkay et al., 2011). Our results showed that bacteria still exhibited significant capacity to produce Hg^0 at ambient concentrations as low as ~5 pM (Fig. 5-

2a). However, we did not determine if *merA* transcription was induced in our samples during the incubation. Further work is needed to elucidate whether threshold concentrations of Hg are applicable to bacteria.

Production kinetics and rates

Mason et al. (1995) examined Hg^0 formation from Hg(II)-treated seawater in diverse cultures of marine microorganisms (mostly phytoplankton, including cyanobacteria), and reported Hg^0 production rates of 0.4–9.7% d^{-1} (corresponding to 0.027–0.48 amol-Hg $cell^{-1}$ d^{-1}), which were comparable with our results (Table 5-1). However, it should be noted that their added Hg(II) concentrations were 0.5 nM which was about 10 times higher than ours. Monperrus et al. (2007) reported that bacterial and/or phytoplanktonic reduction of Hg(II) in surface waters of the Mediterranean Sea ranged from 2.2–12.3% per day, which were also comparable to our study (Table 5-1).

The patterns of Hg^0 evolved from Hg(II)-treated seawater (Figs. 5-4a, 5-5, 5-6a) were very similar to the results from Barkay et al. (1991), where they measured Hg(II) volatilization by an indigenous freshwater microbial community. The first phase had rapid formation rates and the second phase had slower evasion rates (Fig. 5-7). The decline in production rate from Hg(II) treatments was probably because of a decline in bioavailable Hg(II) for the bacteria and/or reactive Hg(II) was converted to a non-reducible form by complexation with dissolved organic matter. The Hg^0 production rates normalized to bacterial abundance were significantly higher in SHSW than in SBSW (Fig. 5-7), particularly within the first 48 hours, suggesting that the bacteria in SHSW had a higher capacity to reduce Hg(II). The reaction of Hg(II) reduction from $SHSW_{1\mu m}$ over 96 h seemed to be a mixed order reaction. But treated as a first order reaction, the

calculated rate constant was 1.1×10^{-6} s^{-1}. The reaction for SBSW can perfectly fit the model of a first order reaction and the rate constants were 1.3×10^{-6} s^{-1} for SBSW$_{1\mu m}$ and 2.2 x 10^{-6} s^{-1} for SBSW$_{unfiltered}$. These values are comparable to dark (or low light) incubation results for the Baltic Sea ($1.5 \pm 0.5 \times 10^{-6}$ s^{-1}) (Kuss et al., 2015) and Chesapeake Bay and coastal shelf waters (0.67–1.8×10^{-6} s^{-1}) (Whalin et al., 2007), but rate constants of microbial production can be one to two orders of magnitude lower than those attributable to photochemical transformation (O'Driscoll et al., 2006; Qureshi et al., 2009; Vost et al., 2012; Whalin et al., 2007).

Very few studies reported microbial MeHg demethylation rates and kinetics in seawater. Our calculated Hg^0 evasion rates from MeHg-treated seawater (1.9–4.6% d^{-1}, Table 5-1) were comparable to Hg^0 production rates (2.8–10.9% d^{-1}) reported by Monperrus et al. (2007) in the Mediterranean. The evasion of Hg^0 from MeHg-treated seawater was linear over time (Figs. 5-4b, 5-5, 5-6b), implying a zero-order reaction with an independence of substrate (MeHg) concentrations. Unlike the Hg(II)-treated seawater, the Hg^0 evasion rates from MeHg treatments did not change much over time (Fig. 5-7b). The modest increase over time is probably due to bacterial growth over time as indicated by the low variability in Hg^0 production rate normalized to bacterial densities (Fig. 5-7d). As noted above in Section "*Effects of Temperature and light*", the formation of Hg^0 from MeHg is a two-step reaction involving the demethylation of MeHg to Hg(II), and the subsequent reduction to Hg^0. The demethylating process might be the rate limiting step, resulting in a linear increase of Hg^0 evasion which was very different from the Hg(II)-treated seawater. In order to compare with Hg(II) treatments, here we also used first order kinetics to calculate the rate constants for Hg^0 evasion from MeHg-treated seawater. The calculated values were 0.61×10^{-6} s^{-1} for SHSW$_{1\mu m}$, 0.17×10^{-6} s^{-1} for SBSW$_{1\mu m}$, and 0.47×10^{-6} s^{-1} for SBSW$_{unfiltered}$. Whalin et al. (2007) reported that the rate constants of demethylation in the

water column of Chesapeake Bay were $<1–5\times10^{-6}$ s^{-1} where the demethylation was driven by both photochemical and microbial processes. In a lab study using coastal seawater, rate constants attributable solely to photochemistry were reported to range from 10 to 19×10^{-6} s^{-1} (DiMento and Mason, 2017).

The distribution of Hg species in bacterial cells may influence the kinetics of Hg(II) reduction and MeHg degradation. It has been shown that more MeHg can penetrate into the cytoplasm of phytoplankton cells than Hg(II) (Lee and Fisher, 2016; Mason et al., 1996; Pickhardt and Fisher, 2007). If this is also applicable to bacteria, rapid accumulation of MeHg into bacterial cytoplasm may therefore provide enough substrate (MeHg) to induce demethylation by the organomercurial lyase, resulting in continuous Hg^0 formation. In contrast, only part of the Hg(II) (free ion or neutral species) may be allowed to enter bacterial cells in the beginning of incubations and be reduced by mercuric reductase. Bioavailability of Hg(II) to microorganisms may be lowered because of further complexation of Hg(II) with other ligands (Barkay et al., 1997; Hsu-Kim et al., 2013; Ullrich et al., 2001), explaining why less Hg^0 production was observed at a later stage of incubation. Although MeHg can also form strong complexes with ligands which decrease its bioavailability to microorganisms (Lee and Fisher, 2017b; Ndu et al., 2016), Hg(II) is more prone to form metal complexes than MeHg because of its greater formation constant with ligands. Similar cases can be seen in previous studies regarding MeHg production by Hg-methylating bacteria, where the highest methylation rate can be found in the first few days (Compeau and Bartha, 1984; Hamdy and Noyes, 1975; Ullrich et al., 2001).

Importance of microbial transformation of Hg^0

This study demonstrated for the first time that natural marine bacterioplankton assemblages are capable of rapidly converting MeHg to Hg^0. Once the Hg^0 is formed it can then be released to the overlying air as shown in the experiments that used bubbling to force dissolved gas into the air. In the ocean, however, aeration of surface seawater through winds and turbulence may not result in the same rate of gas evasion from surface waters. Even microbes that remained in coarse-filtered seawater for 6 years in the dark were immediately able to convert some MeHg to Hg^0. Like the production of Hg^0 from Hg(II), this process is related to the microbial biomass, but clear differences between bacterial assemblages from Stony Brook harbor and Southampton exist. The extent to which the microbial conversion of MeHg to Hg^0 that is released to the air results in diminished build-up of MeHg in marine food chains remains to be explored.

It has been suggested that climate change can increase mercury mobilization in the Arctic through increased freshwater discharge and thawing of permafrost. Release of large quantities of Hg has led to elevated atmospheric Hg^0 concentrations in summer months over the Arctic Ocean (Fisher et al., 2012). Extrapolating from the results here that marine bacteria rapidly produced atmospheric Hg^0 from Hg(II) and MeHg dissolved in seawater following long cold storage, it seems plausible that microbes revived from permafrost thawing could generate Hg^0 gas evasion from Arctic waters.

In natural waters, Hg^0 formation is a combination of photochemical and microbial processes. The importance and relative contribution of each process on total Hg^0 formation may vary from one place to another. Some studies concluded that photochemical reduction of Hg(II) was the dominant process; for instance, Rolfhus and Fitzgerald (2004) reported that approximately 70% of bulk reduction was driven photochemically and 20% was by microbial mediation in coastal surface seawater from Long Island Sound. Whalin et al. (2007) also suggested that biotic

124

processes were relatively unimportant to Hg(II) reduction in surface waters of the Chesapeake. Although the photochemical production of Hg^0 can be very efficient, it is limited in the daytime and at the surface ocean. Rapid water column attenuation of sunlight with depth can diminish the importance of the photochemical process, especially in high latitude regions. For example, Poulain et al. (2007) reported that at a depth of 10 m below the surface of the Arctic Ocean, up to 94% of Hg^0 was produced by microbial reduction of Hg(II) rather than photochemical reduction. Kuss et al. (2015) reported that microbial production of Hg^0 under low-light conditions in the Baltic accounted for ~40% of total Hg^0 production. If the microbial transformation of Hg^0 can occur at any depth, the biological reduction of Hg(II) should become a significant source to the total pool of Hg^0 in the water column.

Conclusions

Our results demonstrated the importance of Hg^0 formation through reduction of Hg(II) and degradation of MeHg mediated by natural marine bacteria assemblages. Assuming Hg^0 oxidation and Hg(II) methylation are not pronounced reactions in the water column, the resulting decline in Hg(II) and MeHg concentrations may be beneficial to marine biota. Detection of *merA* in our samples suggested that Hg^0 production by bacteria with *mer*-operon could be the primary pathway. Bacterial community structure in different water types and bioavailability of Hg species to bacteria seemed to be critical factors controlling the Hg^0 formation. Future study should incorporate identification of bacterial community structures which can largely affect the capacity of reduction of Hg(II) and demethylation of MeHg. In addition, other factors such as availability of Hg species to bacteria (complexation with ligands), organic matter supply from phytoplankton, and bacterial grazing by protozoa are not included in our study. Further

investigations are needed to better understand the fate and transformation of Hg species in microbial loops.

Table 5-1. Production of Hg^0 by marine bacteria in SHSW and SBSW in 4-d incubation experiments.

All production rates from treatments with bacteria are corrected for abiotic production (controls). Mean bacterial cell density represents the average bacterial density of all time points. In controls, bacterial cell densities were below detection limit (BDL).

Seawater type	Incubation temp. (°C)	Added Hg species	Total Hg^0 evasion after 4 d (%)	Hg^0 evasion (% d^{-1})	Mean bacterial density (×10^6 cells mL^{-1})	Hg^0 evasion (% d^{-1} ×10^6 cells^{-1})	Hg^0 evasion (amol-Hg d^{-1} cells^{-1})	Rate constant (×10^{-6} s^{-1})
SHSW$_{1\mu m}$	24	Hg(II)	25.1 ± 1.2	6.3 ± 0.3	0.86 ± 0.10	7.3 ± 0.9	0.82 ± 0.10	1.1
SHSW$_{1\mu m}$	24	MeHg	18.5 ± 1.7	4.6 ± 0.4	0.74 ± 0.09	6.2 ± 0.9	0.69 ± 0.11	0.61
SHSW$_{ctrl}$	24	Hg(II)	7.6 ± 3.5	1.9 ± 0.9	BDL	-	-	0.14
SHSW$_{ctrl}$	24	MeHg	0.5 ± 0.4	0.1 ± 0.1	BDL	-	-	<0.01
SHSW$_{1\mu m}$	4	Hg(II)	2.5 ± 2.7	0.6 ± 0.7	0.47 ± 0.07	1.3 ± 1.5	0.20 ± 0.22	0.06
SHSW$_{1\mu m}$	4	MeHg	9.9 ± 0.4	2.5 ± 0.1	0.52 ± 0.11	4.8 ± 1.0	0.56 ± 0.12	0.30
SHSW$_{ctrl}$	4	Hg(II)	5.6 ± 1.4	1.4 ± 0.4	BDL	-	-	0.17
SHSW$_{ctrl}$	4	MeHg	0.2 ± 0.0	0.05 ± 0.01	BDL	-	-	<0.01
SBSW$_{1\mu m}$	24	Hg(II)	42.2 ± 3.1	10.5 ± 0.8	5.02 ± 0.58	2.1 ± 0.3	0.31 ± 0.04	1.3
SBSW$_{1\mu m}$	24	MeHg	7.6 ± 0.2	1.9 ± 0.1	5.26 ± 0.83	0.4 ± 0.1	0.05 ± 0.01	0.17
SBSW$_{unfiltered}$	24	Hg(II)	59.3 ± 5.4	14.8 ± 1.3	5.54 ± 0.39	2.7 ± 0.3	0.39 ± 0.05	2.2
SBSW$_{unfiltered}$	24	MeHg	18.4 ± 0.6	4.6 ± 0.2	5.44 ± 0.38	0.8 ± 0.1	0.12 ± 0.01	0.47
SBSW$_{ctrl}$	24	Hg(II)	11.2 ± 1.3	2.8 ± 0.3	BDL	-	-	0.27
SBSW$_{ctrl}$	24	MeHg	0.4 ± 0.1	0.09 ± 0.03	BDL	-	-	<0.01
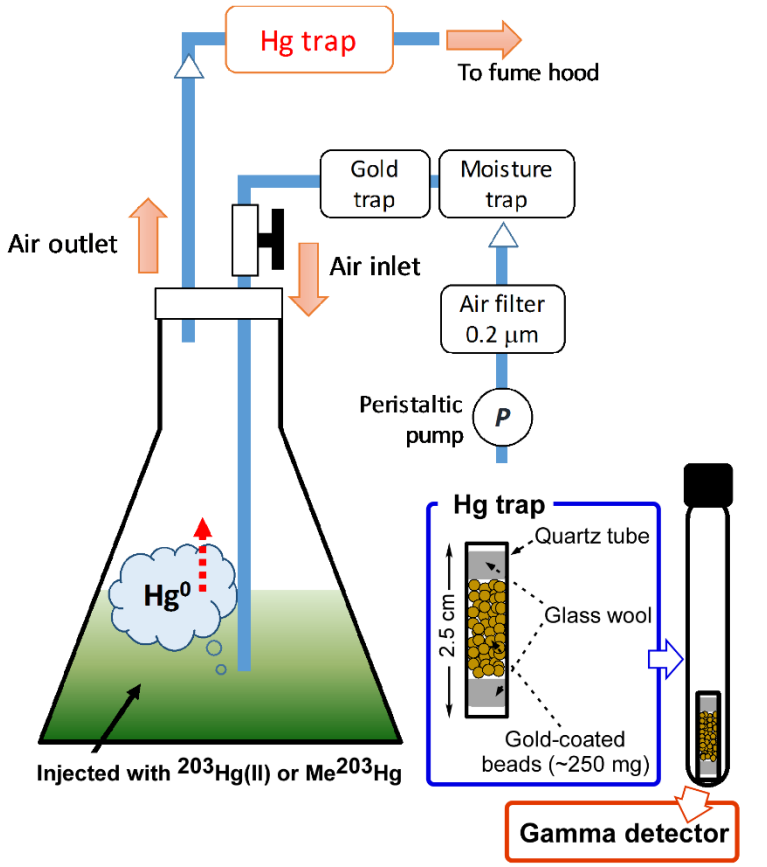
Figure 5-1. Schematic layout of the incubation setting and the Hg trap.
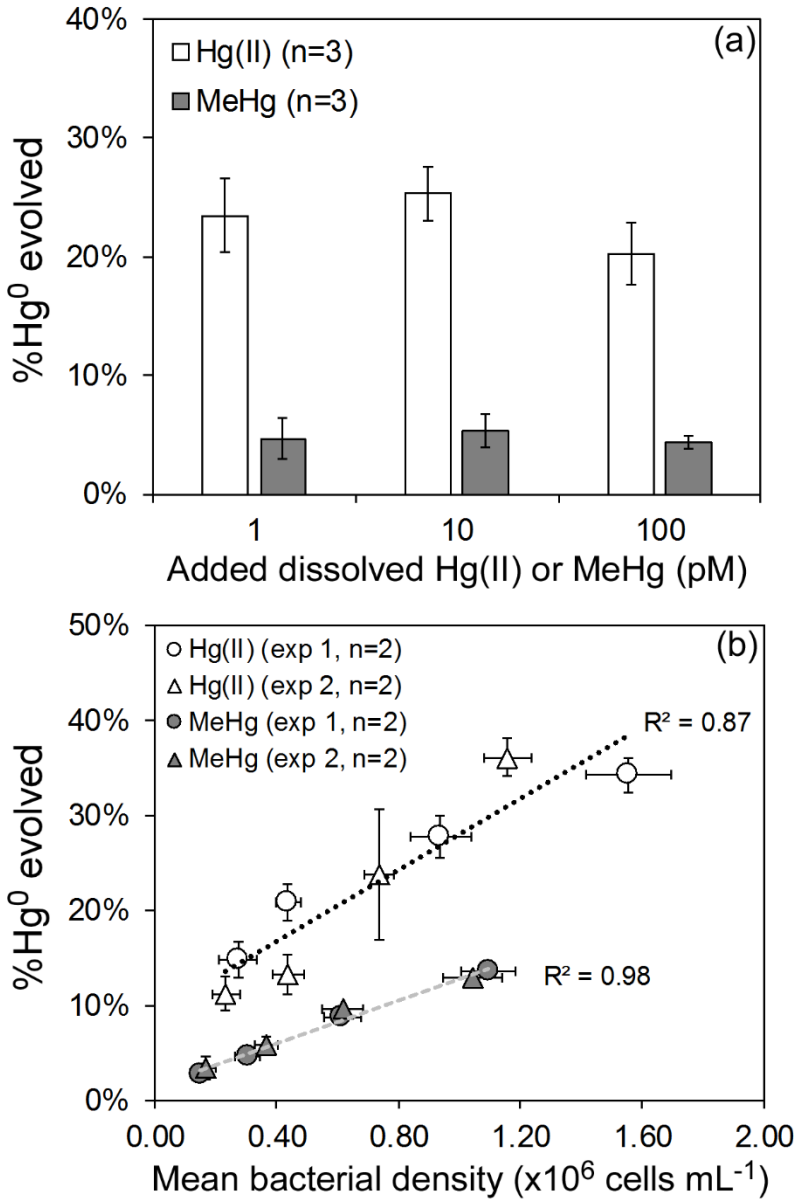
Figure 5-2. Total percentage of Hg⁰ evolved from Hg(II)- and MeHg-treated SHSW after 1-day incubation as a function of (a) dissolved Hg(II) or MeHg concentrations and (b) mean bacterial cell density. Data points are the means from two or three replicate cultures with error bars of one standard deviation. Added concentrations of Hg(II) and MeHg were 10 pM in (b). Note that background concentrations of Hg(II) and MeHg in SHSW were ~5 pM and ~5 fM, respectively.
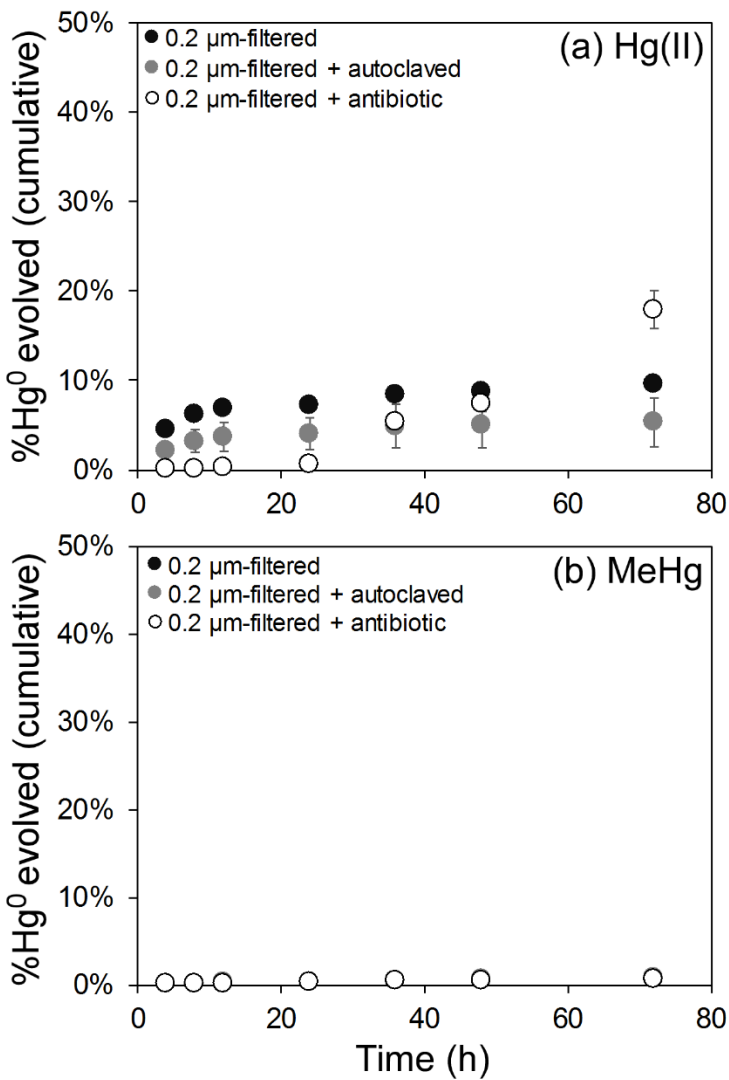
Figure 5-3. Total percentage of Hg⁰ evolved over time at 24°C from different controls (without bacteria) treated with (a) Hg(II) or (b) MeHg. Data points are the means from three replicate cultures with error bars of one standard deviation. Added concentrations of Hg(II) were 54 pM and of MeHg were 56 pM.
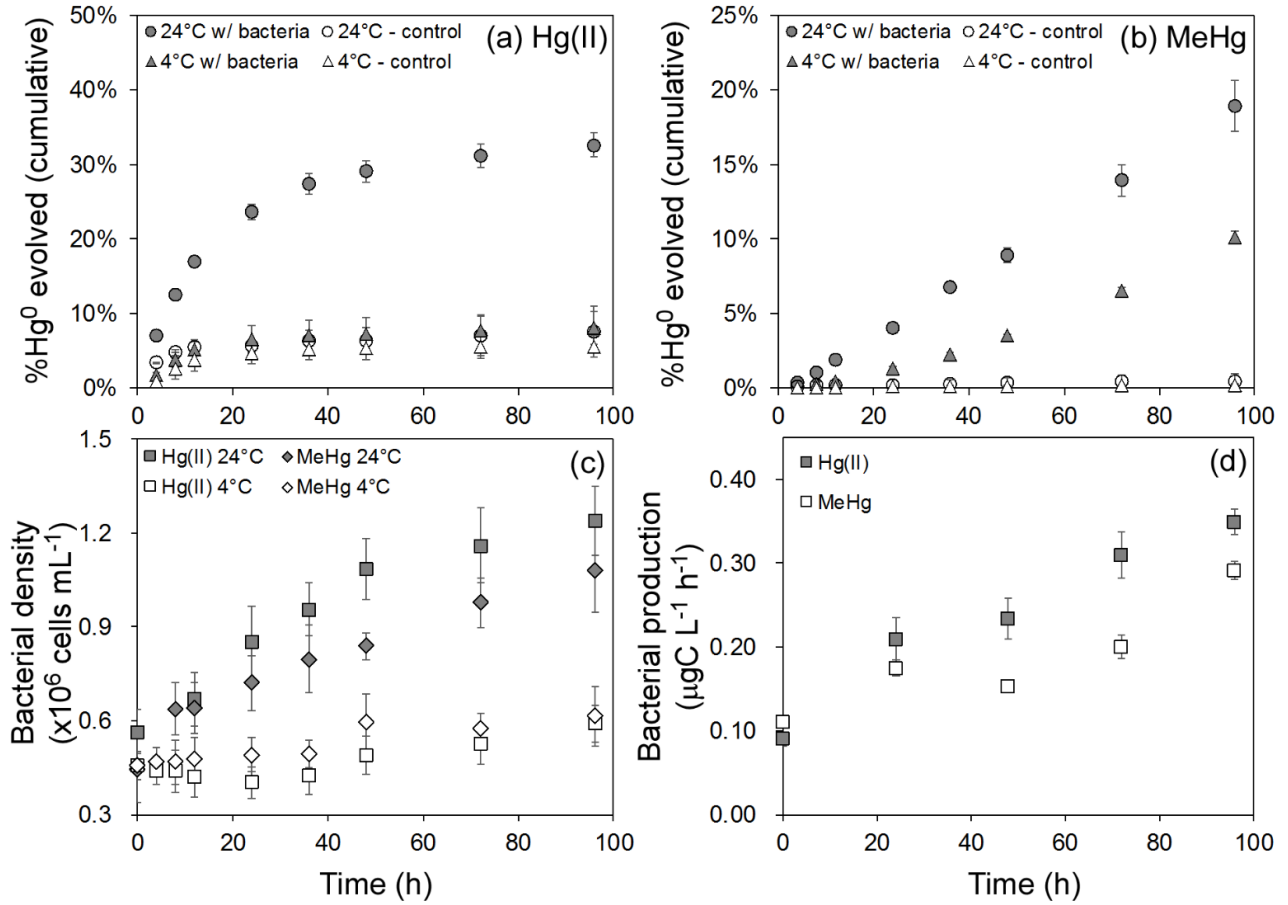
Figure 5-4. Total percentage of Hg⁰ evolved from (a) Hg(II)-treated SHSW and (b) MeHg-treated SHSW at two different temperatures, (c) bacterial cell density, and (d) bacterial production (24°C only) over time. Treatments with bacteria were 1 μm filtered and controls were 0.2 μm filtered. Data points are the means from three replicate cultures with error bars of one standard deviation. Added concentrations of Hg(II) were 56 pM and of MeHg were 55 pM.
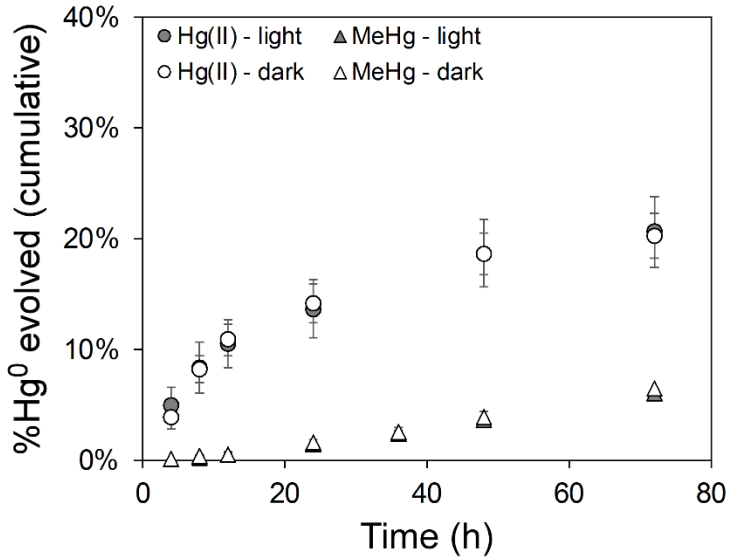
Figure 5-5. Total percentage of Hg⁰ evolved from Hg(II)-treated SHSW and MeHg-treated SHSW under light and dark conditions. Control treatments are not shown. Data points are the means from two replicate cultures with error bars of one standard deviation. Added concentrations of Hg(II) were 45 pM and of MeHg were 70 pM.
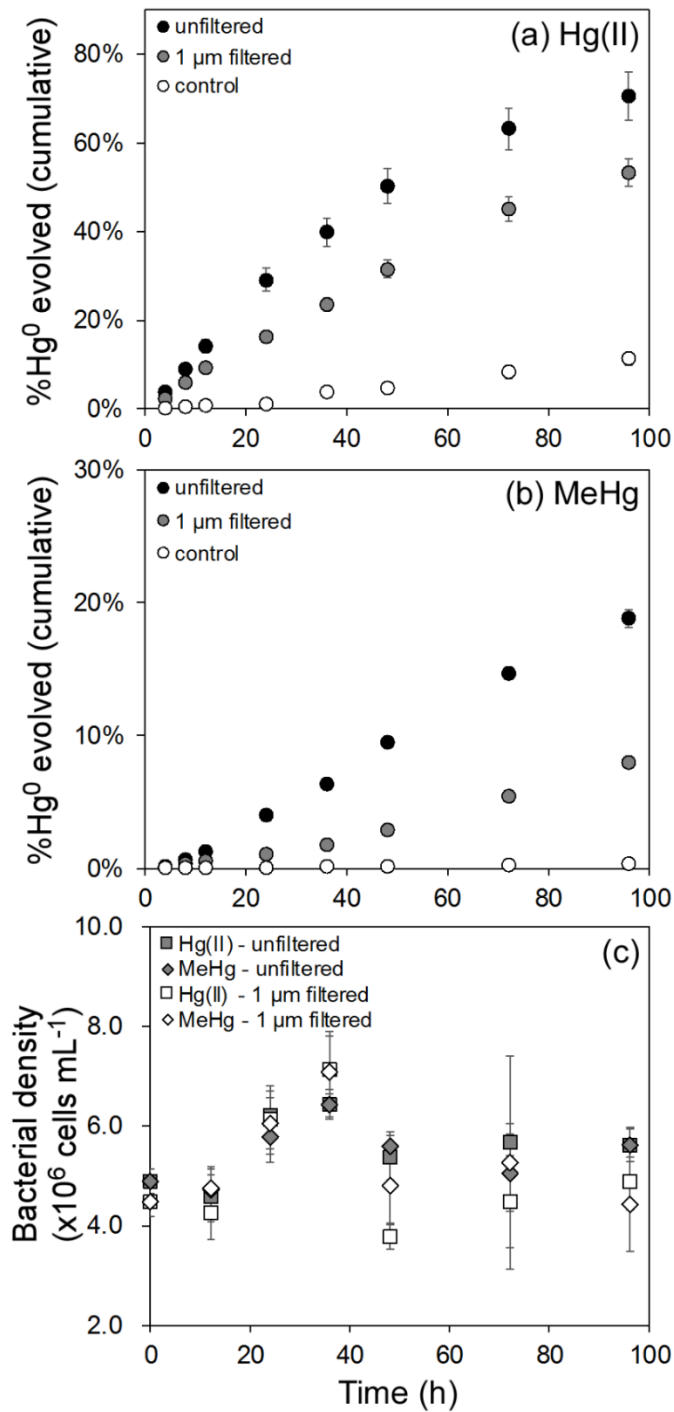
Figure 5-6. Total percentage of Hg⁰ evolved from (a) Hg(II)-treated SBSW and (b) MeHg-treated SBSW, and (c) bacterial cell density at 24°C over time. Data points are the means from two replicate cultures with error bars of one standard deviation. Added concentrations of Hg(II) were 74 pM and of MeHg were 67 pM.
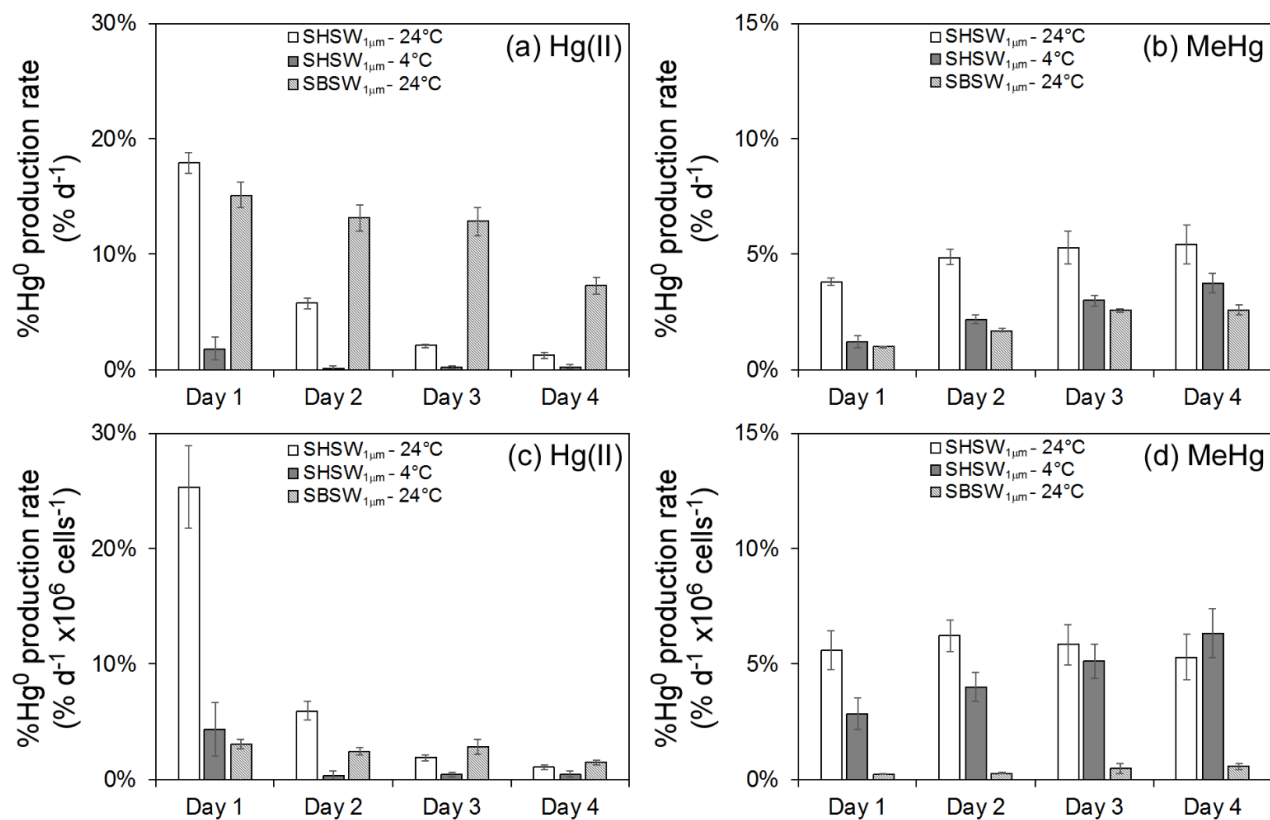
Figure 5-7. Hg⁰ production rate (corrected for controls) at different periods of time. Hg^0 production rate from (a) Hg(II)-treated seawater and (b) MeHg-treated seawater, and Hg^0 production rate normalized to bacterial cell density from (c) Hg(II)-treated seawater and (d) MeHg-treated seawater. All data shown here were for 1 μm-filtered seawater and bars represent means of two or three replicate cultures with error bars of one standard deviation.
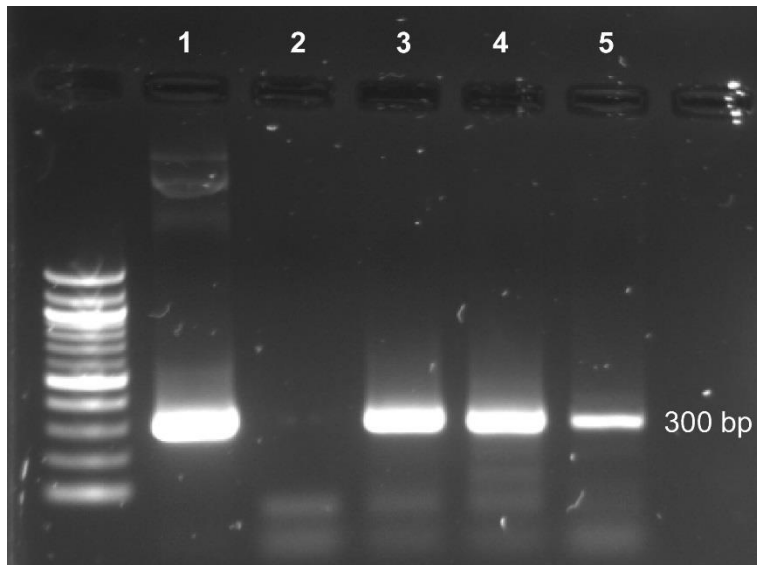
Figure 5-8. Gel picture of *merA* PCR product at 300 bp. (1) positive control, (2) negative control, (3) SHSW with bacteria in *E. huxleyi* cultures, (4) SHSW with bacteria, (5) SBSW with bacteria.

Chapter 6

Declining mercury concentrations in bluefin tuna reflect reduced emissions to the North Atlantic Ocean

Abstract

Tunas are apex predators in marine food webs that can accumulate mercury (Hg) to high concentrations and provide more Hg (~40%) to the U.S population than any other source. We measured Hg concentrations in 1,292 Atlantic bluefin tuna (ABFT, *Thunnus thynnus*) captured in the NW Atlantic from 2004 to 2012. ABFT Hg concentrations and variability increased non-linearly with length, weight, and age, ranging from 0.25 to 3.15 mg kg^{-1}, and declined significantly at a rate of 0.018 ± 0.003 mg kg^{-1} per year, or 19% over an eight-year period from the 1990s to the early 2000s. Notably, this decrease parallels comparably reduced anthropogenic Hg emission rates in North America and North Atlantic atmospheric Hg^0 concentrations during this period, suggesting that recent efforts to decrease atmospheric Hg loading have rapidly propagated up marine food webs to a commercially important species. This is the first evidence to suggest that emission reduction efforts have resulted in lower Hg concentrations in large, long-lived fish.

Introduction

High human consumption and moderate to high species-dependent Hg concentrations cause tunas to provide more Hg (~40%) to the U.S population than any other source (Sunderland, 2007). All tuna species support large international fisheries due to high economic value and popularity as seafood. Relatively high Hg concentrations in larger, long-lived tunas have been posited as a potential health concern for frequent consumers, women of child-bearing age, fetuses, and young children (National Research Council, 2000). Unresolved are tradeoffs between Hg-dependent impacts on human health and health benefits of omega-3 fatty acids, selenium and other nutrients in seafood (Burger and Gochfeld, 2011; Gribble et al., 2016;

Mozaffarian, 2009). Average Hg concentrations reported for different tuna species vary from 0.118 ppm (0.047-0.400 ppm) in canned skipjack tuna to 0.796 ppm (0.057-3.030 ppm) in wild bluefin tuna (Karimi et al., 2012). The long lifespan and highly migratory behavior of ABFT may make them valuable bioindicators of changes in Hg over time on basin-wide scales. In addition, bluefin tunas have enormous economic value, are fished globally, and are iconic species in ocean conservation campaigns.

Monomethylmercury (MeHg), a highly toxic and bioaccumulative form of Hg, is mainly formed by diverse bacteria that methylate inorganic Hg both in sediments and the water column (Fitzgerald et al., 2007; Gilmour et al., 2013; Sunderland et al., 2009). In the open ocean, MeHg levels have recently been reported to be higher in the subsurface oxygen deficit zone than in deeper waters (Bowman et al., 2015; Hammerschmidt and Bowman, 2012; Sunderland et al., 2009). In addition, Lehnherr et al. (2011) suggested that in-situ methylation was the dominant source of MeHg in the mixed layer. Phytoplankton at the base of the food web concentrate (enriched about 10^5 times) both inorganic and methylmercury from ambient seawater and serve as highly enriched sources of mercury for marine food chains (Morel et al., 1998). Unlike inorganic Hg and most other metals, MeHg is transferred efficiently to subsequent trophic levels through diet and eliminated by aquatic animals at extremely low rates (Mathews and Fisher, 2008). Thus MeHg constitutes nearly all Hg in fish (Bloom, 1992; Harris et al., 2003) and muscle tissue concentrations are highest in upper trophic level animals (e.g., tunas, billfish, sharks) (Chen et al., 2008; Karimi et al., 2012). Efficient transfer makes MeHg concentrations in marine predators especially sensitive to food web dynamics, including MeHg levels at the base of the food web (Lee and Fisher, 2016) and in forage fish (Choy et al., 2009), and variation in food chain length (Cabana and Rasmussen, 1994).

Superimposed on ecological complexities are changing seawater Hg concentrations, caused in part by coal-burning, gold mining, and other industrial activities. Recent efforts to reduce atmospheric contamination have resulted in reduced Hg loadings into the atmosphere in North America (Driscoll et al., 2013; Pirrone et al., 2010; Zhang et al., 2016) and decreased concentrations in Atlantic Ocean surface waters (Driscoll et al., 2013; Mason et al., 2012). A recent study reported declining trends of Hg in Atlantic bluefish (*Pomatomus saltatrix*) since the 1970s reflecting a decline in Hg emissions (Cross et al., 2015). Bonito et al. (2016) synthesized available published data of Hg in numerous species of marine fish across the global ocean since 1969. They averaged all species and sizes from different trophic levels and reported a decline in mean Hg concentrations only in Altantic Ocean fish. However, the extent to which recent reductions have affected Hg concentrations in the largest, highest-mercury fish (e.g., long-lived tunas) has not been quantified. Reported Hg concentrations in wild Atlantic bluefin tuna, from different locations have varied widely (Storelli et al., 2002). Few data are available for Hg concentrations in western ABFT (Table 6-1), and prior reports have often been based on small sample sizes that cannot represent populations or rigorously identify temporal trends. Relationships of Hg concentrations with ABFT age, length, weight, sex or habitat have not been comprehensively examined in previous studies, limiting the conclusions that can be drawn from Hg measurements.

We measured total Hg concentrations in 1,292 samples of wild-caught western ABFT for which length, weight, gender, year of capture, and location of capture were known. This unique dataset allows assessment of Hg concentration changes in western ABFT over a time period in which atmospheric loading of Hg from North America declined. We report a decline in ABFT Hg concentrations over the period 2004-2012 that appears to reflect decreasing atmospheric

loading in the North Atlantic Ocean, linking reduced Hg emissions to decreasing Hg concentrations in an apex ocean predator.

Materials and Methods

Sample information

ABFT tissue samples were collected from commercial landings from 2004 to 2012, primarily in the Gulf of Maine (n = 1279) and the Gulf of St. Lawrence (n = 13) by rod and reel and purse seine, for a total of 1,292 samples comprising the LPRC (Large Pelagics Research Center) bluefin biosampling archive. Known capture locations are shown in Fig. 6-1. All tissue was subsampled either from caudal white muscle tissue or from cranial muscle, and stored frozen. Length (curved fork length or CFL in cm: a line tracing the lateral contour of the body from the tip of the upper jaw to the fork of the tail), weight, gender, year of capture, and approximate location of capture were recorded for each individual sampled fish. Body length and weight ranged from 65 to 326 cm (218 ± 30 cm) and 58 to 347 kg (132 ± 54 kg), respectively. The approximate age of western ABFT was estimated from CFL using an empirical growth curve generated from direct age-length observations from otoliths and modal progression data (Restrepo et al., 2010). Uncertainty of age estimation increases in fish beyond 10 years of age (Cort et al., 2013).

Total Hg analysis

All samples were freeze-dried and homogenized prior to Hg analysis. Total Hg concentrations were determined using a DMA-80 direct Hg analyzer (Milestone, Inc.). Water content was determined in all samples (mean water content, 66 ± 7%) and dry weight concentrations were

converted to a wet weight basis based on water content of each sample. Reported Hg

concentrations in ABFT are wet weight concentrations unless otherwise noted. Given that >90%

of Hg in tuna tissue is in the methylated form MeHg, we assumed that total Hg concentrations

represent MeHg concentrations in ABFT. The DMA-80 was calibrated with an Hg standard

solution (VHG Labs, Inc.). Certified reference material (DORM-4, NRCC) was measured to

validate quality assurance. All analyses of Hg in reference material were within certified ranges

(certified value: 0.410 ± 0.055 mg kg^{-1}, measured value: 0.395 ± 0.031 mg kg^{-1}, n = 43).

Calibration checks were performed every ten samples to monitor analyzer stability. To evaluate

precision, duplicate samples were randomly measured in every set of analyses, and duplicate

measurements of Hg concentrations varied by <3%.

Statistical analysis

   In order to assess inter-annual trends of Hg concentrations in ABFT, we grouped samples into

age groups (Table 6-2, age estimated from length, as described above) in one-year increments

and compared mean Hg concentrations in same-aged fish across different years of capture (2004-

2012). Age groups with sample size >50 (9 to 14 years old) were analyzed for temporal trends.

Least squares regressions of same-age ABFT Hg concentration versus year of capture were

performed. Calculated slope values of Hg versus time for each age group were compared using

an F-test for homogeneity of regression slopes. This was followed by an analysis of covariance

(ANCOVA) to test adjusted means for age group effects. To assess the effect of departures from

normality and homogeneity of variances in the data, the analysis was repeated on log

transformed Hg data, and the linear and log-linear models were compared using the MacKinnon-

White-Davidson PE test (MacKinnon et al., 1983). Error structure effects were examined further

by comparing linear model parametric results to bias- and skew-corrected bootstrap confidence intervals (Davison and Hinkley, 1997). Data were resampled 5,000 times with replacement within each age group by year of capture combination. The bias- and skew-corrected 95% confidence interval for the slope [-0.022, -0.015] differed only slightly from the parametric interval, indicating that normality and homogeneity assumption violations had little effect on the results.

Repeating the analysis on log transformed Hg data resolved non-normality and heterogeneity of variance problems, but altered the functional form of the relationship between Hg and year. PE tests comparing linear and log-linear models for each age group could not distinguish between the two models, thus the linear model was accepted because of its simplicity.

We also compared ABFT Hg concentrations by year to assess whether changes could be detected on year-to-year timescales. ABFT Hg concentrations were grouped by year (2004-2012) and compared using the non-parametric Kruskal-Wallis test. Analyses were carried out in MATLAB vR2015a and in R v3.2.2.

Results and Discussion

Total Hg concentrations in ABFT

The mean Hg concentration in ABFT muscle samples was 0.76 ± 0.33 mg kg^{-1} (n = 1292, range 0.25-3.15 mg kg^{-1}). Hg concentrations in ABFT correlated positively with length and age (Fig. 6-2). Hg concentrations did not differ significantly between male and female ABFT (Fig. 6-3) for which sex was identified (n = 609, 47%). Variability of Hg concentrations was lowest among smaller fish (<200 cm), and increased markedly with size, particularly among very large fish (>250 cm) (Figs. 6-2 and 6-4). Using dissolved MeHg concentrations in surface waters of

the Gulf of Maine (3-11 pg L^{-1}) (Sunderland et al., 2012) and recent data in North Atlantic surface water (12 ± 10 pg L^{-1}) (Bowman et al., 2015), bioconcentration factors of MeHg in ABFT (MeHg in fish divided by MeHg in seawater) were up to 10^8.

Temporal trend of Hg concentrations in ABFT

Hg in ABFT declined significantly from 2004 to 2012 within each age group analyzed (ages 9-14 years old, see Methods; Figs. 6-5 and 6-6, Table 6-3). Slopes relating ABFT Hg concentrations to time did not differ significantly across age groups (F = 0.557, df = 5, 981, *p* = 0.733; Fig. 6-7). The overall decline in tissue Hg for the pooled data (see Methods) was 0.018 mg kg^{-1} per year (95% CI = [-0.021, -0.015]), corresponding to an average decline of 19% from 2004 to 2012. Comparison of adjusted regression means in ANCOVA indicated a highly significant age group effect (F = 61.2, df = 5, 986, *p* < 0.001). Our calculated decline rate of Hg in ABFT (~2% y^{-1}) was comparable to that reported for Atlantic bluefish (*Pomatomus saltatrix*) (Cross et al., 2015) and mean Atlantic fish (many species, trophic levels, ages combined) (Bonito et al., 2016).

Figure 6-8 shows that the decline in ABFT Hg parallels declining Hg emissions in North America (-2.8% y^{-1} from 1990 to 2007) (Driscoll et al., 2013; Pirrone et al., 2010), Hg(II) wet deposition fluxes in North America (-1.6% y^{-1} from 1996 to 2013) (Zhang et al., 2016), atmospheric Hg^0 concentrations 12 m above sea surface over the North Atlantic (-2.5% y^{-1} from 1990 to 2009) (Soerensen et al., 2012), and seawater Hg^0 concentrations (-4.3% y^{-1} from 1998 to 2010) (Mason et al., 2001; Soerensen et al., 2012). As there is no long-term record of dissolved MeHg in the North Atlantic, temporal trends in surface seawater Hg^0 concentrations were compared with ABFT Hg levels, although it is recognized that dissolved Hg^0 concentrations are

variable and subject to local conditions at the time of sampling. Over the eight-year period (2004-2012) Hg in ABFT declined by 19%, compared to a 20% decline in Hg^0 in N. Atlantic air for the overlapping eight-year period 2001-2009. Thus, an ABFT of a given age, caught in 2004, spent more of its life exposed to higher 1990s oceanic Hg concentrations than one caught in 2012 (Fig. 6-6). Higher Hg concentrations in seawater in the 1990s presumably propagated up food webs to prey (forage fish, squids: Table 6-4) and ultimately to ABFT, whereas declines in Hg emissions led to reduced Hg at the forage base resulting in gradually declining ABFT Hg concentrations in the early 2000s.

While global Hg emissions to the atmosphere continue to increase due largely to increased coal burning in Asia (Streets et al., 2011), regional declines of atmospheric Hg deposition into the North Atlantic Ocean have resulted from reduced North American Hg emissions in the past few decades (Zhang et al., 2016). This regional decline may explain the 1% per year decrease in Mid-Atlantic Bight bluefish Hg concentrations from 1972 to 2011 (Cross et al., 2015). Declining bluefish Hg indicates that other, more frequently consumed ABFT prey may have experienced similar declines. This reported decline in bluefish was based on relatively few samples from initial study years (n = 54; 1972-1973), compared with many more samples taken ≥20 years later. Trends potentially were driven by a few endmembers for larger fish or for temporal endpoints.

Rates of Hg decline reported here for ABFT are based on year-to-year measurements of sample sizes high enough to discern reliable trends despite observed variability. Inter-annual comparisons reinforce the importance of large sample size across long study periods. For example, Hg in 2004 was no different from 2005-2007, but was much higher than 2008-2012 (Table 6-5a). Because within-year ABFT Hg variability was high and slope of change relatively low, years of data may be required for detection of trends in tunas and other marine species.

Slow changes in tuna Hg may be driven by long (>1 year) histories reflected by muscle Hg of large marine predators. Kwon et al. (2016) reported a biological half-life of Hg in captive Pacific Bluefin tuna (PBFT) of ~500 days. Assuming comparable metabolic rates of ABFT and PBFT and given the larger size of ABFT in this study, Hg levels in ABFT likely represent exposure periods of ≥500 days.

Intra-annual variability of ABFT Hg concentrations was very high, representing 69-85% of the total variability in each age group. Pairwise comparisons of ABFT Hg concentrations between consecutive years were often not significant, emphasizing the need to carry out age-group specific analyses over multiple years to identify temporal trends. Of the consecutive year pairwise comparisons, 63% were nonsignificant at both an individual (Table 6-5a) and family (Table 6-5b) error rate of 0.05. Although requiring large samples and a multiyear time span to identify the negative trend in ABFT Hg concentrations, this trend was consistently observed across all age groups and survived all challenges to the form of the regression model and error structure (see Methods and Table 6-3).

Effects of potential shift in prey composition

Since Hg accumulates in fish over time and ABFT are long-lived, variability in large ABFT may represent time-integrated diet differences. Large ABFT feed on a larger size range of prey than smaller ABFT, and encounter different prey in various ocean regions (Butler et al., 2015; Logan et al., 2015). Thus variability in trophic levels and Hg concentrations of prey for large ABFT are greater than those of smaller ABFT. Similar increasing Hg variability with ABFT size has been observed for other fish species off the east coast of N. America (Taylor et al., 2014).

Shifts in ABFT diet over time provide a putative explanation for observed declines in Hg of western ABFT. Specific prey items are important, prey abundance is not constant, and declines in ABFT Hg could result from shifts to low Hg prey (e.g., menhaden) (Table 6-4). However, diet studies of ABFT completed over the same spatio-temporal range of this study indicate that herring remained a dominant prey component of adult size classes (Logan et al., 2015). It also could be argued that variation of migratory histories within specific ABFT cohorts could affect Hg trends. However, the declining trend in ABFT Hg was consistent across multiple age groups, suggesting that age-specific migratory differences cannot account for this observed decline. Furthermore, Hg concentrations of primary ABFT prey in the east Atlantic (myctophids, anchovy, squids) are comparable to western Atlantic prey (Table 6-4). Regardless, a decrease in bioavailable Hg in the North Atlantic would presumably decrease Hg in pelagic prey items throughout this ocean basin (as has been suggested for bluefish) (Cross et al., 2015), causing lower Hg in ABFT and other apex predators in the Atlantic.

EPA and FDA regulations on total Hg in fish

Nearly all (99%) of our measured ABFT samples were above the EPA fish consumption advisory level issued to protect public health (0.3 mg kg^{-1}) and 16% of them exceeded the FDA limit for human consumption (concentration at which fish can be removed from markets; 1.0 mg kg^{-1}). Larger, older fish more frequently exceeded the FDA limit, as most fish >260 cm in length had concentrations above 1 mg kg^{-1} whereas smaller ABFT (<200 cm) were all below this limit (Fig. 6-9). Thus, for consumers of ABFT, fish size-selection will impact total Hg intake, although total MeHg consumption is a function of frequency and total mass of seafood consumed (including non-ABFT seafood). In addition to total Hg consumed, the presence of possible

146

ameliorative factors such as Se and other nutrients in fish may reduce MeHg risks in seafood consumers, although this still needs further exploration (Gribble et al., 2016; Mozaffarian, 2009) While this study does not consider risks, tunas of various species and sizes are important protein sources for millions of people around the world, and this issue remains an important one to explore in future research so that advice to consumers is accurate.

Conclusions

Declining Hg in ABFT parallels declines of atmospheric Hg concentrations, suggesting that Hg in ABFT is linked to human activities and that recent efforts to decrease atmospheric Hg loading have propagated up marine food webs to commercially exploited apex predators. It also suggests that marine animals can respond concurrently to changes in ocean Hg deposition, and that continued efforts to decrease atmospheric loading of Hg could further lower Hg concentrations in seafood. The declines in ABFT MeHg concentrations observed on a decadal time scale suggest a short residence time for Hg in the mixed layer, which is consistent with water column measurements that suggest a residence time of about 1 year (Lamborg et al., 2014b). This study provides the first evidence that these efforts have positively impacted bluefin tuna. It remains to be investigated if other tuna species have responded similarly. Robust analyses of both prey and predator species, and their ecological relationships, should refine our understanding of regional and temporal benefits of reducing ocean Hg contamination.

Table 6-1. Total Hg in bluefin tuna reported in previous literature.

Capture year	Capture location	Sample size	Length (cm)	Weight (kg)	Total Hg concentration (mg kg^{-1} wet weight)		Reference
					Mean (SD)	Range	
1971	E. Atlantic	6	200-271		0.68 (0.17)	0.46-0.91	Establier, 1972
1975	E. Atlantic	344			0.47	0.10-1.30	Thibaud, 1986
1990	W. Atlantic	14	235-310	194-382	1.14 (0.3)	0.58-1.60	Hellou et al., 1992
1988	Mediterranean	7			0.50	0.07-1.36	Pastor et al., 1994
n/a	Mediterranean	3			0.25 (0.01)		Plessi et al., 2001
n/a	Atlantic	20		6.0-39	0.42 (0.06)		Yamashita et al., 2005
1998	Mediterranean	169		0.33-158	1.02 (0.99)	0.07-4.26	Storelli and Marcotrigiano, 2001
1999	Mediterranean	161		5.3-83	1.18 (0.85)	0.16-2.59	Storelli et al., 2002
2003	Mediterranean	73	54-63	2.9-4.4	0.20 (0.07)	0.13-0.35	Storelli et al., 2005
2003	Mediterranean	14	162-235	50-190	3.03 (0.55)	2.45-4.21	Licata et al., 2005
2003	Mediterranean	29		100-300	0.89*	0.49-1.81	Srebocan et al.,2007
2005	Mediterranean	9	126±12	28±8	1.50		Vizzini et al., 2010
2012	Mediterranean	23	137-252	46-259	0.66 (0.59)	0.14-2.21	Renzi et al., 2014
2008-2012	NW Atlantic	1293	63-326	58-347	0.76 (0.33)	0.25-3.15	This study

*median value reported

Table 6-2. Age groups and their corresponding size ranges

Rounded Age	Estimated age range	Actual size range
y	y	cm
9	8.50 ~ 9.49	178.1 ~ 192.8
10	9.50 ~ 10.49	192.9 ~ 205.7
11	10.50 ~ 11.49	205.8 ~ 216.6
12	11.50 ~ 12.49	216.7 ~ 225.7
13	12.50 ~ 13.49	225.8 ~ 233.5
14	13.50 ~ 14.49	233.6 ~ 240.3

Approximate age was estimated from body length using an empirical growth curve generated from direct age-length observations from otoliths and modal progression data (Restrepo et al., 2010).

Table 6-3. Result of the least squares regression analysis in each age group.

Linear Model

Age group	n	r^2	*p* value	Slope	Upper 95%	Lower 95%
9	238	0.185	<0.001	-0.020	-0.025	-0.014
10	249	0.109	<0.001	-0.020	-0.027	-0.013
11	197	0.122	<0.001	-0.017	-0.023	-0.010
12	137	0.122	<0.001	-0.019	-0.028	-0.010
13	94	0.050	0.031	-0.012	-0.023	-0.001
14	78	0.085	<0.001	-0.023	-0.040	-0.006
Pooled slope	993	0.332	<0.001	-0.018	-0.021	-0.015
Pooled slope (bootstrap)	993	-	-	-0.018	-0.022	-0.015

Log-Linear Model

Age group	n	r^2	*p* value	Slope	Upper 95%	Lower 95%
9	238	0.181	<0.001	-0.035	-0.025	-0.044
10	249	0.100	<0.001	-0.027	-0.017	-0.037
11	197	0.115	<0.001	-0.023	-0.014	-0.032
12	137	0.119	<0.001	-0.024	-0.013	-0.035
13	94	0.050	0.030	-0.016	-0.002	-0.030
14	78	0.088	<0.001	-0.026	-0.007	-0.045
Pooled slope	993	0.350	<0.001	-0.026	-0.021	-0.030

Table 6-4. Preferred prey of ABFT in various ocean regions and their Hg concentrations, as reported in the literature.

Prey common name	Scientific name	Region[*]	Hg (SD) mg kg^{-1} w.w.[†]	Refs[‡]
Atlantic herring	*Clupea harengus*	WNA	0.02 (0.02)	1-3
Atlantic menhaden	*Brevootia tyrannus*	WNA	0.01 (0.01)	2,5
sand lance	*Ammodytes spp.*	WNA	0.04 (0.03)	1-3,6
silver hake	*Merluccius bilinearis*	WNA	0.05 (0.05)	1-3
Atlantic mackerel	*Scomber scombrus*	WNA	0.02 (0.01)	1-3
bluefish	*Pomatomus saltatrix*	WNA	0.35 (0.02)	1-3
anchovy	*Engraulis encrasicolus*	ENA	0.03 (0.02)	6-8
myctophids	*Myctophidae spp.*	MED	0.11 (0.08)	1,8
anchovy	*Engraulis encrasicolus*	MED	0.05 (0.01)	8
sardine	*Sardine pilchardus*	MED	0.09 (0.02)	8
shortfin squid	*Illex coindetii*	MED	0.28 (0.15)	1,8

*WNA (Western North Atlantic); ENA (Eastern North Atlantic); MED (Mediterranean Sea)
†w.w. = wet weight
‡Refs refer to published studies that denote prey as preferred prey for ABFT and report Hg concentrations for prey species. 1: Shimose and Wells (2015); 2: Staudinger (2011); 3: Logan et al. (2015); 4: Burger and Gochfeld (2011); 5: Butler (2007); 6: Logan et al. (2011); 7: Ortiz de Zarate and Cort (1986); 8: Lahaye et al. (2006)

Table 6-5. Year-to-year comparisons of Atlantic bluefin tuna (*Thunnus thynnus*) Hg concentrations.

Total Hg data by year were compared, (a) individual and (b) family error rate, using the non-parametric Kruskal-Wallis test.

(a)	2005	2006	2007	2008	2009	2010	2011	2012
2004	0.07	0.67	0.91	**<0.001**	**<0.001**	**<0.001**	**<0.001**	**<0.001**
2005		0.07	0.09	**0.02**	**0.05**	**<0.001**	**<0.001**	**0.02**
2006			0.64	**0.001**	**0.003**	**<0.001**	**<0.001**	**<0.001**
2007				**<0.001**	**0.001**	**<0.001**	**<0.001**	**<0.001**
2008					0.99	**<0.001**	**<0.001**	0.64
2009						**<0.001**	**<0.001**	0.71
2010							0.06	**<0.001**
2011								**<0.001**

(b)	2005	2006	2007	2008	2009	2010	2011	2012
2004	1.00	1.00	1.00	**0.002**	0.12	**<0.001**	**<0.001**	**<0.001**
2005		1.00	1.00	1.00	1.00	**<0.001**	**<0.001**	1.00
2006			1.00	0.14	0.47	**<0.001**	**<0.001**	0.11
2007				**0.02**	0.23	**<0.001**	**<0.001**	**0.006**
2008					1.00	**<0.001**	**0.001**	1.00
2009						**0.004**	0.10	1.00
2010							1.00	**<0.001**
2011								**<0.001**
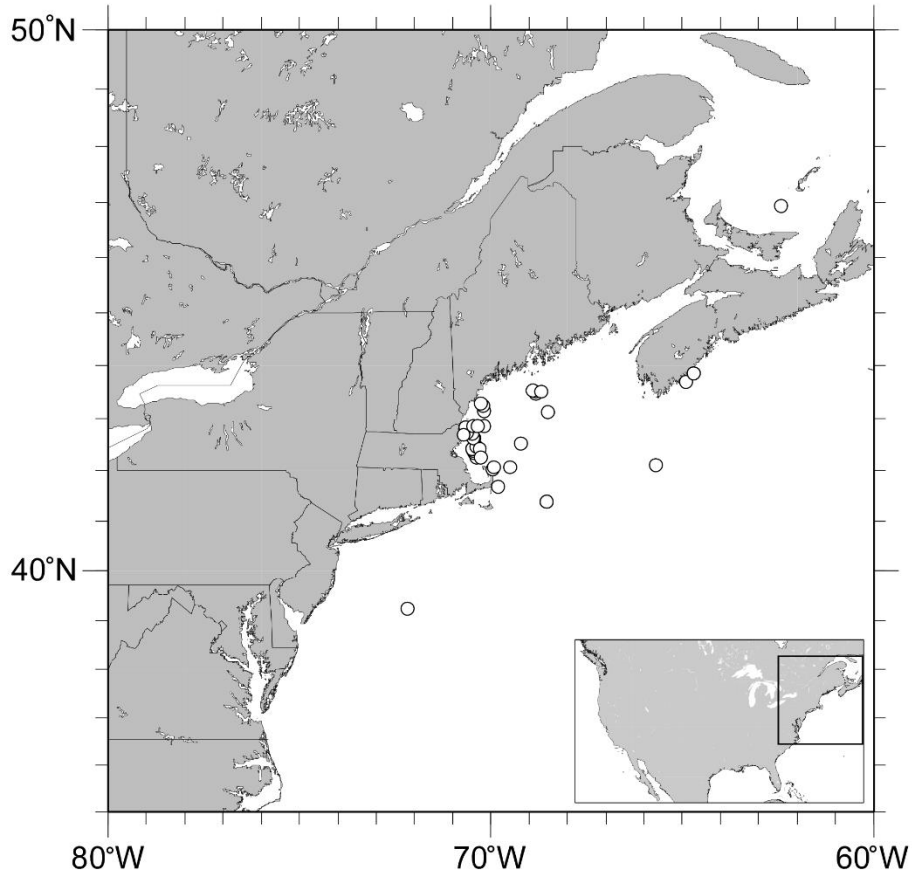
Figure 6-1. Known capture locations of ABFT. Note that several known catch locations have specific region names although no specific coordinates were provided. These include Stellwagen Bank, Ipswich Bay, Jeffrey's Ledge, Whaleback, and Hellhole in Gulf of Maine and Prince Edward Island in Gulf of St. Lawrence. A few ABFT were captured outside the Gulf of Maine in waters off Nova Scotia and oceanic waters off the Northeastern U.S. coast.
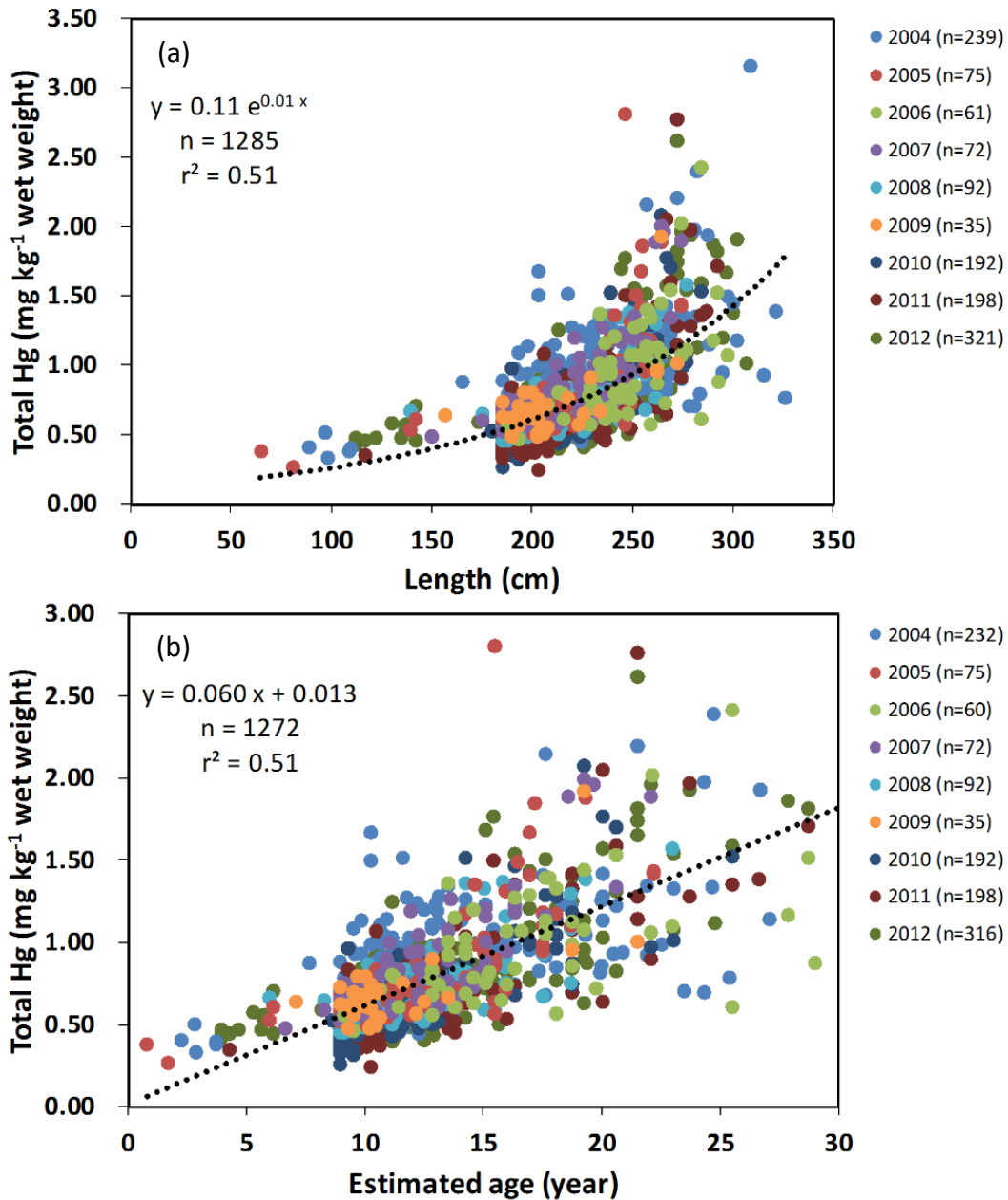
Figure 6- 2. Relationship between total Hg in ABFT and individual ABFT (a) length and (b) estimated age. Circles represent individual Hg measurements with color indicating year of capture (2004 to 2012). Stippled black lines show (a) exponential and (b) linear fits to data. Estimation of age beyond 30 years using length-age algorithms is highly uncertain, thus ABFT estimated >30 years old are not shown.
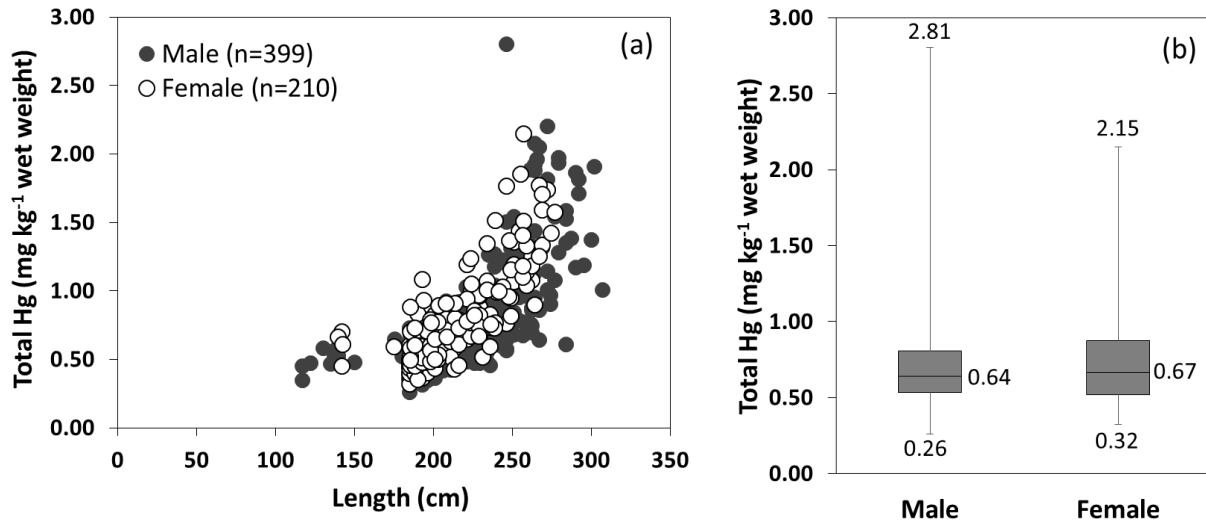
Figure 6-3. Comparison of Hg concentration in male and female ABFT. (a) Total Hg in male and female ABFT as a function of length (curved fork length, cm). (b) Box plot of Hg in male and female ABFT with values of median, maximum and minimum. Average Hg concentrations were 0.74 ± 0.34 mg kg^{-1} in males (n = 399) and 0.76 ± 0.33 mg kg^{-1} in females (n = 210). Hg concentrations in males and females were not significantly different from one another ($p = 0.6$).
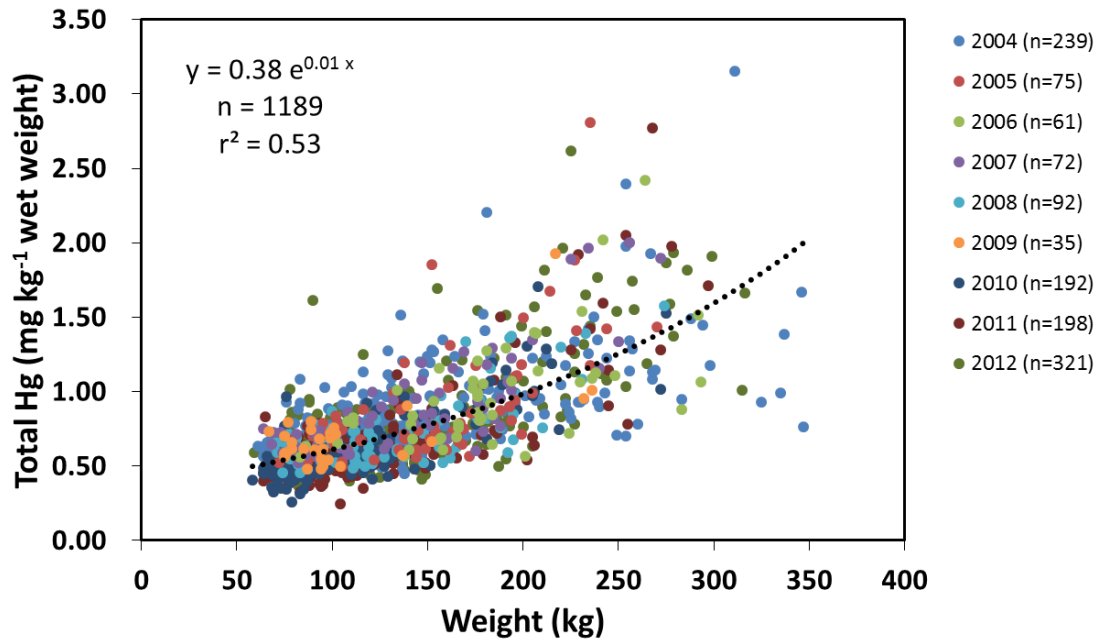
Figure 6-4. Relationship between total Hg in ABFT and weight. Weight here refers to dressed weight: weight of the fish after removal of gills, viscera, head, and fins. Stippled black line shows exponential fit to data.
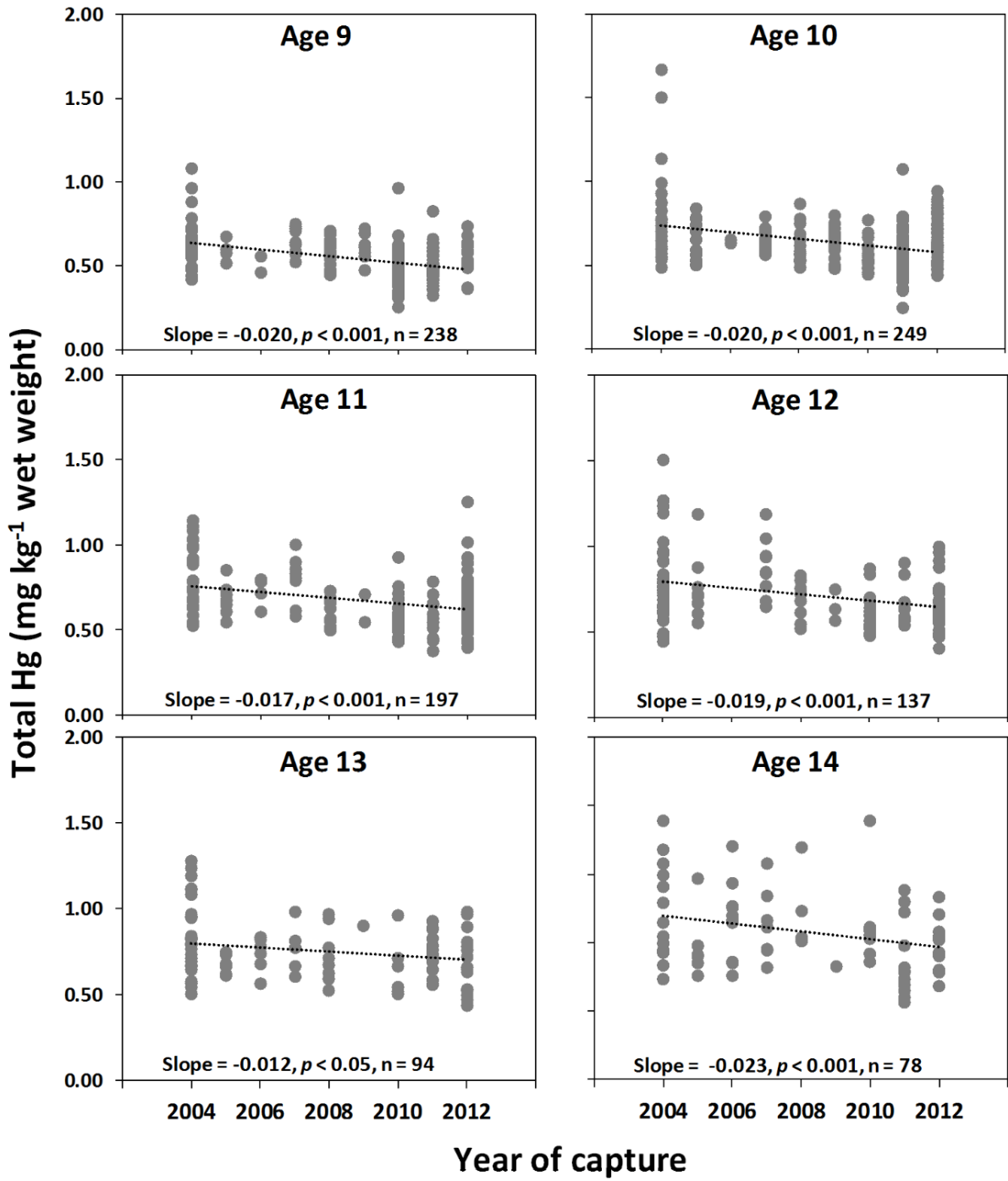
Figure 6-5. Hg concentrations in same-age ABFT decrease from 2004-2012. For each age group, circles represent Hg measurements for individual fish, and stippled line shows linear fit to data. All slopes were negative and significant (see individual panels for *p*-value of trend for each age class). Corresponding fish length of each age group is presented in Table 6-2.

157
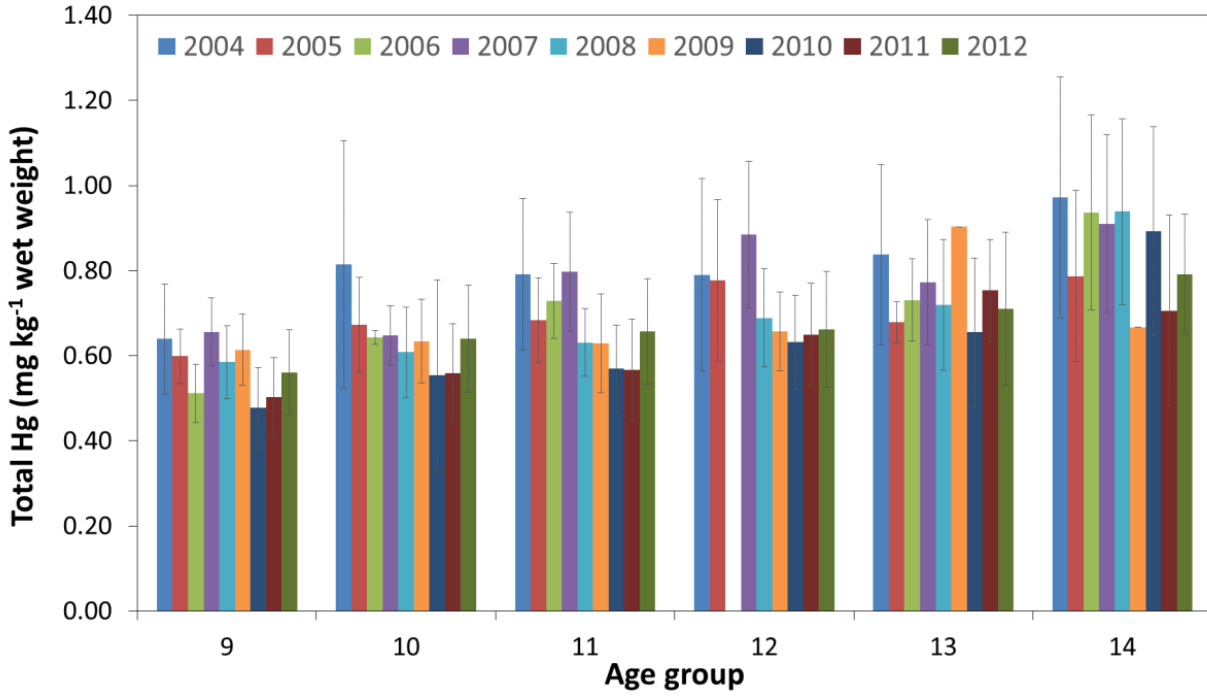
Figure 6-6. Total Hg in ABFT in age groups 9 to 14 years old. Bar color indicates year of capture. Error bars show 1 SD. Blank space in age group 12 indicates no samples collected in 2006.
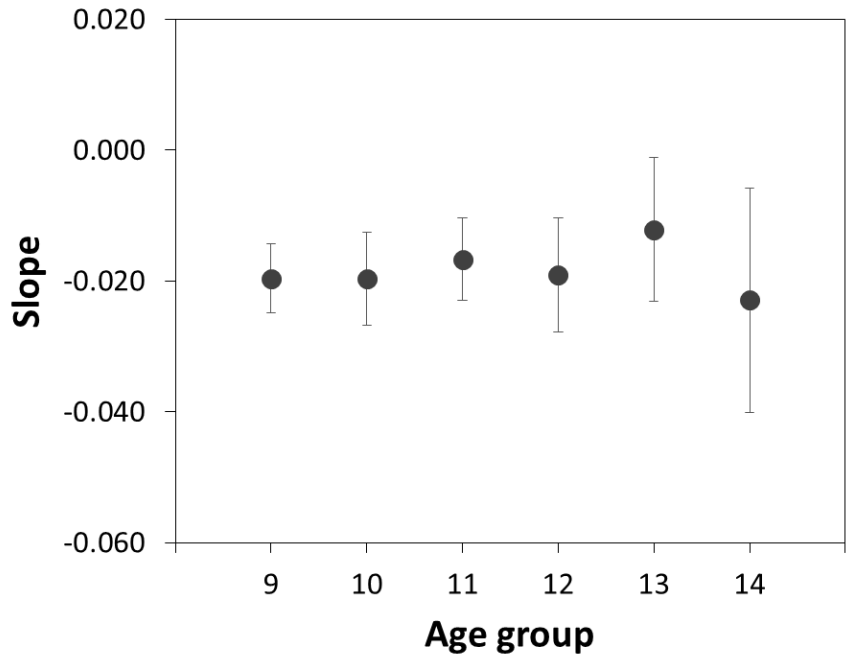
Figure 6-7. Comparison of slopes across age groups 9-14 years. Error bars show 95% confidence interval. There were no significant differences in slope between age groups (F-test for homogeneity of regression slopes, $p = 0.733$).
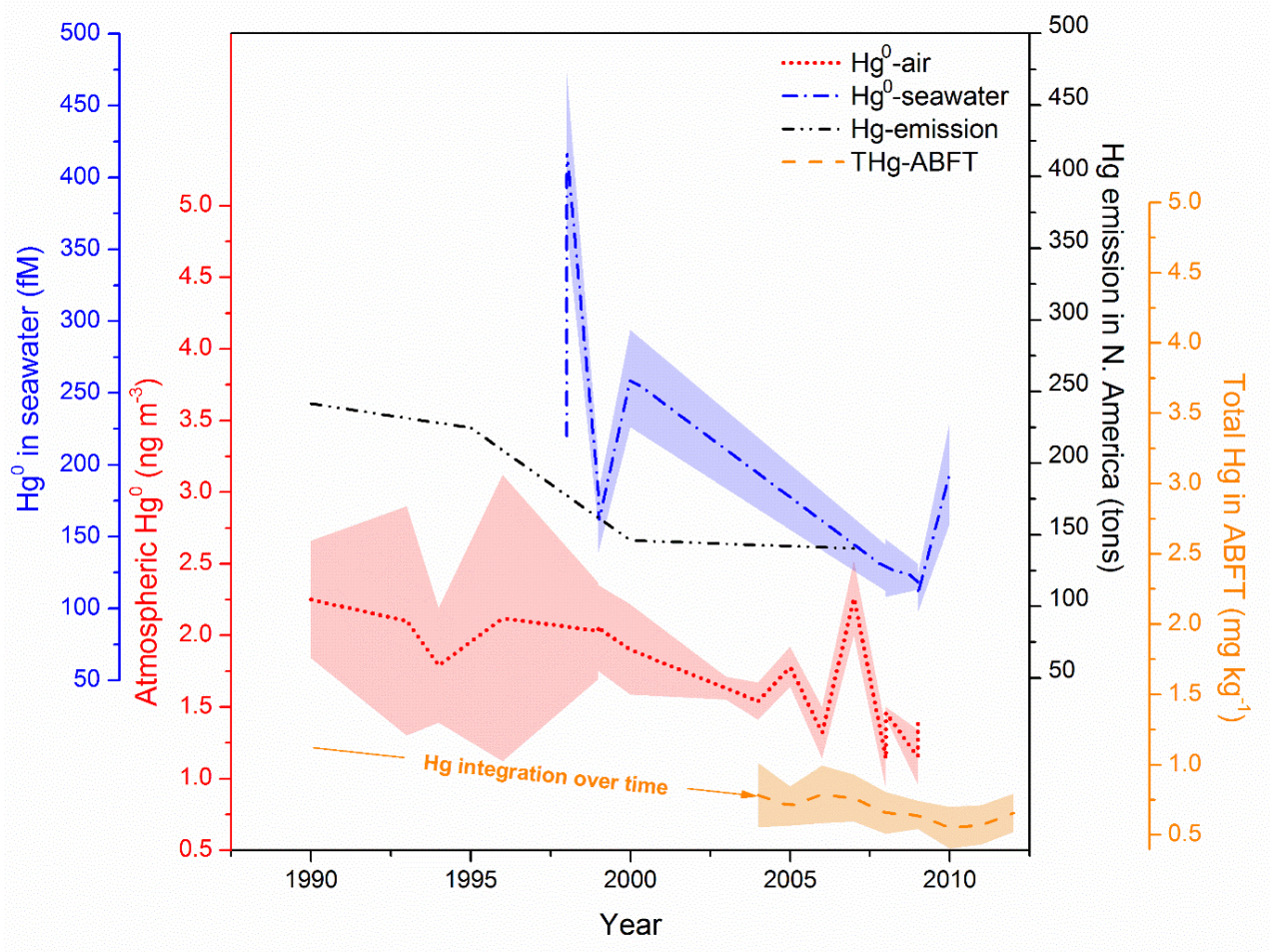
Figure 6-8. Temporal trends of anthropogenic Hg emission in N. America (n = 4), atmospheric Hg^0 above the N. Atlantic (n = 18), dissolved gaseous Hg^0 in N. Atlantic surface water (n = 10), and total Hg in ABFT caught in the Gulf of Maine (n = 993, age group 9 to 14). Shaded areas show variability (1 SD) around measurements. Note that Hg in ABFT was an integration of Hg accumulated over the entire lifetime of the fish.
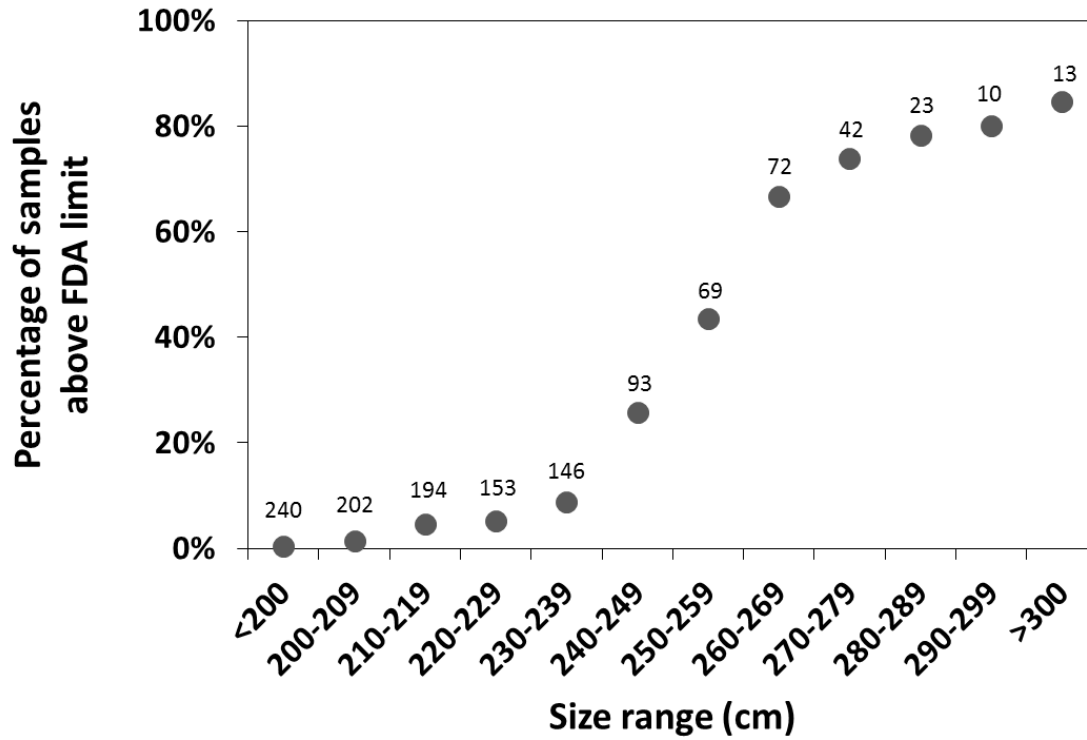
Figure 6-9. Percentage of ABFT muscle samples above FDA limit (1.0 mg kg^{-1}) for different fish size ranges. Numbers above each point represent the sample size for each size group.

Chapter 7

Conclusions

My thesis considered MeHg interactions with marine organisms at different trophic levels in marine food chains. Given that humans are mainly exposed to MeHg through seafood consumption, research on MeHg accumulation and bioavailability to aquatic organisms, and subsequent MeHg biomagnification in food webs has been motivated principally by public health concerns. Phytoplankton as a primary producer in aquatic food chains can accumulate many metals to a great extent from ambient waters and serve as highly enriched sources of these metals for herbivorous animals. Surprisingly, very few studies have addressed algal uptake of MeHg in marine environments. In this thesis, I examined the bioaccumulation of MeHg in six species of marine phytoplankton which have different size, surface area, and cell wall composition. This is the first study reporting the MeHg uptake by diverse marine phytoplankton and how environmental conditions influence algal accumulation. I found that the extent of MeHg uptake by marine algae mainly tracked the surface area-to-volume ratios of algal cells, which is consistent with findings for many other metals. Small cyanobacteria such as *Synechococcus bacillaris* showed great enrichment of MeHg, with concentration factors exceeding 10^6. Although temperature, light, and nutrient concentrations can affect phytoplankton growth, the initial uptake rate constants were not influenced. This suggests that algal MeHg uptake was probably not driven by metabolic activities and was primarily through passive sorption to the cell surfaces. Temperature had significant effects on MeHg uptake by dinoflagellate *P. minimum*, suggesting an active uptake for this species. Because this dinoflagellate species is known to be mixotrophic, it is possible that they acquired MeHg bound to organic matter or colloidal and nanoscale particles through phagocytosis. Limited by finite mass of MeHg in each culture flask, a "biodilution" effect induced by excess algal growth was eventually observed during incubation. However, with the exception of a massive algal bloom event, the biodilution effect would not be

163

expected to occur in most marine environments because algal biomass densities are usually too low to exhaust dissolved MeHg or even draw them to less than 50% of concentrations in the absence of algal cells. Chloride is abundant in seawater, and the MeHg-Cl complex has a higher lipophilicity than other species such as MeHg-OH. Previous studies suggested that increasing Cl concentration can lead to greater MeHg enrichment in algal cells (Kim et al., 2014; Mason et al., 1996). I also found this to be the case, with MeHg accumulation in a diatom *T. pseudonana* being proportional to Cl concentrations. MeHg concentration factors in seawater with high chloride concentrations (550 mM, salinity = 35‰) were about ~2.3 times greater than those in seawater with low chloride (6 mM, salinity = ~3.5‰). Overall, surface area-to-volume ratios of algal cells have the most pronounced effects on MeHg accumulation in phytoplankton, and salinity can moderately affect MeHg bioavailability to phytoplankton. Temperature, light, and nutrients have no direct influences on MeHg uptake. Thus, seasonal variations in the species composition of coastal phytoplankton assemblages may ultimately result in different degrees of MeHg biomagnification in the food chain, with highest levels expected to be inversely related to the cell size of the dominant phytoplankton species.

It has been suggested that dissolved organic matter (DOM) can alter the bioavailability of MeHg through metal-ligand complexation, just as it does for many other metals. However, quantifying the precise amount the DOM reduces bioavailability is probably impossible because of the diversity and uncertain composition of DOM in waters from one place to another, resulting in the difficulty in associating MeHg bioavailability with DOM's concentration and composition. In this thesis, I systematically investigated how MeHg-DOM complexation affects MeHg uptake by a marine diatom *T. pseudonana*. Because Hg, including MeHg, tends to bind most strongly

with sulfur ligands, organic matter containing sulfur was selected in this study. I found that amino acids such as glycine, cysteine, and even methionine had no effects on algal MeHg uptake when their concentrations were at environmentally realistic levels. Although cysteine contains a thiol (-SH) functional group, a decline of algal MeHg uptake was observed only when high concentrations (>100 nM) of cysteine were added. However, glutathione can effectively reduce MeHg uptake at environmentally realistic concentrations. As low as 10 nM of glutathione reduced MeHg's concentration factor in *T. pseudonana* by ~30%. Glutathione is a commonly seen biogenic organic matter in marine environments and is probably associated with phytoplankton productivity. A significant decline in algal MeHg accumulation with glutathione addition may imply that other similar biogenic thiols such as phytochelatin (an oligomer of glutathione), glutamine-cysteine, and γ-glutamylcysteine (a precursor of glutathione) may also have comparable influences. During a massive algal bloom, in addition to the potential bio-dilution effect, the release of these compounds may also reduce MeHg accumulation in phytoplankton. Humic acid can also effectively reduce algal MeHg accumulation by ~15% and ~25% with humic acid addition of 0.1 and 0.5 mg-C L^{-1}, respectively. This suggests the terrestrial input of DOM (mainly humic substances) may substantially reduce algal uptake of MeHg in estuarine and coastal waters, and this in turn may explain why MeHg concentration factors in seston in coastal areas are often found to be low. By examining algal MeHg uptake in seawater containing different concentrations of naturally occurring DOM, I concluded that MeHg accumulation in *T. pseudonana* was inversely correlated with bulk dissolved organic carbon (DOC) concentrations. MeHg accumulation in *T. pseudonana* at a DOC concentration of 40 μM (open ocean waters) was ~3 times higher than at a DOC concentration of 400 μM (coastal waters with very high DOM input). Overall, this study demonstrated that naturally occurring

DOM, particularly some thiol-containing compounds, effectively reduced MeHg accumulation in phytoplankton.

Considering all the factors affecting MeHg uptake by phytoplankton, it is possible to attempt a comparison of phytoplankton bioaccumulation of MeHg in coastal and open ocean waters based on my data. These comparisons are based on broad generalizations that do not apply to all waters, of course, but they may still provide a set of expectations of patterns of MeHg bioaccumulation in different waters. Surface area-to-volume ratio of algal cells and DOC concentrations are the two factors most affecting MeHg uptake by phytoplankton. Generally, open-ocean algal communities are dominated by smaller cells than coastal regions, hence for equal concentrations of mercury in surface waters, algal concentration factors of MeHg in the open ocean can be expected to exceed those of coastal cells, possibly by up to two orders of magnitude. In addition, DOC concentrations in the open ocean are typically lower than in coastal waters, the concentration factor of MeHg in algae can be up to 3-fold higher in oligotrophic regions of the open ocean than in coastal waters. The modest effect of salinity on MeHg accumulation can be ignored between oceanic and coastal waters. Since temperature and light have no direct effects on algal MeHg uptake, they can also be ignored in this comparison. Combining the effects of algal sizes and DOC concentrations, the concentration factors of MeHg in open ocean algae may be expected to be ~100 to ~300 times higher than in coastal algae, which is comparable to field observations reported in Table 2-4. However, although the concentration factors of MeHg in coastal algae are typically lower, the total MeHg accumulation in coastal phytoplankton and in their predator at higher trophic levels may be higher because the coastal waters may have higher concentrations of MeHg because Hg loadings from anthropogenic input are often greater in

coastal regions and subsequent *in-situ* production of MeHg from sediments would also be expected to be higher there.

Another issue addressed in my thesis is the trophic transfer of MeHg from phytoplankton to zooplankton. Understanding this process is important because MeHg is highly assimilated in animals and consequently builds up in marine food chains, leading to higher concentrations in upper trophic level animals than their prey. Many other metals have been comprehensively studied in terms of their trophic transfer at the bottom of aquatic food chains, but MeHg has not been similarly studied with respect to assimilation and retention in marine zooplankton, and very few studies have thoroughly investigated the trophic transfer of MeHg from phytoplankton to zooplankton. By feeding different algal foods to a calanoid copepod *Acartia tonsa*, I determined the assimilation efficiencies and efflux rates of MeHg in these copepods. Despite the different algal diets used, the copepod's assimilation efficiencies of MeHg ranged from 58% to 79%, and were proportional to the cytoplasmic fraction of MeHg in the algal cells. The efflux rate constants of MeHg (0.11-0.22 d^{-1}) following dietary uptake were significantly lower than those of Hg(II) (0.47-0.66 d^{-1}). In addition, the efflux rate constants following the aqueous uptake were about 0.21 d^{-1}. By using these measured parameters, I calculated the trophic transfer factors (TTFs) of Hg(II) and MeHg in these copepods. As expected, the TTFs were always larger than one for MeHg, suggesting biomagnification of MeHg from phytoplankton to zooplankton. In contrast, the TTFs of Hg(II) were consistently lower than 0.2, indicating that Hg(II) was unable to build up in food chains. I also used these parameters to assess the relative importance of MeHg sources (diet or water) for copepods. In general, the uptake from diet can account for at least 50% of the MeHg intake in copepods if the seawater-algae bioconcentration factor of MeHg

was ~10^5. If an algal diet with a MeHg bioconcentration factor over 10^6 (mostly found in open ocean waters), over 90% of a copepod's MeHg body burden was derived from the diet. In addition, I established a model using the measured bioaccumulation parameters to predict the MeHg concentrations in zooplankton when MeHg concentrations in water and phytoplankton (or microseston) are known. Although comprehensive field studies for MeHg in waters and seston are few, my model-predicted MeHg concentrations in copepods matched most of the independent measurements for copepods in coastal (Long Island Sound) and open ocean waters (Pacific and Atlantic Oceans). Combined with my earlier results in chapter 2 that MeHg concentration factors in diverse marine phytoplankton relate to algal cell size (surface area-to-volume ratios), the MeHg concentrations in both phytoplankton and zooplankton now can be accurately estimated with only a few measured parameters.

Hg transformation, converting Hg(II) and MeHg to Hg^0, in seawater is tightly associated with photochemical and microbial processes. Although the photochemical reaction is significant because of its higher rate constant, it is limited to the daytime and surface ocean depths. Rapid attenuation of sunlight with depth can decrease the effectiveness of the photochemical processes, especially in high latitude regions. If the microbial transformation of Hg can occur at any depth, the biological production of Hg^0 should become a significant source to the total pool of Hg^0 in the water column. However, the relative importance of microbial-mediated conversion of Hg^0 from either Hg(II) or monomethylmercury (MeHg) throughout the water column remains unclear. In addition, it has been suggested that microbial transformation of Hg^0 can directly degrade MeHg and prevent further methylation of Hg(II), and subsequently reduce MeHg concentrations in waters, which is beneficial to aquatic organisms. In my research described in this thesis, I

developed a rapid and sensitive method to trace the production and subsequent evasion of Hg^0 and related these to the abundance and activity of natural bacterioplankton assemblages in coastal waters. Thus, I related the kinetics of Hg^0 evasion, from either Hg(II) or MeHg as the ultimate source, to microbial activities. I also measured the bacteria production using ^{3}H-leucine incorporation method, and performed conventional PCR analysis to search for Hg-resistant genes in bacteria. I demonstrated that marine bacterioplankton can convert Hg(II) and MeHg to Hg^0 at prevailing ocean temperatures, which can then be released to the overlying air. The rate of gas evasion would presumably depend on the turbulence and aeration of surface waters.

Surprisingly, Hg^0 gas evasion was even observed in coarse-filtered Southampton seawater stored at 4°C for 6 years in the dark that was brought to room temperature over 48 h. This result may imply that microbes revived from low temperature due to climate changes (e.g., thawed permafrost) may be able to quickly transform Hg species (e.g., demethylation or methylation), resulting in perturbations in the global Hg cycling. I found that Hg^0 production rates were independent of dissolved Hg(II) and MeHg concentrations, and were directly proportional to bacterial cell densities. In addition to low temperatures inhibiting Hg^0 formation, bacterial mercuric reductase was also detected in our coastal samples, suggesting that bacterial metabolic activities and enzymatic reactions were responsible for Hg^0 gas formation. Hg^0 production rates were very different between Southampton seawater and Stony Brook seawater, even after normalizing to their bacterial densities. This result suggested that the structure of bacterial community residing in these two waters are different, although freshly collected SHSW was not evaluated, so direct comparisons between SHSW and SBSW were not possible from these experiments. Natural microbial assemblages may include archaea, which cannot be distinguished by DAPI staining. However, little is known about the interactions of Hg with archaea and studies

on Hg resistance mechanisms in archaea are sparse. Two very distinct production patterns between Hg(II) and MeHg treatments were observed, suggesting two different pathways of Hg^0 generation. The production of Hg^0 from MeHg seemed not as sensitive to temperature as from Hg(II). These results may be associated with the localization and distribution of Hg(II) and MeHg within bacterial cells. Again, during an algal bloom, in addition to the potential impacts of bio-dilution and elevated DOM complexed with MeHg, enhanced bacterial activity may increase Hg(II) reduction and MeHg degradation, leading to another positive feedback on reducing MeHg accumulation in phytoplankton. Further investigations regarding Hg^0 production mechanisms will be needed in the future. In addition, MeHg transfer among organisms within the microbial loop (e.g., between bacteria and protozoans that feed on them) might be influence the cycling and oceanic residence times of MeHg, although this has not been explored. Further research on this issue to compare with work involving "traditional" food chains (algae-zooplankton-fish) would help complement current knowledge about the fate of MeHg in ocean waters. My findings showed the importance of Hg^0 production and evasion mediated by natural marine bacteria, and the subsequent decline in Hg(II) and MeHg concentrations may have significant implications for the amount of Hg entering marine food webs.

   Once MeHg has entered the marine food chain, its concentrations in biota can increase substantially with increasing trophic level. For instance, large apex pelagic fish such as bluefin tuna can be enriched in MeHg levels up to 10^8 times relative to ambient aqueous MeHg concentrations. Seafood consumption is a major MeHg source for human exposure. Because of public health concerns, many total Hg measurements in various freshwater and marine fish species (including tuna species) have been made in the past few decades. However, modest

sample sizes and the frequent lack of sample information (e.g., fish length, weight, diet, and habitat) precluded further data analyses. In this thesis, I analyzed the total Hg concentrations in muscle tissue in almost 1300 Atlantic bluefin tuna (ABFT, *Thunnus thynnus*) caught primarily in the Gulf of Maine. This data set was unique in part because of the large sample size, but also because there was much ancillary information regarding these tunas. Moreover, there was a wide size spectrum of ABFT, ranging from 65 to 326 cm, with consecutive capture years spanning from 2004 to 2012. These allowed me to investigate the relationships of ABFT MeHg concentrations with their captured location and date, length, weight, and sex. I found the average total Hg concentrations to be 0.76 ± 0.33 mg kg^{-1} (range 0.25–3.15 mg kg^{-1}), which was comparable to some previously published studies. The Hg concentrations were found to increase exponentially or linearly with fish length, weight, and estimated age. For those fish where gender was identified, no differences were observed for Hg concentrations between male and female ABFT. The most striking finding was that Hg in ABFT declined significantly from 2004 to 2012 within the same age fish. The decline rate was about 0.018 mg kg^{-1} per year, corresponding to an average decline of 19% from 2004 to 2012 (~2% per year). This decline was nearly parallel to temporal changes in concentrations of atmospheric Hg^0 above the North Atlantic, dissolved gaseous Hg^0 in North Atlantic surface water, and anthropogenic Hg emissions in North America over the same period of time. This also suggested that Hg in ABFT was linked to human activities and recent efforts of decreasing Hg emission have propagated up marine food webs to large apex predators. It further implies that marine animals can respond rapidly to changes in ocean Hg concentrations. This finding can respond to the statement in the Introduction that "because the higher trophic levels obtain their MeHg mainly from dietary sources, it has been suggested that even a small difference in MeHg enrichment at the base of aquatic food web may

171

have a significant consequence on the overall biomagnification of MeHg at upper trophic levels." This study has provided the very first evidence that human efforts have positively impacted Hg levels in ABFT.

Significance and Implications

This proposal investigated several important processes of MeHg in marine environments and demonstrated the importance of MeHg interactions with biota in marine food chains, enhancing our knowledge of marine biogeochemistry of Hg. This thesis is also the first study to evaluate the impacts of multiple biological factors and environmental variables on MeHg uptake and its subsequent trophic transfer. I have combined laboratory experiments with field data to ensure the validity of my results and discussion. This thesis also pointed out that marine bacteria can play a critical role in converting MeHg to Hg^0 gas, and this process may directly influence aqueous Hg(II) and MeHg concentrations and their build-up in food chains. In addition, marine bacteria respire labile dissolved organic matter (DOM) which is mainly produced and released from plankton. Consequently, the cycling of mercury in marine ecosystems appears to be heavily influenced by microorganisms with the "microbial loop." It would be expected that the influence of microbial processes can also determine the residence time of dissolved Hg species in the water column and the amount of MeHg entering the marine food web. This thesis is also the first study to present the Hg concentrations in numerous individuals of ABFT with known ancillary parameters such as fish size, gender, and location and time of capture. These results suggest the use of migratory fish as bioindicators of Hg levels on a basin-wide scale and will become a useful information regarding public health implications.

The generated data can be applied to a global biogeochemical Hg model (GEOs-Chem) developed at Harvard University. Models are effective tools to formalize our best understanding of processes, make a connection between laboratory and field data and evaluate the relative importance of various processes of MeHg cycling in the ocean. Given the expected changes of anthropogenic Hg emission in the future due to the Minamata treaty, the refined biogeochemical Hg model will be helpful to better predict the fate of Hg in the marine environment and its concentrations in marine biota.

Suggestions for future work

Decipher phytoplankton derived MeHg-binding organic ligands

While conducting the experiment of algal MeHg uptake, it was interesting that the uptake curve reached a plateau after 24 to 48 h of exposure even though more MeHg remained in solution and algal cells kept growing which provided more binding surfaces to MeHg (Figs. 2-1, 3-1). Most of the cultures were axenic therefore it was unlikely that bacterial uptake was competing against algal uptake. As described above in Chapters 2 and 3, one possibility was that phytoplankton-derived DOM formed complexes with MeHg and then reduced the MeHg bioavailability to algal cells. A recent study used a liquid chromatography (LC) coupled by electrospray ionization to a hybrid linear ion trap − Fourier-transform ion cyclotron resonance (FT-ICR) mass spectrometer to successfully identify metabolites produced by a diatom *T. pseudonana* (Longnecker et al., 2015). However, whether the newly released dissolved organic compounds have strong affinities for MeHg remains unclear. To date, very few labs have successfully developed a tandem of high pressure liquid chromatography (HPLC) integrated with inductively coupled plasma mass spectrometer (ICP-MS) to detect dissolved organometallic compounds in seawater. Once key compounds associated with targeted metals are identified, use

of ^1H and ^{13}C nuclear magnetic resonance spectrometer (NMR) can further characterize these compounds. These applications allow us not only to determine the molecular mass and elemental composition of organic-metal compounds, but also to characterize their structures and chemical bonds. For example, Dr. Repeta's group at the Woods Hole Oceanographic Institution has been working on identifying marine organic ligands bound to trace metals. However, their metals of interest are biologically essential metals such as Fe, Co, Ni, Cu, and Zn which have known metabolic pathways in marine phytoplankton and bacteria. Field studies suggested that most of the Hg was complexed by natural organic ligands associated with DOM (Han et al., 2006). The exact organic speciation of Hg (including MeHg) in seawater will be an interesting question to explore because speciation can control Hg bioavailability. However, it will be a great challenge because of its extremely low concentrations. The ultimate goals will be to characterize the primary composition of Hg-organic complexes in seawater, to understand how they vary in different marine environments, to identify their sources (which organisms are responsible for the production), and to assess how Hg-organic ligands influence Hg species acquisition by microorganisms.

MeHg uptake by plankton and the influences of colloidal matter

Hg (both Hg(II) and MeHg) is associated with colloidal material in many different marine environments, and the fraction of Hg-colloid can vary substantially from one place to another (Choe and Gill, 2003; Guentzel et al., 1996; Stordal et al., 1996). Several studies have investigated the bioavailability of metals bound to colloids. For example, Wang and Guo (2000) have found that marine colloidal materials added to cultures of a diatom and dinoflagellate decreased Zn uptake but increased Cr uptake. In addition, the colloidal material might be an

important source of metals to some heterotrophic flagellates (Tranvik et al., 1993). However, no study was ever conducted to investigate whether colloidal Hg or MeHg can affect its bioavailability to algae. In my preliminary experiment, I found that once 0.2 μm-filtered SHSW was injected with dissolved MeHg, about 30% of the MeHg was associated with colloidal matter (1 kDa−0.2 μm) and over 70% of MeHg stayed in the truly dissolved phase (<1 kDa) (Fig. 7-1). If MeHg is injected into 1 kDa-filtered SHSW, most of the MeHg stayed in the truly dissolved phase (Fig. 7-1). Coastal and estuarine waters have received large quantities of terrestrial high-molecular weight (colloidal) organic matter such as humic substances. This thesis has already shown that humic acid can reduce MeHg accumulation in phytoplankton, implying a low bioavailability of colloidal MeHg to algal cells. Further studies should include a systematic investigation (i.e., using more than one cut-off to differentiate colloids' size) on how colloidal Hg species interact with marine phytoplankton.

MeHg distribution and localization within cells

Living particles such as phytoplankton are important carriers of MeHg. In this thesis, I determined the uptake rate constant of MeHg by marine phytoplankton and found that most of the MeHg was inside the algal cells. Zhong and Wang (2009) used washing reagents to remove the cell-surface-bound MeHg and determined the internalization rate of MeHg in diatom cells. These results show that MeHg can rapidly penetrate the cell membrane and accumulate in the cytoplasm of algal cells. However, the exact localization of MeHg and whether MeHg is evenly or heterogeneously distributed in algal cells have not been well studied. Also, the traditional methods to determine cytoplasmic fraction of MeHg include mechanical grinding or sonication and separation through centrifugation. Some issues, for example, re-partitioning between cell

175

wall-bound MeHg and cytoplasmic MeHg may occur during sample processing in these methods. In addition, using washing reagents may also cause potential artifacts. Synchrotron X-ray fluorescence (SXRF) is known to be a powerful tool to visualize the element distribution (e.g., Si, S, Fe, Mn, Ni, Zn…etc) in the cell of microorganisms. Gu et al. (2014) successfully used SXRF technique to map total Hg (mostly Hg(II)) on suspended particles and diatoms in a contaminated freshwater system. They found that Hg was heterogeneously distributed and was mostly found on the surface of algal cells, which agreed with earlier studies. SXRF has been used in hair analyses of animals and humans to assess their MeHg intake (Zareba et al., 2008), and has been used to localize MeHg uptake and accumulation in zebrafish larvae at the tissue and cellular level (Korbas et al., 2008). However, to my knowledge, SXRF has not been used to map MeHg localization in suspended biogenic particles. One difficulty might be tied to the low quantity of any Hg species inside one single cell that is below SXRF's detection limit. Another complication is that SXRF cannot distinguish MeHg from total Hg. Nevertheless, by using this technique, with phytoplankton cells amended with MeHg, it may allow us to determine the partitioning, reactivity, and bioavailability of MeHg more accurately in marine phytoplankton.

MeHg release from planktonic carcasses and fecal pellets

   MeHg accumulation in phytoplankton, and assimilation and release from zooplankton were reported in this thesis. But release of MeHg from living phytoplankton is not examined. Because MeHg penetrates appreciably into algal cytoplasm, it is unlikely that phytoplankton release MeHg efficiently in a short time. The rates of MeHg release from debris of phytoplankton, and from fecal materials and carcasses of zooplankton have not been examined yet. The release of MeHg from decomposing planktonic debris and fecal materials may contribute MeHg input to

176

subsurface remineralization zones, although *in situ* production of MeHg in association with bacterial decomposition of organic matter is thought to be a more important source below surface waters. Lee and Fisher (1992a; 1992b) have studied the degradation and release of many elements from planktonic debris and fecal materials. Similar approaches can apply to MeHg to examine its release rates from materials derived from plankton. Because MeHg is highly assimilated in plankton, it can be expected that MeHg released from decomposing debris should be at rates comparable to that of organic carbon. These processes and their associated parameters are important components for the model of marine Hg cycling, and will be needed to better understand Hg's fate in the ocean.

Potential Hg methylation occurring in the guts of zooplankton and fish

Microbial methylation of Hg(II) is the primary source of MeHg in most aquatic environments. Anaerobic sulfate-reducing and iron-reducing bacteria are thought to be responsible for in situ MeHg production. In a study in the Canadian Arctic, Pućko et al. (2014) calculated the dietary intake of MeHg could account for only ~30% of the MeHg body burden in zooplankton *Calanus hyperboreus*, and they speculated that transformation of MeHg might occur within the species which was mediated by gut microbial communities. It has been suggested that the guts of zooplankton *Calanus* spp. can serve as biogeochemical hotspots where acidic and suboxic/anoxic conditions might support iron dissolution and anaerobic microbial activities (Tang et al., 2011). Therefore, such conditions in the guts may promote *in vivo* Hg methylation by iron-reducing bacteria. If this hypothesis is true for zooplankton, then a similar mechanism is likely to occur in fish guts (Rudd et al., 1980). Thus, the amount and availability of Hg(II) substrate necessary for methylation in the diet may become very important, though Hg(II) does not build up in food

177

webs. Application of multiple stable Hg isotopes may be a better tool to help validate this hypothesis. In addition, the recent discovery of two Hg methylation genes, *hgcA* and *hgcB*, has allowed us to design molecular probes for assessing Hg methylation in the environment (Christensen et al., 2016; Parks et al., 2013). Hence, whether the microbes residing in plankton guts have the potential to methylate Hg(II) can be tested.

Effects of microbial Hg evasion in the presence of phytoplankton

Bacteria and phytoplankton are two major components in the marine microbial loop. They are coexisting in the ocean waters, and how their interactions affect the transformation of Hg species would be an interesting question to explore. The incubation studies in this thesis showed that marine bacteria alone can rapidly reduce Hg(II) and degrade MeHg, generating gaseous Hg^0 and thus removing MeHg from seawater. In contrast, phytoplankton are greatly enriched in MeHg and introduce MeHg into marine food chains, essentially keeping MeHg in the water column. In natural waters, algal cells can compete against bacterial cells in acquiring MeHg. However, phytoplankton cells can be a hotspot hosting bacteria and phytoplankton-derived DOM can fuel bacterial activities, both of which may lead to enhanced Hg^0 evasion. In my preliminary experiments, I inoculated the diatom *T. pseudonana* into seawater containing natural bacterial assemblages, then injected this culture with Hg(II) and MeHg, and examined Hg^0 formation over time. The preliminary results are shown in Fig. 7-2. It was interesting that more Hg(II) reduction was found in seawater containing only bacteria (Fig. 7-2a); in contrast, more MeHg demethylation was found in seawater containing both bacteria and diatoms (Fig. 7-2b). These results indicated that bacteria-algae interactions favored MeHg degradation but went against Hg(II) reduction. Algal growth and bacterial growth are shown in Fig. 7-2c and Fig. 7-2d,

respectively. In Hg(II) treatments (Fig. 7-2a), less Hg^0 formation in the seawater containing algae might be because the algal cells took up aqueous Hg(II) and thus less Hg(II) was available to the bacteria. In MeHg treatments (Fig. 7-2b), more Hg^0 formation in the seawater containing algae might be attributable to enhanced bacterial growth due to more DOM released by algae. The explanation and mechanism behind these observations need further exploration.

Comparison of total Hg in large pelagic fish between ocean basins

Through analyzing the large data set of Hg concentrations in ABFT, I found that ABFT Hg body burdens declined in the past decade. The likely explanation is that anthropogenic Hg emissions from the North America and Europe have decreased due to human efforts, resulting in less Hg deposition in the Atlantic. In Asia, countries like China and India are two major sources of Hg emissions because of their fast-growing industries and increased coal burning. Consequently, the Pacific Ocean may have received increased Hg deposition, and elevated Hg may propagate up the food chain to top predators. Drevnick et al. (2015) reported that the Hg concentrations in Pacific yellowfin tuna (PYFT, *Thunnus albacares*) caught near Hawaii was increasing at a rate of at least 3.8% per year, and they suggested that Hg concentrations in fish are keeping pace with current loading increases to the ocean. However, whether Pacific bluefin tuna (PBFT, *Thunnus orientalis*) shows a similar trend to PYFT is unknown. Because bluefin tuna is a highly migratory species, it might be a better sentinel species than PYFT to evaluate "basin-wide" impacts in response to increasing Hg loading. It is also worthwhile to compare Hg accumulation patterns in bluefin tunas from different ocean basins, for example, Pacific vs. Atlantic. ABFT and PBFT are closely related to each other and are supposed to have very similar Hg accumulation kinetics. But because of the differences in seawater Hg concentration, diet

(prey), fishing pressure and management, and migration route of tunas between the two largest oceans, the Hg accumulation in ABFT might be dissimilar from PBFT. Figure 7-3 shows total Hg in ABFT and PBFT as a function of fish length. It seemed that Hg concentrations in small fish from Atlantic and Pacific were comparable. However, the size spectrum of PBFT available for my analysis was not as wide as ABFT and therefore no further discussion can be made (Fig. 7-3).

In Chapter 6, I concluded that there was no difference between male and female ABFT (Fig. 6-3). Most of my samples were caught in the northwest Atlantic, Gulf of Maine, which is not ABFT's spawning area. Two major spawning areas for ABFT are the Mediterranean Sea and the Gulf of Mexico. Prior to spawning, female ABFT may feed on more prey or have higher assimilation efficiency, resulting in higher Hg accumulation. In Fig. 7-3, I also present Hg concentrations in bluefin tunas caught in the Gulf of Mexico (GBFT). However, limited by its small sample size, no conclusion can be made at this point. More tuna samples with detailed ancillary information are needed in the future to confirm the hypotheses.

Mercury-Selenium molar ratios in marine fish.

This thesis showed that total Hg concentrations in ABFT was positively correlated to fish size. Thus, for consumers of tuna, fish size-selection will impact their total Hg intake, though total MeHg consumption is also a function of frequency and total mass of seafood consumed, including non-ABFT seafood. Recent studies have claimed that selenium (Se)-enriched diets not only prevent MeHg toxicity, but can also rapidly reverse some of its most severe symptoms (Ralston and Raymond, 2010). Studies have also demonstrated that Se at levels usually found in tunas and billfish tend to accumulate together with Hg in marine fish (Burger and Gochfeld,

2011; Kaneko and Ralston, 2007). Studies of maternal populations exposed to diets that contain

Hg in molar excess of Se, such as shark or pilot whale meats, have found adverse child outcomes,

but studies of populations exposed to MeHg by eating Se-enriched ocean fish observe improved

child IQs instead of harm (Ralston and Raymond, 2010). Therefore, a molar Se-Hg ratio of one

or greater in diets might be able to mitigate toxic impacts of MeHg, but this is not yet considered

in FDA advisories, nor is it widely accepted in the "mercury community." In addition to

determining total Hg, I also measured total Se in bluefin tunas (n = 484). Figure 7-4a shows total

Se concentrations in Atlantic and Pacific bluefin tunas as a function of length. Unlike Hg, Se

concentrations were not proportional to length but appeared to be better regulated than Hg.

Because Se concentrations stayed less variable, Hg-Se ratios were mainly controlled by Hg

concentrations and ratios >1 were only found in tunas larger than 200 cm (Fig. 7-4b). I further

separated fish into different size groups and compared the percentage of fish individuals with

Hg:Se ratios >1 in each group (Fig. 7-5). It was clear that Hg-Se ratios >1 increase with fish size.

Future research should specifically focus on dynamics of these interactions in the most

commonly consumed tunas so that advice to seafood consumers is accurate. While FDA

guidelines are static numbers (not related to mass and frequency of intake, as well as other

nutrients like Se), the data generated from this thesis and follow-up analysis in the future can

provide useful information in refining advisory guidelines of seafood consumption.
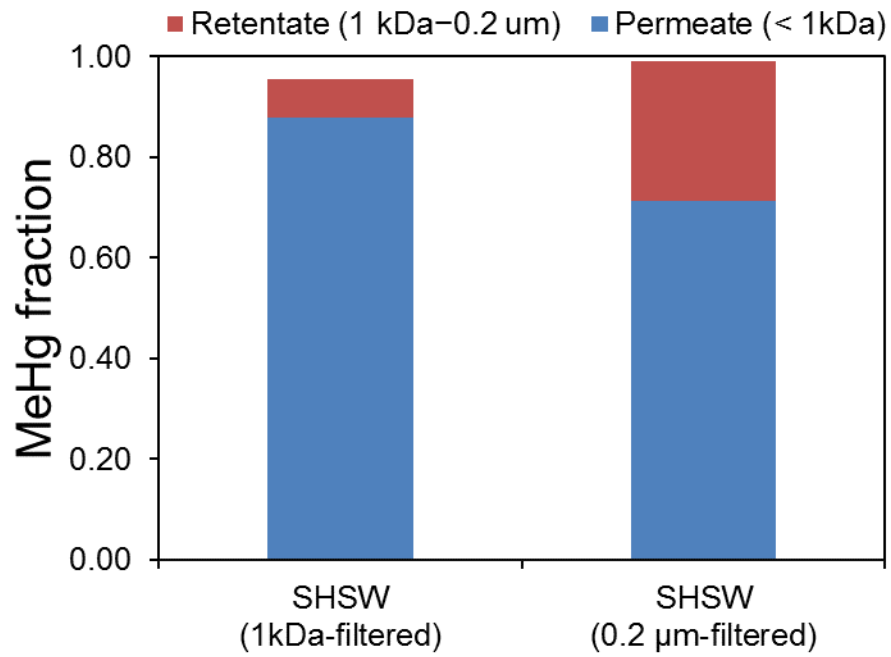
Figure 7-1. MeHg distribution in the collodial phase (1 kDa−0.2 μm) and the truly dissolved phase (<1 kDa).
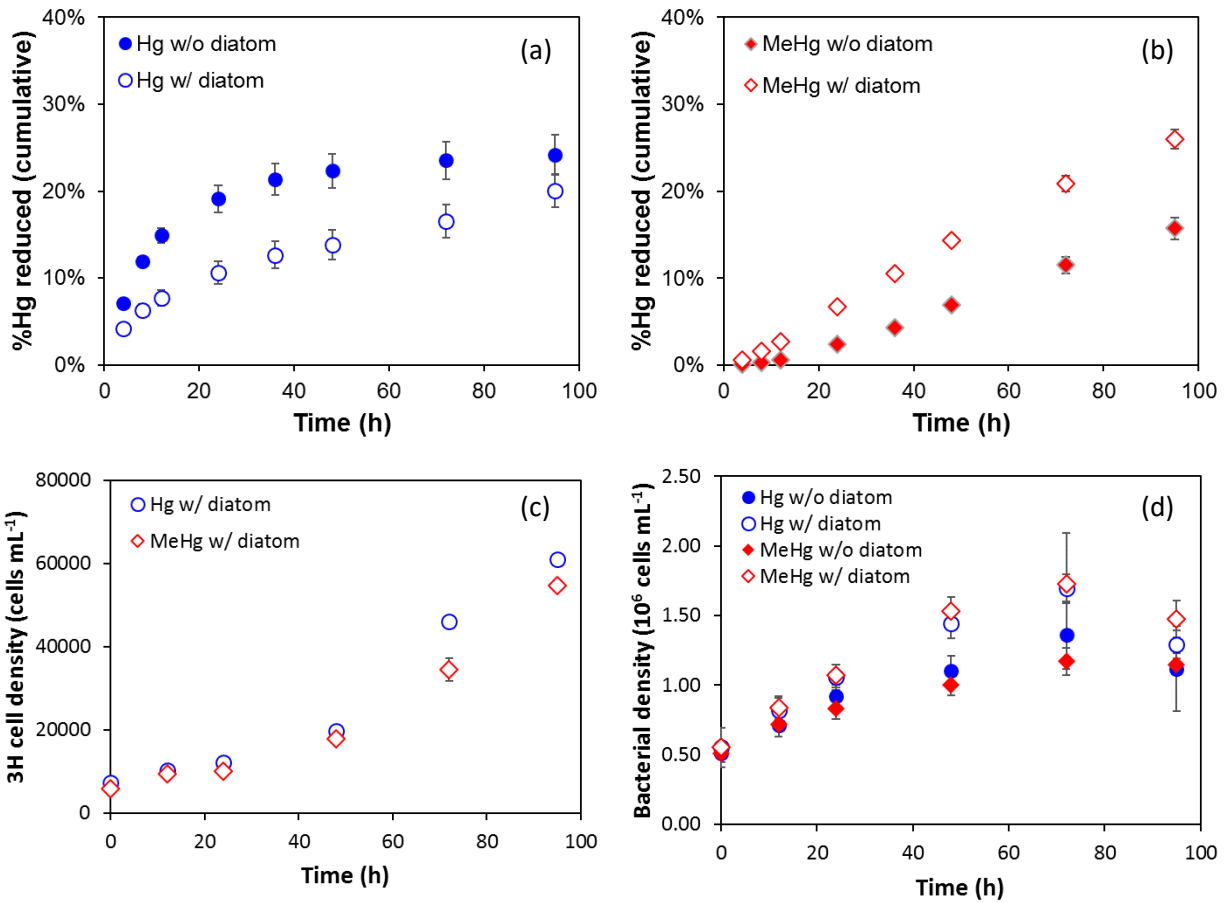
Figure 7-2. Total percentage of Hg⁰ evolved from (a) Hg(II)-treated and (b) MeHg-treated SHSW with and without diatom *T. pseudonana*, (c) diatom cell density and (d) bacterial density in two treatments over time. Treatments with bacteria were 1 μm filtered and controls were 0.2 μm filtered. Data points are the means from three replicate cultures with error bars of one standard deviation. %Hg evolved in controls were subtracted.
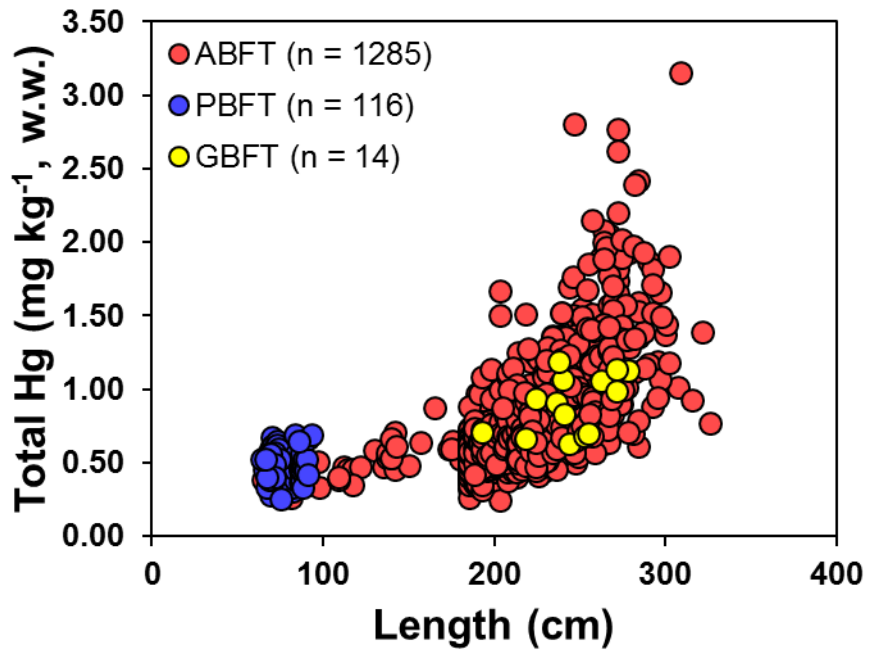
Figure 7-3. Total Hg in bluefin tunas caught from different ocean basins as a function of length. ABFT = bluefin tuna caught near northwest Atlantic; PBFT = bluefin tuna caught off California; GBFT = bluefin tuna caught in Gulf of Mexico.
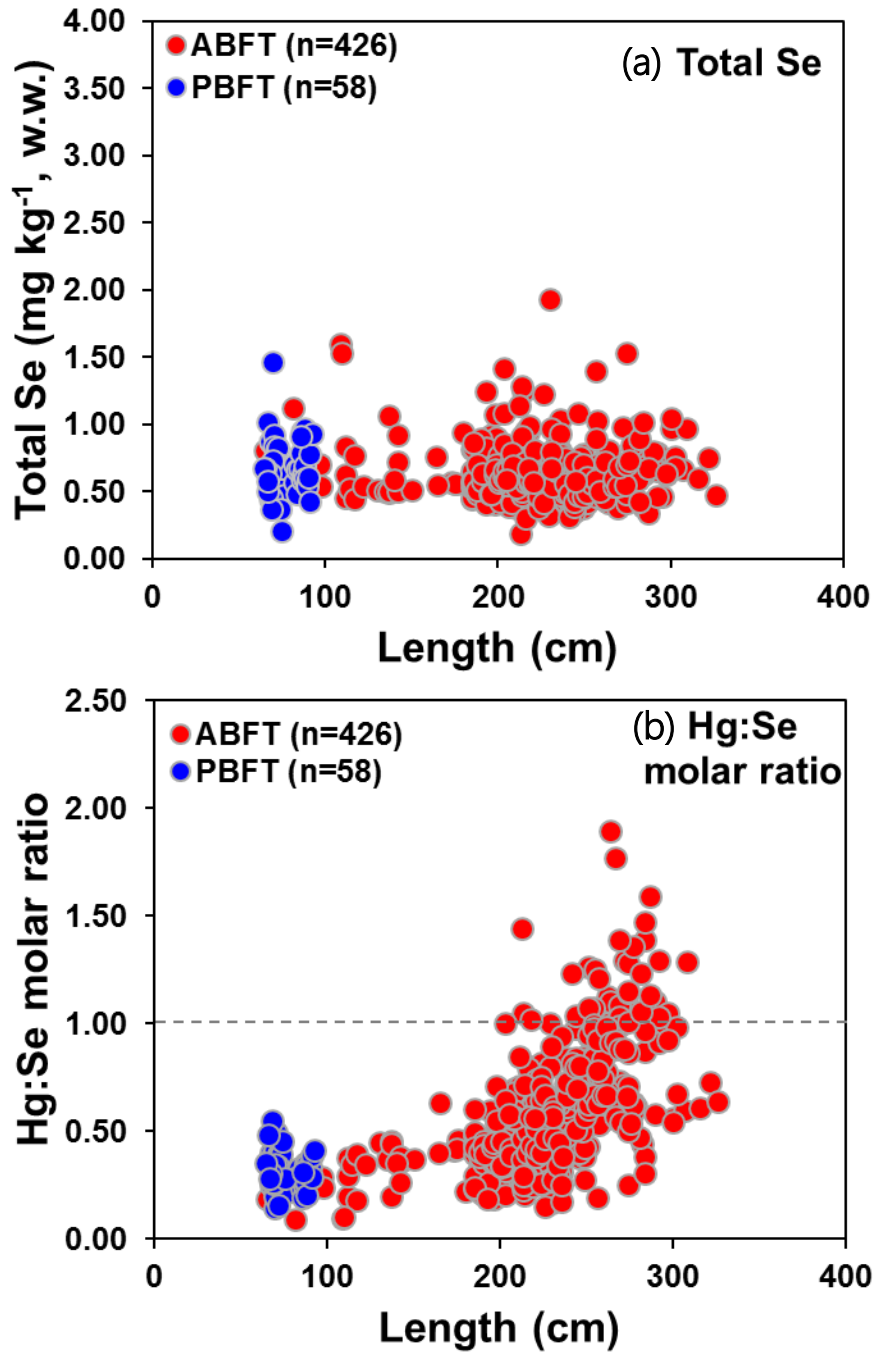
Figure 7-4. (a) Total Se concentrations and (b) Hg-Se ratios in Atlantic and Pacific bluefin tuna as a function of length.
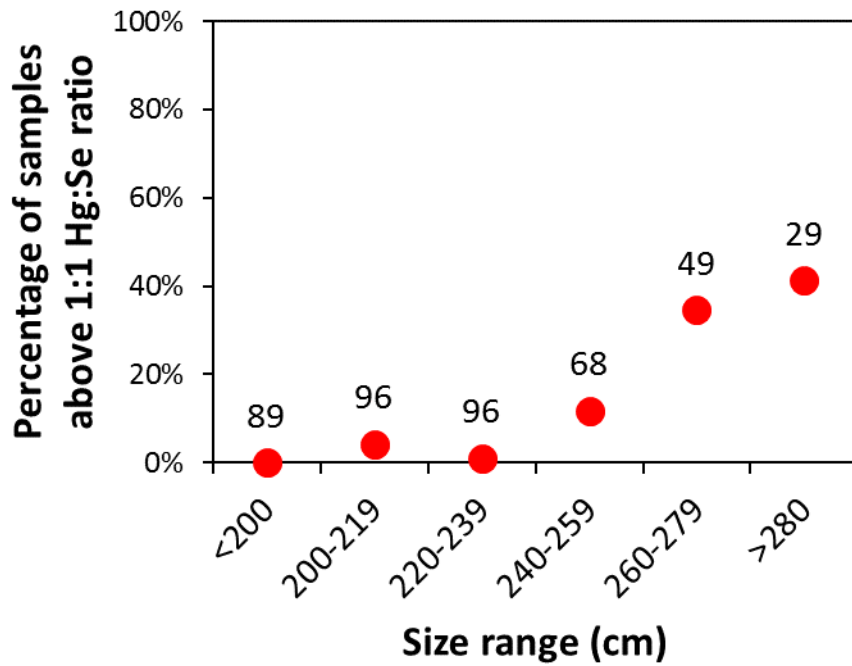
Figure 7-5. Percentage of tuna samples above 1:1 Hg:Se ratio in different fish-size groups. Numbers above data points are sample sizes.

Literature cited

Ahner, B.A., Wei, L., Oleson, J.R. and Ogura, N., 2002. Glutathione and other low molecular weight thiols in marine phytoplankton under metal stress. *Mar. Ecol. Prog. Ser.*, **232**: 93-103.

Al-Farawati, R. and van den Berg, C.M.G., 2001. Thiols in coastal waters of the western North Sea and English Channel. *Environ. Sci. Technol.*, **35(10)**: 1902-1911.

Alderighi, L., Gans, P., Midollini, S. and Vacca, A., 2003. Co-ordination chemistry of the methylmercury(II) ion in aqueous solution: a thermodynamic investigation. *Inorg. Chim. Acta*, **356**: 8-18.

Amirbahman, A., Reid, A.L., Haines, T.A., Kahl, J.S. and Arnold, C., 2002. Association of methylmercury with dissolved humic acids. *Environ. Sci. Technol.*, **36(4)**: 690-695.

Amyot, M., Gill, G.A. and Morel, F.M.M., 1997. Production and loss of dissolved gaseous mercury in coastal seawater. *Environ. Sci. Technol.*, **31(12)**: 3606-3611.

Amyot, M., McQueen, D.J., Mierle, G. and Lean, D.R.S., 1994. Sunlight-induced formation of dissolved gaseous mercury in lake waters. *Environ. Sci. Technol.*, **28(13)**: 2366-2371.

Anderson, T.H. and Taylor, G.T., 2001. Nutrient pulses, plankton blooms, and seasonal hypoxia in western Long Island Sound. *Estuaries*, **24(2)**: 228-243.

Arnold, A.P. and Canty, A.J., 1983. Methylmercury(II) sulfhydryl interactions. Potentiometric determination of the formation constants for complexation of methylmercury(II) by sulfhydryl containing amino acids and related molecules, including glutathione. *Can. J. Chem.*, **61(7)**: 1428-1434.

Baeyens, W., Leermakers, M., Papina, T., Saprykin, A., Brion, N., Noyen, J., De Gieter, M., Elskens, M. and Goeyens, L., 2003. Bioconcentration and biomagnification of mercury and methylmercury in North Sea and Scheldt Estuary fish. *Arch. Environ. Contam. Toxicol.*, **45(4)**: 498-508.

Balcom, P.H., Fitzgerald, W.F., Vandal, G.M., Lamborg, C.H., Rolfhus, K.R., Langer, C.S. and Hammerschmidt, C.R., 2004. Mercury sources and cycling in the Connecticut River and Long Island Sound. *Mar. Chem.*, **90(1-4)**: 53-74.

Barkay, T., Gillman, M. and Turner, R.R., 1997. Effects of dissolved organic carbon and salinity on bioavailability of mercury. *Appl. Environ. Microbiol.*, **63(11)**: 4267-4271.

Barkay, T., Kroer, N. and Poulain, A.J., 2011. Some like it cold: microbial transformations of mercury in polar regions. *Polar Res.*, **30(1)**.

Barkay, T., Liebert, C. and Gillman, M., 1989. Environmental significance of the potential for *mer*(Tn21)-mediated reduction of Hg^{2+} to Hg^0 in natural waters. *Appl. Environ. Microbiol.*, **55(5)**: 1196-1202.

Barkay, T., Miller, S.M. and Summers, A.O., 2003. Bacterial mercury resistance from atoms to ecosystems. *FEMS Microbiol. Rev.*, **27(2-3)**: 355-384.

Barkay, T., Turner, R.R., VandenBrook, A. and Liebert, C., 1991. The relationships of Hg(II) volatilization from a freshwater pond to the abundance ofmer genes in the gene pool of the indigenous microbial community. *Microb. Ecol.*, **21(1)**: 151-161.

Baya, P.A., Hollinsworth, J.L. and Hintelmann, H., 2013. Evaluation and optimization of solid adsorbents for the sampling of gaseous methylated mercury species. *Anal. Chim. Acta*, **786**: 61-9.

Ben-Bassat, D. and Mayer, A.M., 1977. Reduction of mercury chloride by *Chlorella*: evidence for a reducing factor. *Physiol. Plant.*, **40(3)**: 157-162.

Berggreen, U., Hansen, B. and Kiorboe, T., 1988. Food size spectra, ingestion and growth of the copepod *Acartia tonsa* during development: implications for determination of copepod production. *Mar. Biol.*, **99(3)**: 341-352.

Berthon, G., 1995. Critical evaluation of the stability constants of metal complexes of amino acids with polar side chains (Technical Report). *Pure Appl. Chem.*, **67(7)**: 1117-1240.

Block, B.A., Dewar, H., Blackwell, S.B., Williams, T.D., Prince, E.D., Farwell, C.J., Boustany, A., Teo, S.L.H., Seitz, A. and Walli, A., 2001. Migratory movements, depth preferences, and thermal biology of Atlantic bluefin tuna. *Science*, **293(5533)**: 1310-1314.

Block, B.A., Jonsen, I.D., Jorgensen, S.J., Winship, A.J., Shaffer, S.A., Bograd, S.J., Hazen, E.L., Foley, D.G., Breed, G.A., Harrison, A.L., Ganong, J.E., Swithenbank, A., Castleton, M., Dewar, H., Mate, B.R., Shillinger, G.L., Schaefer, K.M., Benson, S.R., Weise, M.J., Henry, R.W. and Costa, D.P., 2011. Tracking apex marine predator movements in a dynamic ocean. *Nature*, **475(7354)**: 86-90.

Block, B.A., Teo, S.L.H., Walli, A., Boustany, A., Stokesbury, M.J.W., Farwell, C.J., Weng, K.C., Dewar, H. and Williams, T.D., 2005. Electronic tagging and population structure of Atlantic bluefin tuna. *Nature*, **434(7037)**: 1121-1127.

Bloom, N.S., 1992. On the chemical form of mercury in edible fish and marine invertebrate tissue. *Can. J. Fish. Aquat. Sci.*, **49(5)**: 1010-1017.

Bloom, N.S., Gill, G.A., Cappellino, S., Dobbs, C., McShea, L., Driscoll, C., Mason, R. and Rudd, J., 1999. Speciation and cycling of mercury in Lavaca Bay, Texas, sediments. *Environ. Sci. Technol.*, **33(1)**: 7-13.

Blum, J.D., Popp, B.N., Drazen, J.C., Choy, C.A. and Johnson, M.W., 2013. Methylmercury production below the mixed layer in the North Pacific Ocean. *Nat. Geosci.*, **6(10)**: 879-884.

Bonito, L.T., Hamdoun, A. and Sandin, S.A., 2016. Evaluation of the global impacts of mitigation on persistent, bioaccumulative and toxic pollutants in marine fish. *PeerJ*, **4**.

Bowman, K.L., Hammerschmidt, C.R., Lamborg, C.H. and Swarr, G., 2015. Mercury in the North Atlantic Ocean: The U.S. GEOTRACES zonal and meridional sections. *Deep Sea Res., Part II*, **116**: 251-261.

Burger, J. and Gochfeld, M., 2011. Mercury and selenium levels in 19 species of saltwater fish from New Jersey as a function of species, size, and season. *Sci. Total Environ.*, **409(8)**: 1418-1429.

Butler, C.M., 2007. Atlantic bluefin tuna (*Thunnus thynnus*) feeding ecology and potential ecosystem effects during winter in North Carolina. Master Thesis, North Carolina State University, Raleigh, NC, 118 pp.

Butler, C.M., Logan, J.M., Provaznik, J.M., Hoffmayer, E.R., Staudinger, M.D., Quattro, J.M., Roberts, M.A., Ingram, G.W., Jr., Pollack, A.G. and Lutcavage, M.E., 2015. Atlantic bluefin tuna *Thunnus thynnus* feeding ecology in the northern Gulf of Mexico: a preliminary description of diet from the western Atlantic spawning grounds. *J. Fish Biol.*, **86(1)**: 365-374.

Cabana, G. and Rasmussen, J.B., 1994. Modelling food chain structure and contaminant bioaccumulation using stable nitrogen isotopes. *Nature*, **372(6503)**: 255-257.

Campbell, P.G.C., 1995. Interactions between trace metals and aquatic organisms: A critique of the free-ion activity model. In: A. Tessier and D.R. Turner (Editors), Metal speciation and bioavailability in aquatic systems. Wiley, Chichester, West Sussex, England, pp. 45-102.

Campbell, P.G.C., Errécalde, O., Fortin, C., Hiriart-Baer, V.P. and Vigneault, B., 2002. Metal bioavailability to phytoplankton—applicability of the biotic ligand model. *Comp. Biochem. Physiol., C: Toxicol. Pharmacol.*, **133(1)**: 189-206.

Carlson, C.A. and Ducklow, H.W., 1995. Dissolved organic carbon in the upper ocean of the central equatorial Pacific Ocean, 1992: Daily and finescale vertical variations. *Deep Sea Res., Part II*, **42(2)**: 639-656.

Chang, S.I. and Reinfelder, J.R., 2000. Bioaccumulation, subcellular distribution, and trophic transfer of copper in a coastal marine diatom. *Environ. Sci. Technol.*, **34(23)**: 4931-4935.

Chapman, C.S., Capodaglio, G., Turetta, C. and van den Berg, C.M.G., 2009. Benthic fluxes of copper, complexing ligands and thiol compounds in shallow lagoon waters. *Mar. Environ. Res.*, **67(1)**: 17-24.

Chen, C.Y., Amirbahman, A., Fisher, N.S., Harding, G., Lamborg, C.H., Nacci, D. and Taylor, D., 2008. Methylmercury in marine ecosystems: spatial patterns and processes of production, bioaccumulation, and biomagnification. *EcoHealth*, **5(4)**: 399-408.

Choe, K.-Y. and Gill, G.A., 2003. Distribution of particulate, colloidal, and dissolved mercury in San Francisco Bay estuary. 2. Monomethyl mercury. *Limnol. Oceanogr.*, **48(4)**: 1547-1556.

Choy, C.A., Popp, B.N., Kaneko, J.J. and Drazen, J.C., 2009. The influence of depth on mercury levels in pelagic fishes and their prey. *Proc. Natl. Acad. Sci.*, **106(33)**: 13865-13869.

Christensen, G.A., Wymore, A.M., King, A.J., Podar, M., Hurt, R.A., Santillan, E.U., Soren, A., Brandt, C.C., Brown, S.D. and Palumbo, A.V., 2016. Development and validation of broad-range qualitative and clade-specific quantitative molecular probes for assessing mercury methylation in the environment. *Appl. Environ. Microbiol.*, **82(19)**: 6068-6078.

Colman, J.A., Nogueira, J.I., Pancorbo, O.C., Batdorf, C.A., Block, B.A. and MacLatchy, D., 2015. Mercury in Pacific bluefin tuna (*Thunnus orientalis*): bioaccumulation and trans-Pacific Ocean migration. *Can. J. Fish. Aquat. Sci.*, **72(7)**: 1015-1023.

Compeau, G. and Bartha, R., 1984. Methylation and demethylation of mercury under controlled redox, pH and salinity conditions. *Appl. Environ. Microbiol.*, **48(6)**: 1203-1207.

Cort, J.L., Deguara, S., Galaz, T., Mèlich, B., Artetxe, I., Arregi, I., Neilson, J., Andrushchenko, I., Hanke, A., Neves dos Santos, M., Estruch, V., Lutcavage, M., Knapp, J., Compeán-Jiménez, G., Solana-Sansores, R., Belmonte, A., Martínez, D., Piccinetti, C., Kimoto, A., Addis, P., Velasco, M., De la Serna, J.M., Godoy, D., Ceyhan, T., Oray, I., Karakulak, S., Nøttestad, L., López, A., Ribalta, O., Abid, N. and Idrissi, M.H., 2013. Determination of L_{max} for Atlantic bluefin tuna,*Thunnus thynnus(L.)*, from meta-analysis of published and available biometric data. *Rev. Fish. Sci.*, **21(2)**: 181-212.

Cossa, D., 2013. Marine biogeochemistry: Methylmercury manufacture. *Nat. Geosci.*, **6(10)**: 810-811.

Cossa, D., Averty, B. and Pirrone, N., 2009. The origin of methylmercury in open Mediterranean waters. *Limnol. Oceanogr.*, **54(3)**: 837-844.

Cossa, D., Harmelin-Vivien, M., Mellon-Duval, C., Loizeau, V., Averty, B., Crochet, S., Chou, L. and Cadiou, J.F., 2012. Influences of bioavailability, trophic position, and growth on methylmercury in hakes (*Merluccius merluccius*) from Northwestern Mediterranean and Northeastern Atlantic. *Environ. Sci. Technol.*, **46(9)**: 4885-93.

Cossa, D., Heimbürger, L.-E., Lannuzel, D., Rintoul, S.R., Butler, E.C.V., Bowie, A.R., Averty, B., Watson, R.J. and Remenyi, T., 2011. Mercury in the Southern Ocean. *Geochim. Cosmochim. Acta*, **75(14)**: 4037-4052.

Costa, M. and Liss, P.S., 1999. Photoreduction of mercury in sea water and its possible implications for Hg^0 air–sea fluxes. *Mar. Chem.*, **68(1)**: 87-95.

Costa, M. and Liss, P.S., 2000. Photoreduction and evolution of mercury from seawater. *Sci. Total Environ.*, **261(1)**: 125-135.

Cross, F.A., Evans, D.W. and Barber, R.T., 2015. Decadal declines of mercury in adult bluefish (1972-2011) from the mid-Atlantic coast of the U.S.A. *Environ. Sci. Technol.*, **49(15)**: 9064-9072.

Davison, A.C. and Hinkley, D.V., 1997. Bootstrap methods and their application. Cambridge series on statistical and probabilistic mathematics. Cambridge university press.

DiMento, B.P. and Mason, R.P., 2017. Factors controlling the photochemical degradation of methylmercury in coastal and oceanic waters. *Mar. Chem.*

Drevnick, P.E., Lamborg, C.H. and Horgan, M.J., 2015. Increase in mercury in Pacific yellowfin tuna. *Environ. Toxicol. Chem.*, **34(4)**: 931-934.

Driscoll, C.T., Mason, R.P., Chan, H.M., Jacob, D.J. and Pirrone, N., 2013. Mercury as a global pollutant: sources, pathways, and effects. *Environ. Sci. Technol.*, **47(10)**: 4967-4983.

Dupont, C.L. and Ahner, B.A., 2005. Effects of copper, cadmium, and zinc on the production and exudation of thiols by *Emiliania huxleyi. Limnol. Oceanogr.*, **50(2)**: 508-515.

Dupont, C.L., Goepfert, T.J., Lo, P., Wei, L. and Ahner, B.A., 2004. Diurnal cycling of glutathione in marine phytoplankton: field and culture studies. *Limnol. Oceanogr.*, **49**: 991-996.

Dupont, C.L., Moffett, J.W., Bidigare, R.R. and Ahner, B.A., 2006. Distributions of dissolved and particulate biogenic thiols in the subartic Pacific Ocean. *Deep Sea Res., Part I*, **53(12)**: 1961-1974.

Ercal, N., Gurer-Orhan, H. and Aykin-Burns, N., 2001. Toxic metals and oxidative stress part I: mechanisms involved in metal-induced oxidative damage. *Curr. Top. Med. Chem.*, **1(6)**: 529-539.

Fisher, J.A., Jacob, D.J., Soerensen, A.L., Amos, H.M., Steffen, A. and Sunderland, E.M., 2012. Riverine source of Arctic Ocean mercury inferred from atmospheric observations. *Nat. Geosci.*, **5(7)**: 499-504.

Fisher, N.S., 1985. Accumulation of metals by marine picoplankton. *Mar. Biol.*, **87(2)**: 137-142.

Fisher, N.S., 1986. On the reactivity of metals for marine phytoplankton. *Limnol. Oceanogr.*, **31(2)**: 443-449.

Fisher, N.S., 2002. Advantages and problems in the application of radiotracers for determining bioaccumulation of contaminants in aquatic organisms. In: P. Borretzen, T. Jolle and P. Strand (Editors), Proc. Intl. Conf. Radioactivity in the Environment. Norwegian Radiation Protection Authority, Monaco, pp. 573-576.

Fisher, N.S., Bjerregaard, P. and Fowler, S.W., 1983a. Interactions of marine plankton with transuranic elements. 1. Biokinetics of neptunium, plutonium, americium, and californium in phytoplankton. *Limnol. Oceanogr.*, **28(3)**: 432-447.

Fisher, N.S., Bohe, M. and Teyssie, J.L., 1984. Accumulation and toxicity of Cd, Zn, Ag, and Hg in four marine phytoplankters. *Mar. Ecol. Prog. Ser.*, **19(3)**: 201-213.

Fisher, N.S., Burns, K.A., Cherry, R.D. and Heyraud, M., 1983b. Accumulation and cellular distribution of ^{241}Am, ^{210}Po, and ^{210}Pb in two marine algae. *Mar. Ecol. Prog. Ser.*, **11**: 233-237.

Fisher, N.S. and Fabris, J.G., 1982. Complexation of Cu, Zn and Cd by metabolites excreted from marine diatoms. *Mar. Chem.*, **11(3)**: 245-255.

Fisher, N.S. and Fowler, S.W., 1987. The role of biogenic debris in the vertical transport of transuranic wastes in the sea. In: T.P. O'Connor, W.V. Burt and I.W. Duedall (Editors), Physicochemical processes and wastes in the ocean: Oceanic processes in marine pollution. Krieger, Malabar, FL, U.S.A, pp. 197-207.

Fisher, N.S., Nolan, C.V. and Fowler, S.W., 1991. Assimilation of metals in marine copepods and its biogeochemical implications. *Mar. Ecol. Prog. Ser.*, **71(1)**: 37-43.

Fisher, N.S. and Reinfelder, J.R., 1995. The trophic transfer of metals in marine systems. In: A. Tessier and D.R. Turner (Editors), Metal speciation and bioavailability in aquatic systems. Wiley, Chichester, West Sussex, England, pp. 363-406.

Fisher, N.S., Teyssie, J.L., Krishnaswami, S. and Baskaran, M., 1987. Accumulation of Th, Pb, U, and Ra in marine phytoplankton and its geochemical significance. *Limnol. Oceanogr.*, **32(1)**: 131-142.

Fitzgerald, W.F., Gill, G.A. and Kim, J.P., 1984. An equatorial Pacific Ocean source of atmospheric mercury. *Science*, **224**: 597-600.

Fitzgerald, W.F. and Lamborg, C.H., 2003. Geochemistry of mercury in the environment. In: H.D. Holland and K.K. Turekian (Editors), Treatise on geochemistry. Elsevier, pp. 1-47.

Fitzgerald, W.F., Lamborg, C.H. and Hammerschmidt, C.R., 2007. Marine biogeochemical cycling of mercury. *Chem. Rev.*, **107(2)**: 641-662.

Fowler, S.W. and Knauer, G.A., 1986. Role of large particles in the transport of elements and organic compounds through the oceanic water column. *Prog. Oceanogr.*, **16(3)**: 147-194.

French, T.D., Houben, A.J., Desforges, J.-P.W., Kimpe, L.E., Kokelj, S.V., Poulain, A.J., Smol, J.P., Wang, X. and Blais, J.M., 2014. Dissolved organic carbon thresholds affect mercury bioaccumulation in Arctic lakes. *Environ. Sci. Technol.*, **48(6)**: 3162-3168.

Gilmour, C.C., Podar, M., Bullock, A.L., Graham, A.M., Brown, S.D., Somenahally, A.C., Johs, A., Hurt, R.A., Jr., Bailey, K.L. and Elias, D.A., 2013. Mercury methylation by novel microorganisms from new environments. *Environ. Sci. Technol.*, **47(20)**: 11810-11820.

Gionfriddo, C.M., Tate, M.T., Wick, R.R., Schultz, M.B., Zemla, A., Thelen, M.P., Schofield, R., Krabbenhoft, D.P., Holt, K.E. and Moreau, J.W., 2016. Microbial mercury methylation in Antarctic sea ice. *Nat. Microbiol.*, **1**: 16127.

Gobler, C.J., Buck, N.J., Sieracki, M.E. and Sañudo-Wilhelmy, S.A., 2006. Nitrogen and silicon limitation of phytoplankton communities across an urban estuary: The East River-Long Island Sound system. *Estuar. Coast. Shelf Sci.*, **68(1-2)**: 127-138.

Gonzalez-Davila, M., Santana-Casiano, J.M., Perez-Pena, J. and Millero, F.J., 1995. Binding of Cu(II) to the surface and exudates of the alga *Dunaliella tertiolecta* in seawater. *Environ. Sci. Technol.*, **29(2)**: 289-301.

Gorski, P.R., Armstrong, D.E., Hurley, J.P. and Krabbenhoft, D.P., 2008. Influence of natural dissolved organic carbon on the bioavailability of mercury to a freshwater alga. *Environ. Pollut.*, **154(1)**: 116-123.

Gorski, P.R., Armstrong, D.E., Hurley, J.P. and Shafer, M.M., 2006. Speciation of aqueous methylmercury influences uptake by a freshwater alga (*Selenastrum capricornutum*). *Environ. Toxicol. Chem.*, **25(2)**: 534-540.

Gosnell, K.J. and Mason, R.P., 2015. Mercury and methylmercury incidence and bioaccumulation in plankton from the central Pacific Ocean. *Mar. Chem.*, **177**: 772-780.

Grandjean, P., Satoh, H., Murata, K. and Eto, K., 2010. Adverse effects of methylmercury: environmental health research implications. *Environ. Health Perspect.*, **118(8)**: 1137-45.

Gribble, M.O., Karimi, R., Feingold, B.J., Nyland, J.F., O'Hara, T.M., Gladyshev, M.I. and Chen, C.Y., 2016. Mercury, selenium and fish oils in marine food webs and implications for human health. *J. Mar. Biol. Assoc. UK*, **96(1)**: 43-59.

Gu, B., Mishra, B., Miller, C., Wang, W., Lai, B., Brooks, S.C., Kemner, K.M. and Liang, L., 2014. X-ray fluorescence mapping of mercury on suspended mineral particles and diatoms in a contaminated freshwater system. *Biogeosciences*: 5259.

Guentzel, J.L., Powell, R.T., Landing, W.M. and Mason, R.P., 1996. Mercury associated with colloidal material in an estuarine and an open-ocean environment. *Mar. Chem.*, **55(1-2)**: 177-188.

Guillard, R.R.L., 1975. Culture of phytoplankton for feeding marine invertebrates. In: W.L. Smith and M.H. Chanley (Editors), Culture of marine invertebrate animals. Plenum Press, pp. 29-60.

Guillard, R.R.L. and Ryther, J.H., 1962. Studies of marine planktonic diatoms: I. *Cyclotella Nana* Hustedt, and *Detonula Confervacea* (Cleve) Gran. *Can. J. Microbiol.*, **8(2)**: 229-239.

Gutknecht, J., 1981. Inorganic mercury (Hg^{2+}) transport through lipid bilayer membranes. *J. Membr. Biol.*, **61(1)**: 61-66.

Haitzer, M., Aiken, G.R. and Ryan, J.N., 2002. Binding of mercury(II) to dissolved organic matter: the role of the mercury-to-DOM concentration ratio. *Environ. Sci. Technol.*, **36(16)**: 3564-3570.

Hamdy, M.K. and Noyes, O.R., 1975. Formation of methyl mercury by bacteria. *Appl. Microbiol.*, **30(3)**: 424-432.

Hammerschmidt, C.R. and Bowman, K.L., 2012. Vertical methylmercury distribution in the subtropical North Pacific Ocean. *Mar. Chem.*, **132-133**: 77-82.

Hammerschmidt, C.R., Finiguerra, M.B., Weller, R.L. and Fitzgerald, W.F., 2013. Methylmercury accumulation in plankton on the continental margin of the northwest Atlantic Ocean. *Environ. Sci. Technol.*, **47(8)**: 3671-7.

Hammerschmidt, C.R. and Fitzgerald, W.F., 2006a. Bioaccumulation and trophic transfer of methylmercury in Long Island Sound. *Arch. Environ. Contam. Toxicol.*, **51(3)**: 416-24.

Hammerschmidt, C.R. and Fitzgerald, W.F., 2006b. Methylmercury cycling in sediments on the continental shelf of southern New England. *Geochim. Cosmochim. Acta*, **70(4)**: 918-930.

Hammerschmidt, C.R. and Fitzgerald, W.F., 2006c. Photodecomposition of methylmercury in an arctic Alaskan lake. *Environ. Sci. Technol.*, **40(4)**: 1212-1216.

Hammerschmidt, C.R., Fitzgerald, W.F., Lamborg, C.H., Balcom, P.H. and Visscher, P.T., 2004. Biogeochemistry of methylmercury in sediments of Long Island Sound. *Mar. Chem.*, **90(1-4)**: 31-52.

Han, S., Gill, G.A., Lehman, R.D. and Choe, K.-Y., 2006. Complexation of mercury by dissolved organic matter in surface waters of Galveston Bay, Texas. *Mar. Chem.*, **98(2)**: 156-166.

Hansell, D.A. and Carlson, C.A., 2002. Biogeochemistry of marine dissolved organic matter. Academic Press.

Harris, H.H., Pickering, I.J. and George, G.N., 2003. The chemical form of mercury in fish. *Science*, **301(5637)**: 1203-1203.

Heyes, A., Mason, R.P., Kim, E.-H. and Sunderland, E., 2006. Mercury methylation in estuaries: Insights from using measuring rates using stable mercury isotopes. *Mar. Chem.*, **102(1-2)**: 134-147.

Hintelmann, H., Welbourn, P.M. and Evans, R.D., 1997. Measurement of complexation of methylmercury(II) compounds by freshwater humic substances using equilibrium dialysis. *Environ. Sci. Technol.*, **31(2)**: 489-495.

Hsu-Kim, H., 2007. Stability of metal−glutathione complexes during oxidation by hydrogen peroxide and Cu(II)-catalysis. *Environ. Sci. Technol.*, **41(7)**: 2338-2342.

Hsu-Kim, H., Kucharzyk, K.H., Zhang, T. and Deshusses, M.A., 2013. Mechanisms regulating mercury bioavailability for methylating microorganisms in the aquatic environment: a critical review. *Environ. Sci. Technol.*, **47(6)**: 2441-2456.

Hudson, R.J.M. and Morel, F.M.M., 1990. lron transport in marine phytoplankton: Kinetics of cellular and medium coordination reactions. *Limnol. Oceanogr.*, **35(5)**: 1002-1020.

Hutchins, D.A., Wang, W.-X. and Fisher, N.S., 1995. Copepod grazing and the biogeochemical fate of diatom iron. *Limnol. Oceanogr.*, **40(5)**: 989-994.

Jawaid, M. and Ingman, F., 1981. Potentiometric studies on the complex formation between methylmercury(II) and some keto-and amino-carboxylic acids. *Talanta*, **28(3)**: 137-143.

Kading, T., 2013. Distribution of thiols in the northwest Atlantic Ocean. Master Thesis, Massachusetts Institute of Technology and Woods Hole Oceanographic Institution, 52 pp.

Kaiser, K. and Benner, R., 2009. Biochemical composition and size distribution of organic matter at the Pacific and Atlantic time-series stations. *Mar. Chem.*, **113(1)**: 63-77.

Kaneko, J.J. and Ralston, N.V., 2007. Selenium and mercury in pelagic fish in the central north Pacific near Hawaii. *Biol. Trace Elem. Res.*, **119(3)**: 242-254.

Karimi, R., Chen, C.Y., Pickhardt, P.C., Fisher, N.S. and Folt, C.L., 2007. Stoichiometric controls of mercury dilution by growth. *Proc. Natl. Acad. Sci.*, **104(18)**: 7477-7482.

Karimi, R., Fisher, N.S. and Folt, C.L., 2010. Multielement stoichiometry in aquatic invertebrates: when growth dilution matters. *Am. Nat.*, **176(6)**: 699-709.

Karimi, R., Fitzgerald, T.P. and Fisher, N.S., 2012. A quantitative synthesis of mercury in commercial seafood and implications for exposure in the United States. *Environ. Health Perspect.*, **120(11)**: 1512-1519.

Kester, D.R., Duedall, I.W., Connors, D.N. and Pytkowicz, R.M., 1967. Preparation of artificial seawater. *Limnol. Oceanogr.*, **12(1)**: 176-179.

Kim, H., Van Duong, H., Kim, E., Lee, B.G. and Han, S., 2014. Effects of phytoplankton cell size and chloride concentration on the bioaccumulation of methylmercury in marine phytoplankton. *Environ. Toxicol.*, **29(8)**: 936-41.

Kim, J.P. and Fitzgerald, W.F., 1986. Sea-air partitioning of mercury in the equatorial Pacific Ocean. *Science*, **231**: 1131-1134.

Kirchman, D.L., 1993. Leucine incorporation as a measure of biomass production by heterotrophic bacteria. In: P.F. Kemp, B.F. Sherr, E.B. Sherr and J.J. Cole (Editors), Handbook of methods in aquatic microbial ecology. CRC Press, pp. 509-512.

Korbas, M., Blechinger, S.R., Krone, P.H., Pickering, I.J. and George, G.N., 2008. Localizing organomercury uptake and accumulation in zebrafish larvae at the tissue and cellular level. *Proc. Natl. Acad. Sci.*, **105(34)**: 12108-12112.

Kraepiel, A.M.L., Keller, K., Chin, H.B., Malcolm, E.G. and Morel, F.M.M., 2003. Sources and variations of mercury in tuna. *Environ. Sci. Technol.*, **37(24)**: 5551-5558.

Krezel, A. and Bal, W., 1999. Coordination chemistry of glutathione. *Acta Biochim. Pol.*, **46**: 567-580.

Kuss, J., Wasmund, N., Nausch, G.n. and Labrenz, M., 2015. Mercury emission by the Baltic Sea: A consequence of cyanobacterial activity, photochemistry, and low-light mercury transformation. *Environ. Sci. Technol.*, **49(19)**: 11449-11457.

Kwon, S.Y., Blum, J.D., Madigan, D.J., Block, B.A. and Popp, B.N., 2016. Quantifying mercury isotope dynamics in captive Pacific bluefin tuna (*Thunnus orientalis*). *Elementa*, **4**.

Laglera, L.M. and van den Berg, C.M.G., 2006. Photochemical oxidation of thiols and copper complexing ligands in estuarine waters. *Mar. Chem.*, **101(1)**: 130-140.

Lahaye, V., Bustamante, P., Dabin, W., Van Canneyt, O., Dhermain, F., Cesarini, C., Pierce, G.J. and Caurant, F., 2006. New insights from age determination on toxic element accumulation in striped and bottlenose dolphins from Atlantic and Mediterranean waters. *Mar. Pollut. Bull.*, **52(10)**: 1219-30.

Lamborg, C.H., Bowman, K.L., Hammerschmidt, C.R., Gilmour, C.C., Munson, K.M., Selin, N.E. and Tseng, C.-M., 2014a. Mercury in the anthropocene ocean. *Oceanography*, **27(1)**: 76-87.

Lamborg, C.H., Fitzgerald, W.F., Skoog, A. and Visscher, P.T., 2004. The abundance and source of mercury-binding organic ligands in Long Island Sound. *Mar. Chem.*, **90(1-4)**: 151-163.

Lamborg, C.H., Hammerschmidt, C.R., Bowman, K.L., Swarr, G.J., Munson, K.M., Ohnemus, D.C., Lam, P.J., Heimbürger, L.-E., Rijkenberg, M.J. and Saito, M.A., 2014b. A global ocean inventory of anthropogenic mercury based on water column measurements. *Nature*, **512(7512)**: 65-68.

Lawson, N.M. and Mason, R.P., 1998. Accumulation of mercury in estuarine food chains. *Biogeochemistry*, **40(2-3)**: 235-247.

Le Gall, A.C. and van den Berg, C.M.G., 1998. Folic acid and glutathione in the water column of the North East Atlantic. *Deep Sea Res., Part I*, **45(11)**: 1903-1918.

Leal, M.F.C., Vasconcelos, M.T.S.D. and van den Berg, C.M.G., 1999. Copper-induced release of complexing ligands similar to thiols by *Emiliania huxleyi* in seawater cultures. *Limnol. Oceanogr.*, **44(7)**: 1750-1762.

Lee, B.-G. and Fisher, N.S., 1992a. Decomposition and release of elements from zooplankton debris. *Mar. Ecol. Prog. Ser.*, **88**: 117-117.

Lee, B.-G. and Fisher, N.S., 1992b. Degradation and elemental release rates from phytoplankton debris and their geochemical implications. *Limnol. Oceanogr.*, **37(7)**: 1345-1360.

Lee, C.-S. and Fisher, N.S., 2016. Methylmercury uptake by diverse marine phytoplankton. *Limnol. Oceanogr.*, **61(5)**: 1626-1639.

Lee, C.-S. and Fisher, N.S., 2017a. Bioaccumulation of methylmercury in a marine copepod. *Environ. Toxicol. Chem.*, **36(5)**: 1287-1293.

Lee, C.-S. and Fisher, N.S., 2017b. Bioaccumulation of methylmercury in a marine diatom and the influence of dissolved organic matter. *Mar. Chem.*, **197**: 70-79.

Lee, S. and Fuhrman, J.A., 1987. Relationships between biovolume and biomass of naturally derived marine bacterioplankton. *Appl. Environ. Microbiol.*, **53(6)**: 1298-1303.

Lehnherr, I., Louis, V.L.S., Hintelmann, H. and Kirk, J.L., 2011. Methylation of inorganic mercury in polar marine waters. *Nat. Geosci.*, **4(5)**: 298-302.

Lehnherr, I. and St. Louis, V.L., 2009. Importance of ultraviolet radiation in the photodemethylation of methylmercury in freshwater ecosystems. *Environ. Sci. Technol.*, **43(15)**: 5692-5698.

Lloyd, N.A., Janssen, S.E., Reinfelder, J.R. and Barkay, T., 2016. Co-selection of mercury and multiple antibiotic resistances in bacteria exposed to mercury in the *Fundulus heteroclitus* gut microbiome. *Curr. Microbiol.*, **73(6)**: 834-842.

Logan, J.M., Golet, W.J. and Lutcavage, M.E., 2015. Diet and condition of Atlantic bluefin tuna (*Thunnus thynnus*) in the Gulf of Maine, 2004–2008. *Environ. Biol. Fishes*, **98(5)**: 1411-1430.

Logan, J.M., Rodríguez-Marín, E., Goñi, N., Barreiro, S., Arrizabalaga, H., Golet, W. and Lutcavage, M., 2011. Diet of young Atlantic bluefin tuna (*Thunnus thynnus*) in eastern and western Atlantic foraging grounds. *Mar. Biol.*, **158(1)**: 73-85.

Longnecker, K., Soule, M.C.K. and Kujawinski, E.B., 2015. Dissolved organic matter produced by *Thalassiosira pseudonana*. *Mar. Chem.*, **168**: 114-123.

Lonsdale, D.J., Cosper, E.M. and Doall, M., 1996. Effects of zooplankton grazing on phytoplankton size-structure and biomass in the lower Hudson River estuary. *Estuaries and Coasts*, **19(4)**: 874-889.

Luengen, A.C., Fisher, N.S. and Bergamaschi, B.A., 2012. Dissolved organic matter reduces algal accumulation of methylmercury. *Environ. Toxicol. Chem.*, **31(8)**: 1712-9.

MacKinnon, J.G., White, H. and Davidson, R., 1983. Tests for model specification in the presence of alternative hypotheses: Some further results. *J. Econometrics*, **21(1)**: 53-70.

Maldonado, M.T. and Price, N.M., 2001. Reduction and transport of organically bound iron by *Thalassiosira oceanica* (Bacillariophyceae). *J. Phycol.*, **37(2)**: 298-310.

Mason, R.P., Choi, A.L., Fitzgerald, W.F., Hammerschmidt, C.R., Lamborg, C.H., Soerensen, A.L. and Sunderland, E.M., 2012. Mercury biogeochemical cycling in the ocean and policy implications. *Environ. Res.*, **119**: 101-117.

Mason, R.P. and Fitzgerald, W.F., 1990. Alkylmercury species in the equatorial Pacific. *Nature*, **347(6292)**: 457-459.

Mason, R.P., Fitzgerald, W.F. and Morel, F.M.M., 1994. The biogeochemical cycling of elemental mercury: anthropogenic influences. *Geochim. Cosmochim. Acta*, **58(15)**: 3191-3198.

Mason, R.P., Lawson, N.M. and Sheu, G.-R., 2001. Mercury in the Atlantic Ocean: factors controlling air–sea exchange of mercury and its distribution in the upper waters. *Deep Sea Res., Part II*, **48(13)**: 2829-2853.

Mason, R.P., Morel, F.M.M. and Hemond, H.F., 1995. The role of microorganisms in elemental mercury formation in natural waters. *Water, Air, Soil Pollut.*, **80(1-4)**: 775-787.

Mason, R.P., Reinfelder, J.R. and Morel, F.M.M., 1996. Uptake, toxicity, and trophic transfer of mercury in a coastal diatom. *Environ. Sci. Technol.*, **30(6)**: 1835-1845.

Mason, R.P. and Sheu, G.-R., 2002. Role of the ocean in the global mercury cycle. *Global Biogeochem. Cycles*, **16(4)**.

Mathews, T. and Fisher, N.S., 2008. Evaluating the trophic transfer of cadmium, polonium, and methylmercury in an estuarine food chain. *Environ. Toxicol. Chem.*, **27(5)**: 1093-1101.

Mauchline, J., 1998. The biology of calanoid copepods. Advance in marine biology. Academic Press, 710 pp.

McIntyre, A.M. and Guéguen, C., 2013. Binding interactions of algal-derived dissolved organic matter with metal ions. *Chemosphere*, **90(2)**: 620-626.

Miles, C.J., Moye, H.A., Phlips, E.J. and Sargent, B., 2001. Partitioning of monomethylmercury between freshwater algae and water. *Environ. Sci. Technol.*, **35(21)**: 4277-4282.

Moingt, M., Bressac, M., Bélanger, D. and Amyot, M., 2010. Role of ultra-violet radiation, mercury and copper on the stability of dissolved glutathione in natural and artificial freshwater and saltwater. *Chemosphere*, **80(11)**: 1314-1320.

Monperrus, M., Tessier, E., Amouroux, D., Leynaert, A., Huonnic, P. and Donard, O.F.X., 2007. Mercury methylation, demethylation and reduction rates in coastal and marine surface waters of the Mediterranean Sea. *Mar. Chem.*, **107(1)**: 49-63.

Monteiro, L.R., Costa, V., Furness, R.W. and Santos, R.S., 1996. Mercury concentrations in prey fish indicate enhanced bioaccumulation in mesopelagic environments. *Mar. Ecol. Prog. Ser.*: 21-25.

Mopper, K. and Kieber, D.J., 1991. Distribution and biological turnover of dissolved organic compounds in the water column of the Black Sea. *Deep Sea Res., Part A*, **38**: S1021-S1047.

Morel, F.M.M., Kraepiel, A.M.L. and Amyot, M., 1998. The chemical cycle and bioaccumulation of mercury. *Annu. Rev. Ecol. Syst.*, **29**: 543-566.

Morel, F.M.M. and Price, N.M., 2003. The biogeochemical cycles of trace metals in the oceans. *Science*, **300(5621)**: 944-947.

Mozaffarian, D., 2009. Fish, mercury, selenium and cardiovascular risk: current evidence and unanswered questions. *Int. J. Environ. Res. Public Health*, **6(6)**: 1894-1916.

Munson, K.M., Lamborg, C.H., Swarr, G.J. and Saito, M.A., 2015. Mercury species concentrations and fluxes in the Central Tropical Pacific Ocean. *Global Biogeochem. Cycles*, **29(5)**: 656-676.

National Research Council, 2000. Toxicological effects of methylmercury. National Academy Press, Washington, D.C.

Nazaret, S., Jeffrey, W.H., Saouter, E., Von Haven, R. and Barkay, T., 1994. *merA* gene expression in aquatic environments measured by mRNA production and Hg(II) volatilization. *Appl. Environ. Microbiol.*, **60(11)**: 4059-4065.

Ndu, U., Barkay, T., Schartup, A.T., Mason, R.P. and Reinfelder, J.R., 2016. The effect of aqueous speciation and cellular ligand binding on the biotransformation and bioavailability of methylmercury in mercury-resistant bacteria. *Biodegradation*, **27(1)**: 29-36.

Ndu, U., Mason, R.P., Zhang, H., Lin, S. and Visscher, P.T., 2012. Effect of inorganic and organic ligands on the bioavailability of methylmercury as determined by using a *mer-lux* bioreporter. *Appl. Environ. Microbiol.*, **78(20)**: 7276-82.

NIST, 2004. NIST standard reference database 46: NIST critically selected stability constants of metal complexes database ver. 8. National Institute of Standards and Technology.

Nriagu, J.O., 1994. Mechanistic steps in the photoreduction of mercury in natural waters. *Sci. Total Environ.*, **154(1)**: 1-8.

O'Driscoll, N.J. and Evans, R.D., 2000. Analysis of methyl mercury binding to freshwater humic and fulvic acids by gel permeation chromatography/hydride generation ICP-MS. *Environ. Sci. Technol.*, **34(18)**: 4039-4043.

O'Driscoll, N.J., Poissant, L., Canario, J., Ridal, J. and Lean, D.R.S., 2007. Continuous analysis of dissolved gaseous mercury and mercury volatilization in the upper St. Lawrence River: Exploring temporal relationships and UV attenuation. *Environ. Sci. Technol.*, **41(15)**: 5342-5348.

O'Driscoll, N.J., Siciliano, S.D., Lean, D.R.S. and Amyot, M., 2006. Gross photoreduction kinetics of mercury in temperate freshwater lakes and rivers: application to a general model of DGM dynamics. *Environ. Sci. Technol.*, **40(3)**: 837-843.

Onyido, I., Norris, A.R. and Buncel, E., 2004. Biomolecule− mercury interactions: Modalities of DNA base− mercury binding mechanisms. remediation strategies. *Chem. Rev.*, **104(12)**: 5911-5930.

Oremland, R.S., Culbertson, C.W. and Winfrey, M.R., 1991. Methylmercury decomposition in sediments and bacterial cultures: involvement of methanogens and sulfate reducers in oxidative demethylation. *Appl. Environ. Microbiol.*, **57(1)**: 130-137.

Ortiz de Zarate, V. and Cort, J.L., 1986. Stomach contents study of immature bluefin tuna in the Bay of Biscay, International council for the exploration of the sea council meeting documents.

Osborn, A.M., Bruce, K.D., Strike, P. and Ritchie, D.A., 1997. Distribution, diversity and evolution of the bacterial mercury resistance (*mer*) operon. *FEMS Microbiol. Rev.*, **19(4)**: 239-262.

Parks, J.M., Johs, A., Podar, M., Bridou, R., Hurt, R.A., Smith, S.D., Tomanicek, S.J., Qian, Y., Brown, S.D. and Brandt, C.C., 2013. The genetic basis for bacterial mercury methylation. *Science*, **339(6125)**: 1332-1335.

Pickhardt, P.C. and Fisher, N.S., 2007. Accumulation of inorganic and methylmercury by freshwater phytoplankton in two contrasting water bodies. *Environ. Sci. Technol.*, **41(1)**: 125-131.

Pickhardt, P.C., Folt, C.L., Chen, C.Y., Klaue, B. and Blum, J.D., 2002. Algal blooms reduce the uptake of toxic methylmercury in freshwater food webs. *Proc. Natl. Acad. Sci.*, **99(7)**: 4419-23.

Pickhardt, P.C., Folt, C.L., Chen, C.Y., Klaue, B. and Blum, J.D., 2005. Impacts of zooplankton composition and algal enrichment on the accumulation of mercury in an experimental freshwater food web. *Sci. Total Environ.*, **339(1-3)**: 89-101.

Pirrone, N., Cinnirella, S., Feng, X., Finkelman, R.B., Friedli, H.R., Leaner, J., Mason, R., Mukherjee, A.B., Stracher, G.B., Streets, D.G. and Telmer, K., 2010. Global mercury emissions to the atmosphere from anthropogenic and natural sources. *Atmos. Chem. Phys.*, **10(13)**: 5951-5964.

Poulain, A.J., Aris-Brosou, S., Blais, J.M., Brazeau, M., Keller, W.B. and Paterson, A.M., 2015. Microbial DNA records historical delivery of anthropogenic mercury. *ISME J*, **9(12)**: 2541.

Poulain, A.J., Ni Chadhain, S.M., Ariya, P.A., Amyot, M., Garcia, E., Campbell, P.G.C., Zylstra, G.J. and Barkay, T., 2007. Potential for mercury reduction by microbes in the high arctic. *Appl. Environ. Microbiol.*, **73(7)**: 2230-2238.

Pućko, M., Burt, A., Walkusz, W., Wang, F., Macdonald, R.W., Rysgaard, S., Barber, D.G., Tremblay, J.-É. and Stern, G.A., 2014. Transformation of mercury at the bottom of the

Arctic food web: An overlooked puzzle in the mercury exposure narrative. *Environ. Sci. Technol.*, **48(13)**: 7280-7288.

Qureshi, A., O'Driscoll, N.J., MacLeod, M., Neuhold, Y.-M. and Hungerbühler, K., 2009. Photoreactions of mercury in surface ocean water: Gross reaction kinetics and possible pathways. *Environ. Sci. Technol.*, **44(2)**: 644-649.

Rabenstein, D.L., 1973. Nuclear magnetic resonance studies of the acid-base chemistry of amino acids and peptides. I. Microscopic ionization constants of glutathione and methylmercury-complexed glutathione. *J. Am. Chem. Soc.*, **95(9)**: 2797-2803.

Rabenstein, D.L., 1978. The aqueous solution chemistry of methylmercury and its complexes. *Acc. Chem. Res.*, **11(3)**: 100-107.

Rainbow, P.S., 1997. Ecophysiology of trace metal uptake in crustaceans. *Estuar. Coast. Shelf Sci.*, **44(2)**: 169-176.

Ralston, N.V. and Raymond, L.J., 2010. Dietary selenium's protective effects against methylmercury toxicity. *Toxicology*, **278(1)**: 112-23.

Ravichandran, M., 2004. Interactions between mercury and dissolved organic matter—a review. *Chemosphere*, **55(3)**: 319-31.

Reinfelder, J.R. and Fisher, N.S., 1991. The assimilation of elements ingested by marine copepods. *Science*, **251(4995)**: 794-796.

Reinfelder, J.R. and Fisher, N.S., 1994. The assimilation ofelements ingested by marine planktonic bivalve larvae. *Limnol. Oceanogr.*, **39(1)**: 12-20.

Reinfelder, J.R., Fisher, N.S., Luoma, S.N., Nichols, J.W. and Wang, W.X., 1998. Trace element trophic transfer in aquatic organisms: A critique of the kinetic model approach. *Sci. Total Environ.*, **219(2)**: 117-135.

Restrepo, V.R., Diaz, G.A., Walter, J.F., Neilson, J.D., Campana, S.E., Secor, D. and Wingate, R.L., 2010. Updated estimate of the growth curve of western Atlantic bluefin tuna. *Aquat. Living Resour.*, **23(4)**: 335-342.

Rijstenbil, J.W., Dehairs, F., Ehrlich, R. and Wijnholds, J.A., 1998. Effect of the nitrogen status on copper accumulation and pools of metal-binding peptides in the planktonic diatom *Thalassiosira pseudonana*. *Aquat. Toxicol.*, **42(3)**: 187-209.

Robinson, J.B. and Tuovinen, O.H., 1984. Mechanisms of microbial resistance and detoxification of mercury and organomercury compounds: physiological, biochemical, and genetic analyses. *Microbiol. Rev.*, **48(2)**: 95.

Rolfhus, K.R. and Fitzgerald, W.F., 2001. The evasion and spatial/temporal distribution of mercury species in Long Island Sound, CT-NY. *Geochim. Cosmochim. Acta*, **65(3)**: 407-418.

Rolfhus, K.R. and Fitzgerald, W.F., 2004. Mechanisms and temporal variability of dissolved gaseous mercury production in coastal seawater. *Mar. Chem.*, **90(1)**: 125-136.

Rouleau, C. and Block, M., 1997. Fast and high-yield synthesis of radioactive $CH_3{}^{203}Hg$ (II). *Appl. Organomet. Chem.*, **11(9)**: 751-753.

Rudd, J.W., Furutani, A. and Turner, M.A., 1980. Mercury methylation by fish intestinal contents. *Appl. Environ. Microbiol.*, **40(4)**: 777-782.

Schaefer, J.K. and Morel, F.M.M., 2009. High methylation rates of mercury bound to cysteine by *Geobacter sulfurreducens*. *Nat. Geosci.*, **2(2)**: 123-126.

Schaefer, J.K., Yagi, J., Reinfelder, J.R., Cardona, T., Ellickson, K.M., Tel-Or, S. and Barkay, T., 2004. Role of the bacterial organomercury lyase (*merB*) in controlling methylmercury accumulation in mercury-contaminated natural waters. *Environ. Sci. Technol.*, **38(16)**: 4304-4311.

Schartup, A.T., Balcom, P.H., Soerensen, A.L., Gosnell, K.J., Calder, R.S., Mason, R.P. and Sunderland, E.M., 2015a. Freshwater discharges drive high levels of methylmercury in Arctic marine biota. *Proc. Natl. Acad. Sci.*, **112(38)**: 11789-11794.

Schartup, A.T., Ndu, U., Balcom, P.H., Mason, R.P. and Sunderland, E.M., 2015b. Contrasting effects of marine and terrestrially derived dissolved organic matter on mercury speciation and bioavailability in seawater. *Environ. Sci. Technol.*, **49(10)**: 5965-72.

Selin, N.E., 2009. Global biogeochemical cycling of mercury: A review. *Annu. Rev. Environ. Resour.*, **34(1)**: 43-63.

Sellers, P., Kelly, C.A., Rudd, J.W.M. and MacHutchon, A.R., 1996. Photodegradation of methylmercury in lakes. *Nature*, **380(6576)**: 694.

Sharma, V.K., Moulin, A., Millero, F.J. and De Stefano, C., 2006. Dissociation constants of protonated cysteine species in seawater media. *Mar. Chem.*, **99(1)**: 52-61.

Sherr, B., Sherr, E. and del Giorgio, P., 2001. Enumeration of total and highly active bacteria. In: J.H. Paul (Editor), Methods in microbiology. Academic, pp. 129-159.

Shiah, F.-K. and Ducklow, H.W., 1994. Temperature and substrate regulation of bacterial abundance, production and specific growth rate in Chesapeake Bay, USA. *Mar. Ecol. Prog. Ser.*: 297-308.

Shimose, T. and Wells, R.J.D., 2015. Feeding Ecology of Bluefin Tunas. In: T. Kitagawa and S. Kimura (Editors), Biology and Ecology of Bluefin Tuna. CRC Press, Boca Raton, FL, U.S.A, pp. 78-98.

Simkiss, K. and Taylor, M.G., 1995. Transport of metals across membranes. In: A. Tessier and D.R. Turner (Editors), Metal speciation and bioavailability in aquatic systems. Wiley, Chichester, pp. 1-44.

Soerensen, A.L., Jacob, D.J., Streets, D.G., Witt, M.L.I., Ebinghaus, R., Mason, R.P., Andersson, M. and Sunderland, E.M., 2012. Multi-decadal decline of mercury in the North Atlantic atmosphere explained by changing subsurface seawater concentrations. *Geophys. Res. Lett.*, **39(21)**.

Staudinger, M.D., 2011. Species- and size-specific variability of mercury concentrations in four commercially important finfish and their prey from the northwest Atlantic. *Mar. Pollut. Bull.*, **62(4)**: 734-40.

Stewart, G.M. and Fisher, N.S., 2003a. Bioaccumulation of polonium-210 in marine copepods. *Limnol. Oceanogr.*, **48(5)**: 2011-2019.

Stewart, G.M. and Fisher, N.S., 2003b. Experimental studies on the accumulation of polonium-210 by marine phytoplankton. *Limnol. Oceanogr.*, **48(3)**: 1193-1201.

Stordal, M.C., Gill, G.A., Wen, L.S. and Santschi, P.H., 1996. Mercury phase speciation in the surface waters of three Texas estuaries: Importance of colloidal forms. *Limnol. Oceanogr.*, **41(1)**: 52-61.

Storelli, M., Stuffler, R.G. and Marcotrigiano, G., 2002. Total and methylmercury residues in tuna-fish from the Mediterranean Sea. *Food Addit. Contam.*, **19(8)**: 715-720.

Streets, D.G., Devane, M.K., Lu, Z., Bond, T.C., Sunderland, E.M. and Jacob, D.J., 2011. All-time releases of mercury to the atmosphere from human activities. *Environ. Sci. Technol.*, **45(24)**: 10485-10491.

Suda, I., Suda, M. and Hirayama, K., 1993. Degradation of methyl and ethyl mercury by singlet oxygen generated from sea water exposed to sunlight or ultraviolet light. *Arch. Toxicol.*, **67(5)**: 365-368.

Sunda, W.G., 1989. Trace metal interactions with marine phytoplankton. *Biological Oceanography*, **6(5-6)**: 411-442.

Sunda, W.G. and Huntsman, S.A., 1998. Processes regulating cellular metal accumulation and physiological effects: Phytoplankton as model systems. *Sci. Total Environ.*, **219(2)**: 165-181.

Sunderland, E.M., 2007. Mercury exposure from domestic and imported estuarine and marine fish in the U.S. seafood market. *Environ. Health Perspect.*, **115(2)**: 235-242.

Sunderland, E.M., Amirbahman, A., Burgess, N.M., Dalziel, J., Harding, G., Jones, S.H., Kamai, E., Karagas, M.R., Shi, X. and Chen, C.Y., 2012. Mercury sources and fate in the Gulf of Maine. *Environ. Res.*, **119**: 27-41.

Sunderland, E.M., Gobas, F.A.P.C., Branfireun, B.A. and Heyes, A., 2006. Environmental controls on the speciation and distribution of mercury in coastal sediments. *Mar. Chem.*, **102(1-2)**: 111-123.

Sunderland, E.M., Krabbenhoft, D.P., Moreau, J.W., Strode, S.A. and Landing, W.M., 2009. Mercury sources, distribution, and bioavailability in the North Pacific Ocean: Insights from data and models. *Global Biogeochem. Cycles*, **23(2)**.

Swarr, G.J., Kading, T., Lamborg, C.H., Hammerschmidt, C.R. and Bowman, K.L., 2016. Dissolved low-molecular weight thiol concentrations from the US GEOTRACES North Atlantic Ocean zonal transect. *Deep Sea Res., Part I*, **116**: 77-87.

Tang, D., Hung, C.-C., Warnken, K.W. and Santschi, P.H., 2000. The distribution of biogenic thiols in surface waters of Galveston Bay. *Limnol. Oceanogr.*, **45(6)**: 1289-1297.

Tang, D., Shafer, M.M., Karner, D.A. and Armstrong, D.E., 2005. Response of nonprotein thiols to copper stress and extracellular release of glutathione in the diatom *Thalassiosira weissflogii*. *Limnol. Oceanogr.*, **50(2)**: 516-525.

Tang, D., Shafer, M.M., Karner, D.A., Overdier, J. and Armstrong, D.E., 2004. Factors affecting the presence of dissolved glutathione in estuarine waters. *Environ. Sci. Technol.*, **38(16)**: 4247-4253.

Tang, K.W., Glud, R.N., Glud, A., Rysgaard, S. and Nielsen, T.G., 2011. Copepod guts as biogeochemical hotspots in the sea: Evidence from microelectrode profiling of *Calanus* spp. *Limnol. Oceanogr.*, **56(2)**: 666-672.

Taylor, D.L., Kutil, N.J., Malek, A.J. and Collie, J.S., 2014. Mercury bioaccumulation in cartilaginous fishes from Southern New England coastal waters: Contamination from a trophic ecology and human health perspective. *Mar. Environ. Res.*, **99**: 20-33.

Thomann, R.V., 1981. Equilibrium model of fate of microcontaminants in diverse aquatic food chains. *Can. J. Fish. Aquat. Sci.*, **38(3)**: 280-296.

Thurman, E.M., 1985. Aquatic humic substances. In: E.M. Thurman (Editor), Organic geochemistry of natural waters. Springer, pp. 273-361.

Tranvik, L.J., Sherr, E.B. and Sherr, B.F., 1993. Uptake and utilization of 'colloidal DOM' by heterotrophic flagellates in seawater. *Mar. Ecol. Prog. Ser.*: 301-309.

Ullrich, S.M., Tanton, T.W. and Abdrashitova, S.A., 2001. Mercury in the aquatic environment: a review of factors affecting methylation. *Crit. Rev. Environ. Sci. Technol.*, **31(3)**: 241-293.

Vallee, B.L. and Ulmer, D.D., 1972. Biochemical effects of mercury, cadmium, and lead. *Annu. Rev. Biochem.*, **41(1)**: 91-128.

Vetriani, C., Chew, Y.S., Miller, S.M., Yagi, J., Coombs, J., Lutz, R.A. and Barkay, T., 2005. Mercury adaptation among bacteria from a deep-sea hydrothermal vent. *Appl. Environ. Microbiol.*, **71(1)**: 220-226.

Vost, E.E., Amyot, M. and O'Driscoll, N.J., 2012. Photoreactions of mercury in aquatic systems. In: G. Liu, Y. Cai and N.J. O'Driscoll (Editors), Environmental chemistry and toxicology of mercury. Wiley, Hoboken, New Jersey, pp. 193-218.

Vraspir, J.M. and Butler, A., 2009. Chemistry of marine ligands and siderophores. *Ann. Rev. Mar. Sci.*, **1**: 43-63.

Wang, W.-X. and Dei, R.C.H., 2001a. Effects of major nutrient additions on metal uptake in phytoplankton. *Environ. Pollut.*, **111(2)**: 233-240.

Wang, W.-X. and Dei, R.C.H., 2001b. Metal uptake in a coastal diatom influenced by major nutrients (N, P, and Si). *Water Res.*, **35(1)**: 315-321.

Wang, W.-X. and Fisher, N.S., 1998. Accumulation of trace elements in a marine copepod. *Limnol. Oceanogr.*, **43(2)**: 273-283.

Wang, W.-X. and Fisher, N.S., 1999. Assimilation efficiencies of chemical contaminants in aquatic invertebrates: A synthesis. *Environ. Toxicol. Chem.*, **18(9)**: 2034-2045.

Wang, W.-X. and Guo, L., 2000. Bioavailability of colloid-bound Cd, Cr, and Zn to marine plankton. *Mar. Ecol. Prog. Ser.*, **202**: 41-49.

Wang, W.-X., Reinfelder, J.R., Lee, B.-G. and Fisher, N.S., 1996. Assimilation and regeneration of trace elements by marine copepods. *Limnol. Oceanogr.*, **41(1)**: 70-81.

Watras, C.J., Back, R.C., Halvorsen, S., Hudson, R.J.M., Morrison, K.A. and Wente, S.P., 1998. Bioaccumulation of mercury in pelagic freshwater food webs. *Sci. Total Environ.*, **219(2)**: 183-208.

Whalin, L., Kim, E.-H. and Mason, R.P., 2007. Factors influencing the oxidation, reduction, methylation and demethylation of mercury species in coastal waters. *Mar. Chem.*, **107(3)**: 278-294.

Williams, J.J., Dutton, J., Chen, C.Y. and Fisher, N.S., 2010. Metal (As, Cd, Hg, and CH_3Hg) bioaccumulation from water and food by the benthic amphipod *Leptocheirus plumulosus*. *Environ. Toxicol. Chem.*, **29(8)**: 1755-61.

Winterbourn, C.C. and Metodiewa, D., 1999. Reactivity of biologically important thiol compounds with superoxide and hydrogen peroxide. *Free Radic. Biol. Med.*, **27(3)**: 322-328.

Yu, H., Chu, L. and Misra, T.K., 1996. Intracellular inducer Hg^{2+} concentration is rate determining for the expression of the mercury-resistance operon in cells. *J. Bacteriol.*, **178(9)**: 2712-2714.

Zareba, G., Cernichiari, E., Goldsmith, L.A. and Clarkson, T.W., 2008. Validity of methyl mercury hair analysis: mercury monitoring in human scalp/nude mouse model. *J. Appl. Toxicol.*, **28(4)**: 535-542.

Zhang, J., Wang, F., House, J.D. and Page, B., 2004. Thiols in wetland interstitial waters and their role in mercury and methylmercury speciation. *Limnol. Oceanogr.*, **49(6)**: 2276-2286.

Zhang, Y., Jacob, D.J., Horowitz, H.M., Chen, L., Amos, H.M., Krabbenhoft, D.P., Slemr, F., Louis, V.L.S. and Sunderland, E.M., 2016. Observed decrease in atmospheric mercury explained by global decline in anthropogenic emissions. *Proc. Natl. Acad. Sci.*, **113(3)**: 526-531.

Zhong, H. and Wang, W.-X., 2009. Controls of dissolved organic matter and chloride on mercury uptake by a marine diatom. *Environ. Sci. Technol.*, **43(23)**: 8998-9003.